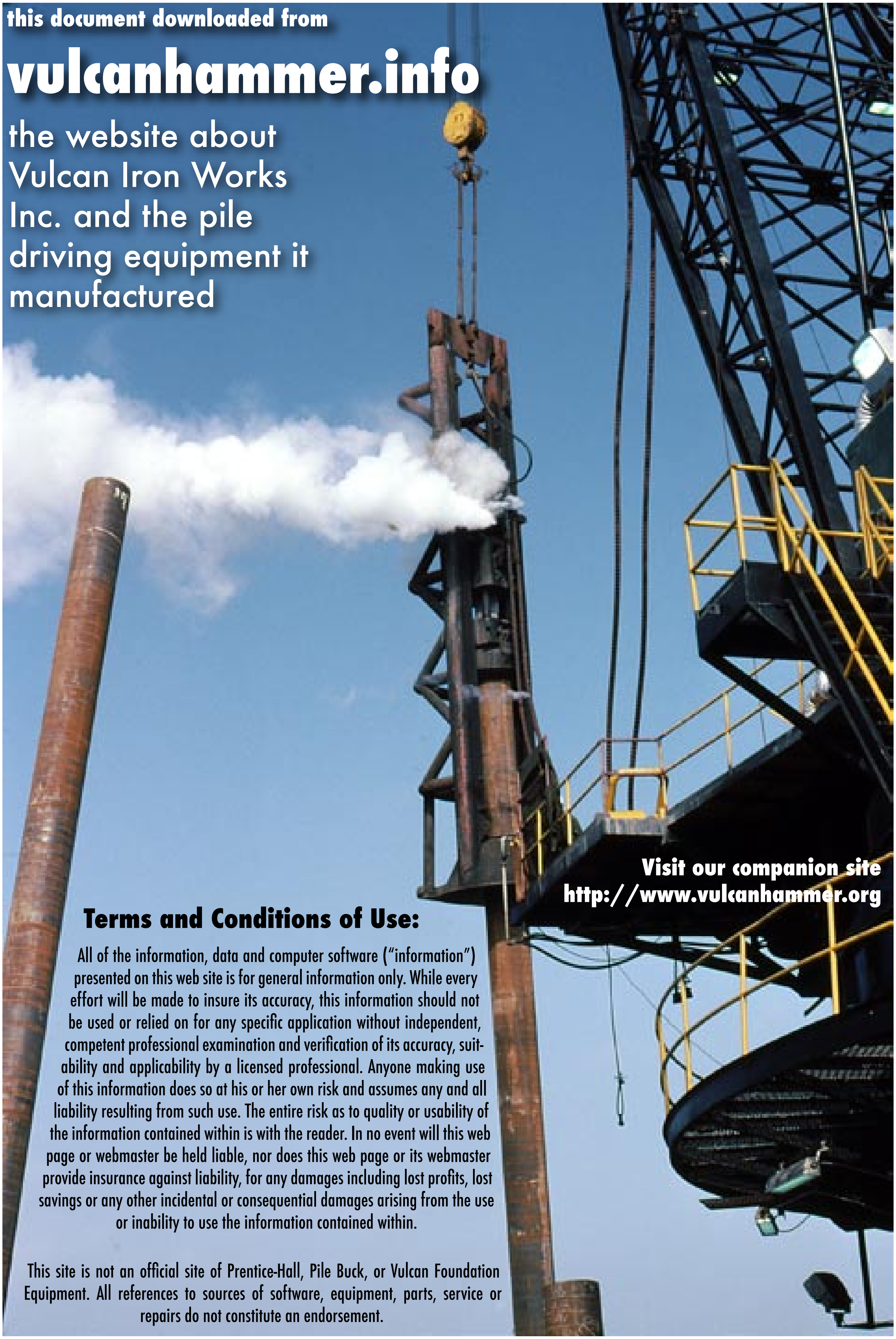

16 State House Station
Augusta, Maine 04333

MaineDOT

Transportation Research Division

Technical Report 15-08

Experimental Evaluation and Design of Unfilled and Concrete-Filled FRP Composite Piles

Task 3 - FRP Composite Pile Flexural Testing

Final Report – Task 3, June 2014

Technical Report Documentation Page

1. Report No. ME 15-08	2.	3. Recipient's Accession No.
4. Title and Subtitle Experimental Evaluation and Design of Unfilled and Concrete-Filled FRP Composite Piles Task 3 – FRP Composite Pile Flexural Testing		5. Report Date June 2014 6.
7. Author(s) Dale Lawrence Roberto Lopez-Anido Thomas Sandford Keenan Goslin Xenia Rofes		8. Performing Organization Report No. AEWC Report Number 15-2-1199
9. Performing Organization Name and Address University of Maine – Advanced Structures and Composites Center		10. Project/Task/Work Unit No. 11. Contract © or Grant (G) No. Contract # 20130731*535
12. Sponsoring Organization Name and Address Maine Department of Transportation		13. Type of Report and Period Covered 14. Sponsoring Agency Code
15. Supplementary Notes		

16. Abstract (Limit 200 words)

The overall goal of this project is the experimental evaluation and design of unfilled and concrete-filled FRP composite piles for load-bearing in bridges. This report covers Task 3, FRP Composite Pile Flexural Testing.

Hollow and concrete filled fiber reinforced polymer (FRP) piles were tested in four point bending to examine degradation in stiffness, ultimate strength, and loss of concrete-FRP composite action due to pile driving and cyclic loading. Testing showed a high level of variability in the ultimate strength of the piles, but all driven and load-cycled samples broke within the upper and lower bounds of the control piles. This series of tests showed no degradation in stiffness during static tests in the piles due to driving or cyclic loading. However, driving and cyclic loading appear to affect composite action between the FRP shell and concrete.

17. Document Analysis/Descriptors Bridge piles, fiber reinforced polymer composites, flexural testing		18. Availability Statement	
19. Security Class (this report)	20. Security Class (this page)	21. No. of Pages 162	22. Price

Technical Report

FRP Composite Pile Flexural Testing

Submitted by:
Dale Lawrence, Roberto Lopez-Anido[1], Thomas Sandford,
Keenan Goslin and Xenia Rofes

University of Maine's Advanced Structures and Composites Center
Report Number: 15-2-1199

Project: Experimental Evaluation and Design of Unfilled and Concrete-Filled FRP Composite Piles

Prepared for:
Dale Peabody P.E.
Director of Transportation Research
Maine Dept. of Transportation
16 State House Station
Augusta, Maine 04333

June 2nd, 2014

[1] Department of Civil and Environmental Engineering, University of Maine
rla@maine.edu Phone: (207) 581-2119

Table of Contents

1. Executive Summary

Hollow and concrete filled fiber reinforced polymer (FRP) piles were tested in four point bending to examine degradation in stiffness, ultimate strength, and loss of concrete-FRP composite action due to pile driving and cyclic loading. Testing showed a high level of variability in the ultimate strength of the piles, but all driven and load-cycled samples broke within the upper and lower bounds of the control piles. This series of tests showed no degradation in stiffness during static tests in the piles due to driving or cyclic loading. However, driving and cyclic loading appear to affect composite action between the FRP shell and concrete.

2. References

1. Lawrence, Dale et al. "Guide Specifications for Unfilled and Concrete-Filled FRP Composite Piles."
2. Lawrence, Dale et al. "FRP Composite Pile Driving at the Richmond-Dresden Bridge Over the Kennebec River", ASCC technical report 14-14-1199. 2014.
3. Advanced Structures and Composites Center Work Instruction WI-T-96: Four Point Flexural Test for 24" Piles.
4. Davol, A., Burgueno, R. and Seible. F. (2001). Flexural Behavior of Circular Concrete Filled FRP Shells. Journal of Structural Engineering: July 2001.
5. ASTM D6109-13 Flexural Properties of Unreinforced and Reinforced Plastic Lumber and Related Products.

3. Materials and Sample Description

FRP piles were manufactured in July of 2013 by Harbor Technologies LLC with a nominal diameter of 24 inches and nominal length of 40 feet. The FRP shell consists a stitched E-glass fabric with 0, 90, and +/-45 degree fibers and a polyester resin. Concrete-filled piles have 4 layers of reinforcement which gives a nominal shell thickness of 1/2 inch and hollow piles have 8 layers of reinforcement which gives a nominal shell thickness of 1 inch.

Specifications for dimensional tolerances and physical properties were established prior to the manufacturing of FRP piles. All piles fell within the range of acceptable dimensions. Additional details on the specifications can be seen in Reference 1.

Driven piles were delivered to the Richmond-Dresden bridge site (MDOT PIN 12674) in early August 2013. This set of piles contained (1) 4 ply pile and (3) 8 ply piles. On August 14, 2013, (1) 4 ply pile (Pile A) was completely filled with concrete and (1) 8 ply pile (Pile B) had a 4 foot concrete plug cast at its toe. All driven piles were stored on site until pile driving took place on August 28, 2013. Piles remained in the ground until they could be removed and shipped to the University of Maine on October 15, 2013, and November 8, 2013.

Baseline and load-cycled piles were delivered to the Richmond-Dresden bridge site on in early September. This set of piles contained (4) 4 ply piles and (2) 8 ply piles. On September 27, 2013, (4) 4 ply piles were filled with concrete. Piles remained on site until they could be shipped to the University of Maine on October 15, 2013 and November 8, 2013.

Driven and undriven piles were tested in flexure at the University of Maine to evaluate their flexural strength, and examine the effects of pile driving and cyclic loading on their structural capacity. The flexural testing of undriven piles corresponds with sub-task 1.2 of the proposal for this research program while the testing of driven piles corresponds with sub-task 1.4. A summary of the piles' construction, and test condition can be seen in Table 1.

Table 1: Summary of Specimen Construction and Test Condition

Driving Designation	Number of Plys in Shell	Type of Concrete	Type of Testing	Pile ID	Driven?	Fatigued?	Delivered Length	Harbor Tech Designation
A	4	F	B	Pile A-4FB	Yes	No	40'-5"	1
B	8	P	B	Pile B-8PB	Yes	No	39'-1"	6
C	8	HF	B	Pile C-8HFB	Yes	No	34'-11"	4
D	8	H	A	Pile D-8HA	Yes	No	34'-5"	5
E	4	F	B	Pile E-4FB	No	Yes	40'-0"	4
F	4	F	B	Pile F-4FB	No	Yes	40'-0"	5
G	4	F	B	Pile G-4FB	No	No	40'-0"	2
H	4	F	B	Pile H-4FB	No	No	40'-0"	3
I	8	H	B	Pile I-8HB	No	No	40'-1"	8
J	8	H	B	Pile J-8HB	No	No	40'-0"	7

F	Filled
P	Concrete Plug
HF	Driven Hollow then Filled
H	Hollow

B	Bending
A	Axial

All driven piles showed various levels of damage from driving and/or extraction. A summary of this damage and a summary of driving can be seen in Reference 2.

4. Test Setup

4.1. General Test Setup

All piles were tested in a four-point bending configuration that can be seen in Figure 1. The span length for each test was 33 feet. The load was applied using a single 300 kip actuator with a spreader beam. Load points were at the 1/3 points of the span (11 feet), except for Pile C when load points were adjusted to create higher moments.

Figure 1: Flexural Test Configuration

Saddles with a curvature equal to that of the piles were used at loading points and end supports to distribute load over the pile. Each saddle was lined with neoprene to aid in load distribution and a plastic sheet to allow lateral translation. These saddles were mounted on pinned supports that allowed rotations associated with the large expected deflections. A saddle and pinned support can be seen in Figure 2.

Figure 2: Saddle and Support Configuration

4.2. Static vs. Load-Cycled Tests

Static piles were loaded to failure by controlling the rate of displacement. Piles were loaded at a rate of 1.5 inches per minute for the first 15 inches of deflection. Then the loading rate was transitioned to 1 inch per minute using a sinusoidal ramp. A plot of the loading profile can be seen in Figure 3.

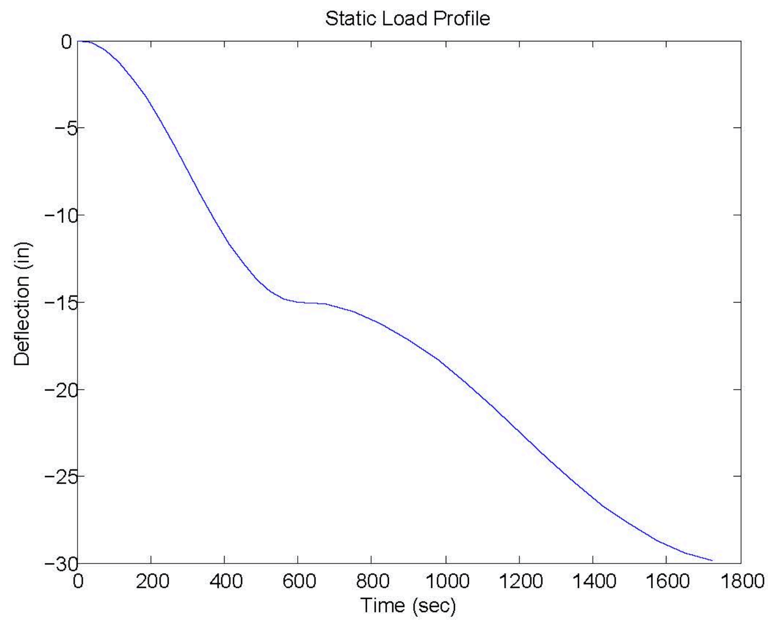

Figure 3: Static Loading Profile

Load-cycled piles were loaded to 50 percent of the average ultimate load of the previously tested piles. This load was determined to be 75 kips. The piles were cycled between 7.5 kips and 75 kips for 10,000 cycles at a frequency of 0.05 Hz. After 10,000 cycles, the piles were rotated 180 degrees about their longitudinal axis and subjected to an additional 10,000 cycles. Then, the piles were tested statically to failure. Strain and displacement measurements were taken at the maximum and minimum load of each cycle. Data was collected over the entire loading cycle for 10 cycles every 1,000 cycles. A plot of the loading profile can be seen in Figure 4.

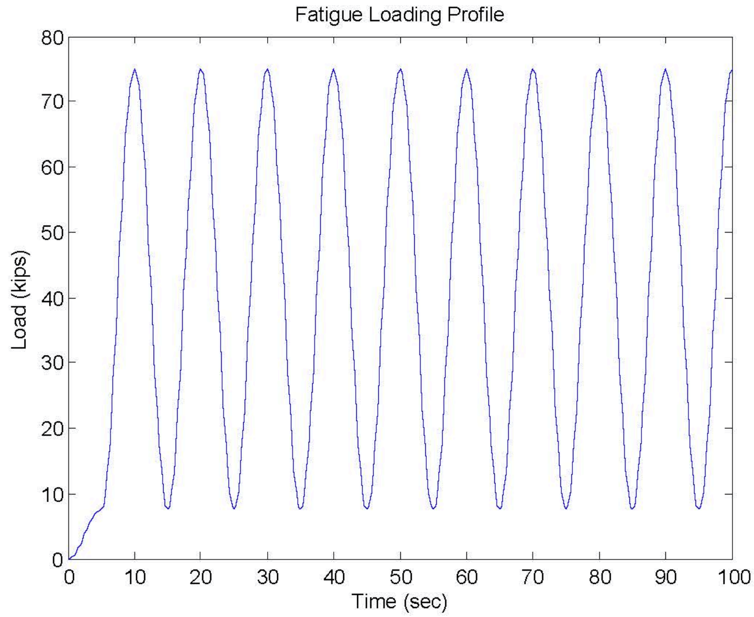

Figure 4: Cyclic Loading Profile

4.3. Instrumentation

All piles were instrumented with 2 sets of 3 strain gages oriented in the longitudinal direction of the pile. Each set of strain gages has 1 gage at the extreme tension fiber (Strain 1 & 5), 1 gage at the mid-height of the cross section (Strain 2 & 6), and 1 gage at the extreme compression fiber (Strain 3 & 7). This can be seen in Figure 5. An additional strain gage was oriented in the hoop direction (Strain 4) at the midspan of the pile. This can be seen in Figure 6.

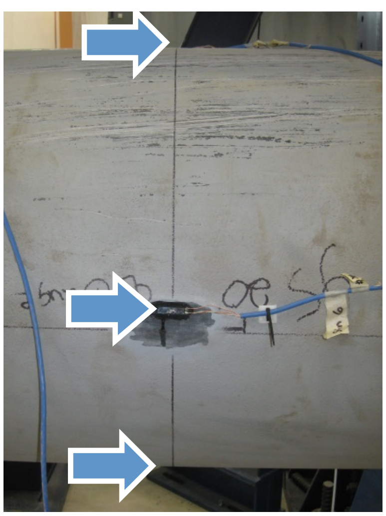

Figure 5: Typical Longitudinal Strain Gage

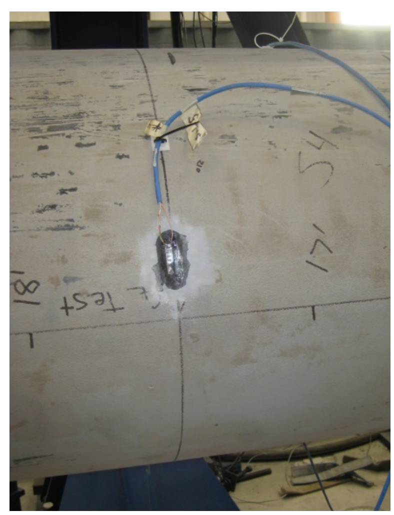

Figure 6: Typical Hoop Strain Gage

Deflections were measured at the mid-point of the span (SP-3) and both loading points (SP-2 & 4) using Celesco SP2-50 sting potentiometers (string pots). This can be seen in Figure 7. Lateral translations were measured at each support using Celesco SP2-25 string pots (SP-1 & 5). This can be seen in Figure 8. All measurements were taken at the mid-height of the cross section.

Figure 7: Vertical Deflection Measurement

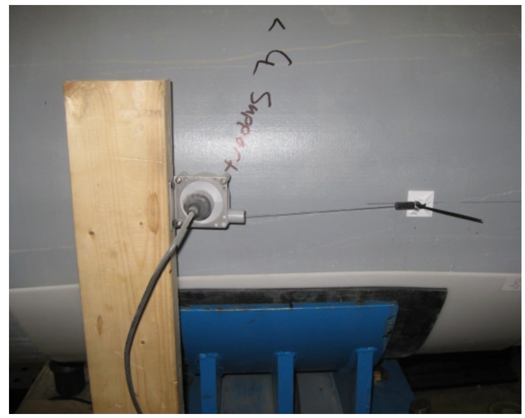

Figure 8: Lateral Translation Measurement

Axial rotation was measured at each pinned end support using +/- 60-degree TURK B2N60H-Q20L60-2LU3/S97 inclinometers (Inc-100 & 200). This can be seen in Figure 9.

Figure 9: Longitudinal Rotation Measurement

For hollow piles, ovalization of the piles was measured using Celesco SP2-4 string pots mounted inside the piles. This can be seen in Figure 10. For concrete-filled piles, the same string pot was used to determine concrete-to-shell composite action by measuring relative displacement of the concrete to the FRP shell (SP-100 & SP-200). This can be seen in Figure 11.

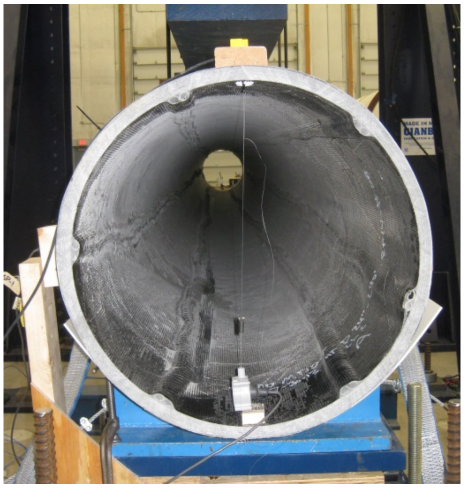

Figure 10: Ovalization Measurement

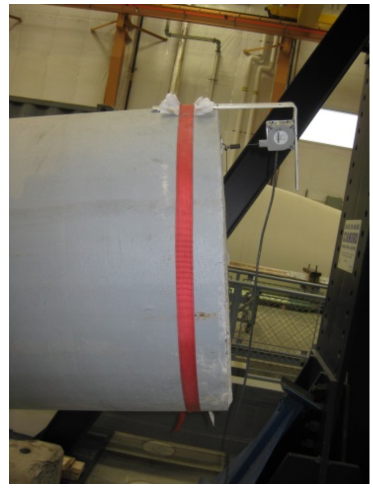

Figure 11: Concrete Composite Action Measurement

Additional details about the test setup and procedures can be seen in Reference 3.

5. Test Predictions

Concrete filled pile capacities were predicted using the Burgueno model (Reference 4). This model calculates failure based on an ultimate strain and elastic modulus that are input from coupon level material tests. This model incorporates confinement of the concrete and axial loading. The Burgueno model determines the moment-curvature interaction of the pile from which the ultimate moment capacity and an effective stiffness are obtained.

Deflections were predicted using the Moment-Area method. First, the pile length was broken into 1-inch increments. Then, the moment diagram of the pile was calculated using beam equations for a beam with 2 equal point loads. Next, the rotation of each beam element was calculated by finding the area under M/EI diagram. The rotation of the beam elements was multiplied by their length to find deflection.

6. Hollow Piles

All hollow piles were constructed with 8 layers of reinforcing. Testing was conducted on 2 baseline piles and 1 driven pile. The driven pile had a 4 foot concrete plug cast at its toe prior to driving. The concrete plug was removed before flexural testing.

6.1. Baseline Piles

<u>Pile I-8HB</u>

Pile I failed by compression at a load of 122 kips, and a corresponding moment of 673 kip*ft. It is believed that the layers of E-glass reinforcement delaminated, and then buckled locally. The failure occurred approximately 1 foot from the nearest loading point (inside the constant moment region) and can be seen in Figure 12.

Figure 12: Compression Failure of Pile I-8HB

Pile J-8HB

Pile J failed by compression at a load of 90 kips and a corresponding moment of 492 kip*ft. It is believed that the layers of E-glass reinforcement delaminated, and then buckled locally. The failure occurred at the midspan of the pile and can be seen in Figure 13.

Figure 13: Compression Failure of Pile J-8HB

6.2. Driven Piles

Pile B-8PB

Pile B failed by compression at a load of 109 kips and a corresponding moment of 599 kip*ft. It is believed that the layers of E-glass reinforcement delaminated, and then buckled locally. The failure occurred approximately 1 foot from the nearest loading point (inside the constant moment region) can be seen in Figure 14. Upon further investigation, this pile contained both folds in the reinforcing fabric and pockets of high resin content located near the failure. This is pictured, and discussed further in Section 6.4.

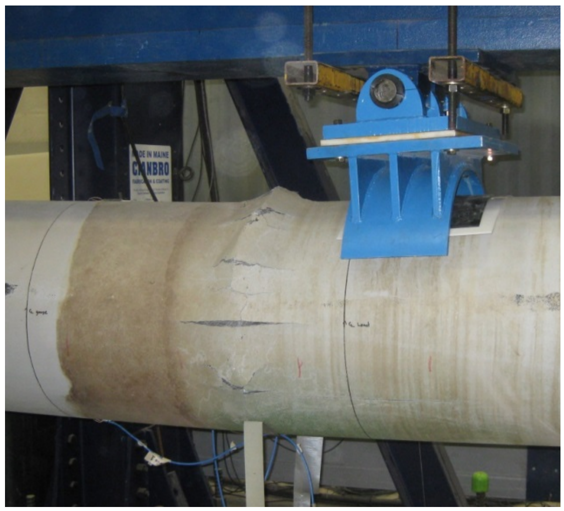

Figure 14: Compression Failure of Pile B-8PB

6.3. Summary of Hollow Piles

Table 2 shows a summary of the maximum loads and deflections seen during the hollow pile tests.

Table 2: Maximum Loads and Deflections of Hollow Piles

Pile ID	Driven	Max Load at Actuator (kip)	Maximum Deflection (Mid-Span) (inches)	Maximum Deflection (Load Point) (inches)
Pile I - 8HB	No	122.4	7.31	7.48
Pile J - 8HB	No	89.5	6.34	5.50
Pile B - 8PB	Yes	109.0	8.03	6.98

The following plots compare the flexural test results of the hollow piles. Load-deflection relationships can be seen in Figure 15, and moment-curvature relationships can be seen in Figure 16.

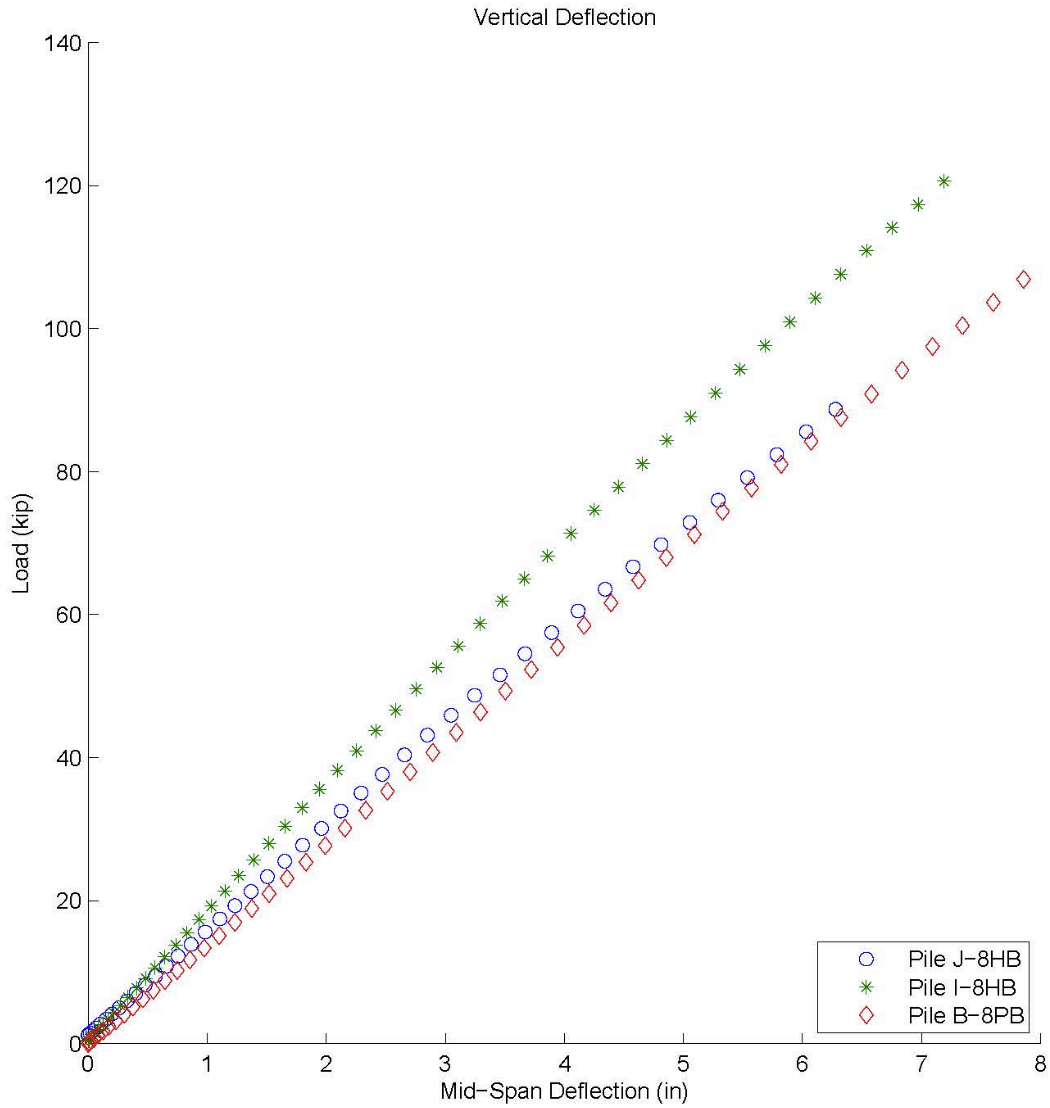

Figure 15: Load-Deflection of Hollow Piles

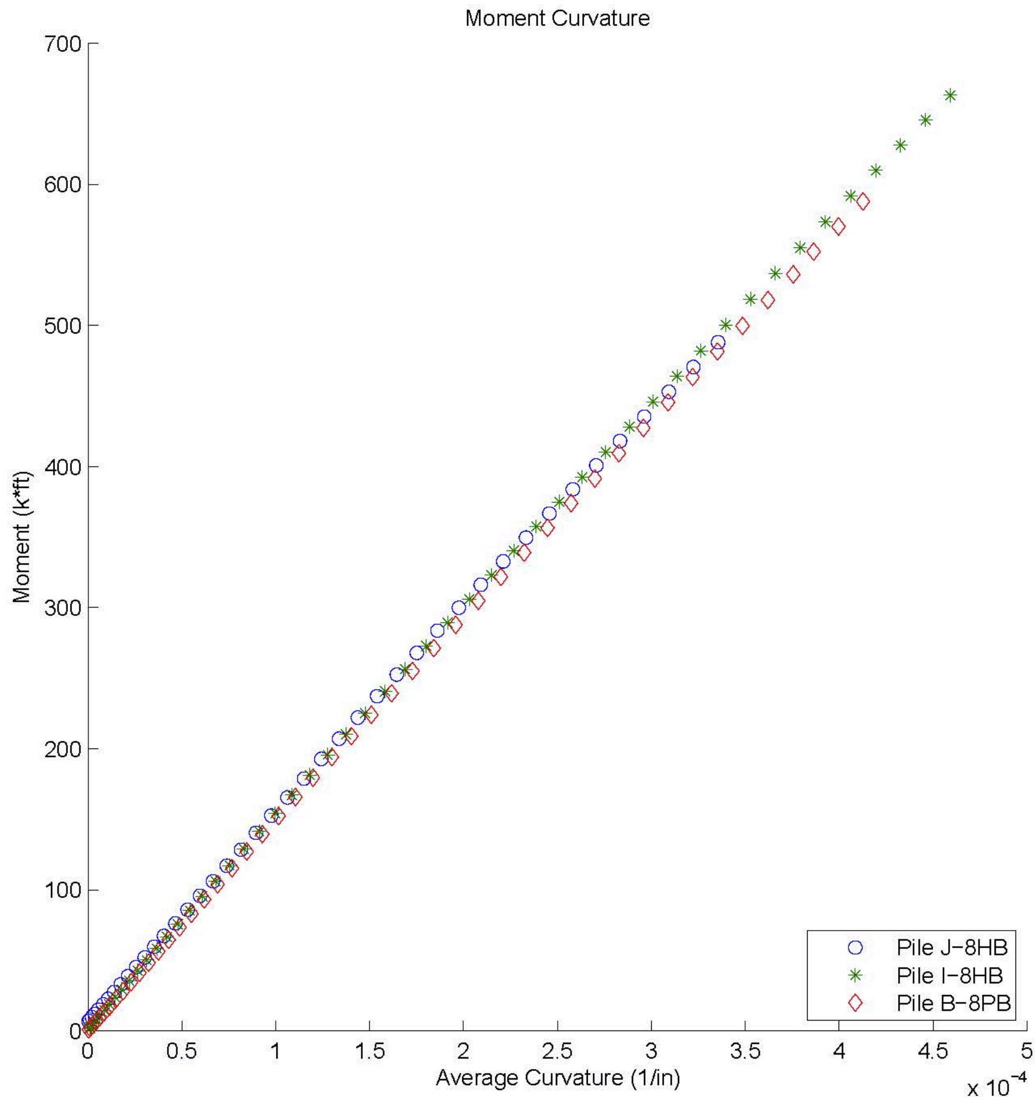

Figure 16: Moment-Curvature of Hollow Piles

6.4. Discussion of Hollow Piles

Defects in the pile could create stress concentration as a load is distributed through the pile. This could be caused by folds in the reinforcing fabric, as seen in Figure 17, or misalignment of fibers, as seen in Figure 18. The misalignment of fibers in Figure 18 led to a reduction in coupon tensile strength of 34.6 percent coupled with 3000 hours of water absorption conditioning at 100 degrees Fahrenheit. Similar coupons without misaligned fibers and identical conditioning lost 13.1 percent of their capacity compared to baseline tests.

of Pile B

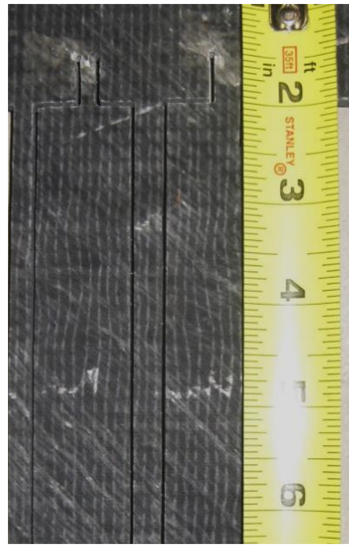

bers in Tension

Variations in wall thickness could represent areas with less reinforcing than others. This may be caused by shifting of the reinforcing fabric during fabrication, as seen in Figure 19, or areas of high resin content, as seen in Figure 20.

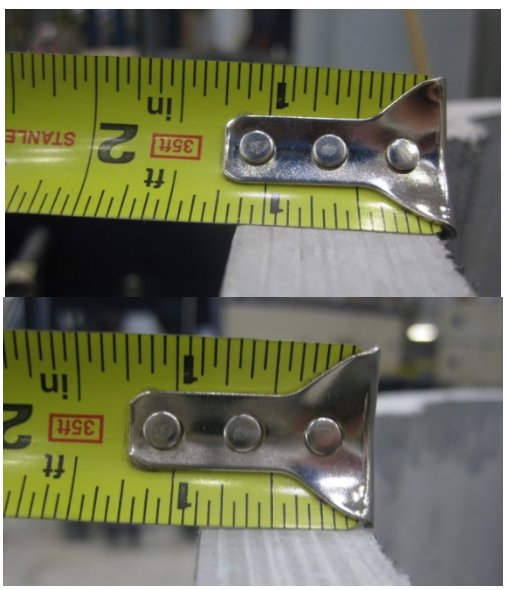

Figure 19: Variation in Thickness

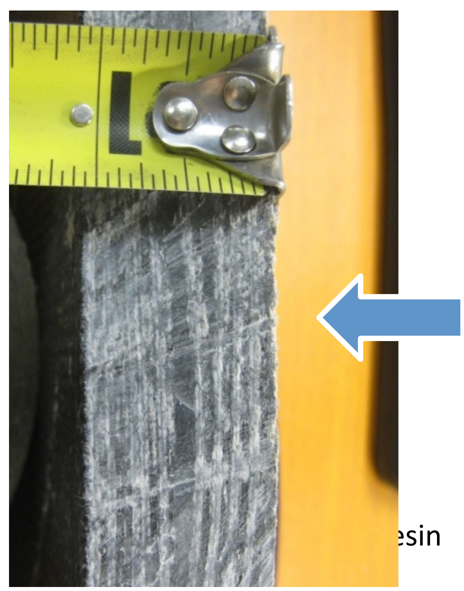

esin

7. Concrete-Filled Piles

All concrete-filled piles were constructed using 4 layers of reinforcement. Testing was conducted on 2 baseline piles, 1 driven pile, and 2 load-cycled piles.

7.1. Baseline Piles

Pile G-4FB

Pile G failed at a load of 200 kips and a corresponding moment of 1,099 kip*ft. when fibers on the tension face appeared to rupture. The failure occurred approximately 1 foot from the nearest loading point (outside the constant moment region) and can be seen in Figure 21, and Figure 22.


Figure 21: Tension Failure of Pile G-4FB


Figure 22: Cut at Failure of Pile G-4FB

Strain data for this test was not collected over +/- 5000 microstrain due to an error in the data collection system.

Pile H-4FB

Pile H failed at a load of 119 kips and a corresponding moment of 652 kip*ft. when fibers on the tension face appeared to rupture. The failure occurred at the midspan of the pile and can be seen in Figure 23, and Figure 24.


Figure 23: Tension Failure of Pile H-4FB

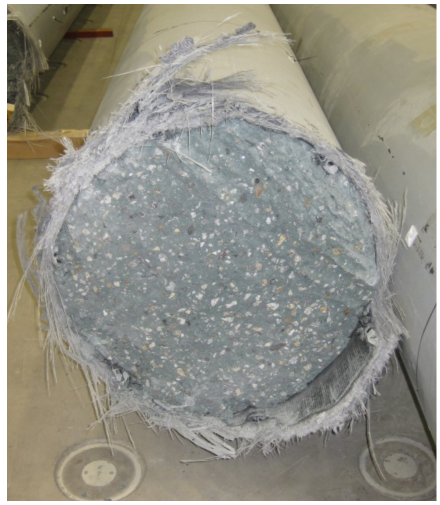
Figure 24: Cut at Failure of Pile H-4FB

Strain data for this test was not collected over +/- 5000 microstrain due to an error in the data collection system.

7.2. Driven Piles

Pile A-4FB

Pile A failed at a load of 174 kips and a corresponding moment of 958 kip*ft. when fibers on the tension face appeared to rupture. The failure occurred approximately 2 feet from the nearest loading point (inside the constant moment region) and can be seen in Figure 25, and Figure 26.

Figure 25: Tension Failure of Pile A-4FB

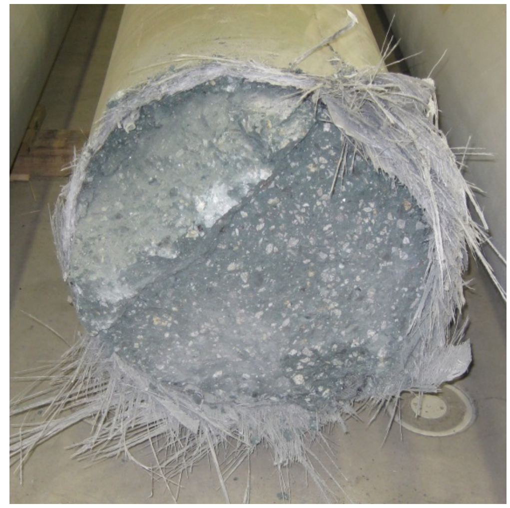

Figure 26: Cut at Failure of Pile A-4FB

A compression wrinkle developed outside of the constant moment region at an approximate load of 155 kips and corresponding moment of 853 kip*ft. The compression wrinkle can be seen in Figure 27. After testing, the FRP shell was cut at the compression wrinkle and a crack that goes through the entire cross section of concrete was discovered. It is believed that this crack occurred during driving. The crack can be seen in Figure 28.

Figure 27: Compression Wrinkle

Figure 28: Crack in Pile A's Concrete at Compression Wrinkle

When this compression wrinkle occurred, the concrete moved with respect to the shell of the pile. The concrete displacement measurement during the test was unreliable, but the concrete displacement measured after the test was 0.245 inches at the end of the pile. The movement at the end of the pile can be seen in Figure 29.

Figure 29: Loss of Composite Action in Pile A

Test data was lost for portions of this test due to an error in the data collection system. Data was recovered for the failure of the pile and when composite action was lost.

7.3. Load-Cycled Piles

Pile E-4FB

Pile E was cycled according to the procedure described in 4.2. During cyclic loading, Pile E developed small cracks along the tension face. These cracks can be seen in Figure 30.

Figure 30: Cracks Due to Cyclic Loading

During the static test to failure after cyclic loading, Pile E initially showed a compression failure at 158 kips and the load dropped to 149 kips. The load started to rise again to 158 kips and a corresponding moment of 871 kip*ft. where the pile appeared to fail in tension. The failure occurred at the midspan of the pile and can be seen in Figure 31 and Figure 32.

Figure 31: Tension Failure of Pile E-4FB

Figure 32: Cut at Failure of Pile E-4FB

Pile F-4FB

Pile F was cycled according to the procedure described in 4.2. During the static test to failure after cyclic loading, Pile F failed at a load of 127 kips and a corresponding moment of 699 kip*ft. when fibers on the tension face appeared to rupture. The failure occurred at the midspan of the pile and can be seen in Figure 33.

Figure 33: Tension Failure of Pile F-4FB

7.4. Summary of Concrete-Filled Piles

Table 3 shows a summary of the maximum loads and deflections seen during the concrete-filled pile tests.

Table 3: Maximum Loads and Deflections of Concrete-Filled Piles

Pile ID	Driven	Max Load at Actuator (kip)	Maximum Deflection (Mid-Span) (inches)	Maximum Deflection (Load Point) (inches)
Pile H - 4FB	No	119.7	9.30	9.36
Pile G - 4FB	No	199.8	21.69	18.72
Pile A - 4FB	Yes	174.2	19.48	17.00
Pile F - 4FB*	No	127.1	9.98	8.56
Pile E - 4FB*	No	158.3	14.28	12.14

*Load-Cycled Test

The following plots compare the flexural test results of the concrete filled piles. Load-deflection relationships can be seen in Figure 34, and moment-curvature relationships can be seen in Figure 35.

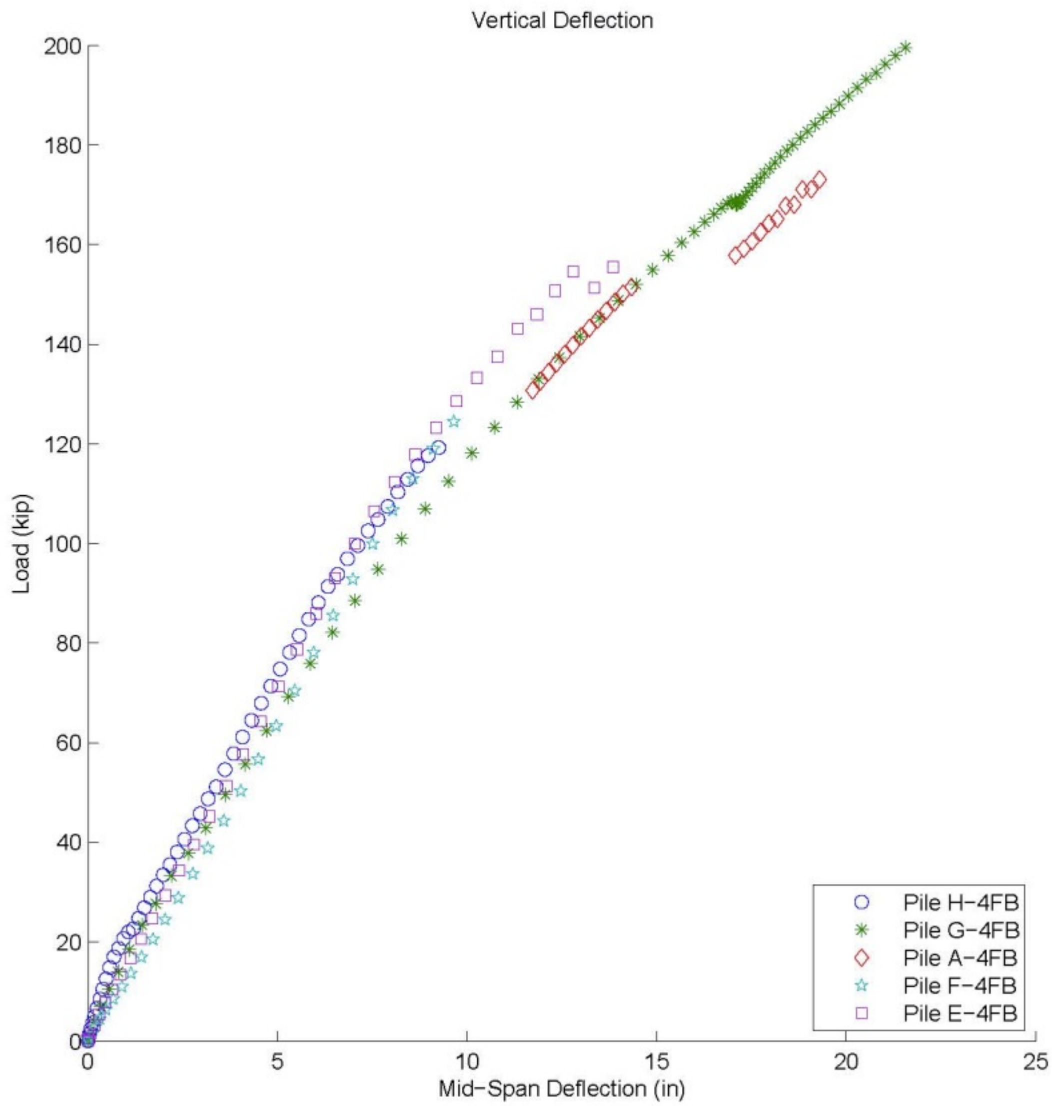

Figure 34: Load-Deflection of Filled Piles

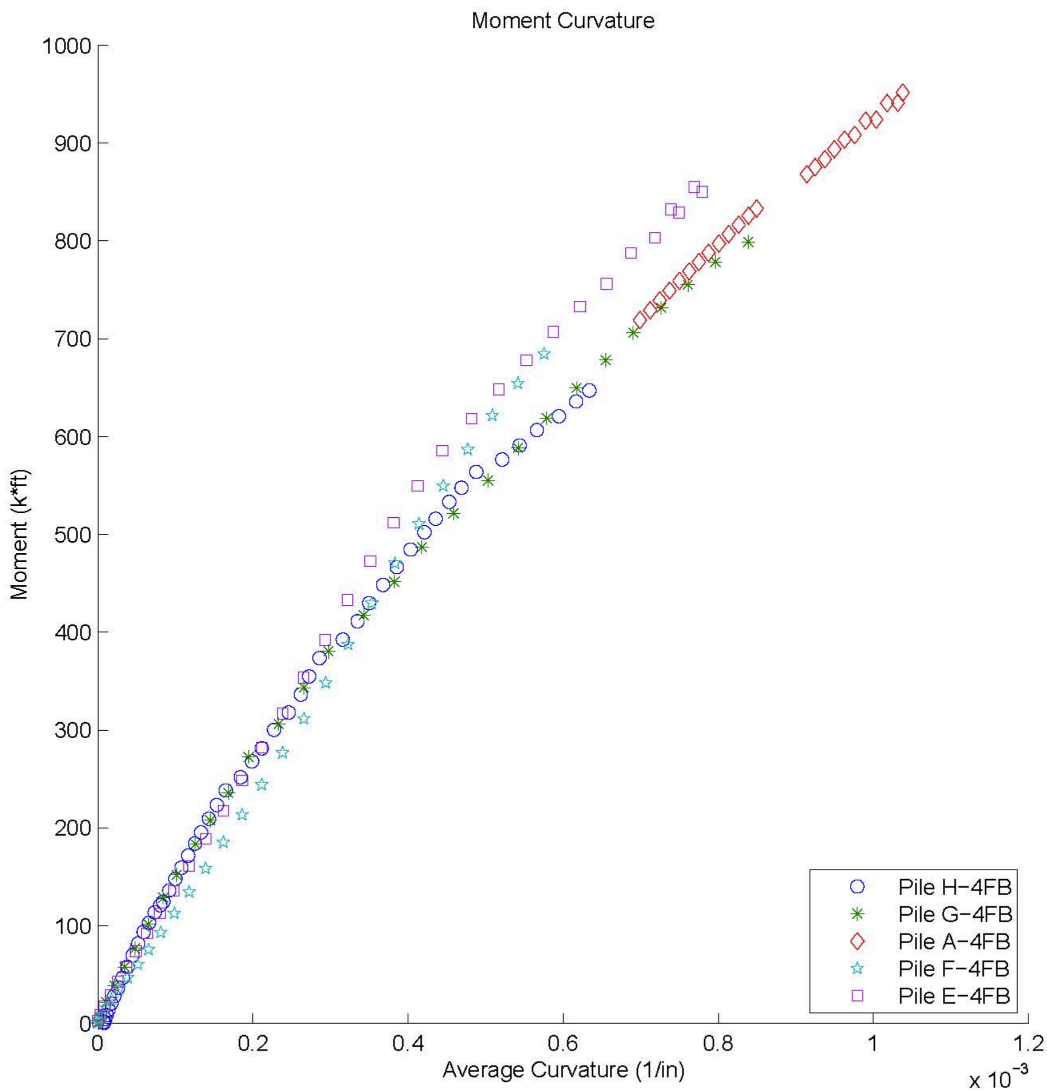

Figure 35: Moment-Curvature of Filled Piles

7.5. Discussion of Concrete-Filled Piles

Concrete-filled piles were cut for disposal after testing. The cut piles showed no significant gaps between the concrete and FRP shell. It should be noted that MDOT Class A concrete with no expansive additive was used to fill the piles. A typical cut can be seen in Figure 36.

Figure 36: Concrete-FRP Interface

Concrete-filled piles showed little variation in shell thickness, no folds in the reinforcement, and no large pockets of resin at the locations of cuts for disposal.

8. Pile C-8HFB Tests

Pile C is the only concrete-filled pile constructed with 8 layers of reinforcement. This pile was initially driven hollow, filled with concrete, and then restruck.

Pile C was tested 3 times. This pile was initially tested using the typical four-point bend set up described in section 4.1. The pile had a difference in diameter of 1/4 inch when the cross section was measured top to bottom versus side to side for the first 2 tests. The pile was rotated 90 degrees to test along the weak axis for the third test to increase the probability of failure.

8.1. Test 1

The first test of Pile C went to the capacity of the test setup. The load cell reached its capacity at an applied load of 300 kips and corresponding moment of 1650 kip*ft., ending the test. The pile developed a series of hairline cracks along the tension face at two points: 2.5 feet from the nearest load point (inside the constant moment region) and 3.5 feet from the nearest load point (outside the constant moment region). These cracks can be seen in Figure 37, and Figure 38.

Figure 37: Cracks in Constant Moment Region

Figure 38:Cracks Out of Constant Moment Region

8.2. Test 2

Pile C was then retested. The loading points were moved inward 1 foot toward the midspan; from 11 feet from the end supports to 12 feet from the end supports. This resulted in a 150 kip*ft. increase in potential applied moment. The load cell reached its capacity again at an applied load of 300 kips and corresponding moment of 1800 kip*ft., ending the test.

8.3. Test 3

Pile C was then tested a third time. The loading points were adjusted to 13 feet from the end supports. Composite action was lost during the test. It is believed that this occurred when there was a loud crack at an approximate load of 185 kips. The concrete displacement measurement at this load was 0.04 inches. The sliding of the concrete at failure was greater (approximately 2.25 inches), and can be seen in Figure 39.

Figure 39: Loss of Composite Action in Pile C

Pile C failed by compression at a load of 263 kips and a corresponding moment of 1,710 kip*ft. The pile was able to fail in compression because the concrete slid relative to the FRP shell, creating a void in the pile at failure. The failure can be seen in Figure 40.

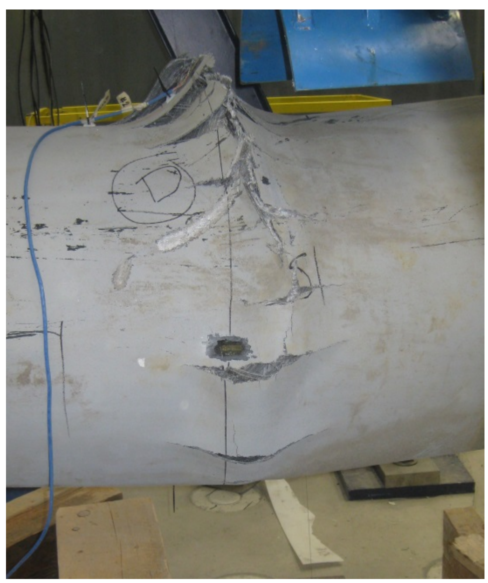

Figure 40: Compression Failure of Pile C-8HFB

8.4. Summary of Pile C Tests

Table 4 shows a summary of the maximum loads and deflection seen during the tests of Pile C.

Table 4: Maximum Loads and Deflections of Pile C Tests

Test Number	Pile ID	Driven	Max Load at Actuator (kip)	Maximum Deflection (Mid-Span) (inches)	Maximum Deflection (Load Point) (inches)
1	Pile C - 8HFB	Yes	300+	17.88	15.44
2	Pile C - 8HFB	Yes	300+	18.72	16.90
3	Pile C - 8HFB	Yes	262.9	21.23	19.93

The following plots compare the flexural test results of the 3 different tests for Pile C. Load-deflection relationships can be seen in Figure 41, and moment curvature relationships can be seen in Figure 42.

The loading points were adjusted for each test of Pile C. This means load-deflection plots for each trial are not comparable. The plot has been included as Figure 41 for completeness.

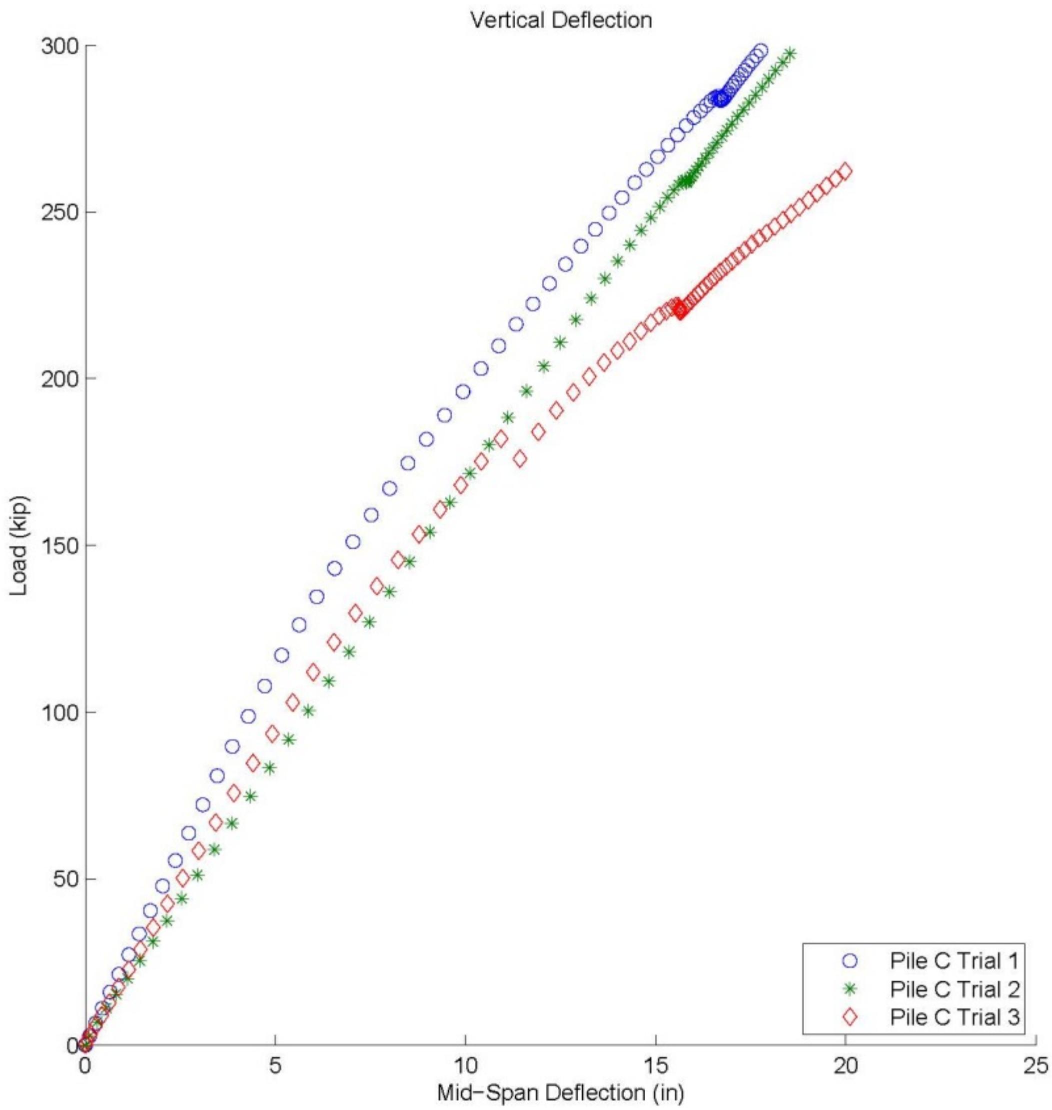

Figure 41: Load Deflection of Pile C Tests

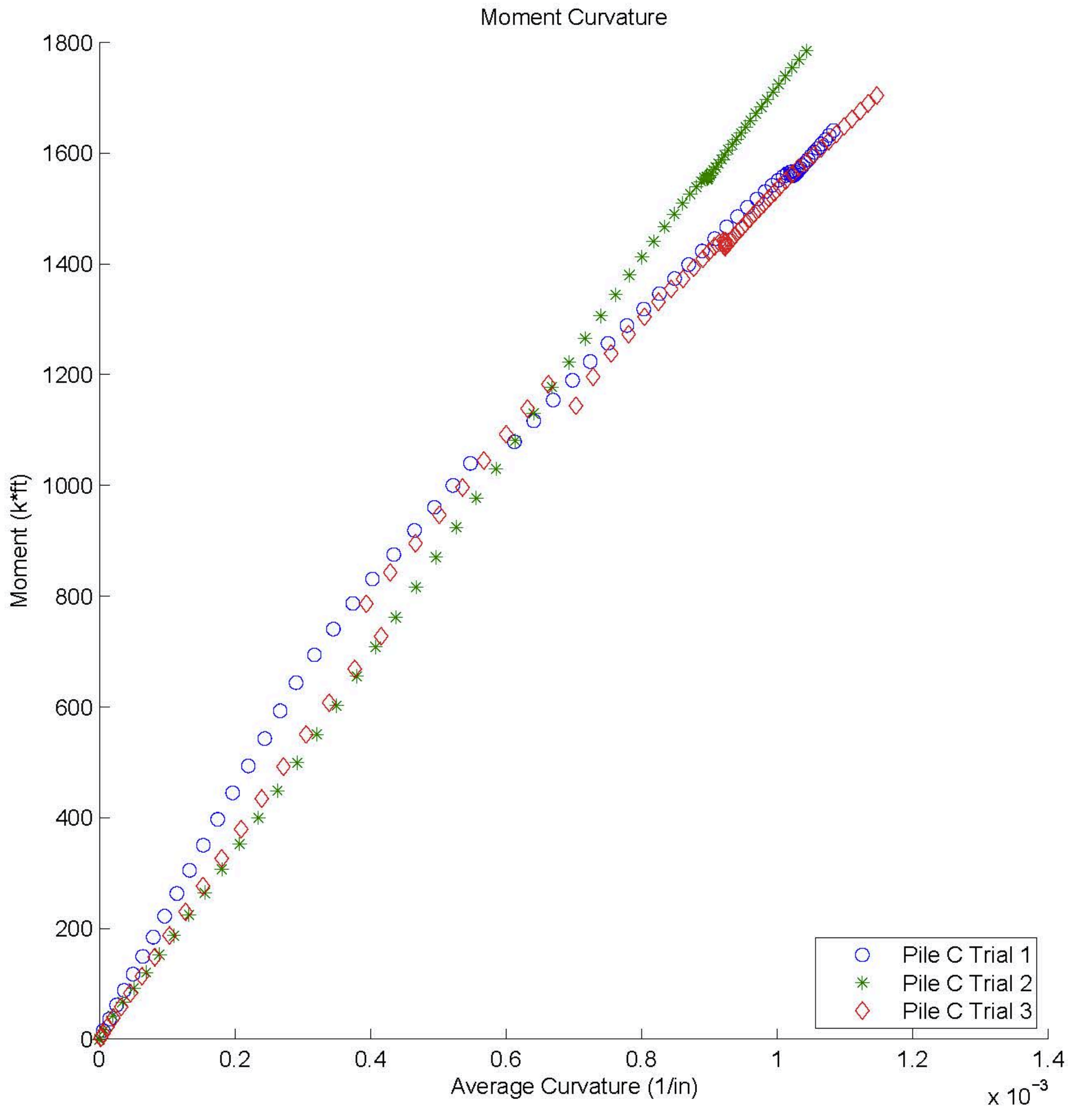

Figure 42: Moment-Curvature of Pile C Tests

8.5. Discussion of Pile C Tests

During the third test of Pile C, composite action was lost at an approximate load of 185 kips. This test saw higher hoop strains than the previous tests of Pile C and all other concrete-filled piles. A plot of hoop strain for Pile C tests can be seen in Figure 43.

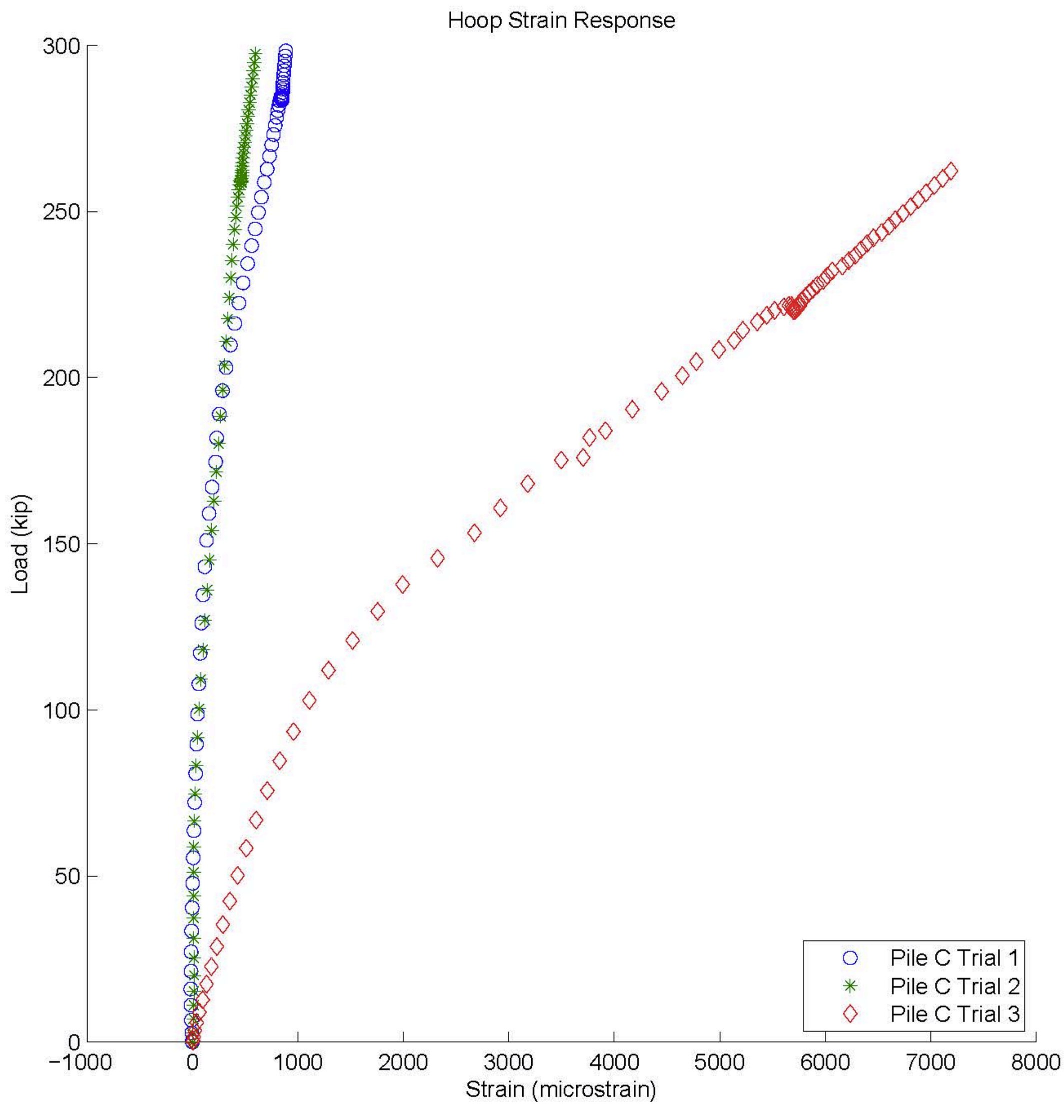

Figure 43: Hoop Strain in Pile C Tests

9. Load-Cycled Tests

9.1. Summary of Load-Cycled Tests

The following plots compare the flexural test results for initial and ultimate testing of load-cycled piles. Load-deflection relationships can be seen in Figure 44, and moment-curvature relationships can be seen in Figure 45. Note that the line for Pile F initial deflection is based after 10 cycles, since no static test was conducted prior to cyclic loading. The concrete cracked on the tension face during the first 10 cycles, therefore the initial apparent deflection and curvature, taken at approximately 8 kips, is higher than that of Pile E.

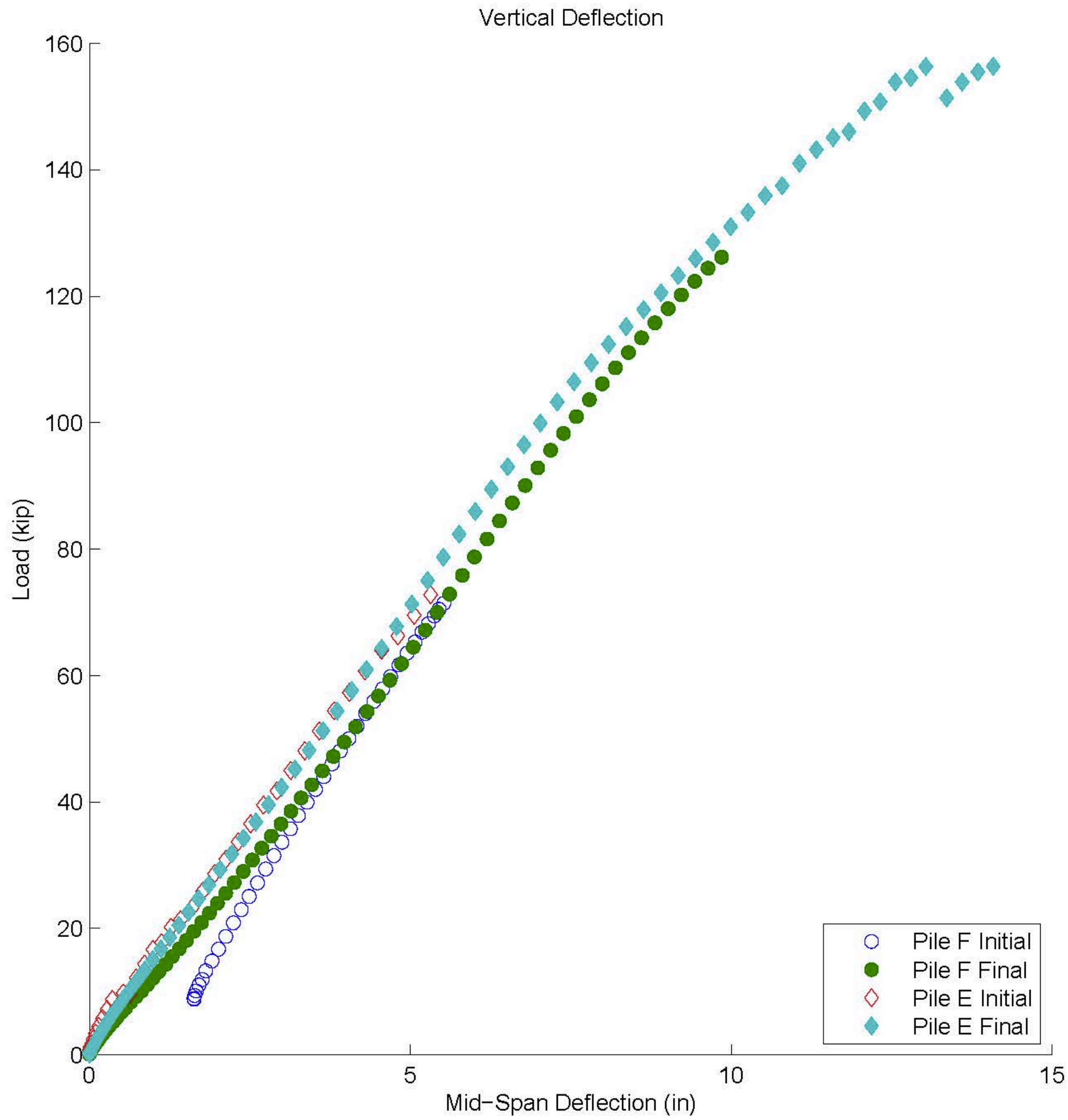

Figure 44: Load-Deflection of Load Cycled Piles

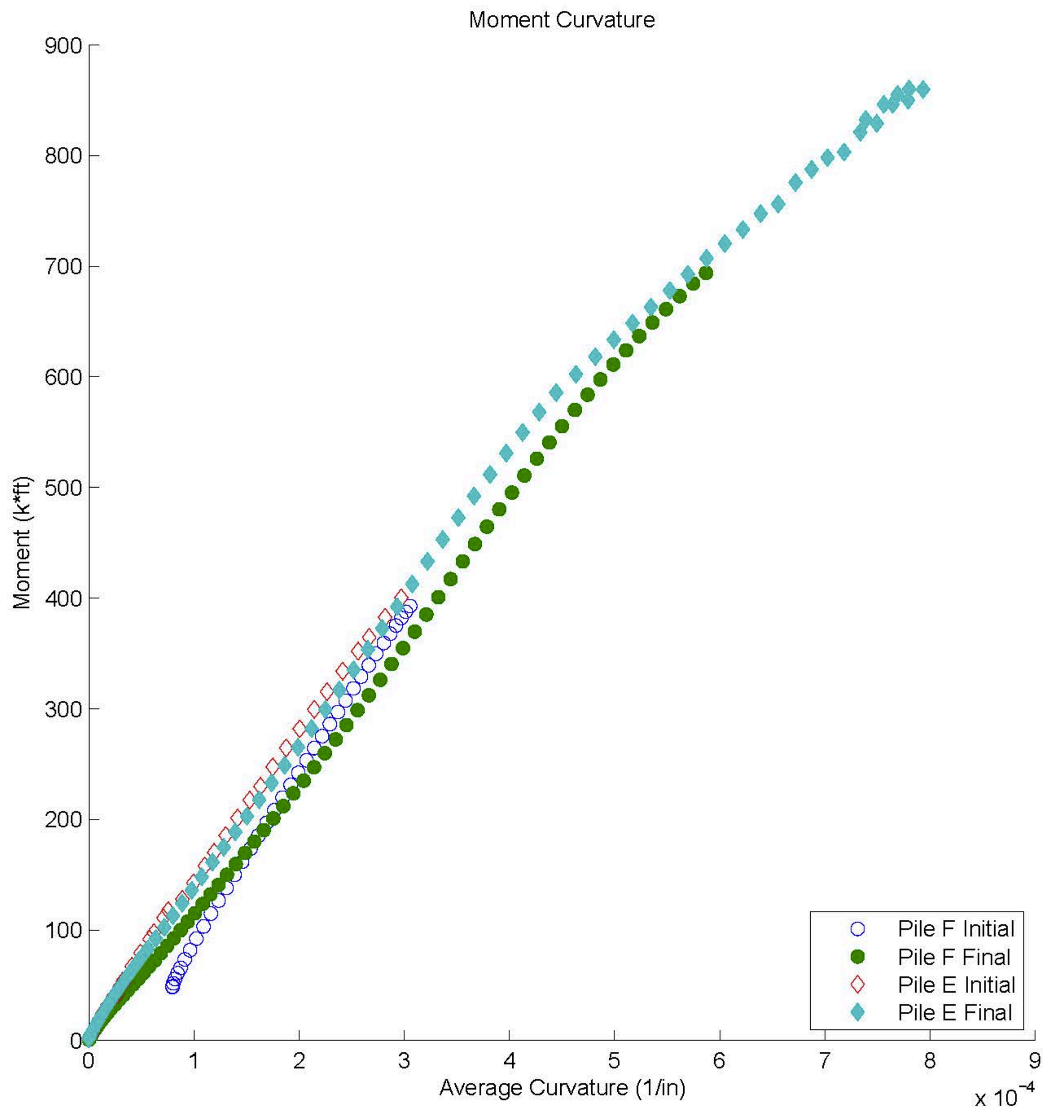

Figure 45: Moment-Curvature of Load-Cycled Piles

Details of ultimate failure tests for load-cycled piles are presented in Section 7.3.

9.2. Discussion of Load-Cycled Tests

Load-cycled piles saw an increase in deflection over time. Some of this may be attributed to permanent deflections in the concrete and loss of composite action. When the piles were rotated 180 degrees after 10,000 cycles, the piles had a slight camber. A plot of the increase in deflection with time can be seen in Figure 46, and Figure 47.

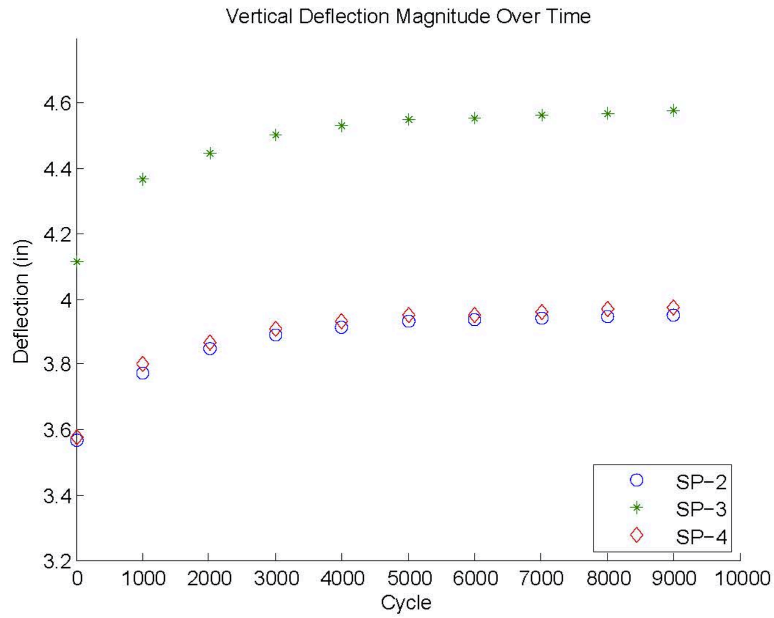

Figure 46: Increased Deflection for Cycles 1 to 10,000

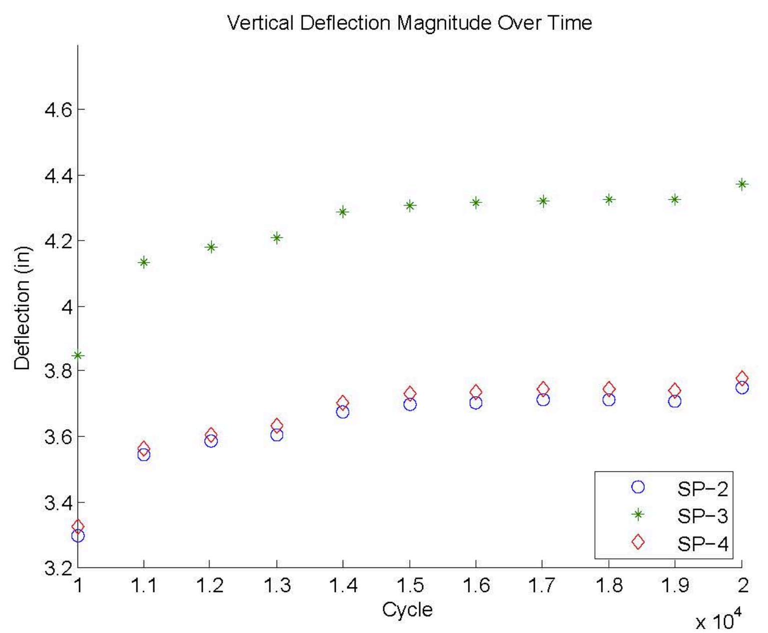

Figure 47: Increased Deflection for Cycles 10,000 to 20,000

There was a noticeable difference between stiffness measured during static tests and stiffness measured during cyclic loading. Pile E-4FB showed a decrease of 1.3 percent between initial and ultimate static tests, but showed a decrease of 10.1 percent between initial and ultimate load-cycled tests. Pile F-4FB showed a decrease of 14.3 percent between initial and ultimate load-cycled tests. There was no initial static test for Pile F.

Stiffness loss due to dynamic loading appears to occur over the first 5,000 cycles of load-cycled tests. After this initial loss in stiffness, the stiffness remains relatively constant. Please note that the beam was rotated 180 degrees after 10,000 cycles, resulting in an apparent increase in stiffness. The loss of dynamic stiffness can be seen in Figure 48, and Figure 49.

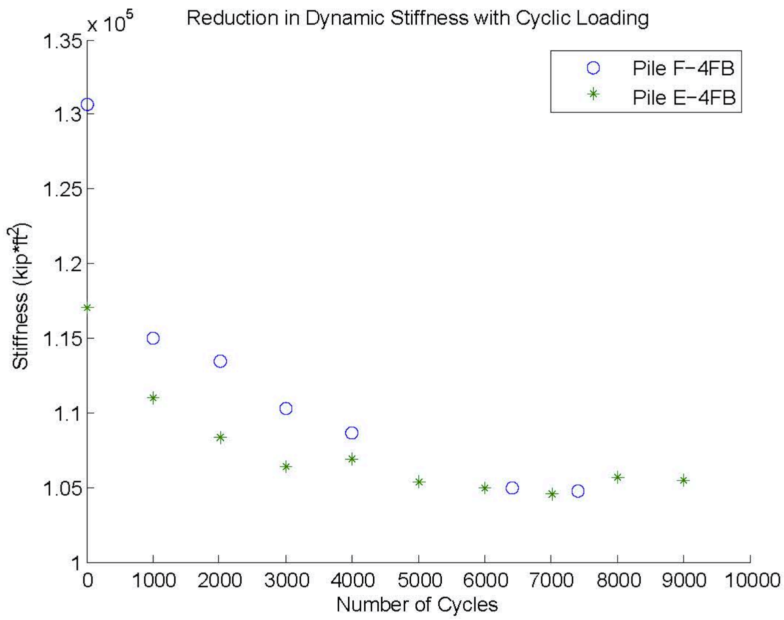

Figure 48: Decrease in Dynamic Stiffness for Cycles 1 to 10,000

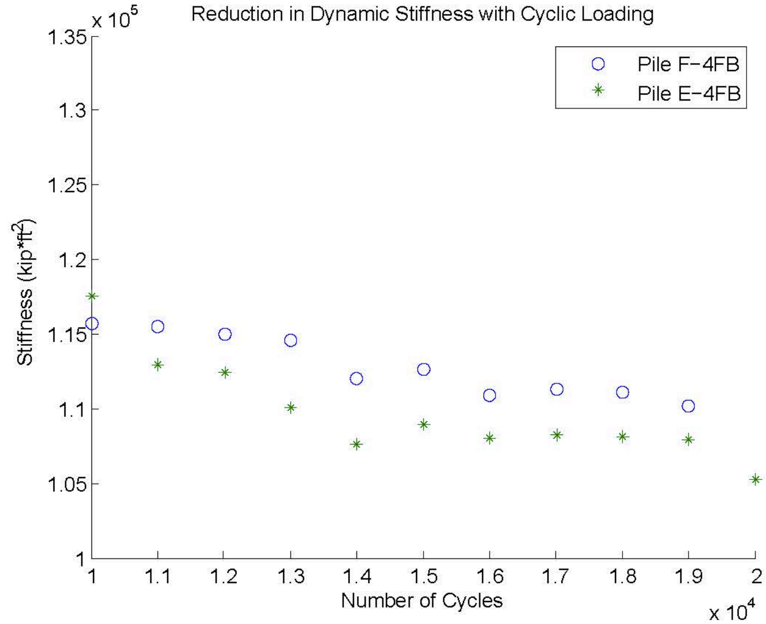

Figure 49: Decrease in Dynamic Stiffness for Cycles 10,000 to 20,000

10. Summary of All Test Results

A summary of all tests can be seen in Table 5. As a reminder, pile ID extension identifies the piles as: 4 or 8 ply; hollow, fully filled before driving, filled with a concrete plug before driving, or driven hollow and then filled (H, F, P, or HF respectively); Bending or axial test (B or A).

Table 5: Summary of Bending Test Ultimate Loads and Deflections

Test Number	Pile ID	Driven	Max Load at Actuator (kip)	Maximum Deflection (Mid-Span) (inches)	Maximum Deflection (Load Point) (inches)
1	Pile I - 8HB	No	122.4	7.31	7.48
2	Pile J - 8HB	No	89.5	6.34	5.50
3	Pile B - 8PB	Yes	109.0	8.03	6.98
4	Pile H - 4FB	No	119.7	9.30	9.36
5	Pile G - 4FB	No	199.8	21.69	18.72
6	Pile A - 4FB	Yes	174.2	19.48	17.00
7	Pile C - 8HFB	Yes	300+	17.88	15.44
8	Pile C - 8HFB	Yes	300+	18.72	16.90
9	Pile C - 8HFB	Yes	262.9	21.23	19.93
10	Pile F - 4FB*	No	127.1	9.98	8.56
11	Pile E - 4FB*	No	158.3	14.28	12.14

*Load-Cycled Test

11. Data Analysis Methods

Stiffness was calculated using the load and deflection between 10% and 40% of the ultimate strength of the piles in accordance with Reference 5. Loads and deflections were used with linear-elastic beam equations to calculate stiffness.

Curvature was calculated by fitting a straight line through each set of 3 longitudinal strain gages. When a gage failed prematurely, the curvature was calculated by fitting a straight line to the remaining strain gages. For these calculations, the strain gages were assumed to be located exactly at the ultimate tension fiber, mid-height of the cross section, and ultimate compression fiber and no rotation about the longitudinal axis of the pile occurred during testing. Stiffness was also calculated using this curvature between 10% and 40% of the ultimate strength of each pile to validate the stiffness found using the linear-elastic beam equations.

A summary of stiffness values can be seen in Table 6.

Table 6: Pile Stiffness Values

Test Number	Pile ID	EI (Moment Curvature) (kip*ft^2)	EI (Beam Deflections) (kip*ft^2)	Percent Difference from Beam Deflection EI	EI (From Coupon Properties) (kip*ft^2)
1	Pile I - 8HB	1.25E+05	No Data	No Data	1.01E+05
2	Pile J - 8HB	1.25E+05	1.24E+05	0.5%	1.01E+05
3	Pile B - 8PB	1.23E+05	1.11E+05	10.2%	1.01E+05
4	Pile H - 4FB	1.13E+05	No Data	No Data	8.90E+04
5	Pile G - 4FB	9.53E+04	8.66E+04	9.1%	8.87E+04
6	Pile A - 4FB	No Data			
7	Pile C - 8HFB	1.81E+05	1.72E+05	5.1%	1.38E+05
8	Pile C - 8HFB	1.45E+05	1.28E+05	11.9%	1.35E+05
9	Pile C - 8HFB	1.48E+05	1.41E+05	4.7%	1.36E+05
10	Pile F - 4FB*	9.65E+04	1.01E+05	-5.0%	8.82E+04
11	Pile E - 4FB*	1.07E+05	9.96E+04	7.1%	8.74E+04

*Load-Cycled Test

Stiffness was also calculated using moment and deflection in 2 kip*ft. increments using linear-elastic beam equations. The beam is assumed to behave linearly over the small increment of moment. This method was used to show degradation in stiffness over the duration of the test.

When comparing separate pile tests, all redundant measurements were averaged to make plots easier to read.

12. Discussion

The testing showed a large variability in the ultimate capacity of the piles. Some possible causes of this are variation in the roundness of the pile, defects along the length of the pile, and variations in the thickness of the shell over the length of the pile. Some of these defects are discussed in Section 6.4.

A variation in the roundness of the piles will affect the load distribution on the pile and create local areas of high stress under the load head. This variation in roundness was seen in hollow and concrete-filled piles, but it is believed that hollow piles were able to conform to the load heads, which distributed the applied load better. Hollow piles saw ovalizations up to 0.5 inches (Pile I). An example of variation in the roundness of piles can be seen in Figure 50.

Figure 50: Variation in Roundness of Piles

Piles were inspected for internal defects upon cutting for disposal. Folds and resin pockets seen in hollow piles were not seen in concrete-filled piles. It appears that the manufacturing process produces more defects in piles with thicker walls. It should be noted that cuts in the piles were made every 5 feet, so defects may have been missed.

Pile A and C both lost composite action during flexural testing. These were the only piles driven while filled with concrete. Pile A was filled with concrete prior to initial driving and was not restruck. Pile C was initially driven hollow then filled with concrete prior to being restruck. It is believed that tensile forces during driving caused cracking in the concrete, which created a failure plane for the concrete to slide at. It is also possible that cracks through the cross section of Pile C are the result of rotating the pile 90 degrees for its third test.

Some error in measurements may be attributed to laying out strain gage and string pot locations. Laser levels, pipe layout rules, and hand levels were used to limit these errors. This may explain some of the small variation between sets of strain gages and string pots at loading points.

Saddles at loading points shifted during some tests. This may have caused more loads to apply to one side of the pile. Saddles did not move more than approximately 2 inches during any test. A large portion of this saddle movement may have occurred when the piles failed and contacted the spreader beam. It is not believed that this caused a significant effect due to the relatively large span length (33 feet). The saddle movement can be seen in Figure 51.

Figure 51: Movement of Saddle at Loading Point After Failure

Piles did not meet the failure strains seen during coupon level testing. This is believed to be a result of defects discussed above. A summary of failure strains and corresponding moments can be seen in Table 7. The percentage in bold denotes the failure mode of the pile. Note that that strain data was not collected over +/- 5000 microstrain for Pile H and Pile G due to an error in the data collection system.

Table 7: Flexural Strength of Piles

Test Number	Pile ID	Max Moment (kip*ft)	Max Comp. Strain (microstrain)	Max Tensile Strain (microstrain)	Percent of Coupon Compressive Strain	Percent of Coupon Tensile Strain
1	Pile I - 8HB	673.0	-5.41E+03	5.40E+03	**25.7%**	21.2%
2	Pile J - 8HB	492.2	-4.09E+03	4.09E+03	**19.4%**	16.0%
3	Pile B - 8PB	599.3	-4.93E+03	4.95E+03	**23.4%**	19.4%
4	Pile H - 4FB	658.5	No Strain Data at Failure			
5	Pile G - 4FB	1099.2				
6	Pile A - 4FB	958.1	-8.74E+03	1.69E+04	41.5%	**66.2%**
7	Pile C - 8HFB	1650+	-8.95E+03	1.53E+04	42.5%	60.0%
8	Pile C - 8HFB	1800+	-9.22E+03	1.65E+04	43.8%	64.9%
9	Pile C - 8HFB	1708.7	-5.95E+03	1.32E+04	**28.2%**	51.6%
10	Pile F - 4FB*	699.2	-4.59E+03	9.75E+03	21.8%	**38.2%**
11	Pile E - 4FB*	870.6	-5.76E+03	1.26E+04	27.3%	**49.4%**

*Load-Cycled Test

13. Conclusions

Testing showed that piles driven while filled with concrete and piles subjected to multiple loadings appeared to lose composite action during flexural testing. This may be an artifact of tensile stress during driving or microcracking in the concrete during repetitive loading. This loss of composite action appears to have caused Pile C to fail in compression at a lower moment than it had sustained in previous tests. It is believed that concrete filled piles would not be able to achieve this failure mode if being used in an application with large axial loads (such as bridge applications). This was seen in Pile A, when the pile lost composite action, but confinement at the end of the pile (provided by the metal driving shoe) prevented the concrete from sliding more than 0.245 inches. Pile A showed a compression wrinkle at the local area of concrete movement, but ultimately failed in tension approximately 12 feet from the compression wrinkle after a 105 kip*ft increase in moment.

The series of tests conducted did not show a reduction in ultimate strength or stiffness between undriven, driven, and load-cycled piles. The baseline variability of the undriven piles created a broad range in ultimate strength for both the concrete filled (119.7 kips to 199.8 kips) and hollow pile (89.5kips to 122.4 kips) strength. The strength results for all driven and load-cycled piles fell within the baseline strength range for both hollow and concrete-filled piles, making any potential trend in pile degradation inconclusive.

Appendix A: Test Results for Pile A – 4FB

Test Results for Pile A – 4FB

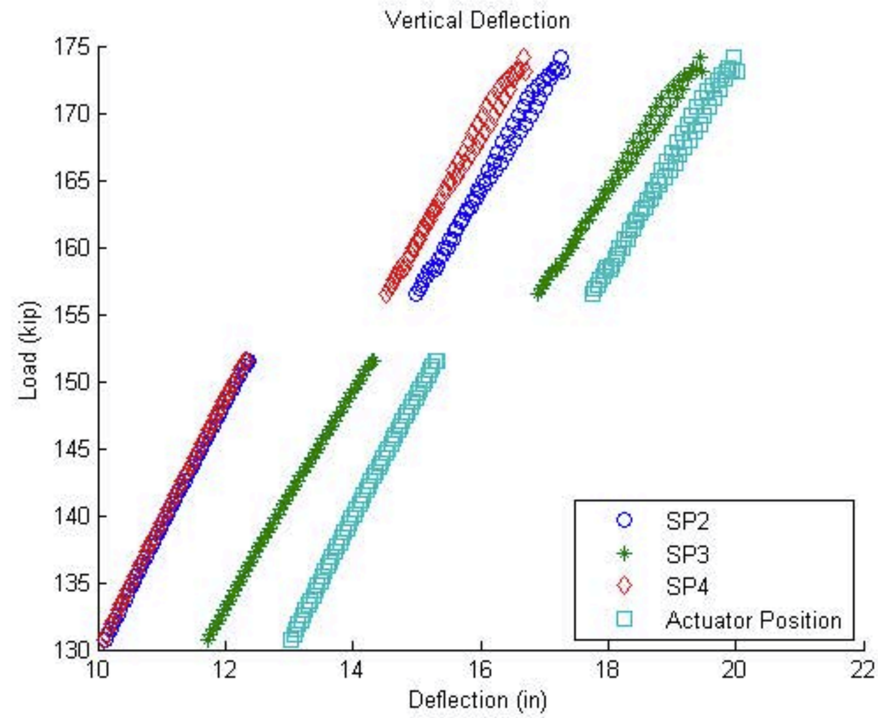

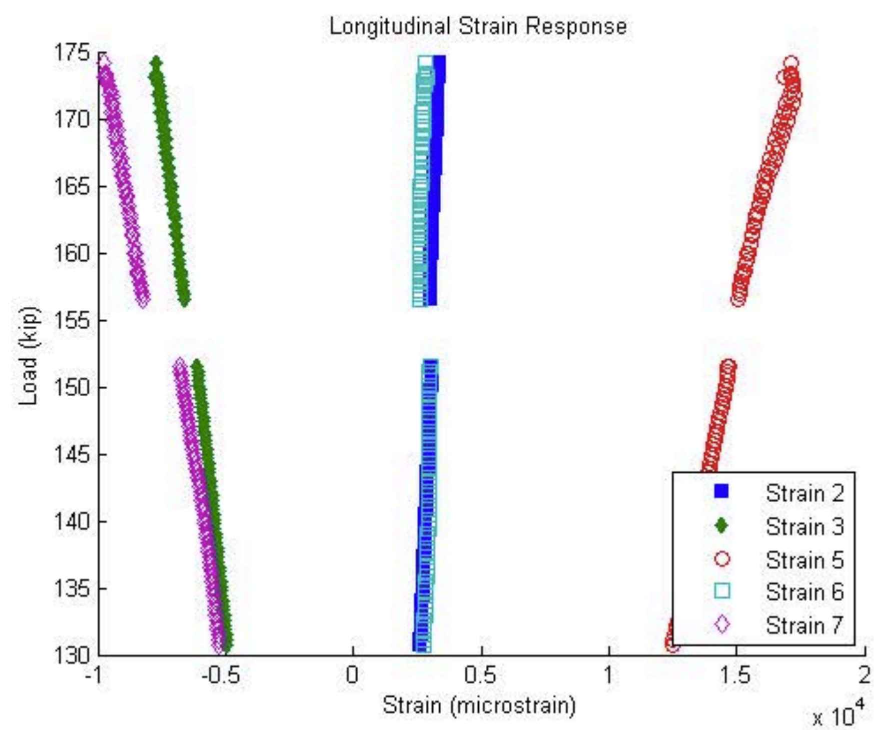

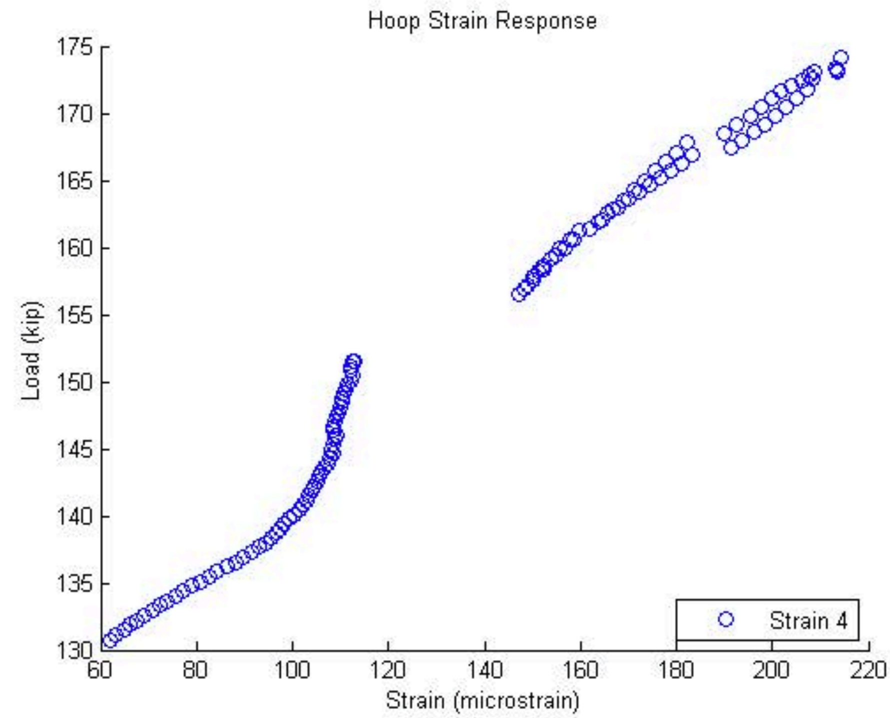
Hoop Strain Response
Load (kip)
Strain (microstrain)
Strain 4
175
170
165
160
155
150
145
140
135
130
60
80
100
120
140
160
180
200
220

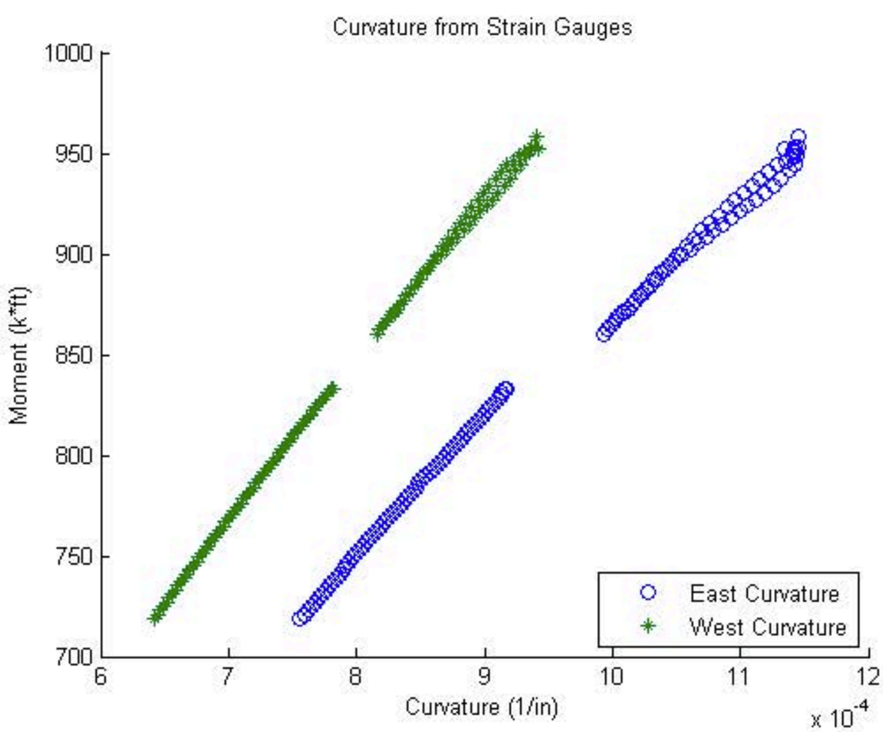
Curvature from Strain Gauges
Moment (k*ft)
Curvature (1/in)
x 10^-4
East Curvature
West Curvature
1000
950
900
850
800
750
700
6
7
8
9
10
11
12

Test Results for Pile A – 4FB

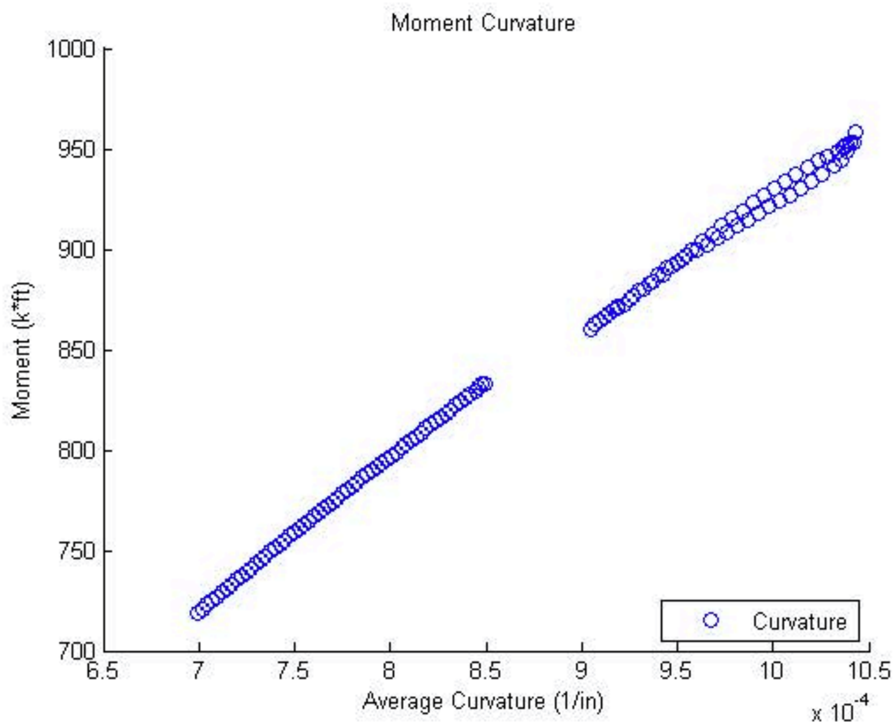

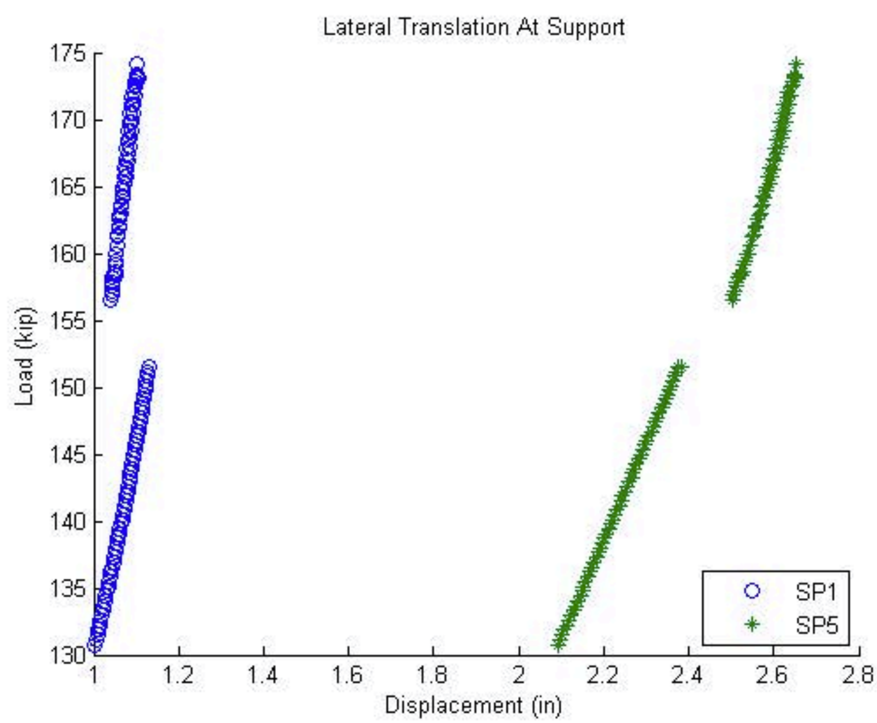

Test Results for Pile A – 4FB

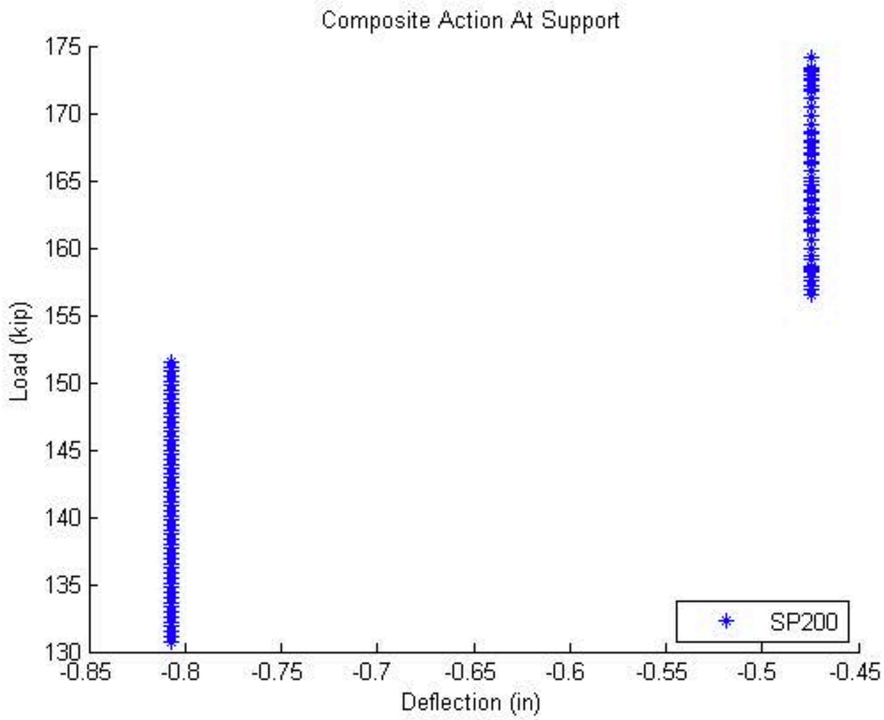

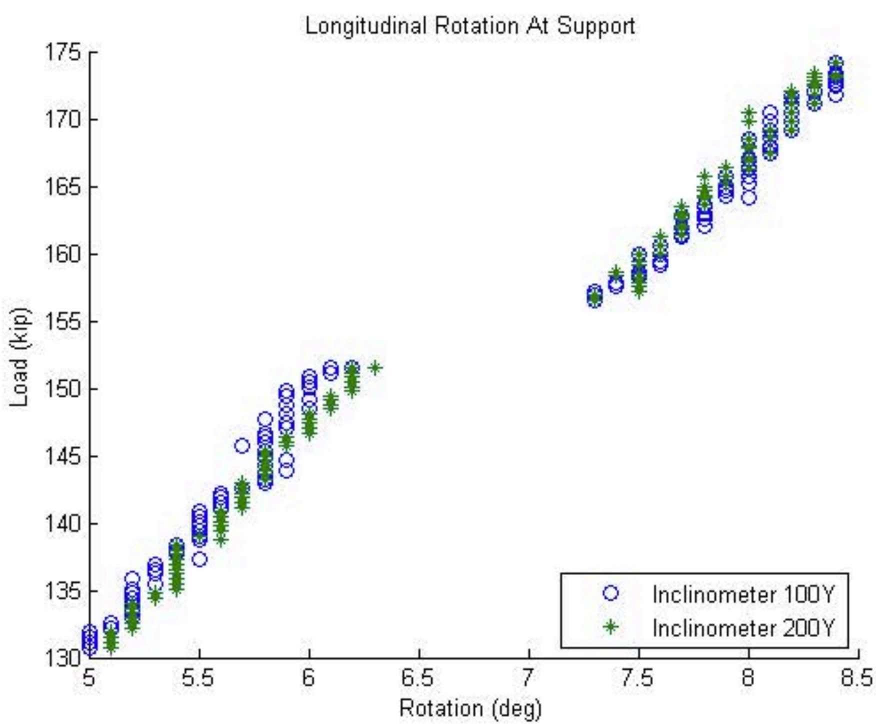

Test Results for Pile A – 4FB

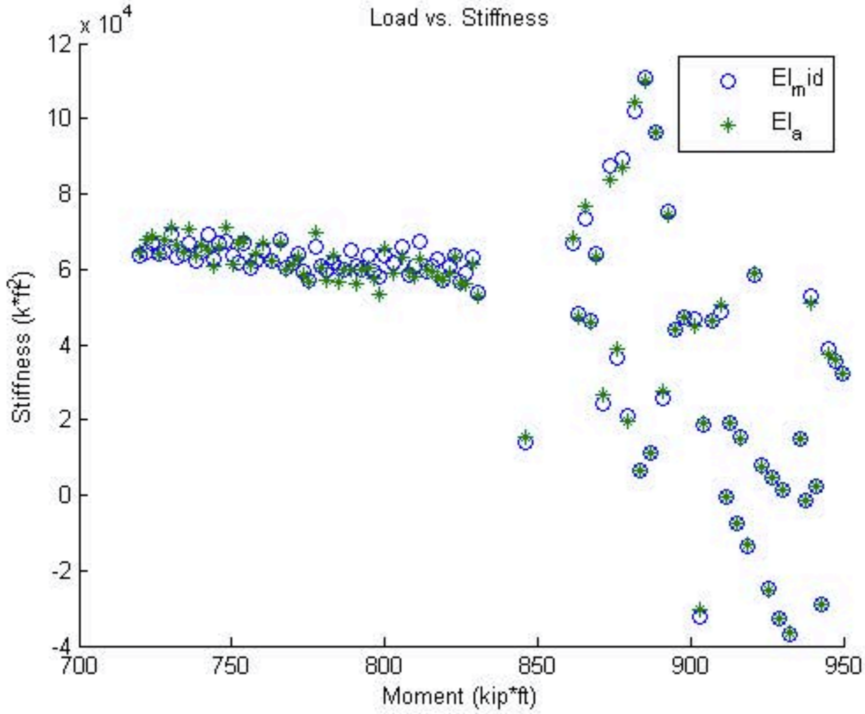

Appendix B: Test Results for Pile B – 8PB

Test Results for Pile B – 8PB

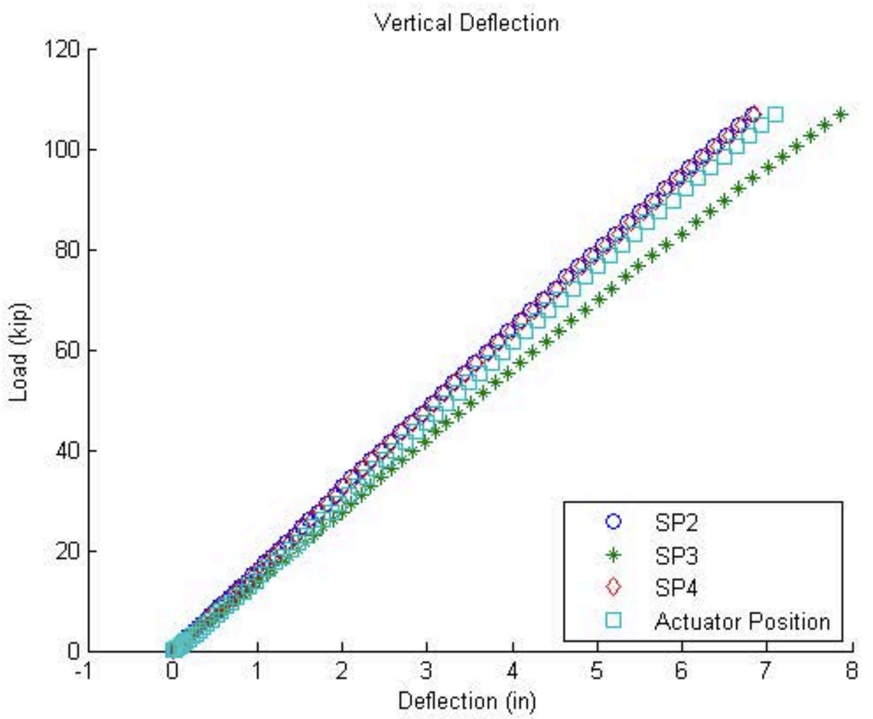

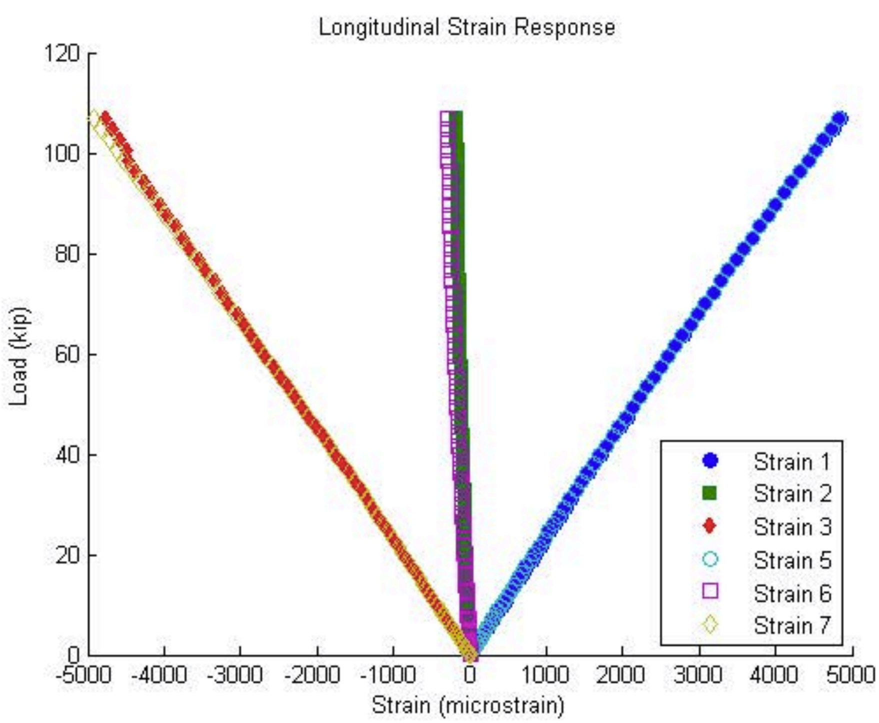

Test Results for Pile B – 8PB

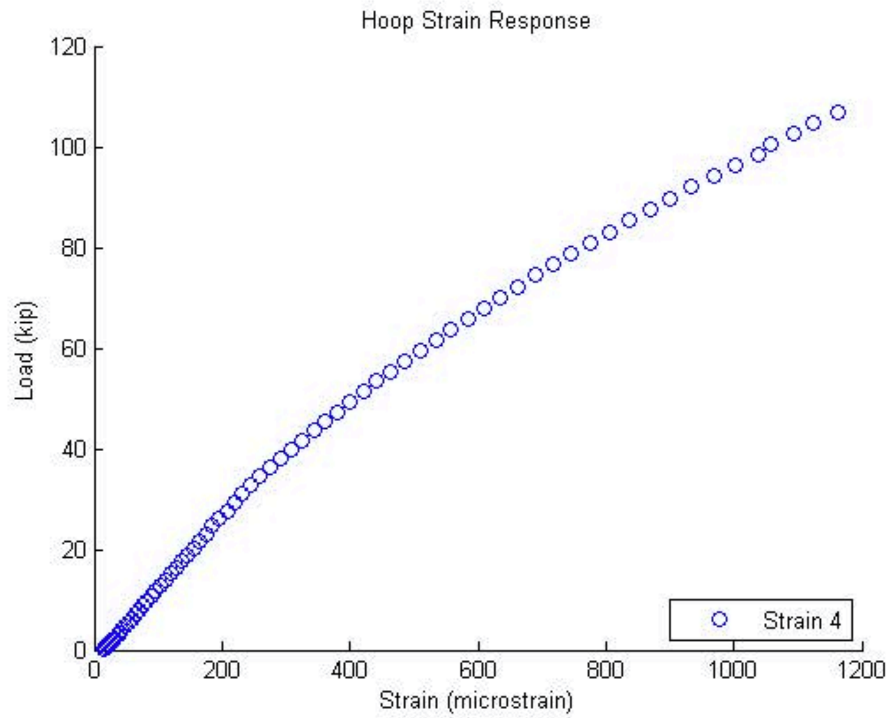

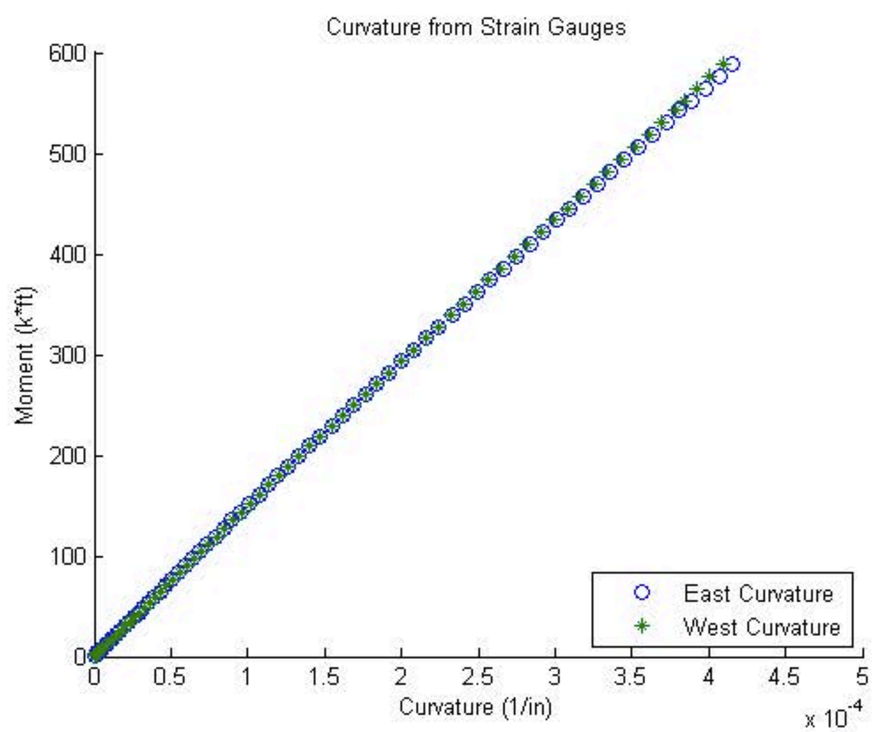

Test Results for Pile B – 8PB

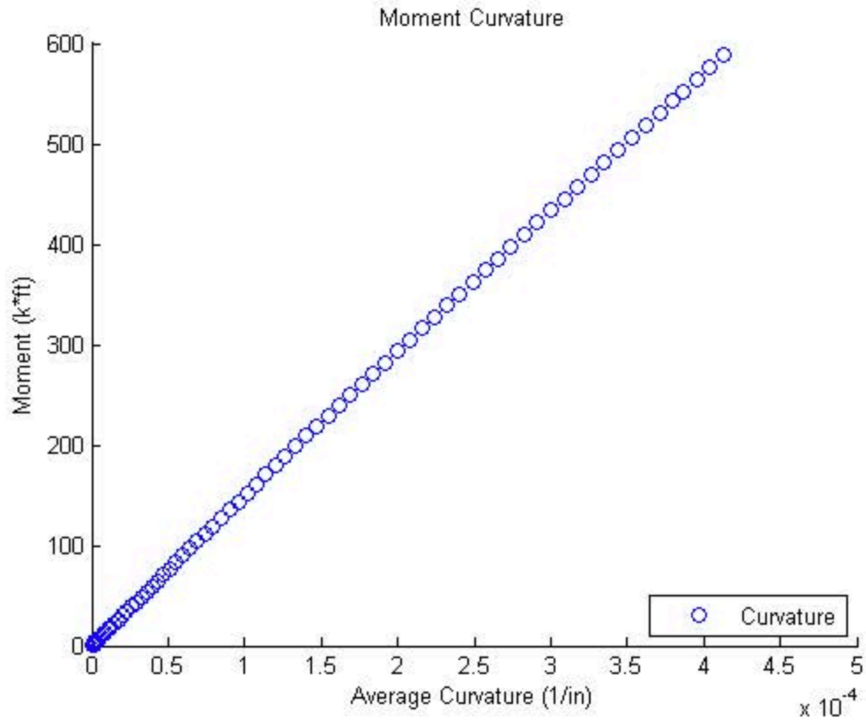

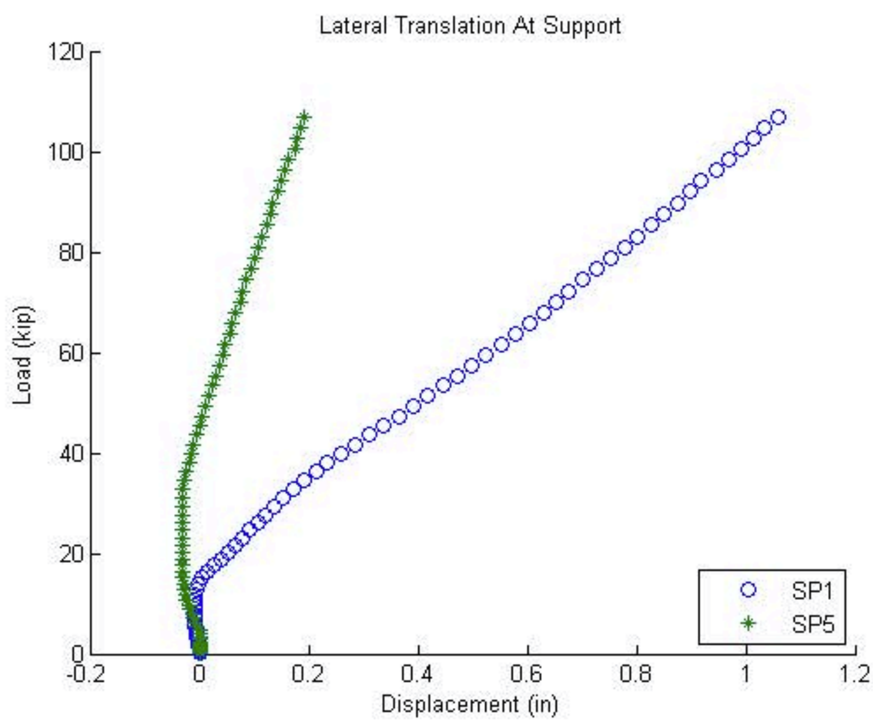

Test Results for Pile B – 8PB

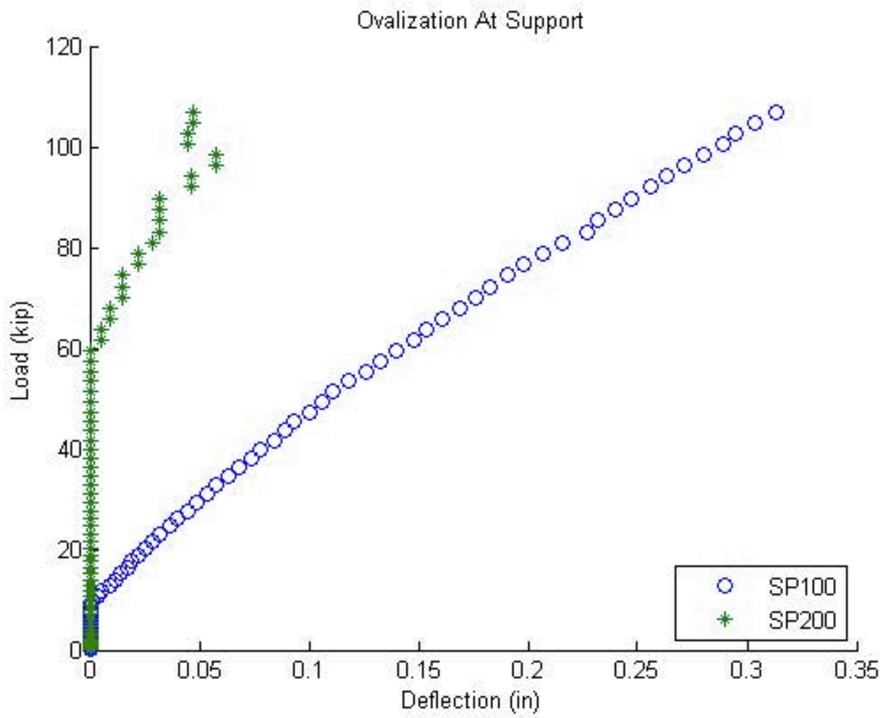

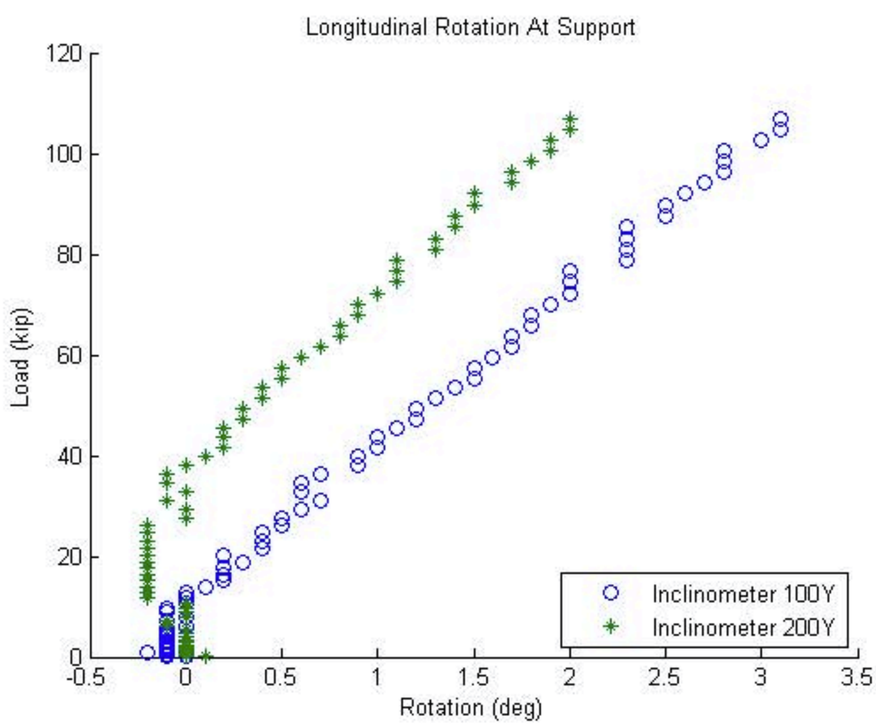

Appendix C: Test Results for Pile C – 8HFB Trial 1

Test Results for Pile C – 8HFB Trial 1

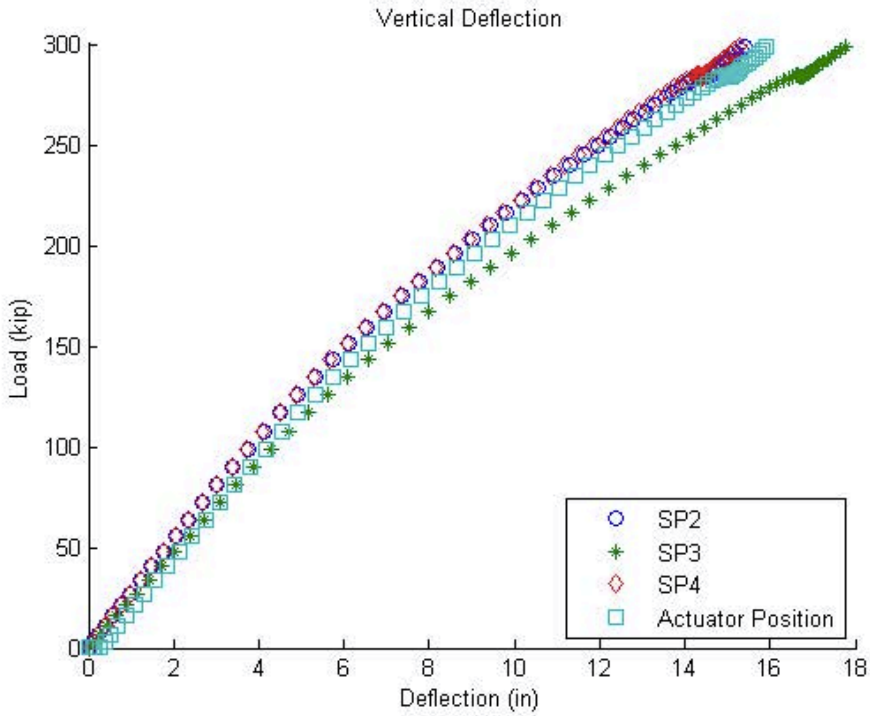

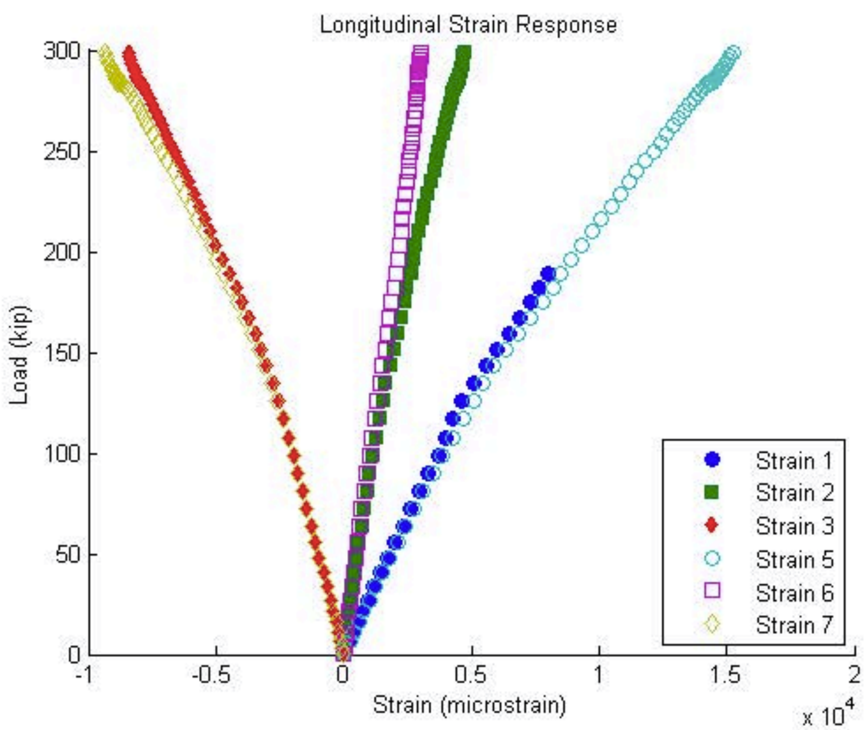

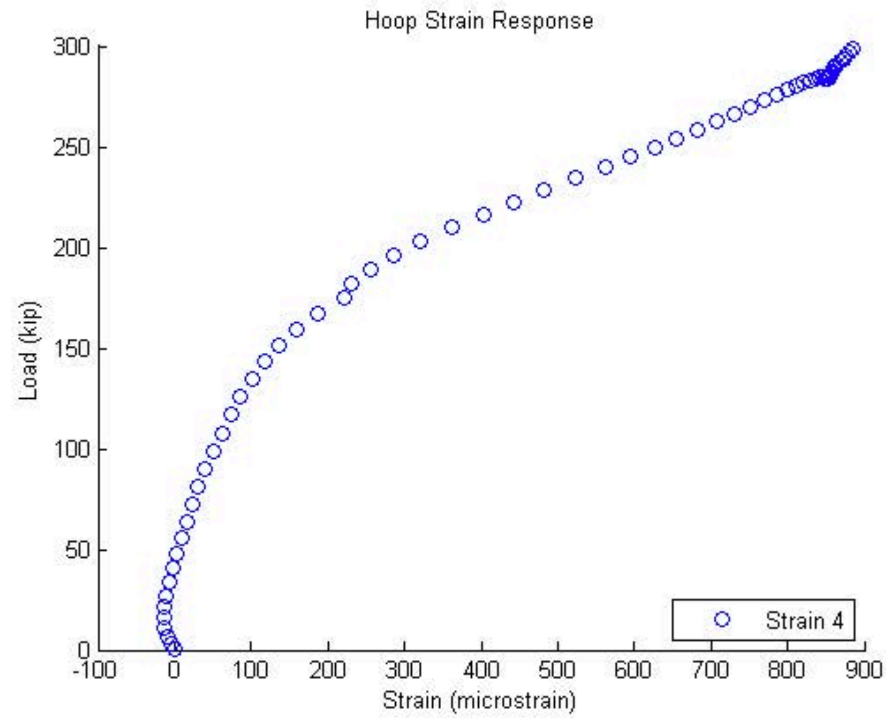
Hoop Strain Response
Load (kip)
Strain (microstrain)
Strain 4
300
250
200
150
100
50
0
-100
0
100
200
300
400
500
600
700
800
900

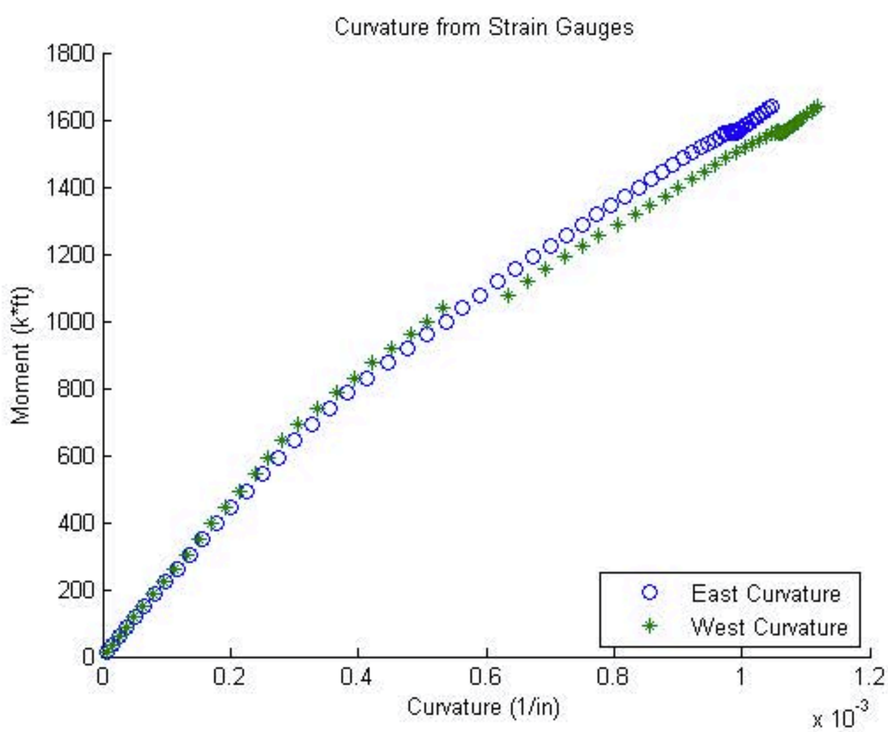
Curvature from Strain Gauges
Moment (k*ft)
Curvature (1/in)
x 10^-3
East Curvature
West Curvature
1800
1600
1400
1200
1000
800
600
400
200
0
0
0.2
0.4
0.6
0.8
1
1.2

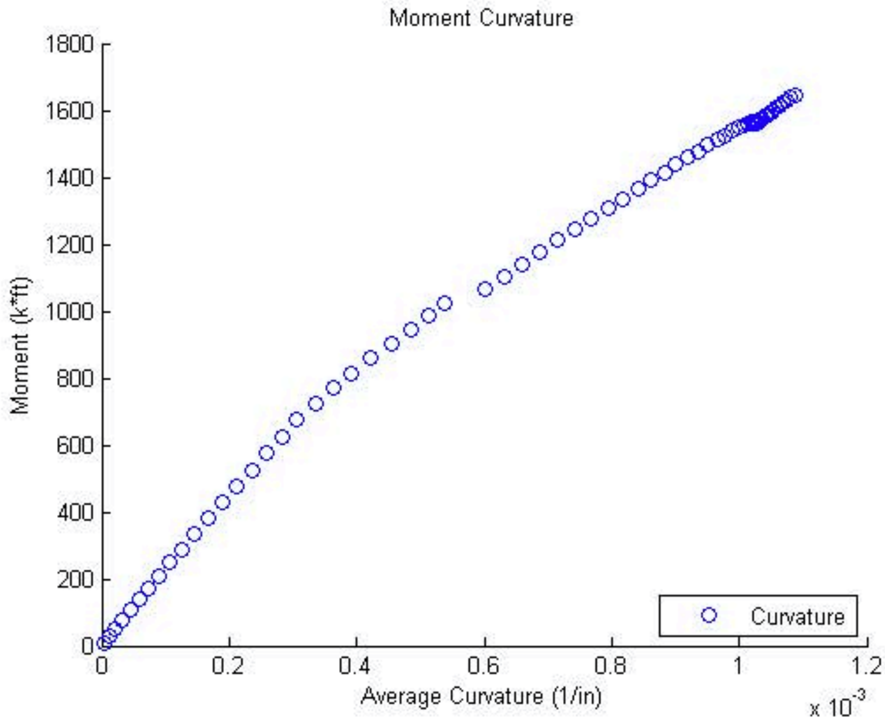
Moment Curvature
Moment (k*ft)
Average Curvature (1/in)
x 10-3
Curvature
0
200
400
600
800
1000
1200
1400
1600
1800
0
0.2
0.4
0.6
0.8
1
1.2

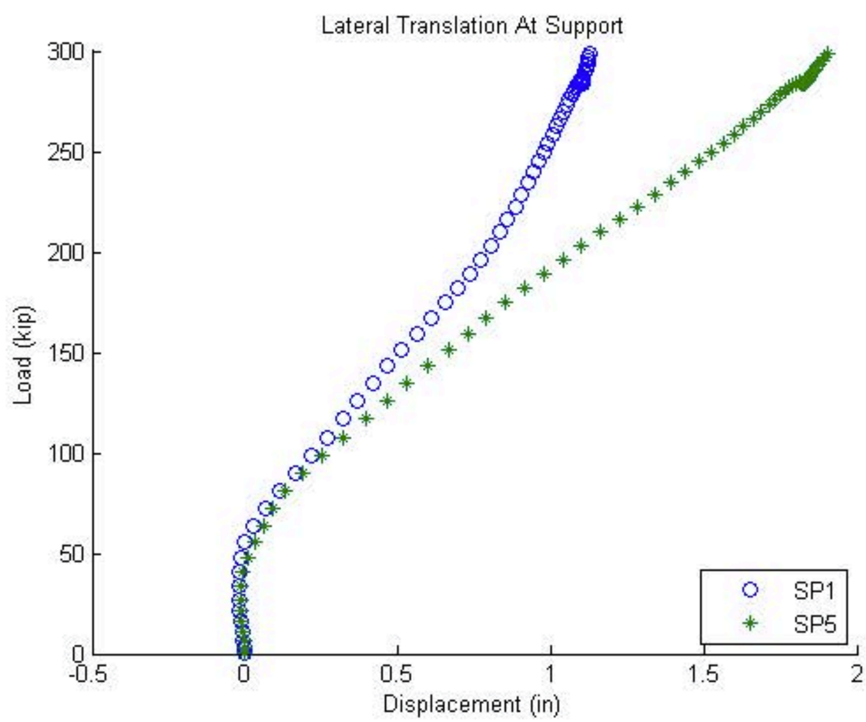
Lateral Translation At Support
Load (kip)
Displacement (in)
SP1
SP5
0
50
100
150
200
250
300
-0.5
0
0.5
1
1.5
2

Test Results for Pile C – 8HFB Trial 1

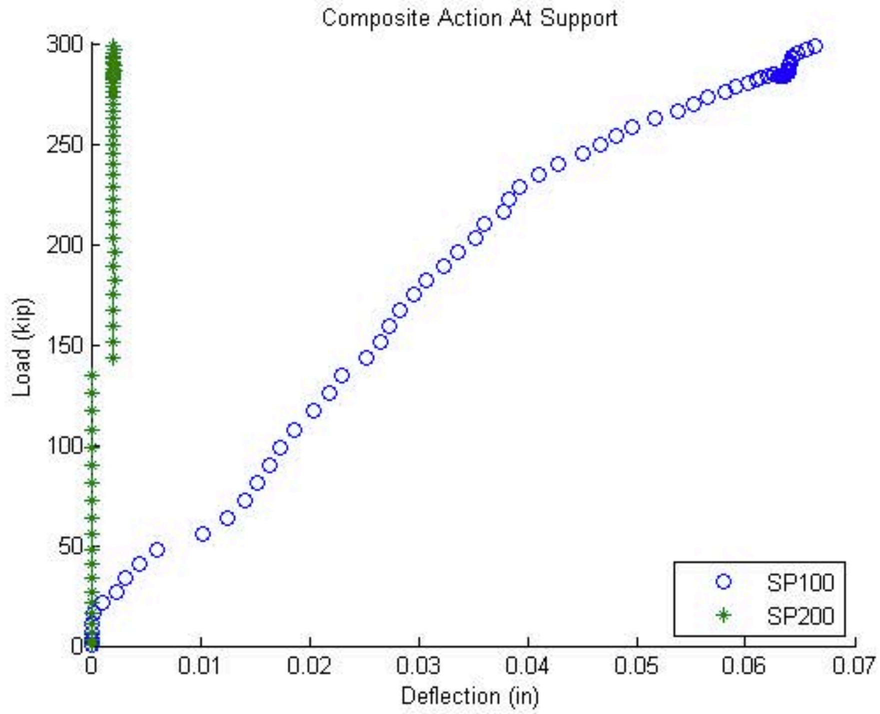

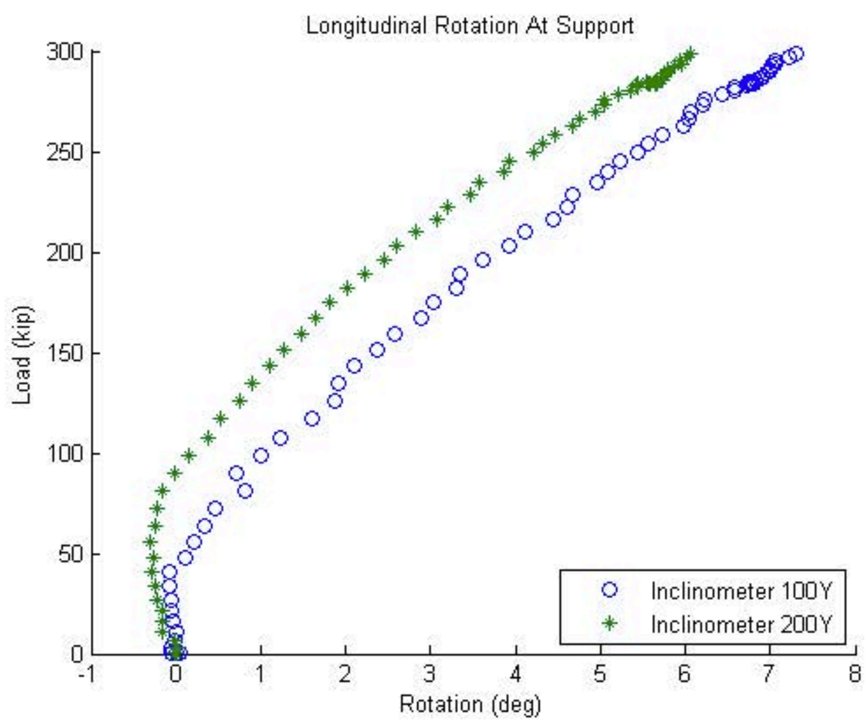

Test Results for Pile C – 8HFB Trial 1

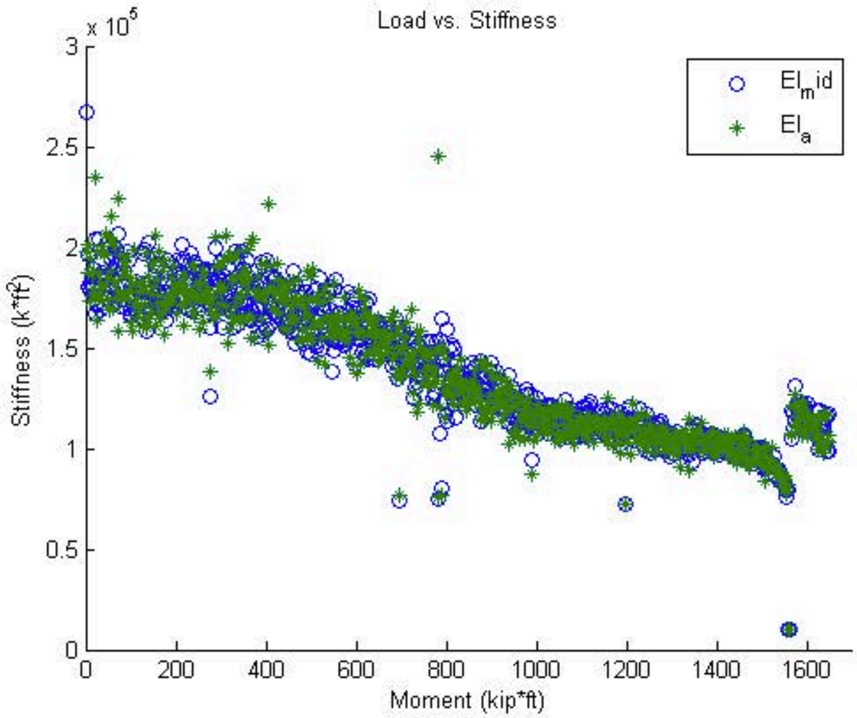

Appendix D: Test Results for Pile C – 8HFB Trial 2

Test Results for Pile C – 8HFB Trial 2

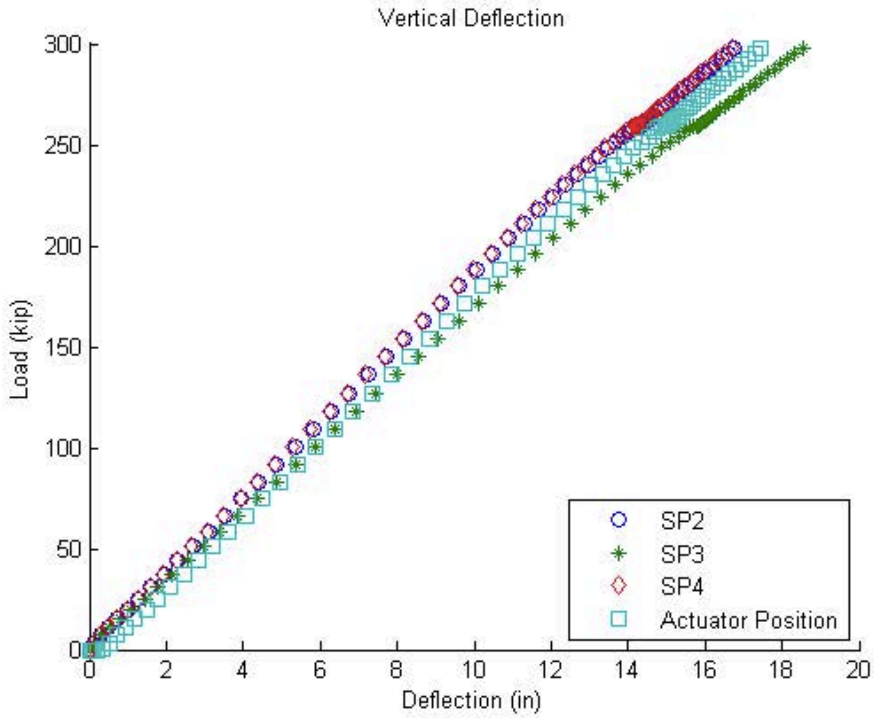

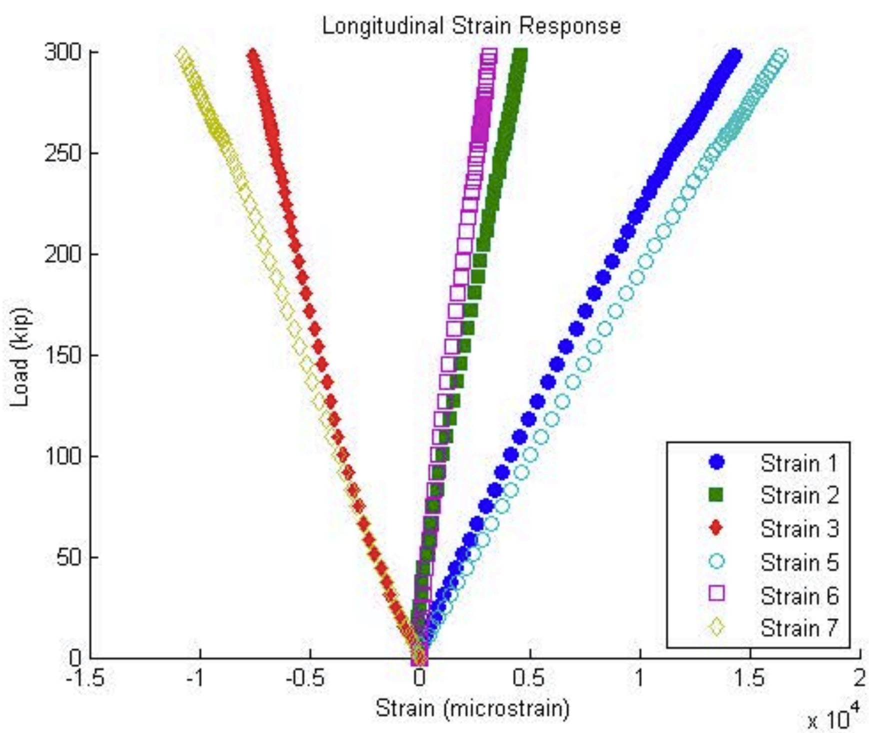

Test Results for Pile C – 8HFB Trial 2

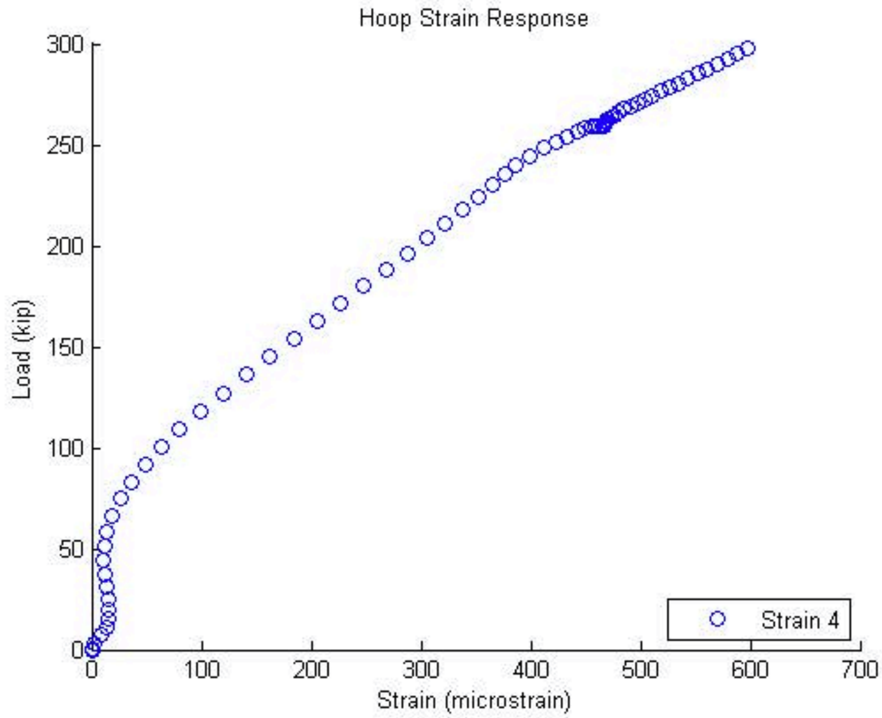

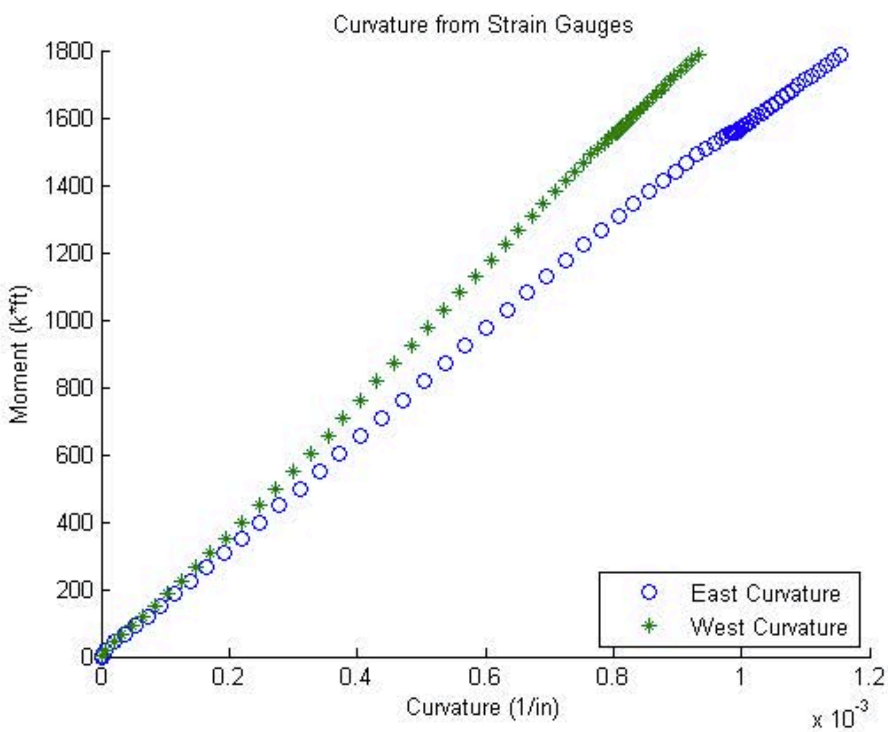

Test Results for Pile C – 8HFB Trial 2

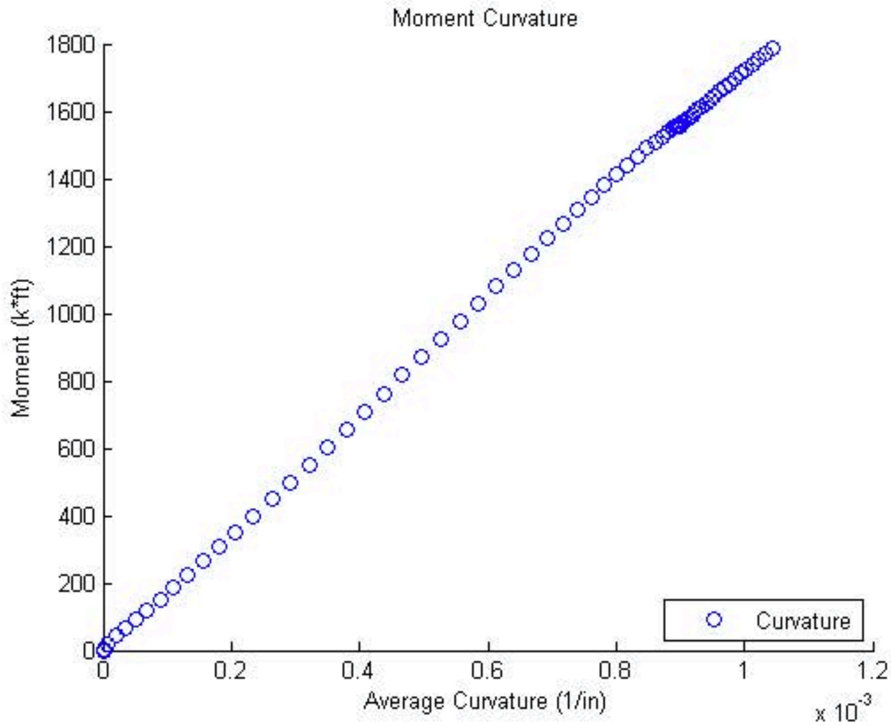

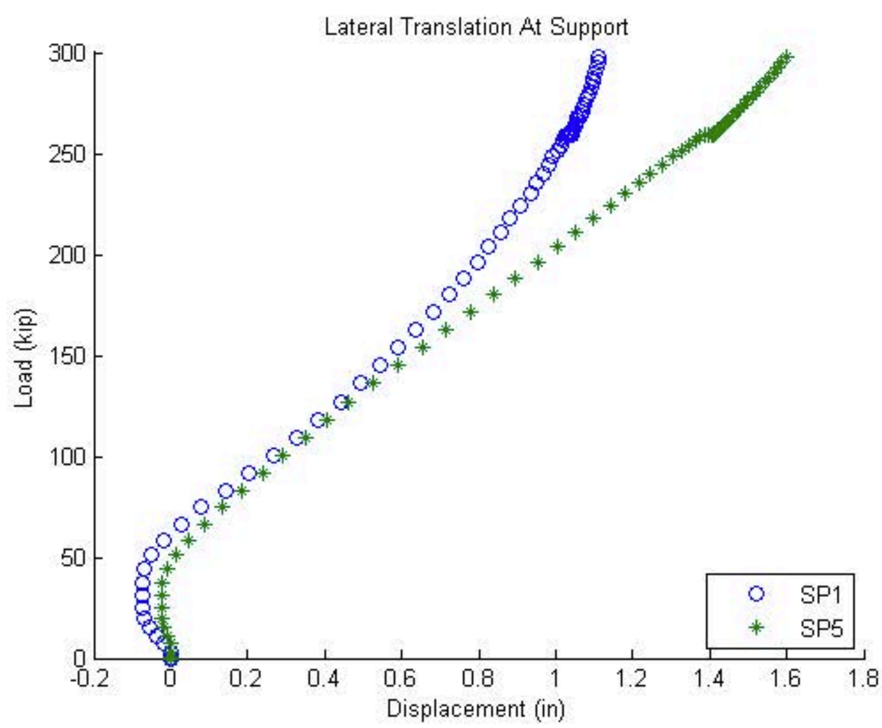

Test Results for Pile C – 8HFB Trial 2

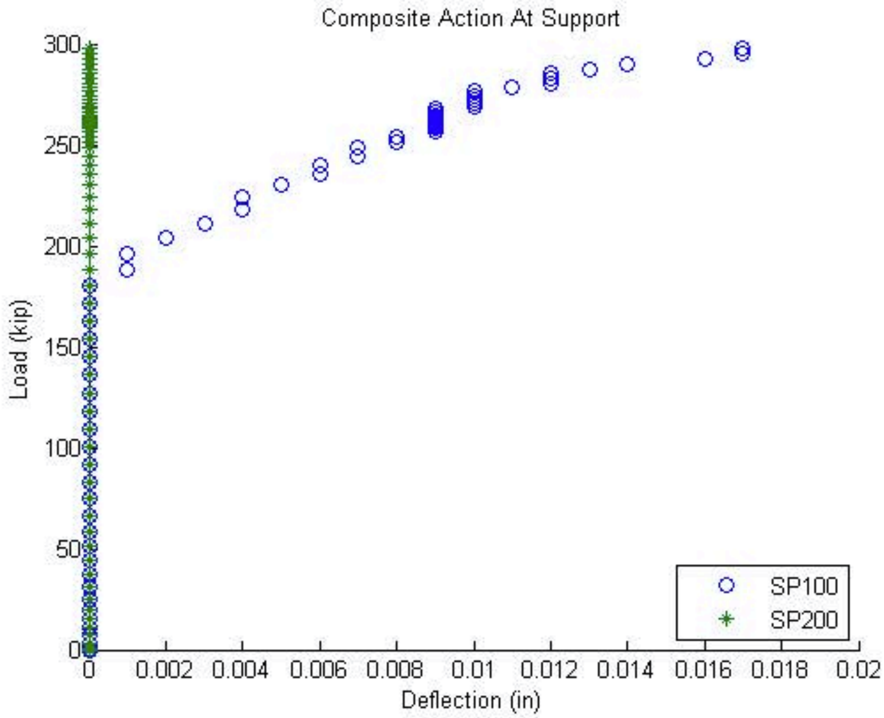

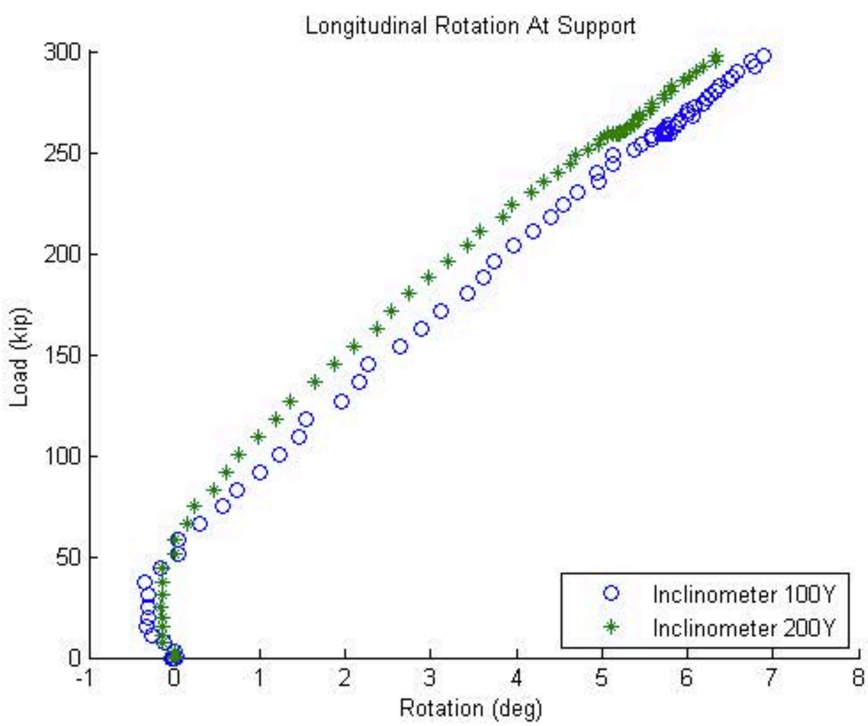

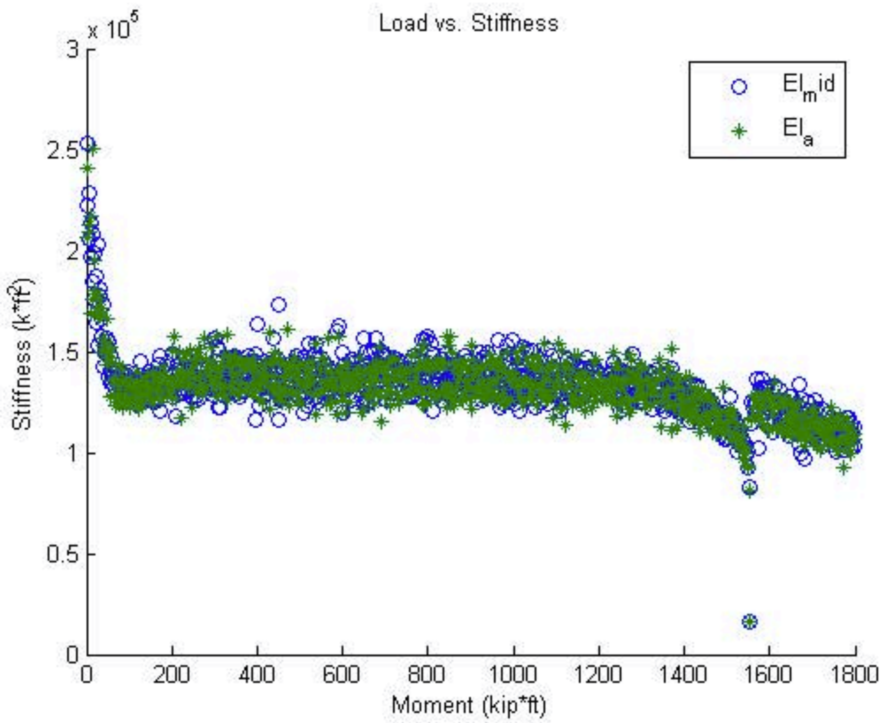
Load vs. Stiffness
x 10^5
Stiffness (k*ft²)
Moment (kip*ft)
EI_mid
EI_a
0
0.5
1
1.5
2
2.5
3
0
200
400
600
800
1000
1200
1400
1600
1800

Appendix E: Test Results for Pile C – 8HFB Trial 3

Test Results for Pile C – 8HFB Trial 3

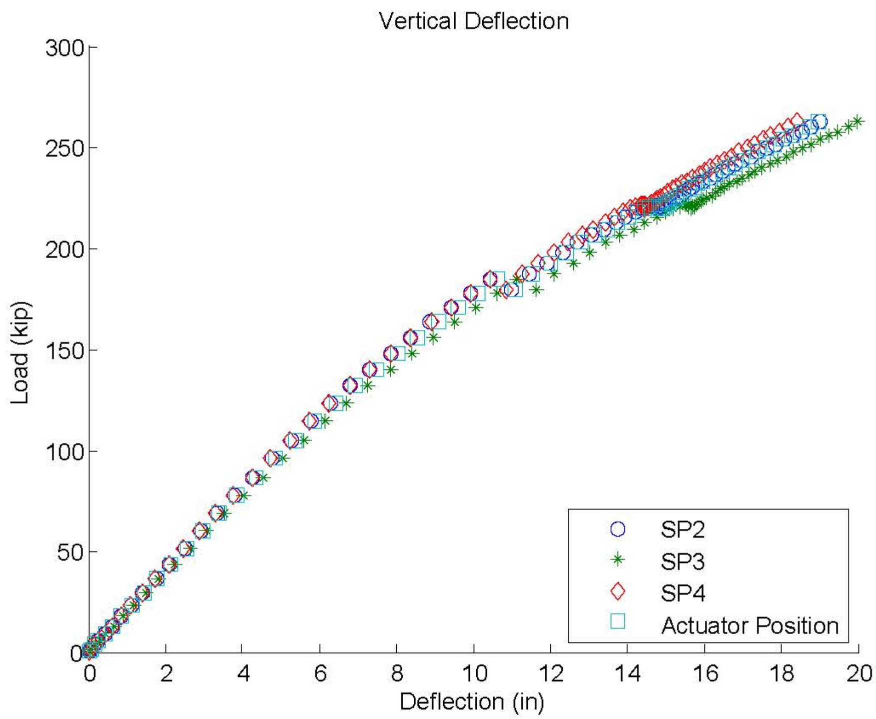

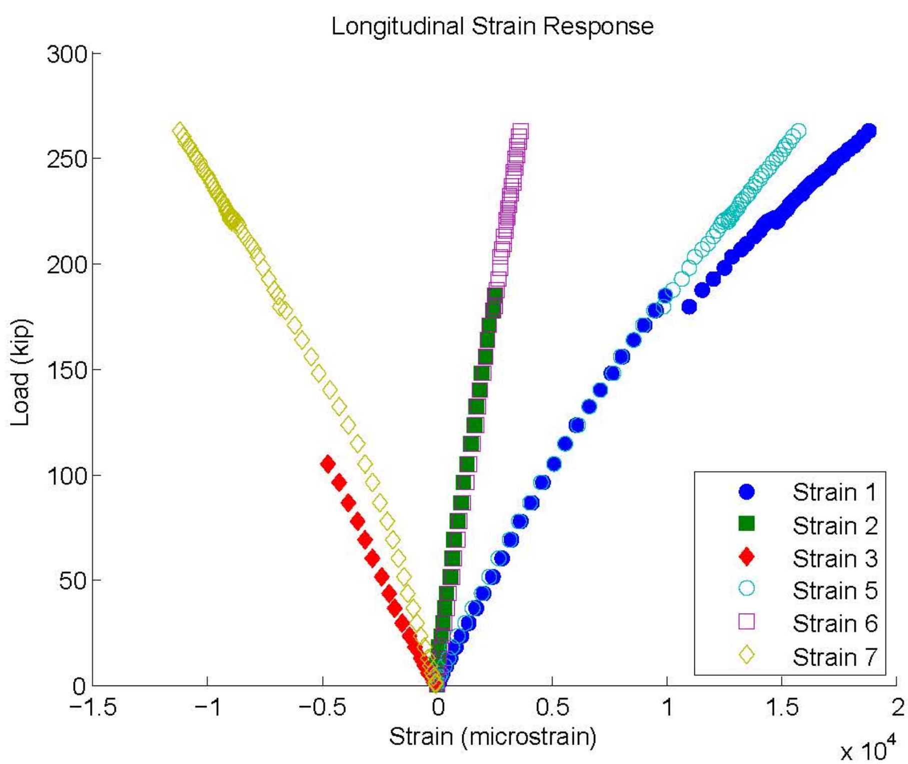

Test Results for Pile C – 8HFB Trial 3

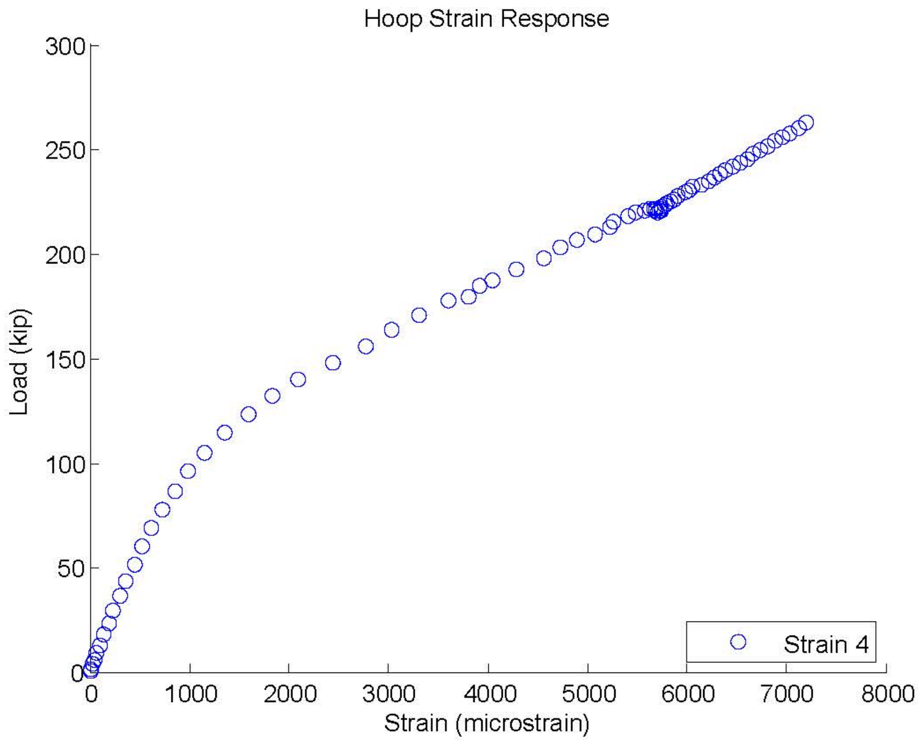

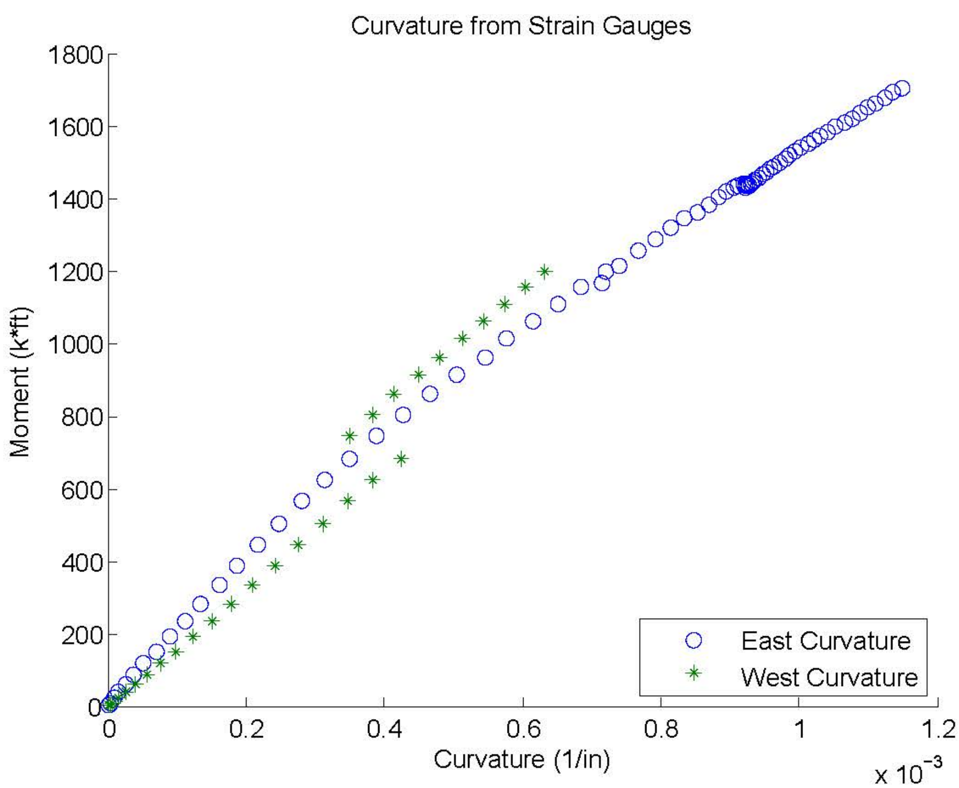

Test Results for Pile C – 8HFB Trial 3

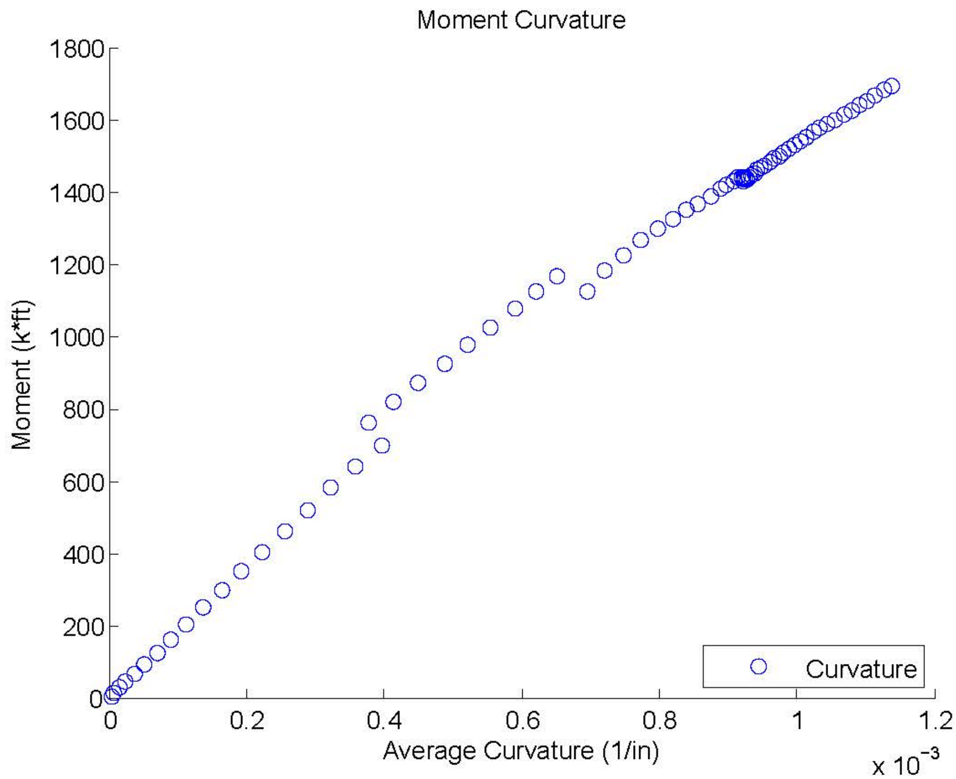

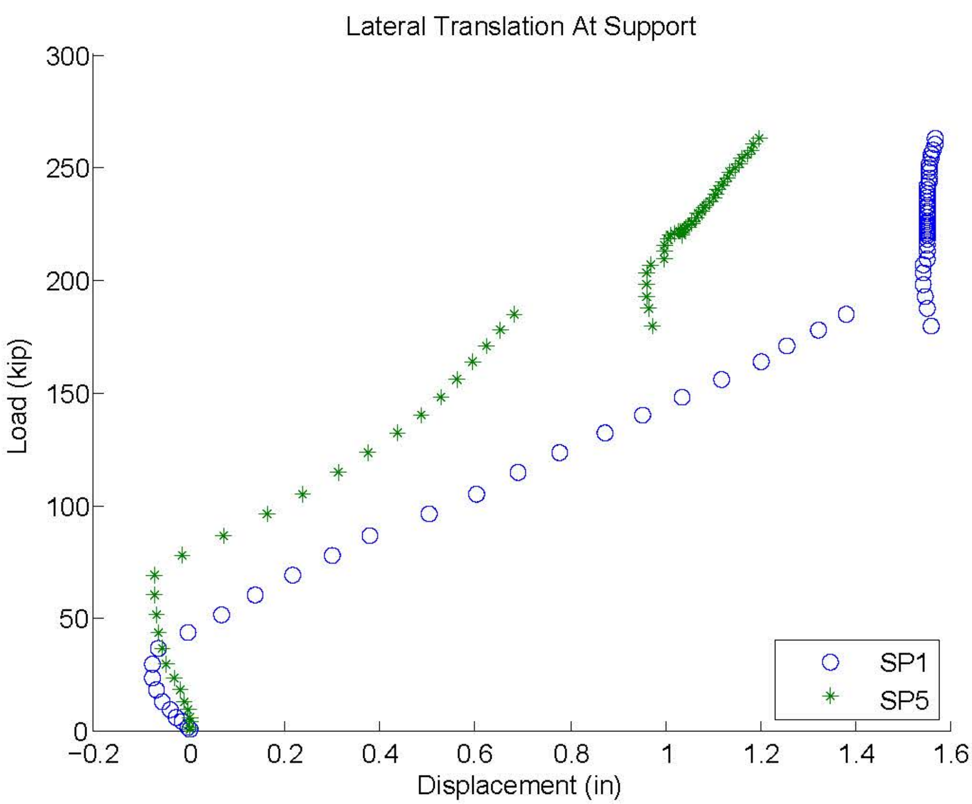

Test Results for Pile C – 8HFB Trial 3

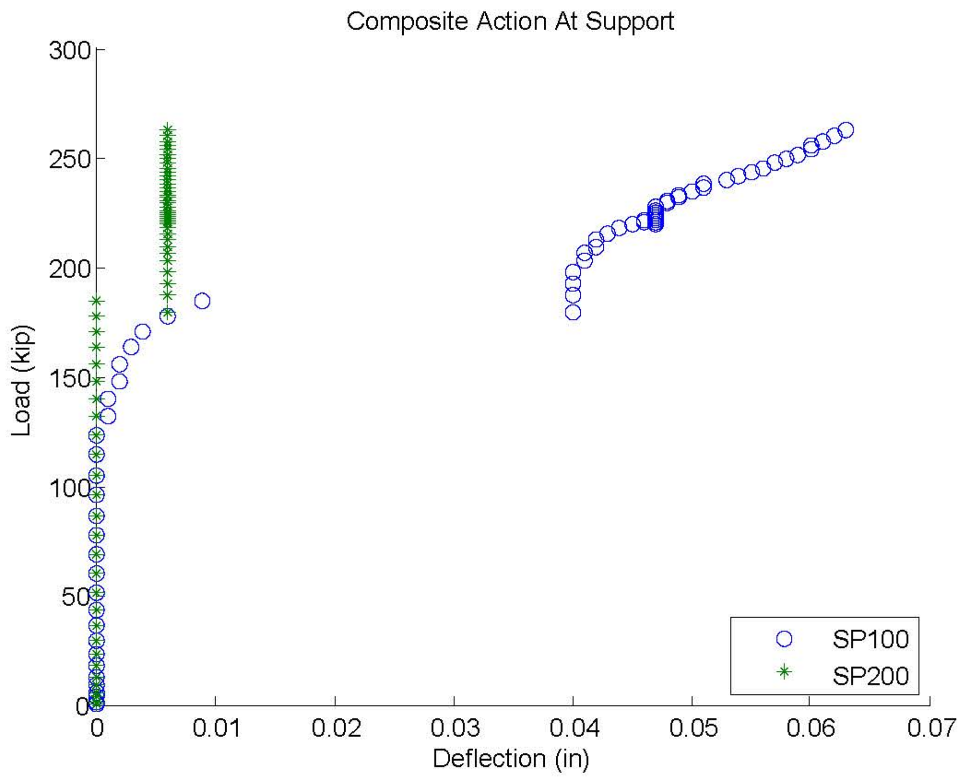

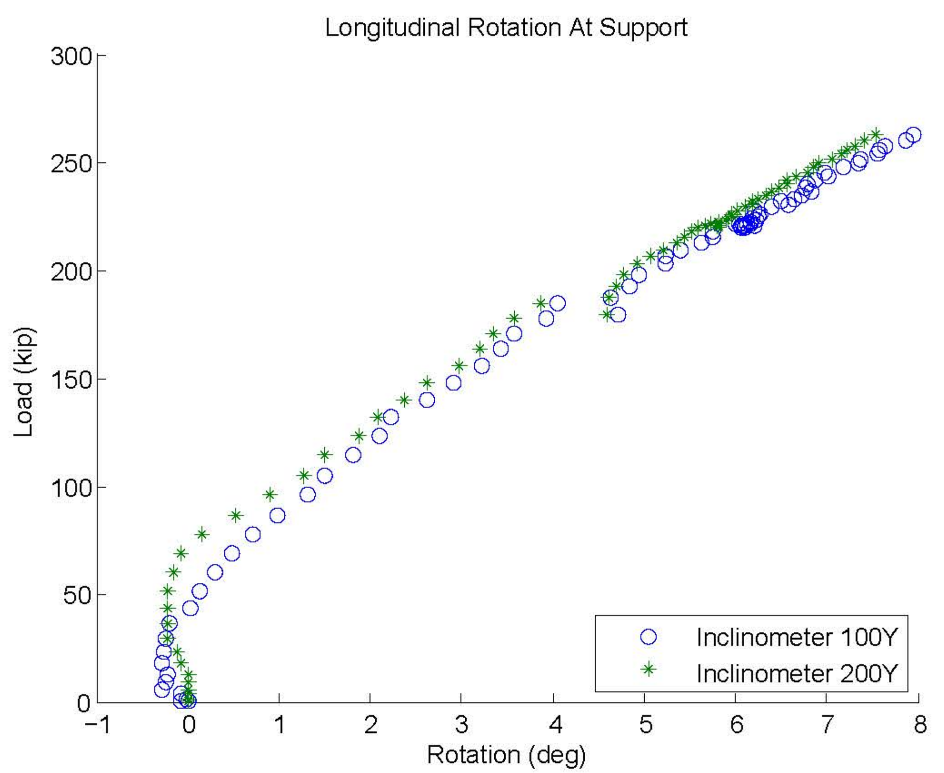

Test Results for Pile C – 8HFB Trial 3

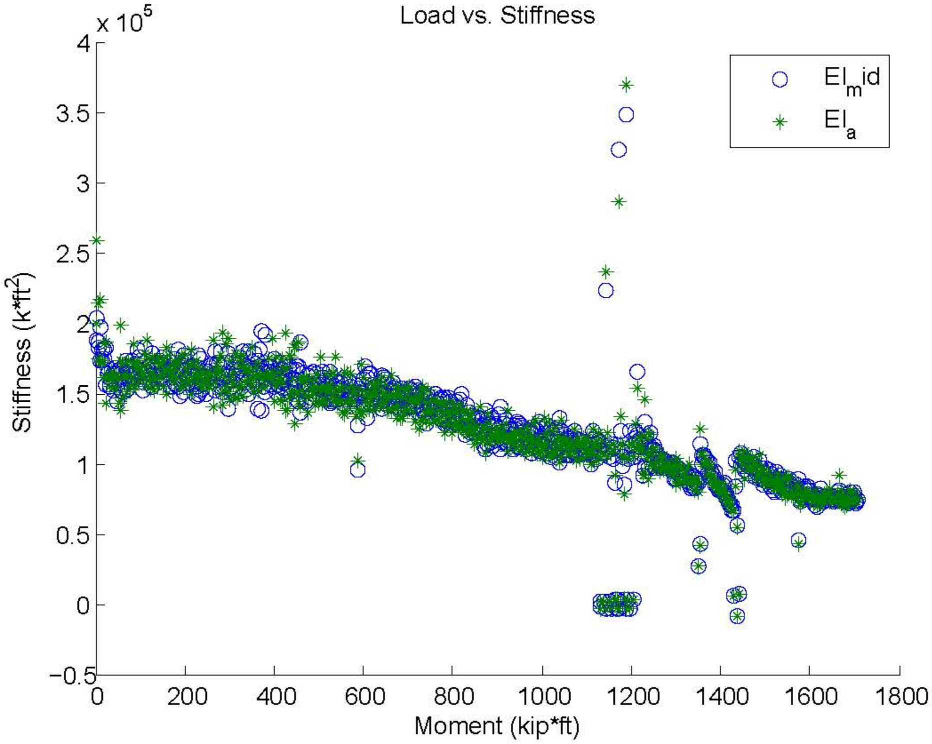

Appendix F: Test Results for Initial Loading of Pile E – 4FB

Test Results for Initial Loading of Pile E – 4FB

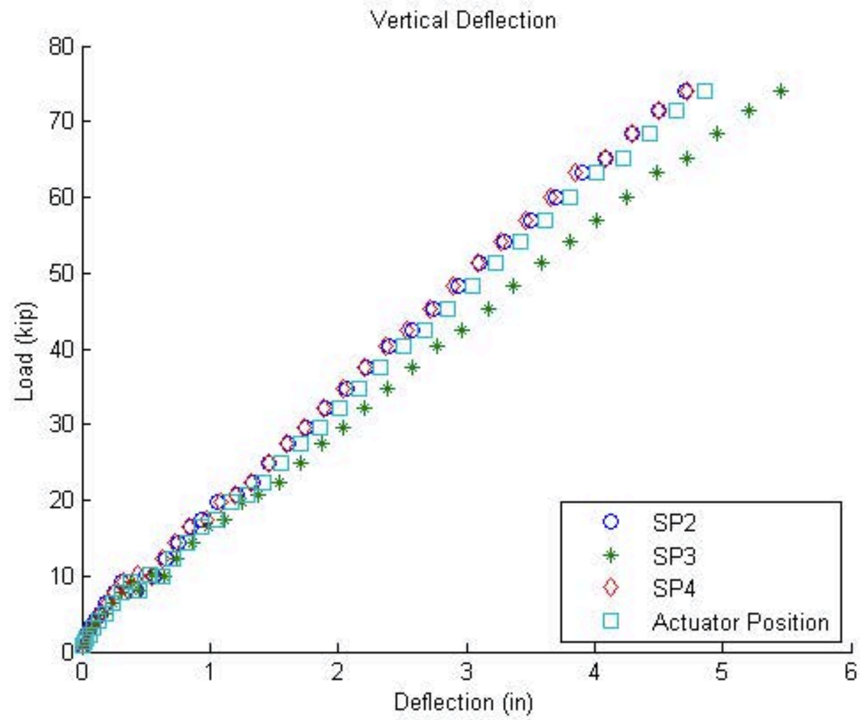

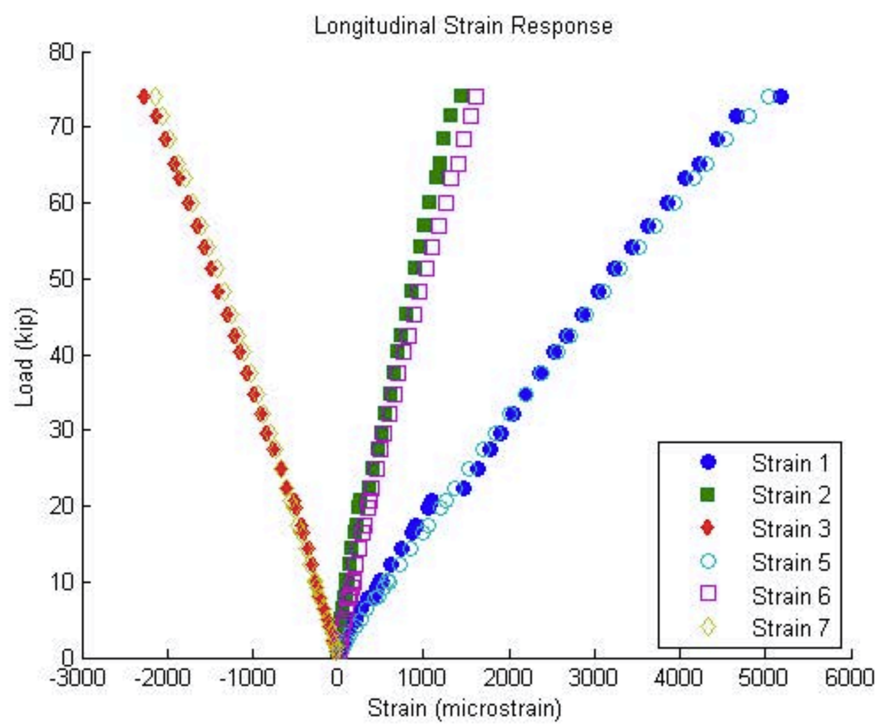

Test Results for Initial Loading of Pile E – 4FB

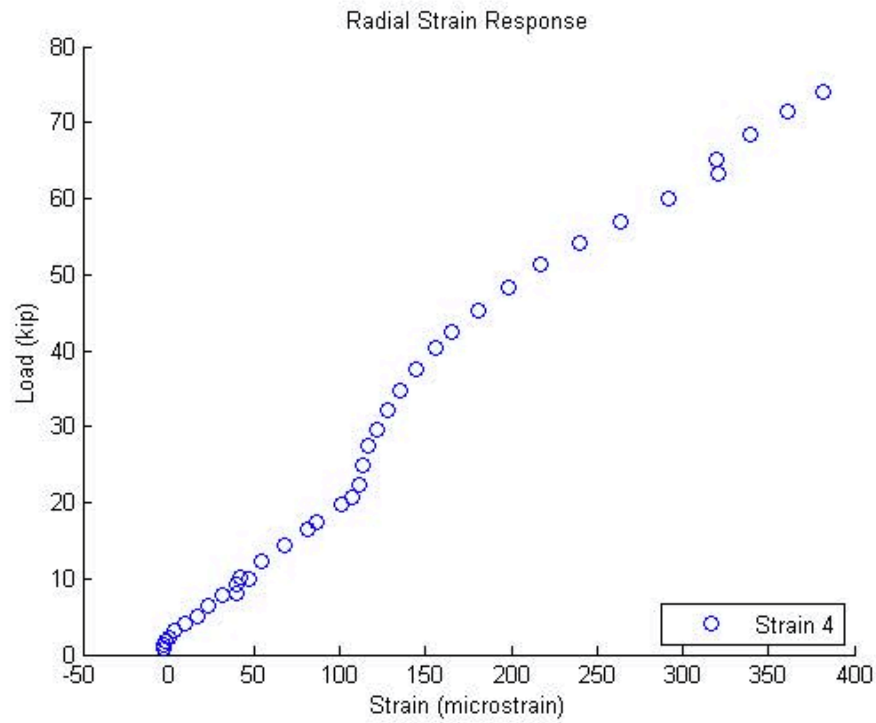

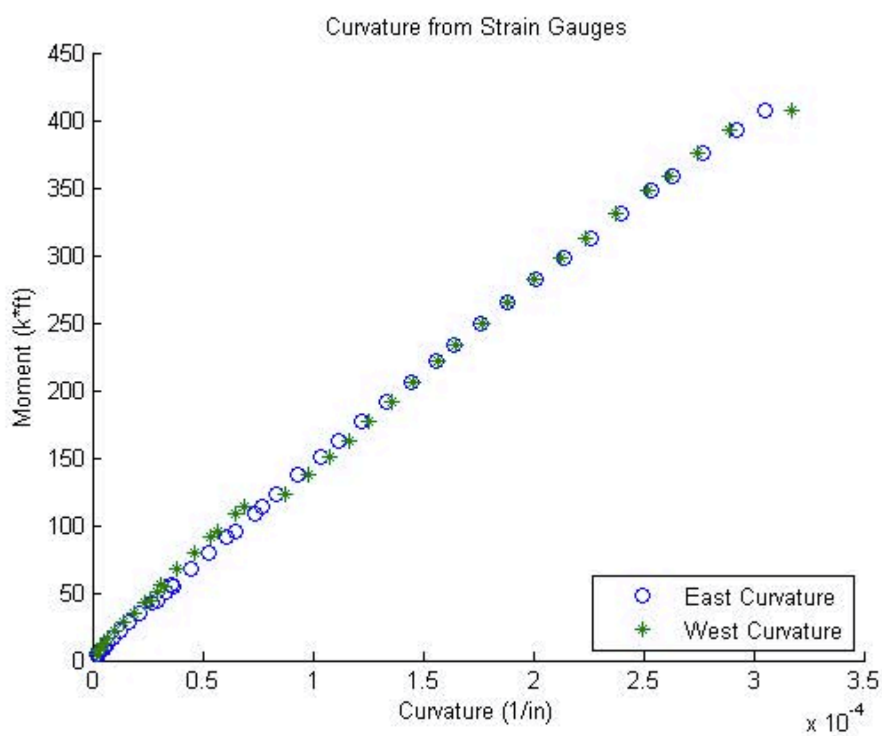

Test Results for Initial Loading of Pile E – 4FB

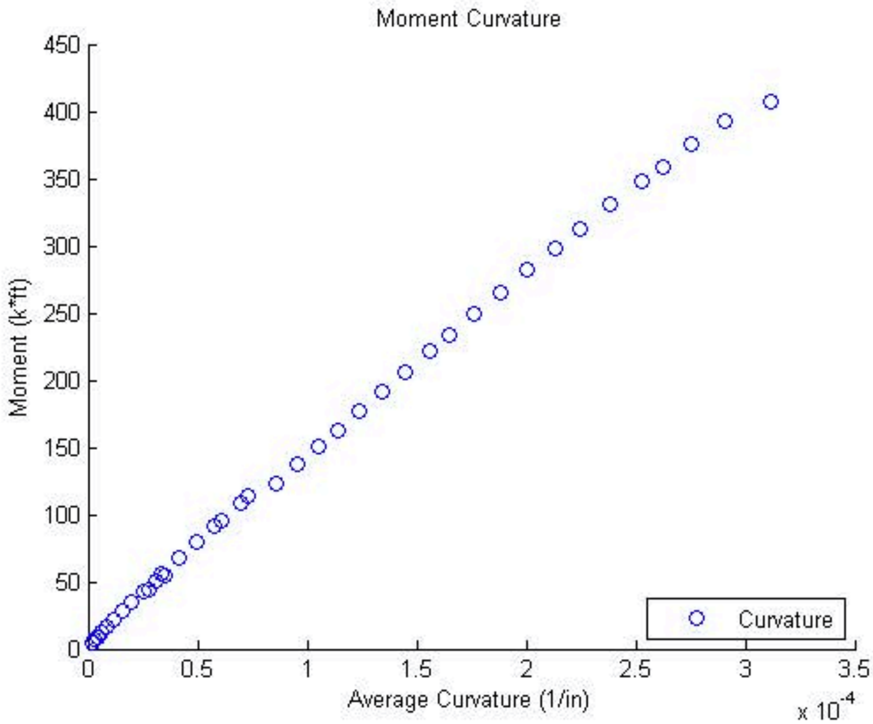

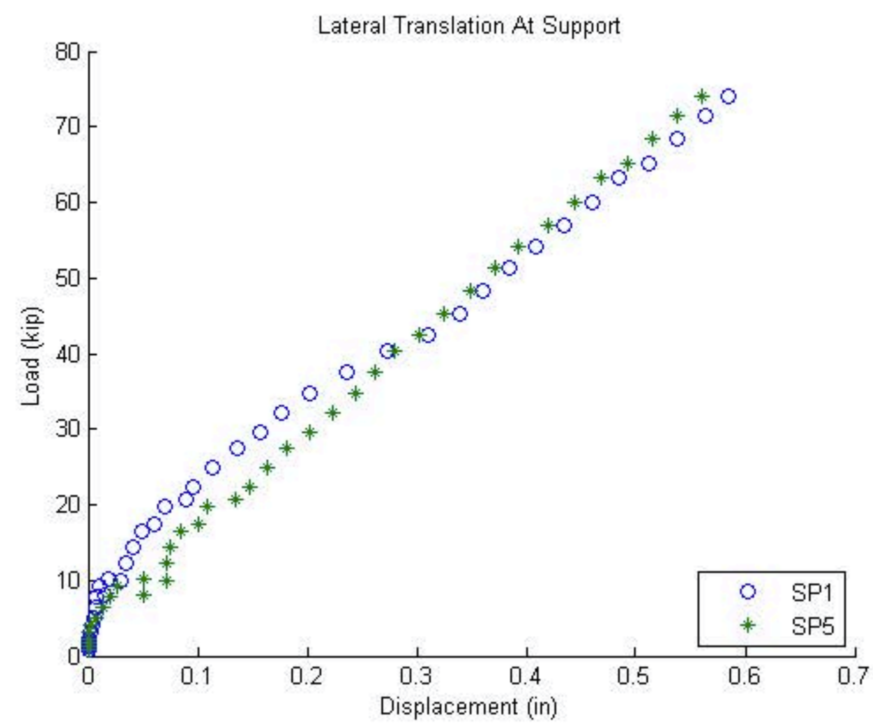

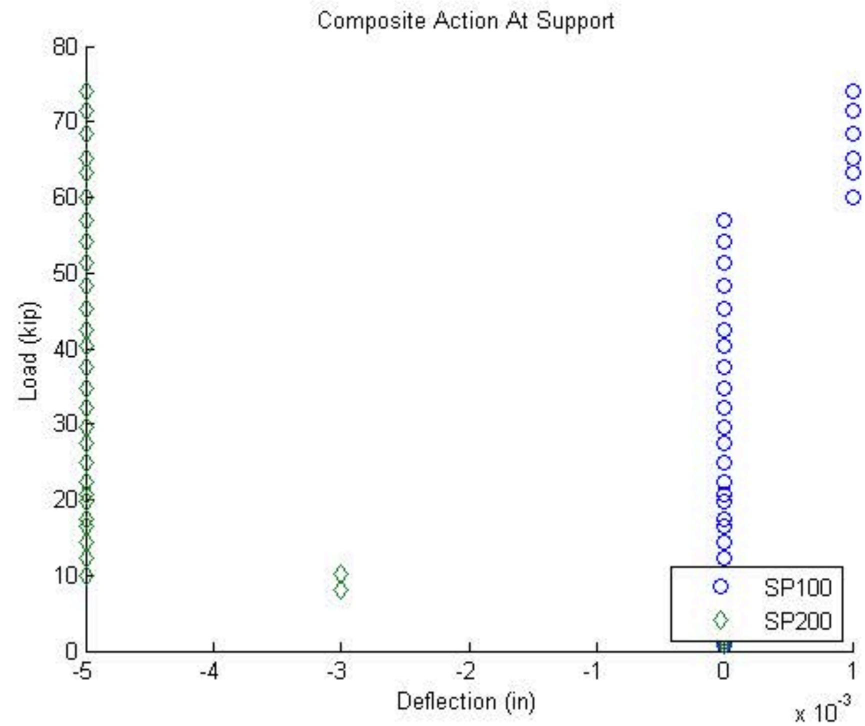
Composite Action At Support
Load (kip)
Deflection (in)
x 10^-3
SP100
SP200
80
70
60
50
40
30
20
10
0
-5
-4
-3
-2
-1
0
1

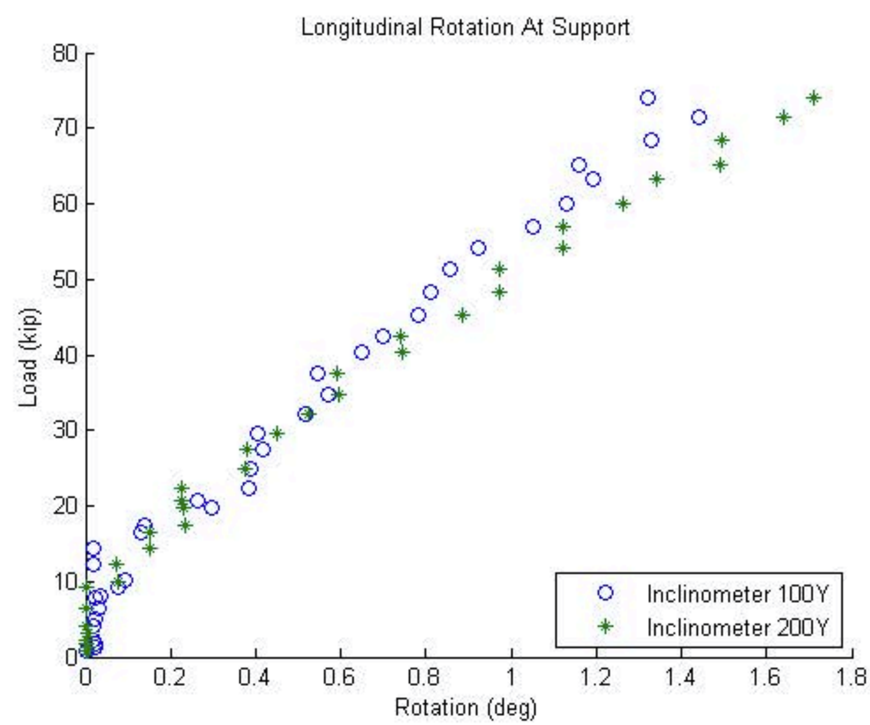
Longitudinal Rotation At Support
Load (kip)
Rotation (deg)
Inclinometer 100Y
Inclinometer 200Y
80
70
60
50
40
30
20
10
0
0.2
0.4
0.6
0.8
1
1.2
1.4
1.6
1.8

Test Results for Initial Loading of Pile E – 4FB

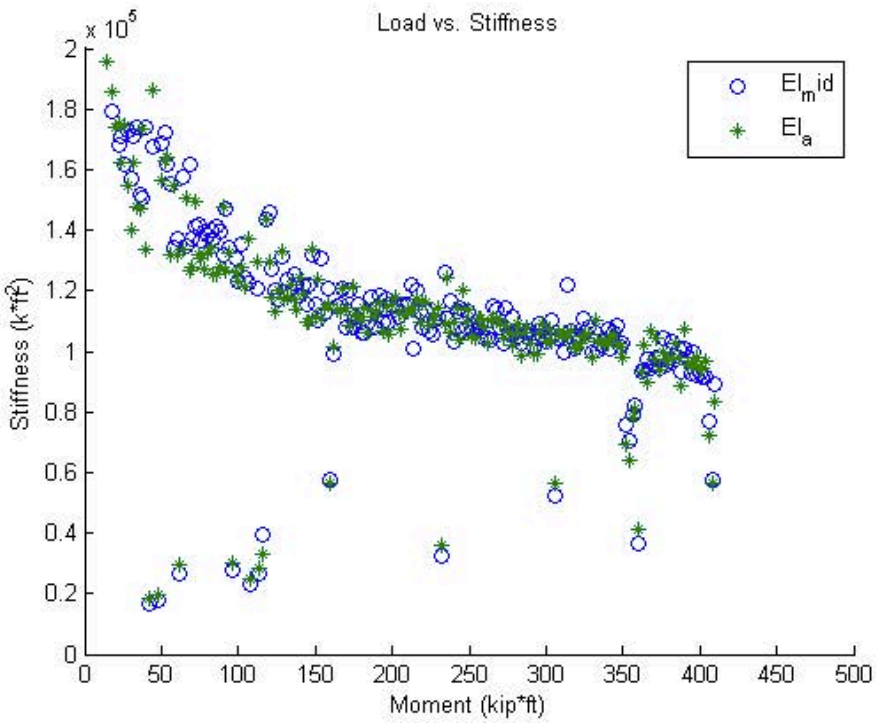

Appendix G: Test Results for Ultimate Loading of Pile E - 4FB

Test Results for Ultimate Loading of Pile E - 4FB

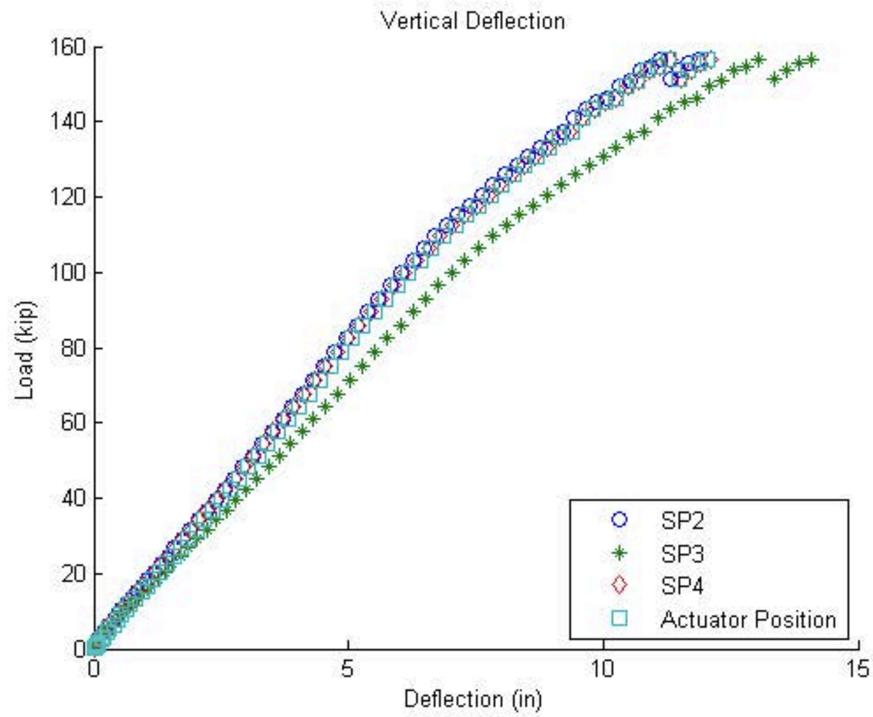

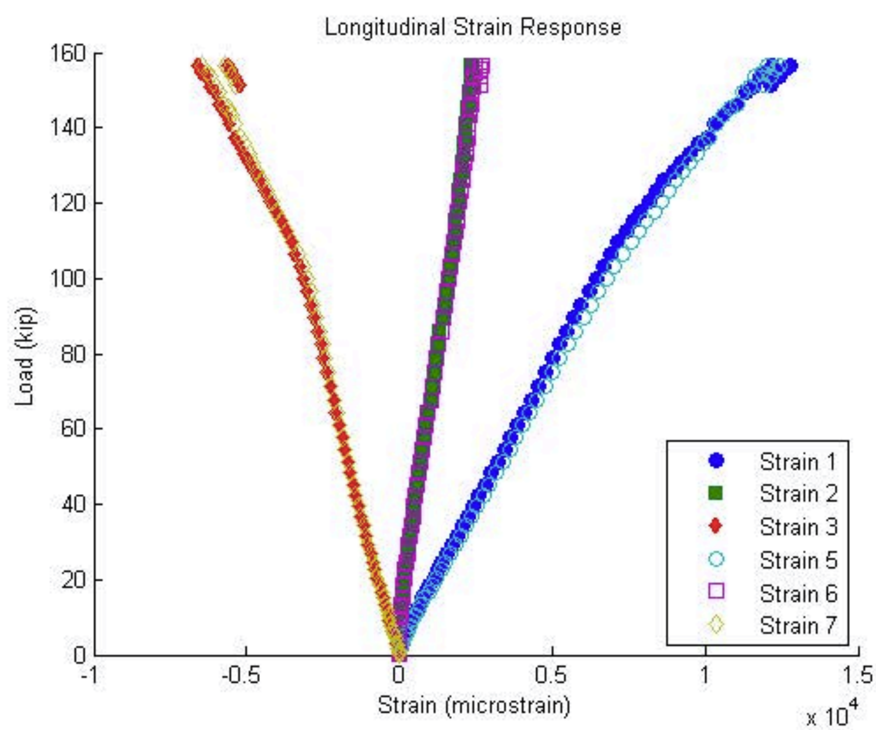

Test Results for Ultimate Loading of Pile E - 4FB

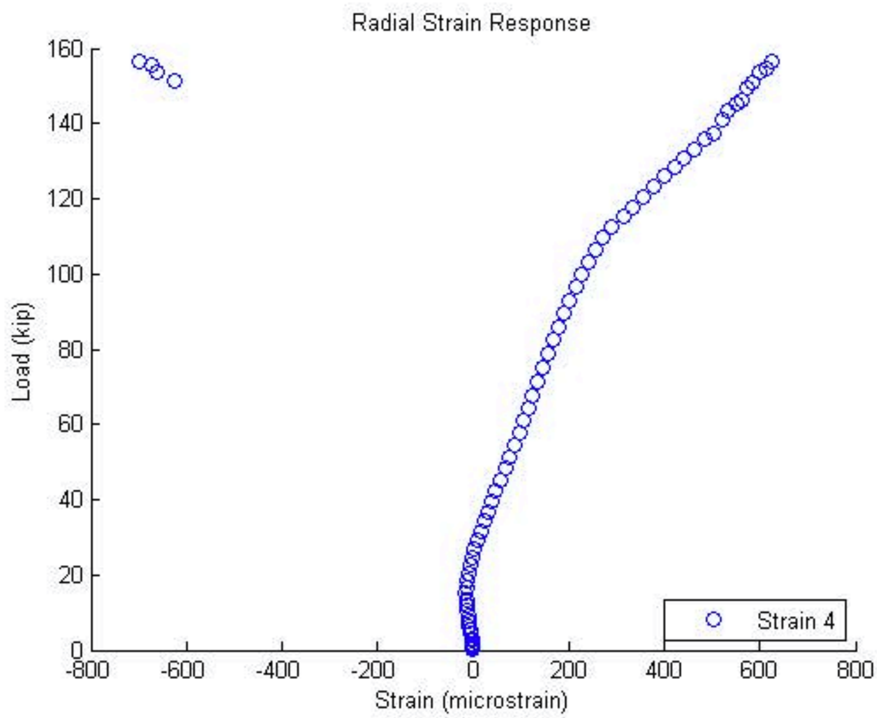

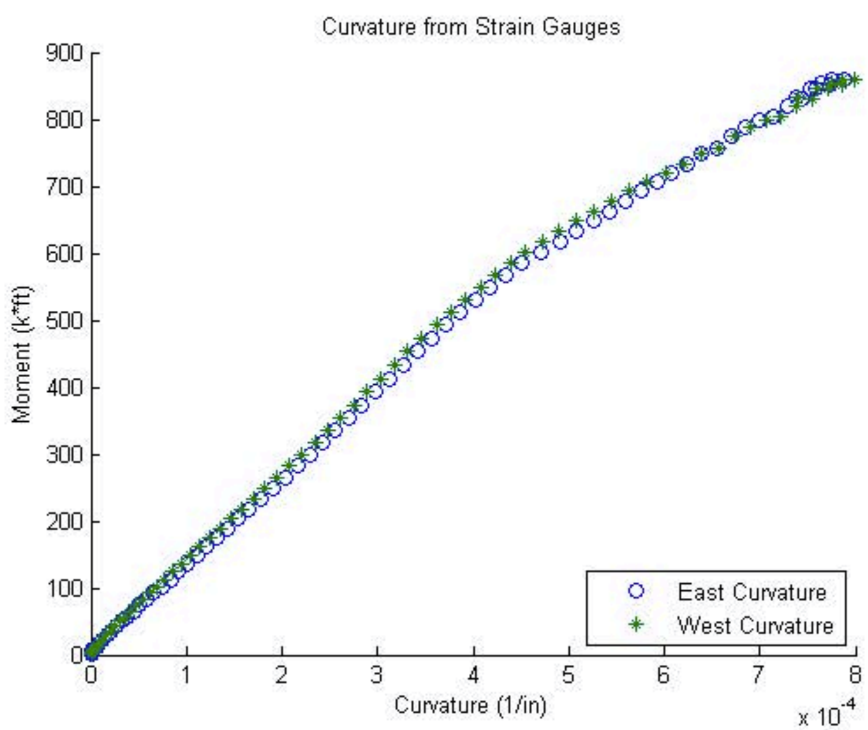

Test Results for Ultimate Loading of Pile E - 4FB

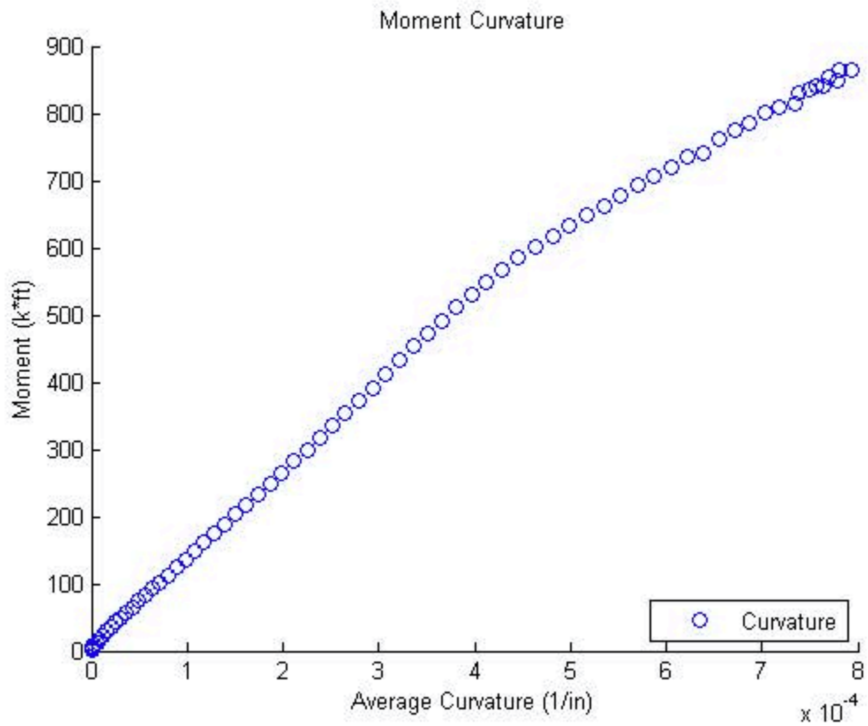

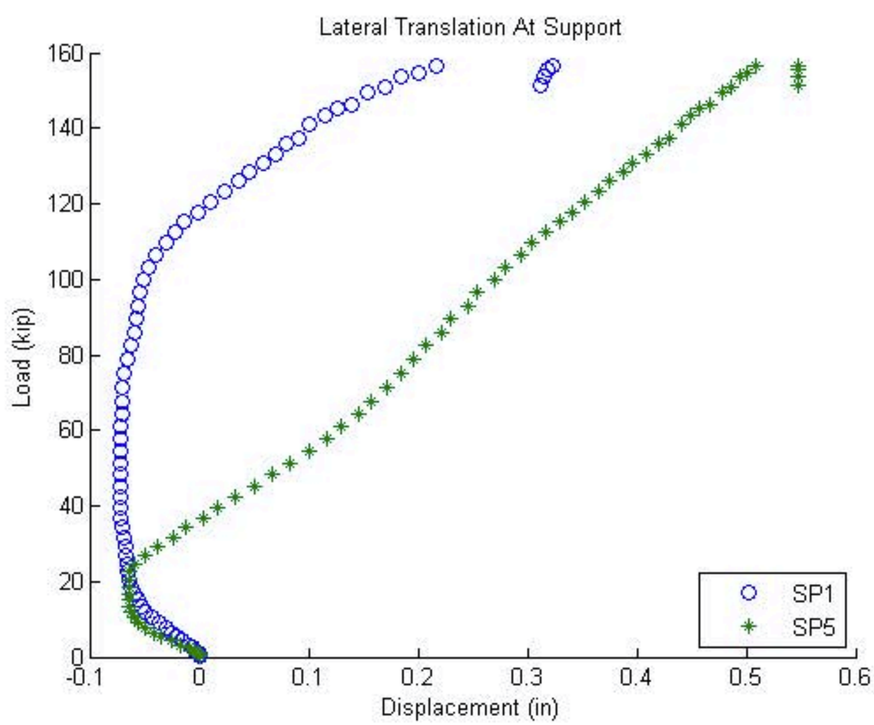

Test Results for Ultimate Loading of Pile E - 4FB

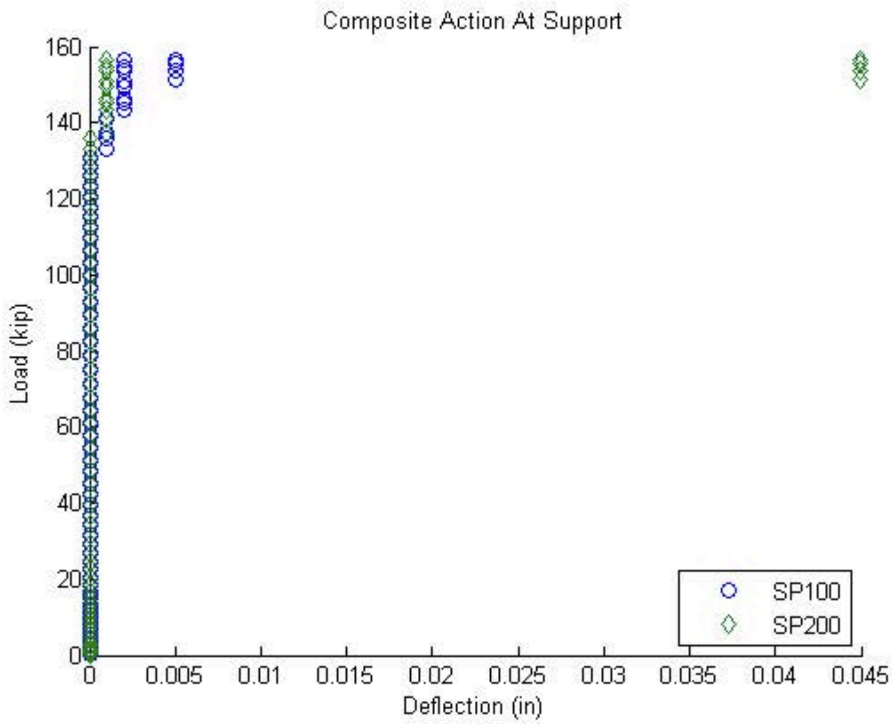

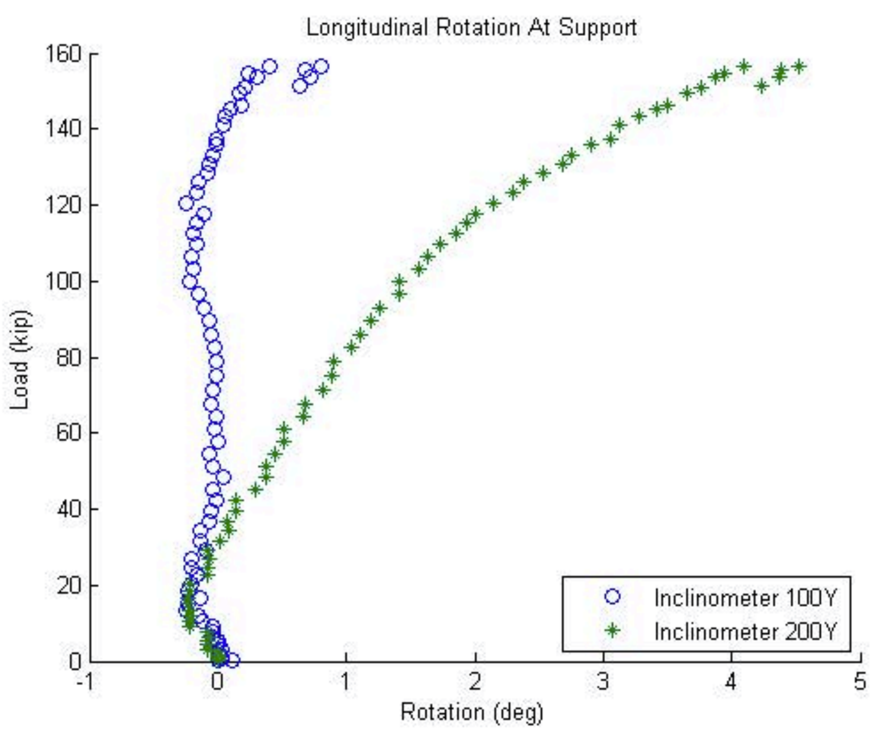

Test Results for Ultimate Loading of Pile E - 4FB

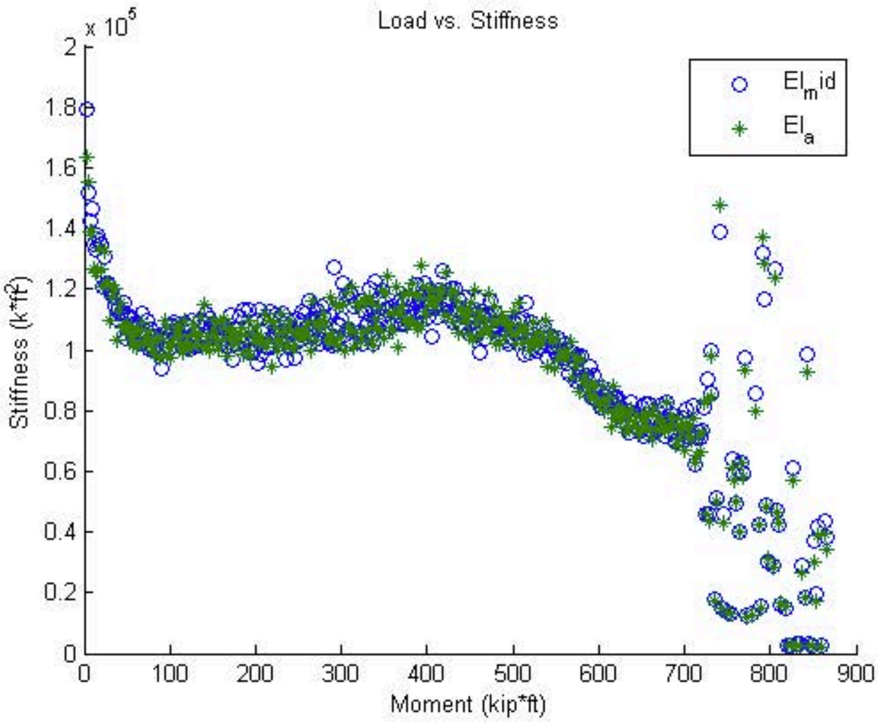

Appendix H: Test Results for First 10 Cycles of Pile E – 4FB

Test Results for First 10 Cycles of Pile E – 4FB

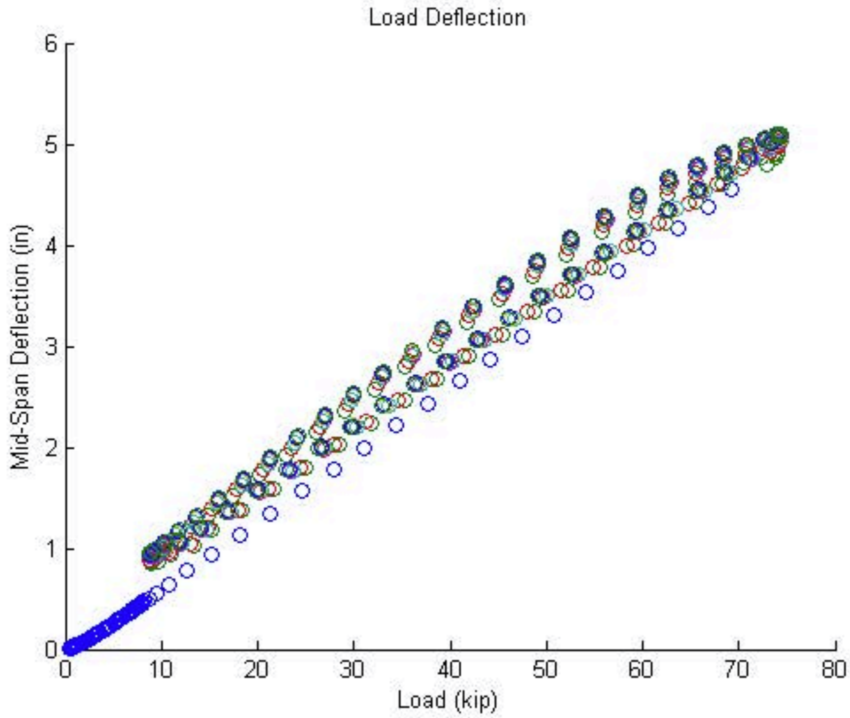

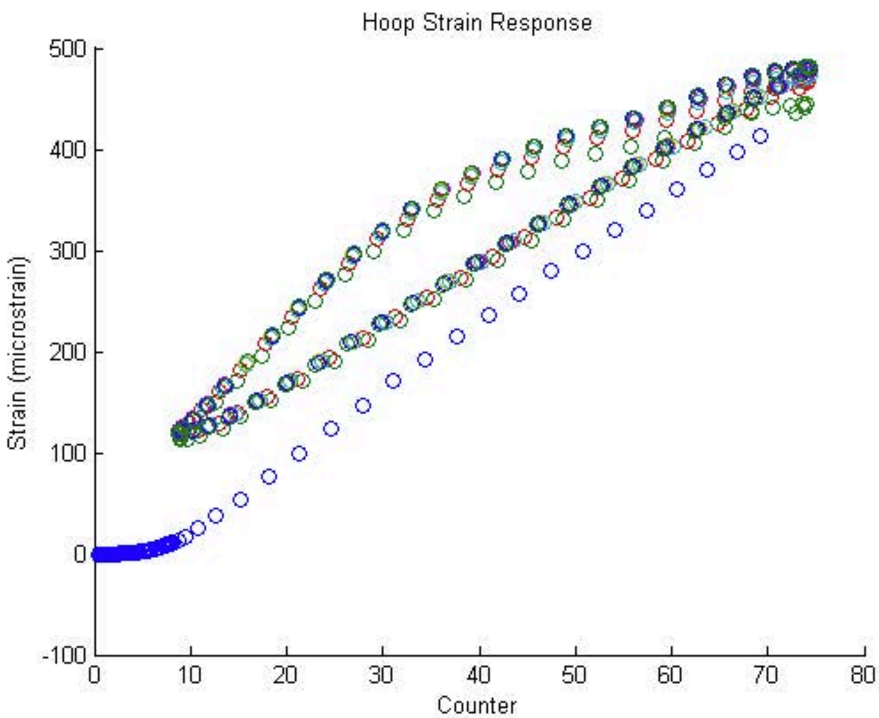

Test Results for First 10 Cycles of Pile E – 4FB

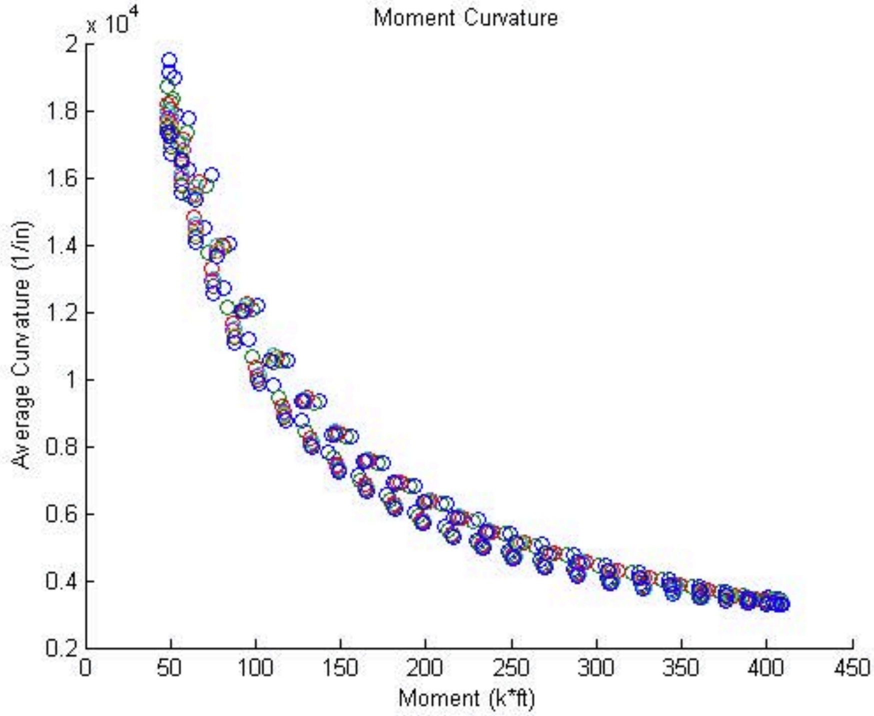

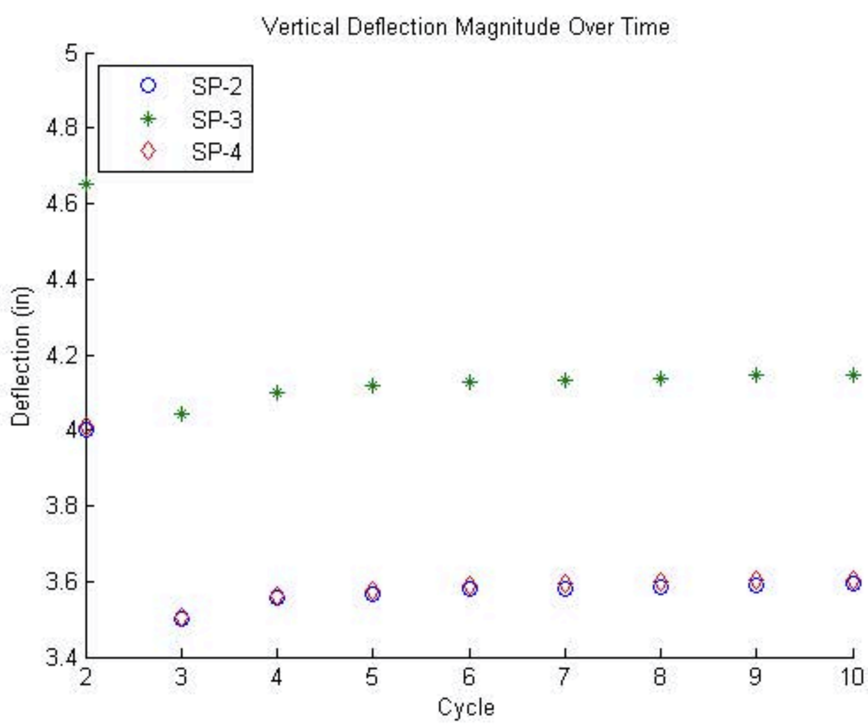

Test Results for First 10 Cycles of Pile E – 4FB

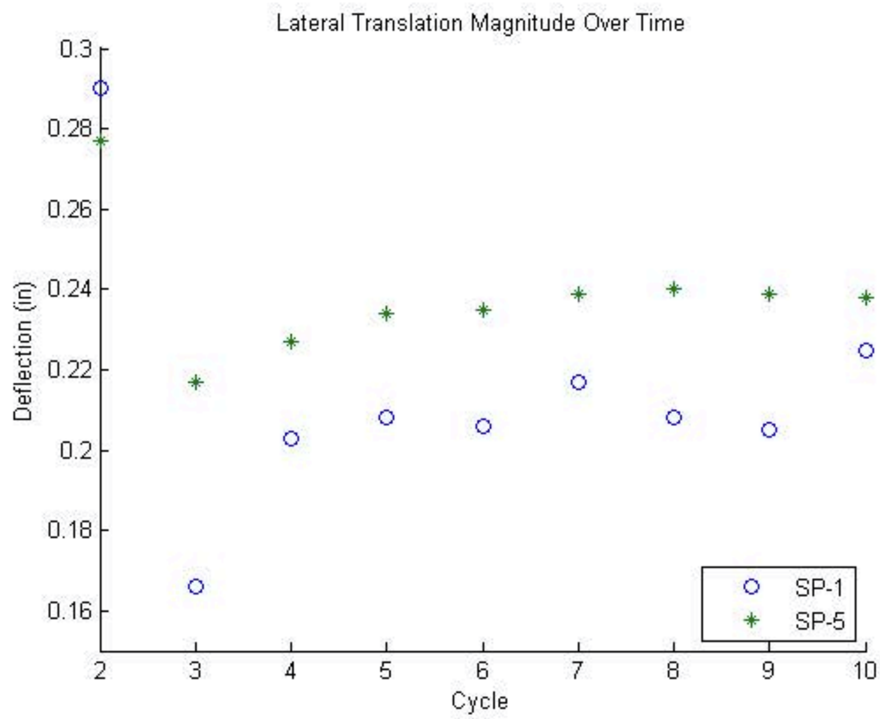

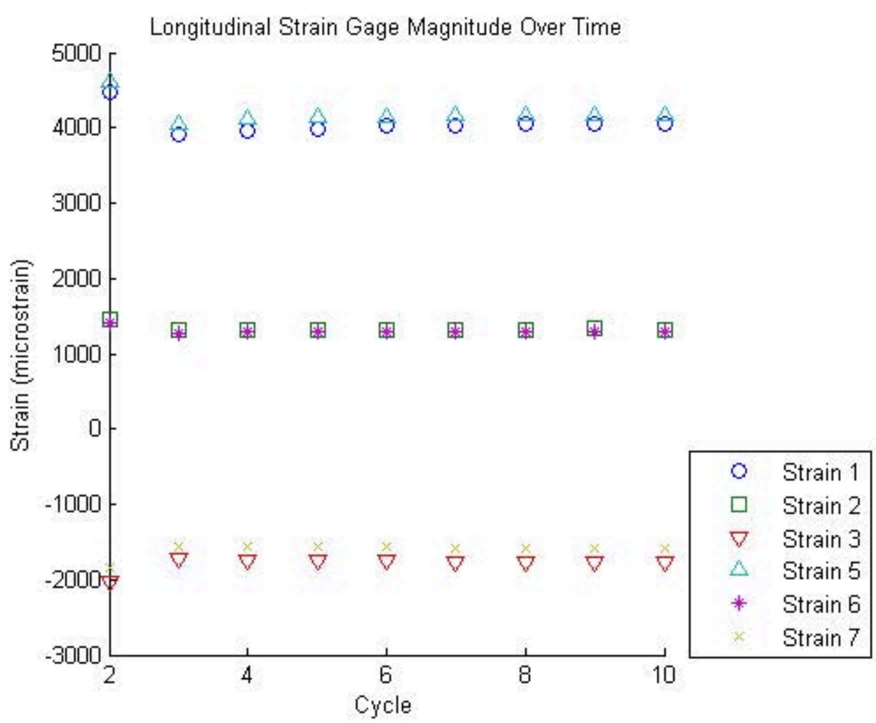

Test Results for First 10 Cycles of Pile E – 4FB

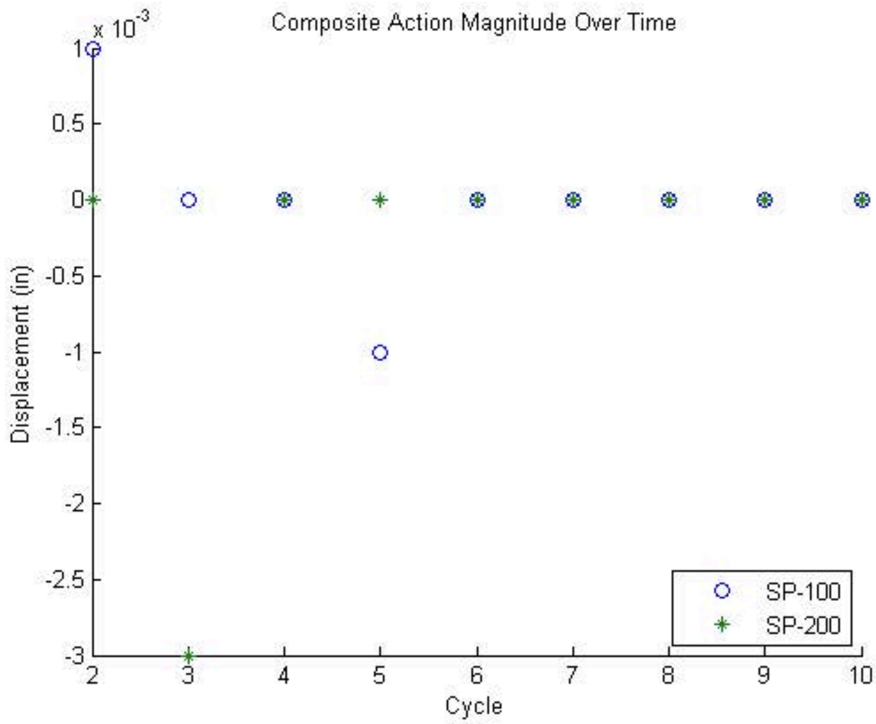

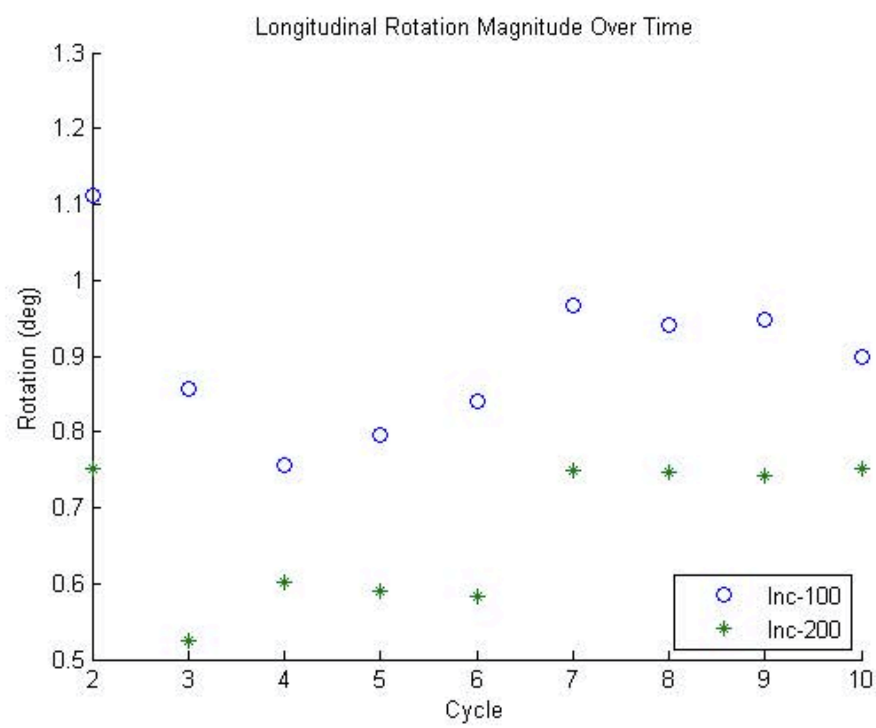

Test Results for First 10 Cycles of Pile E – 4FB

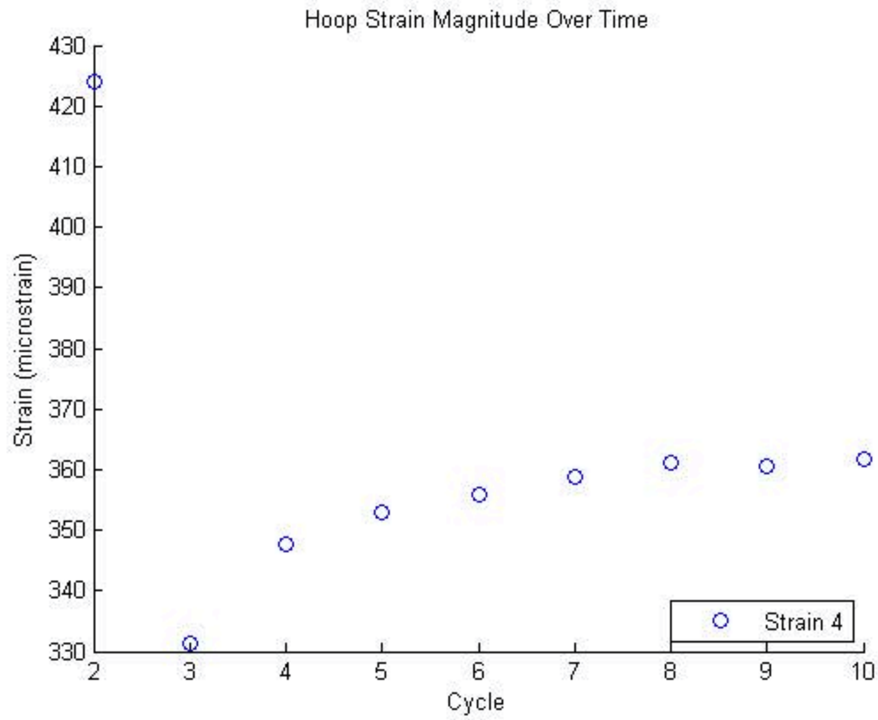

Appendix I: Test Results for Every 1,000 Cycles of Pile E – 4FB

Test Results for Every 1,000 Cycles of Pile E – 4FB

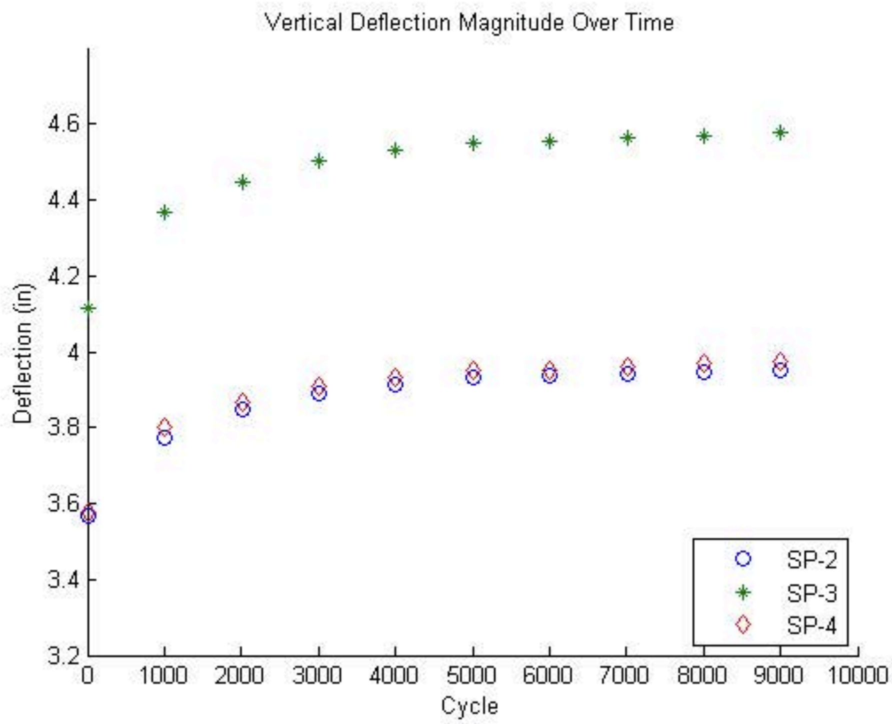

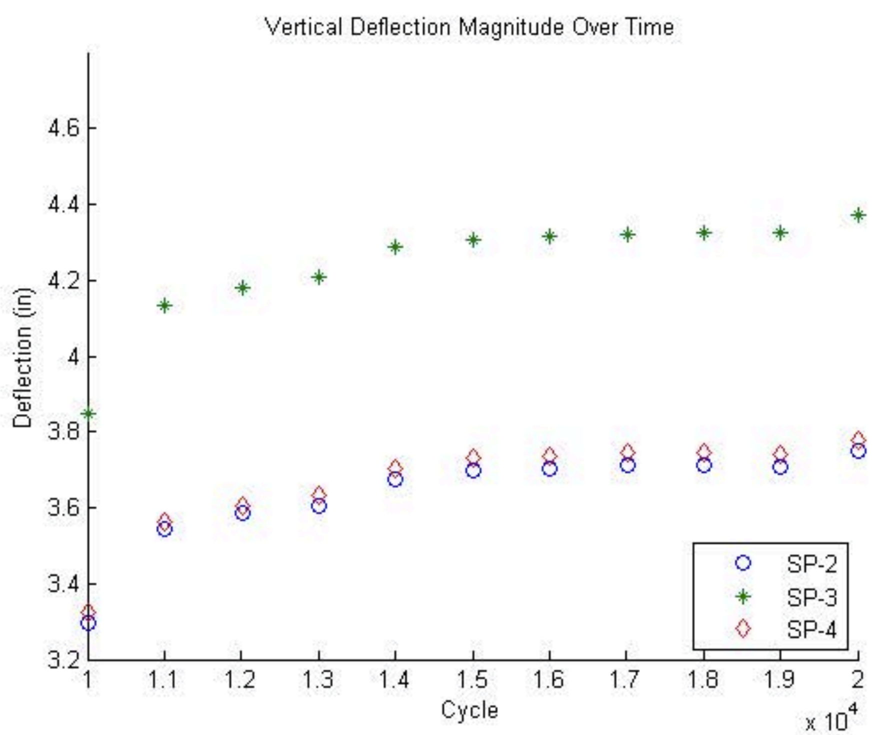

Test Results for Every 1,000 Cycles of Pile E – 4FB

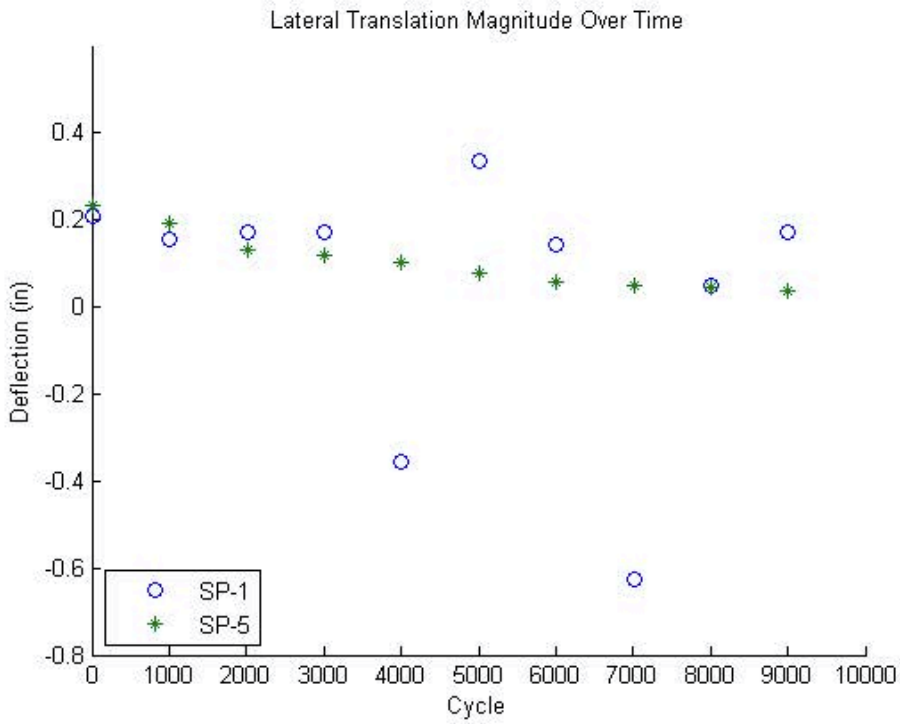

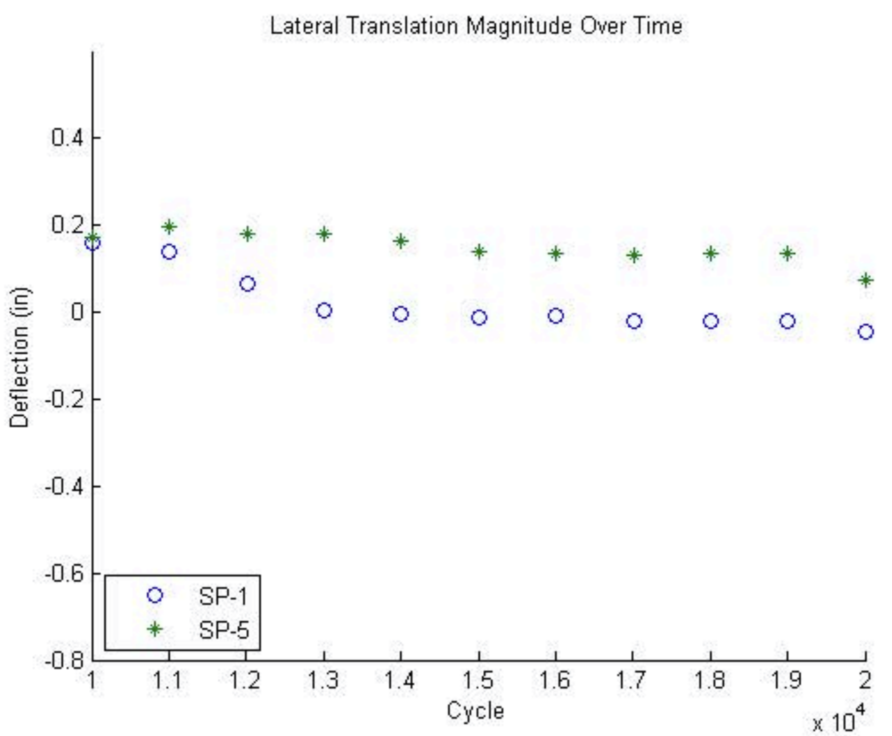

Test Results for Every 1,000 Cycles of Pile E – 4FB

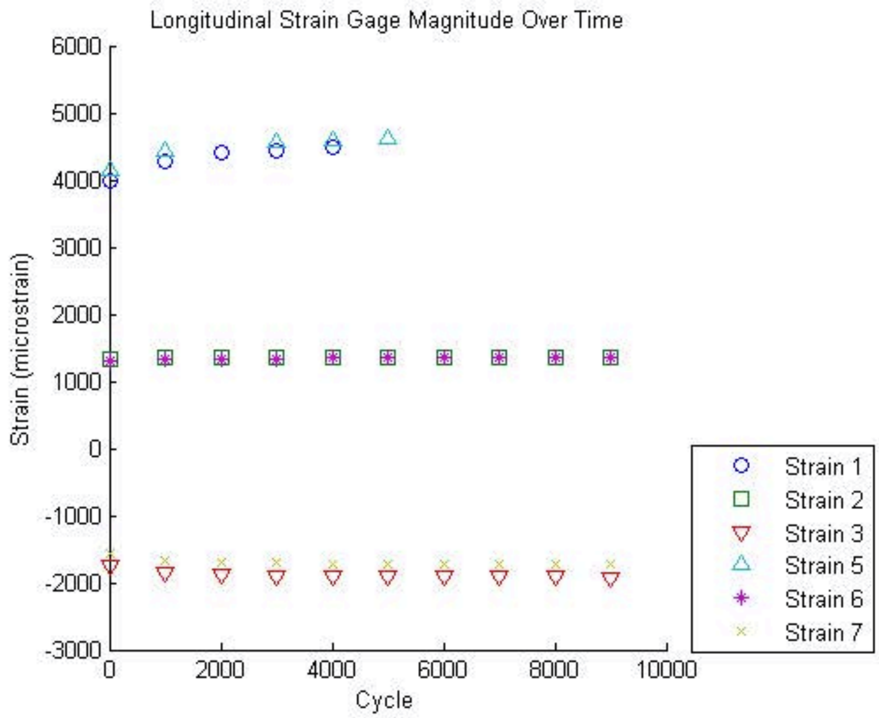

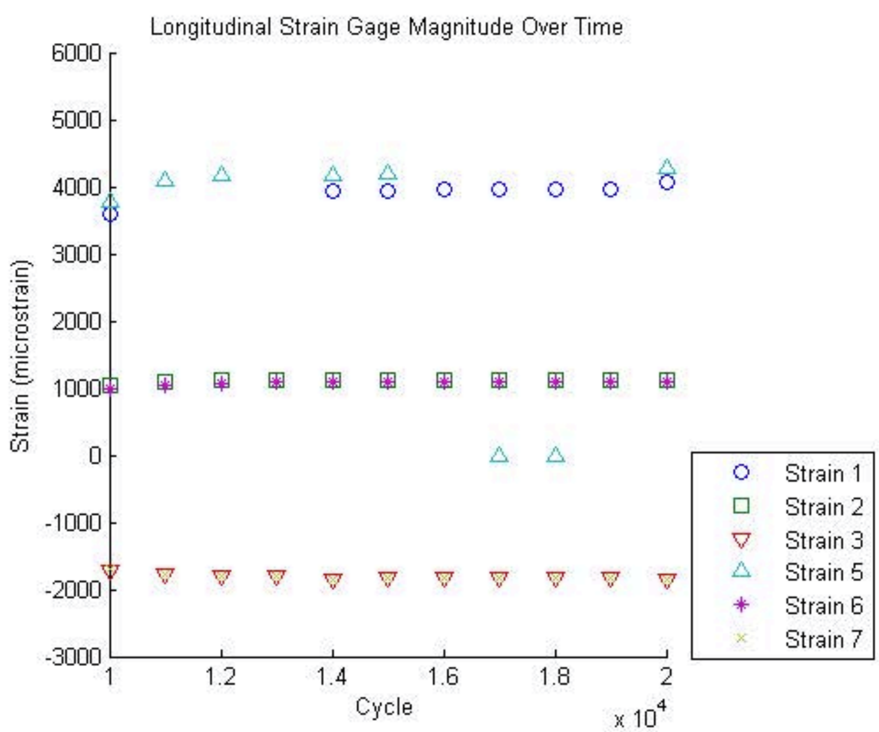

Test Results for Every 1,000 Cycles of Pile E – 4FB

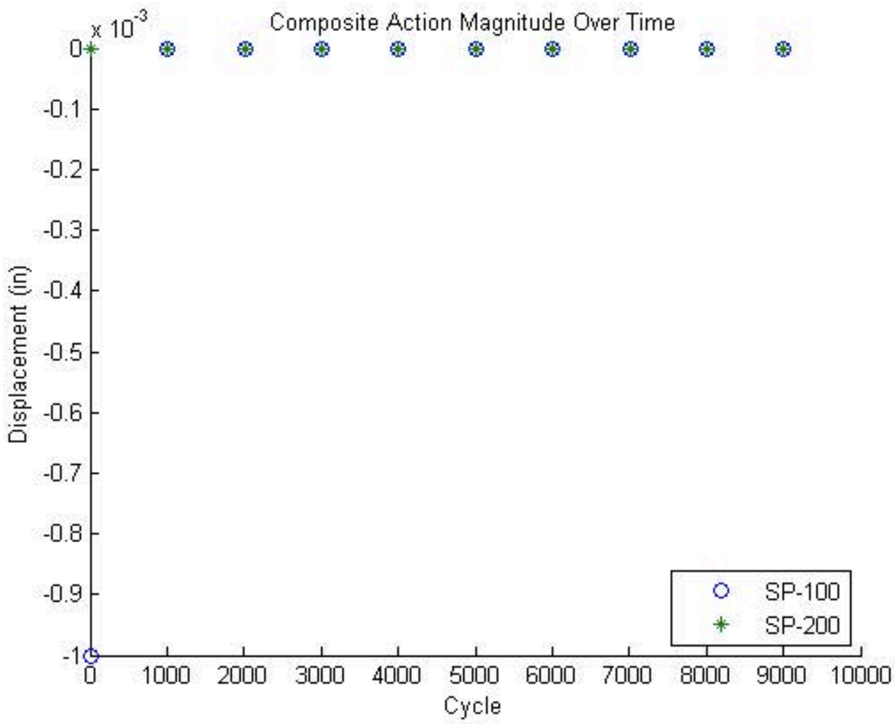

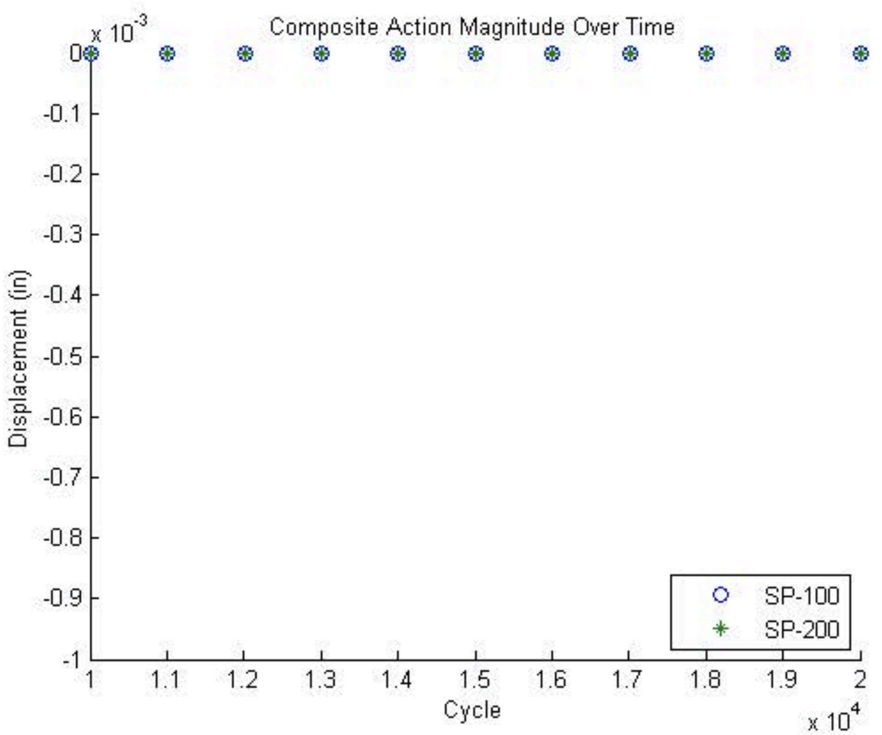

Test Results for Every 1,000 Cycles of Pile E – 4FB

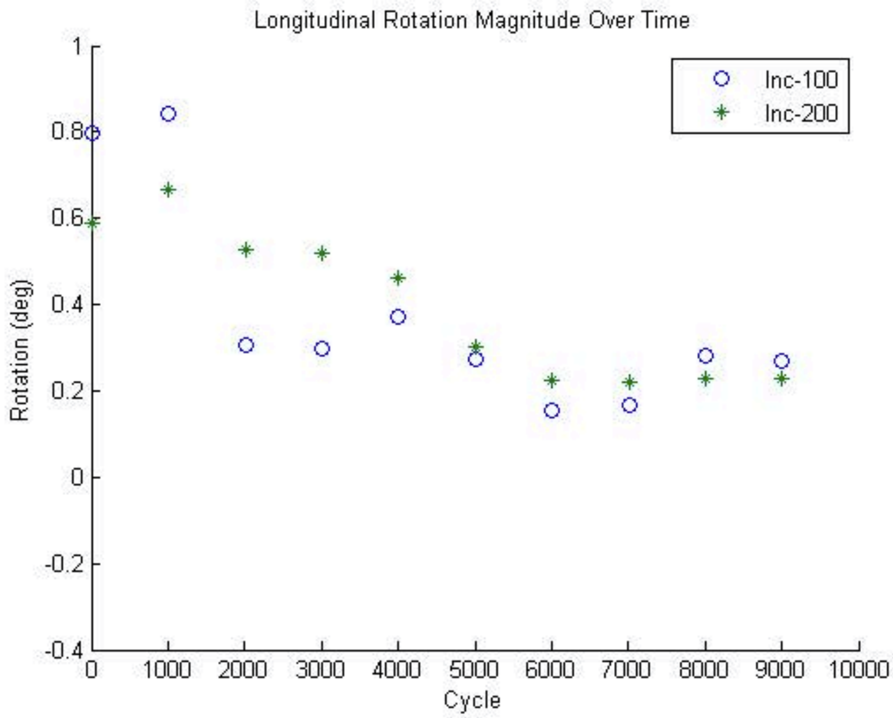

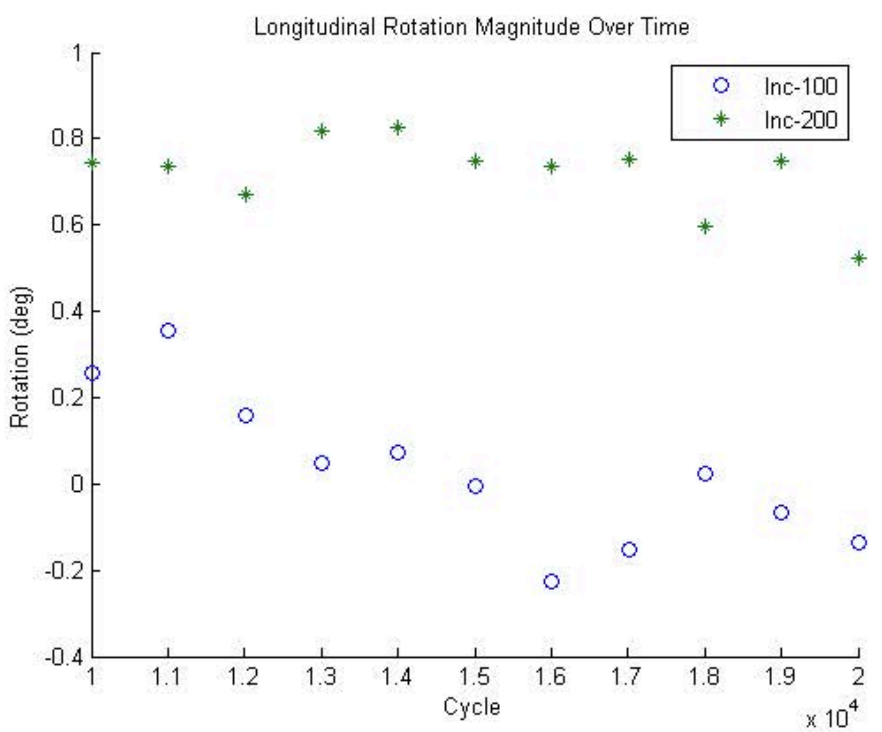

Test Results for Every 1,000 Cycles of Pile E – 4FB

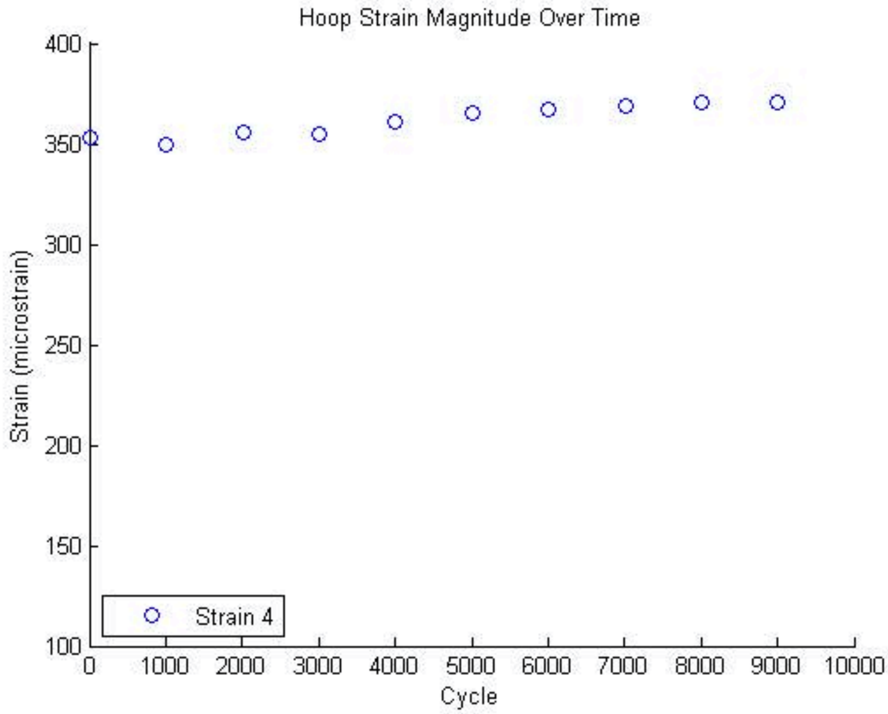

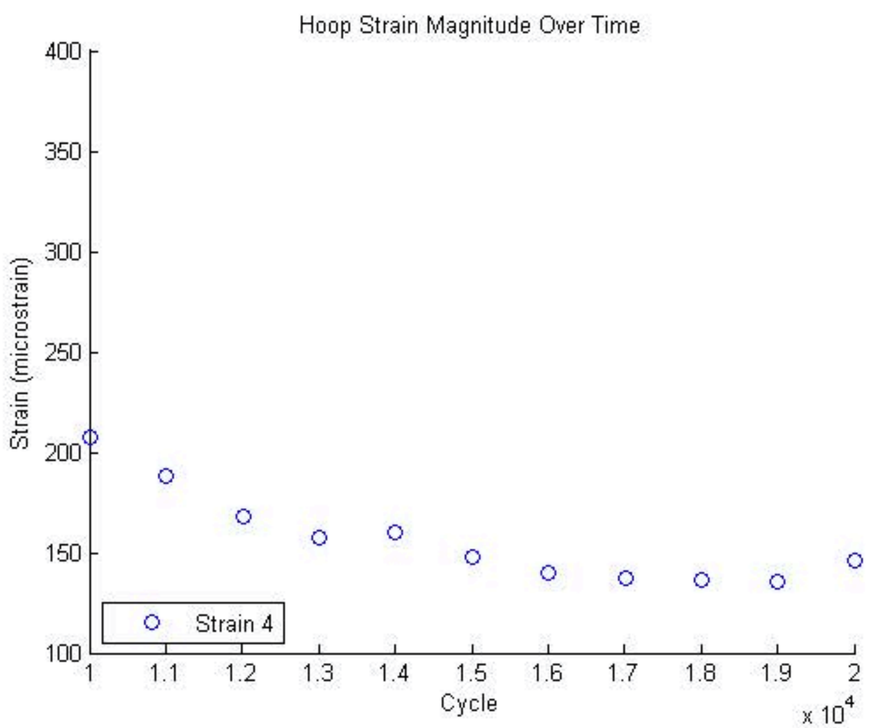

Appendix J: Test Results for Initial Loading Pile F – 4FB

Test Results for Initial Loading Pile F – 4FB

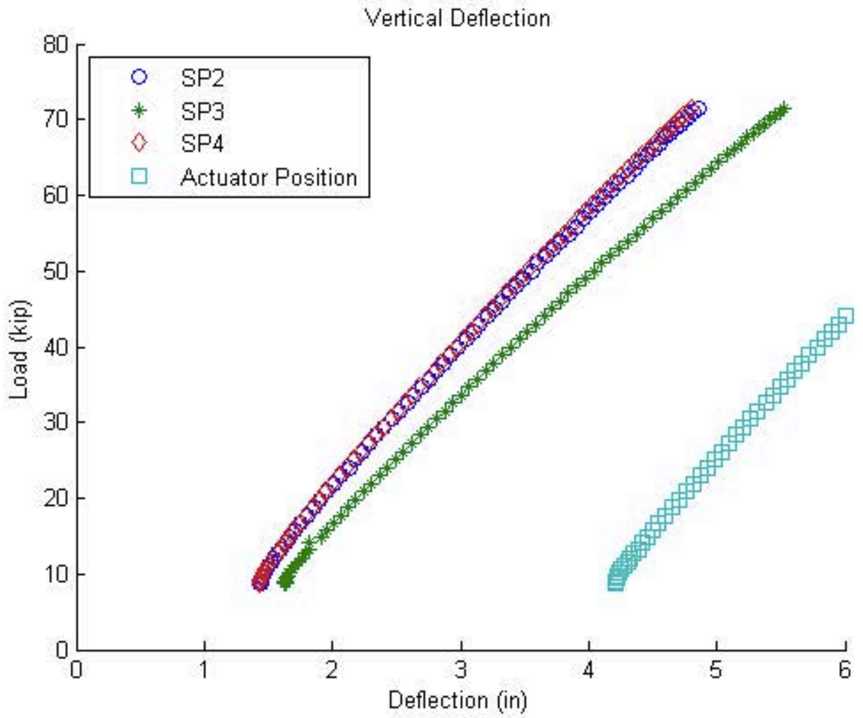

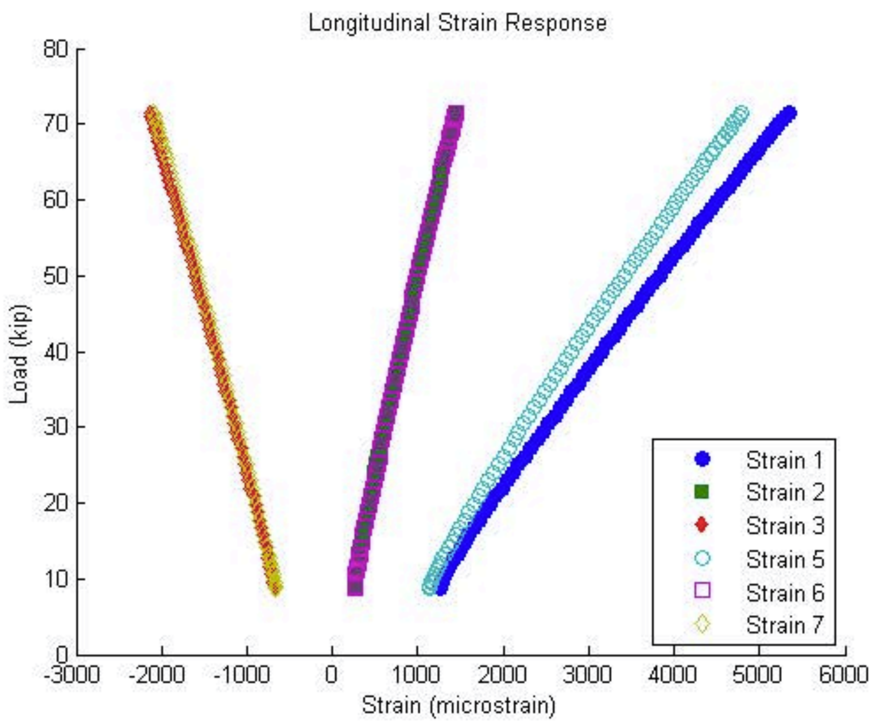

Test Results for Initial Loading Pile F – 4FB

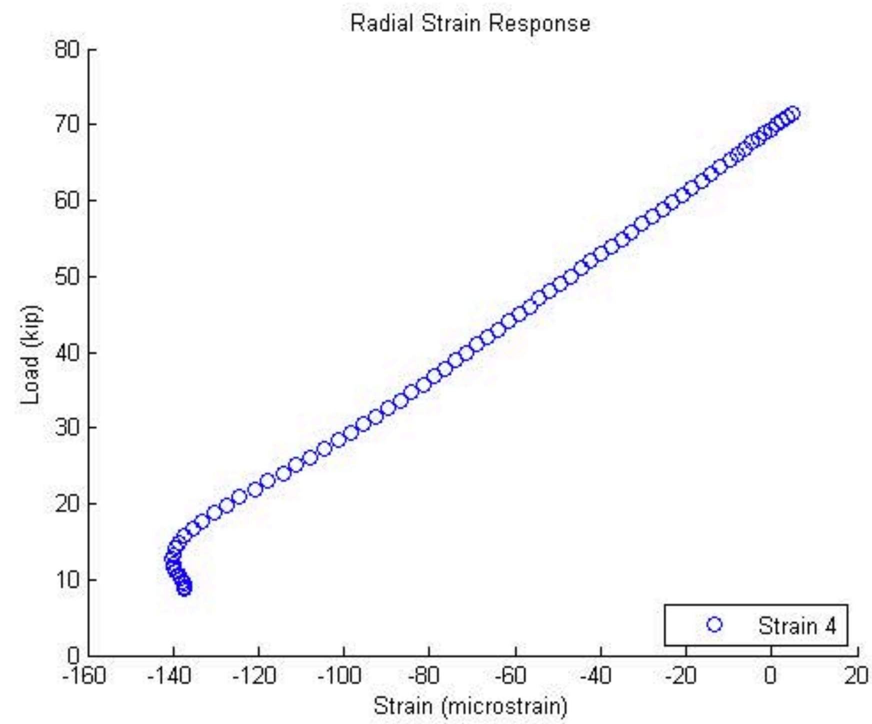

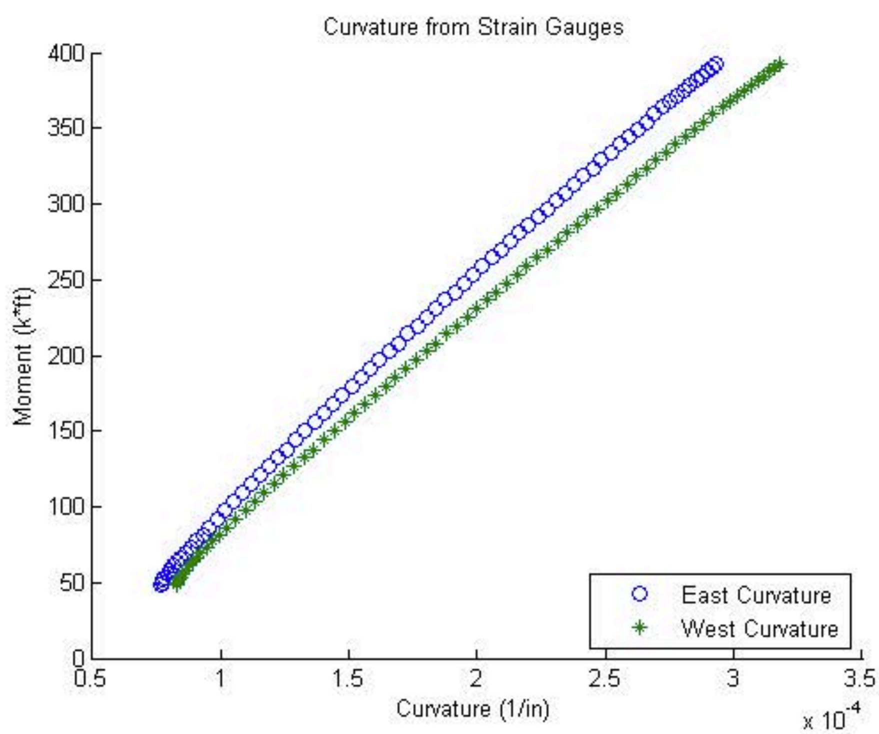

Test Results for Initial Loading Pile F – 4FB

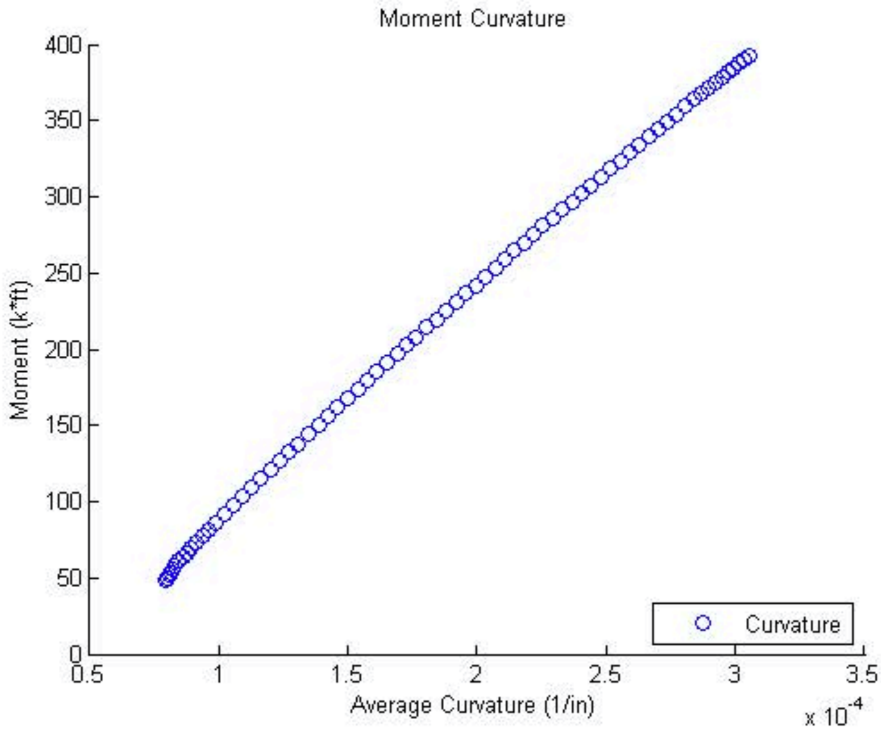

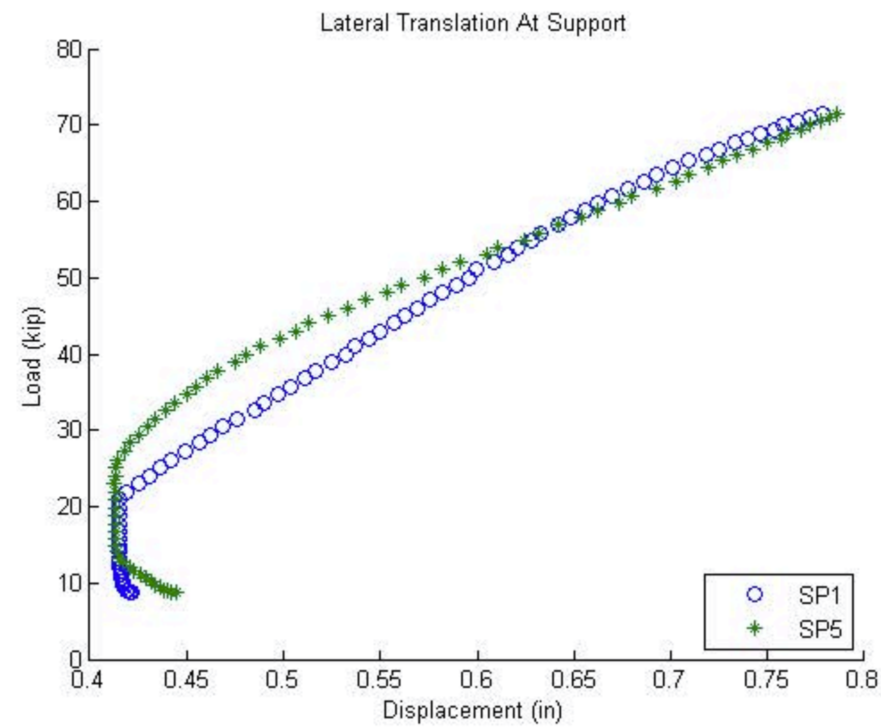

Test Results for Initial Loading Pile F – 4FB

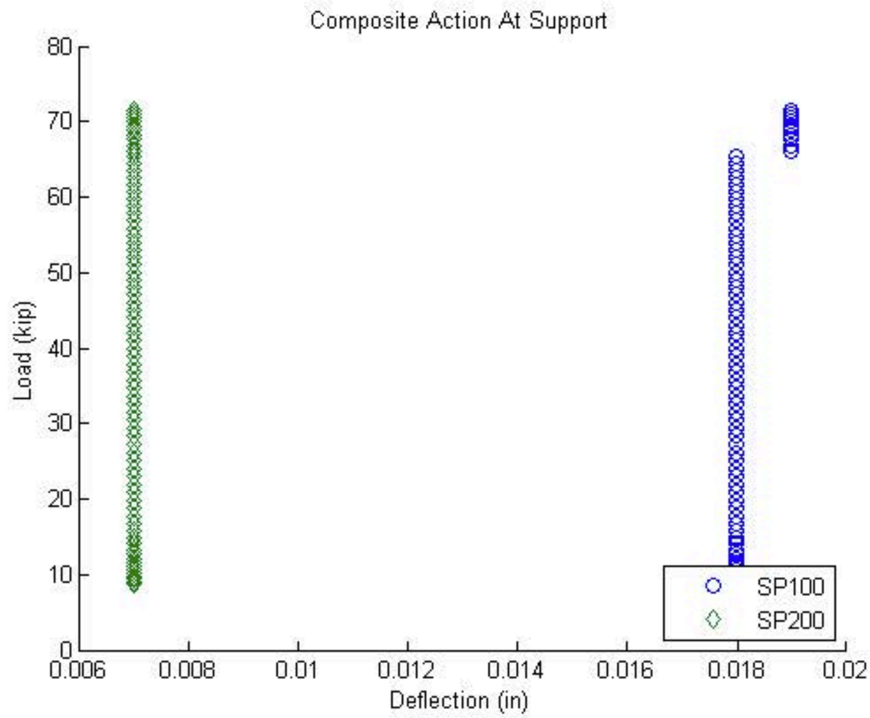

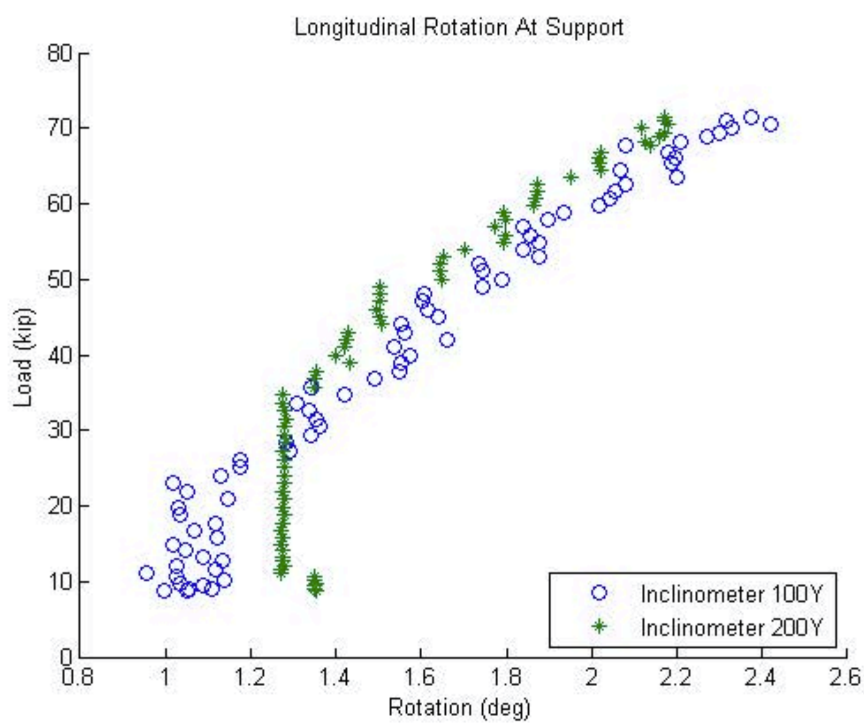

Test Results for Initial Loading Pile F – 4FB

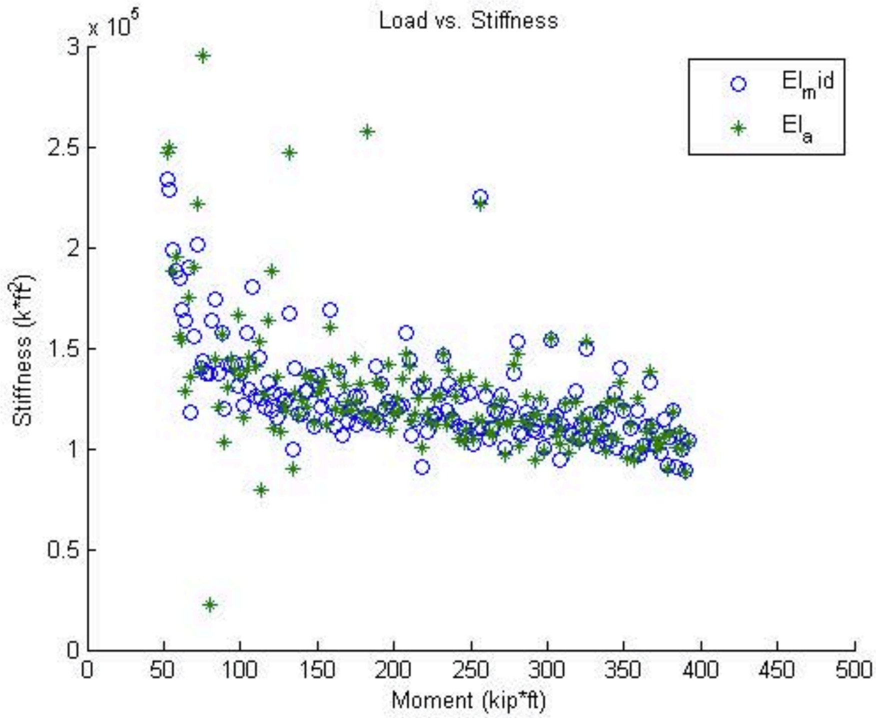

Appendix K: Test Results for Ultimate Loading of Pile F - 4FB

Test Results for Ultimate Loading of Pile F - 4FB

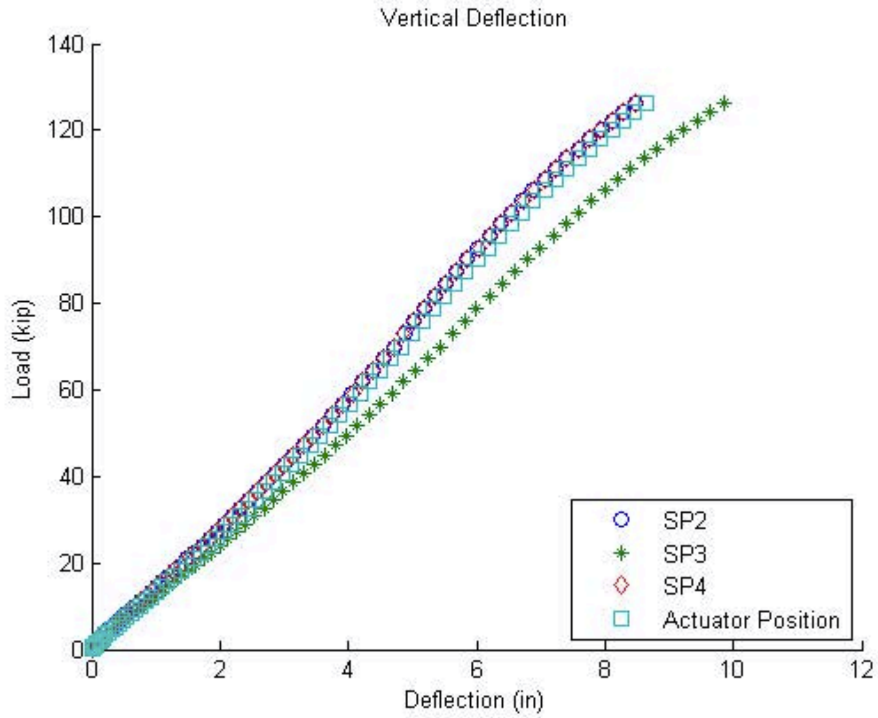

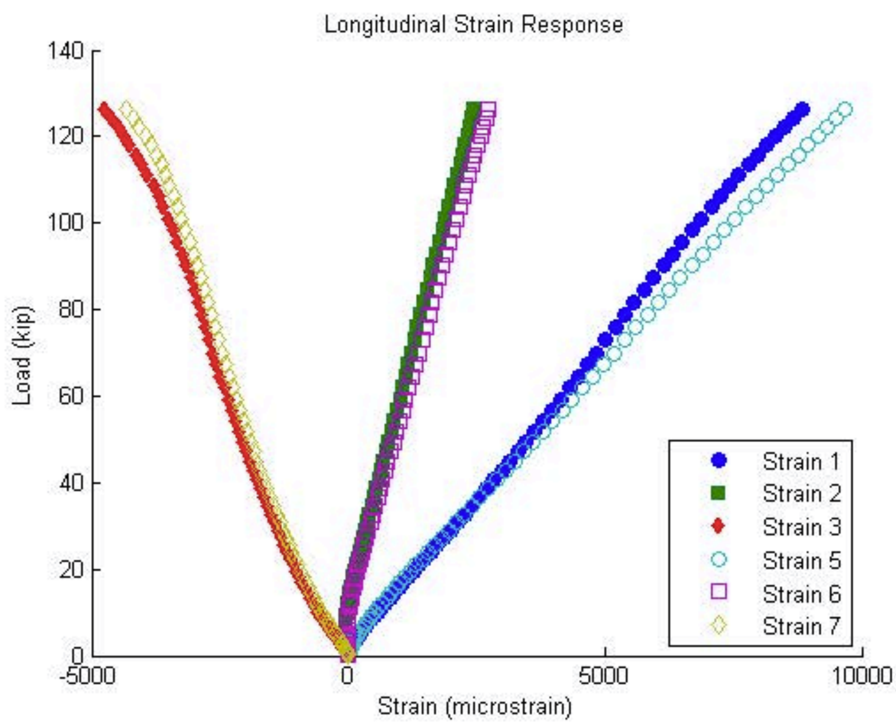

Test Results for Ultimate Loading of Pile F - 4FB

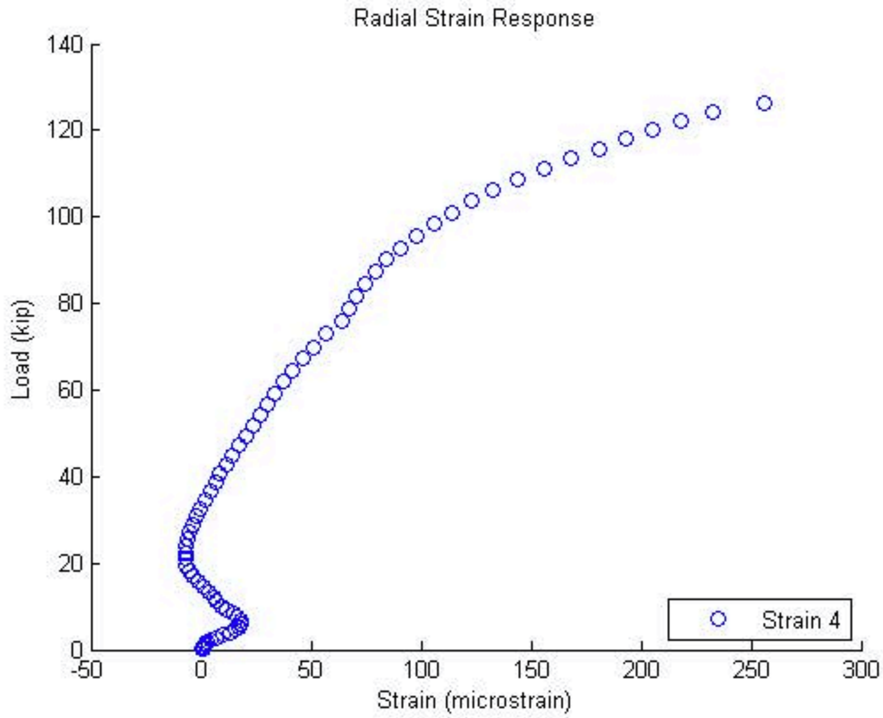

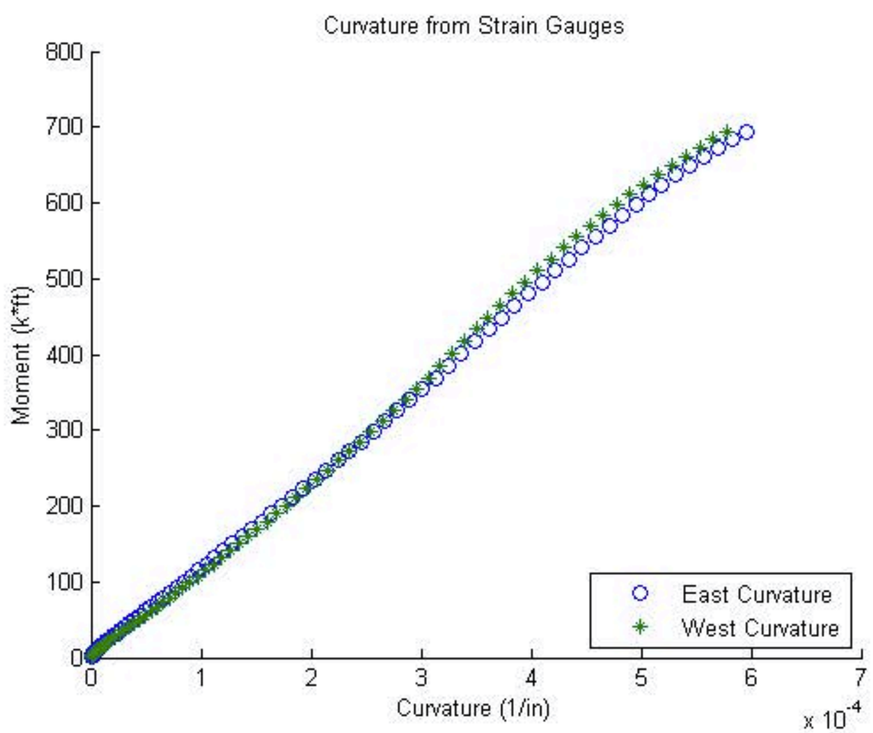

Test Results for Ultimate Loading of Pile F - 4FB

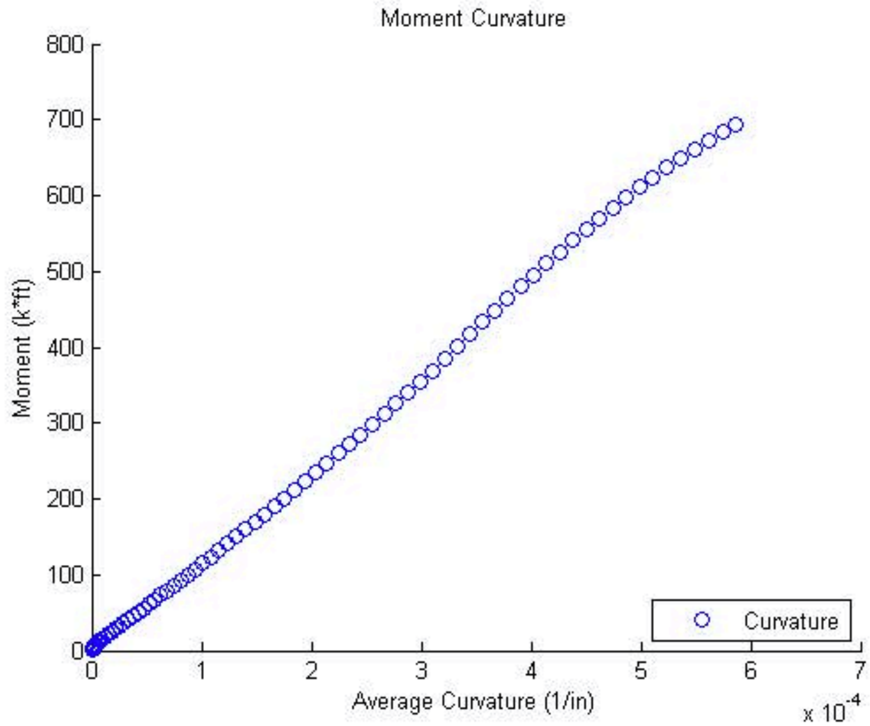

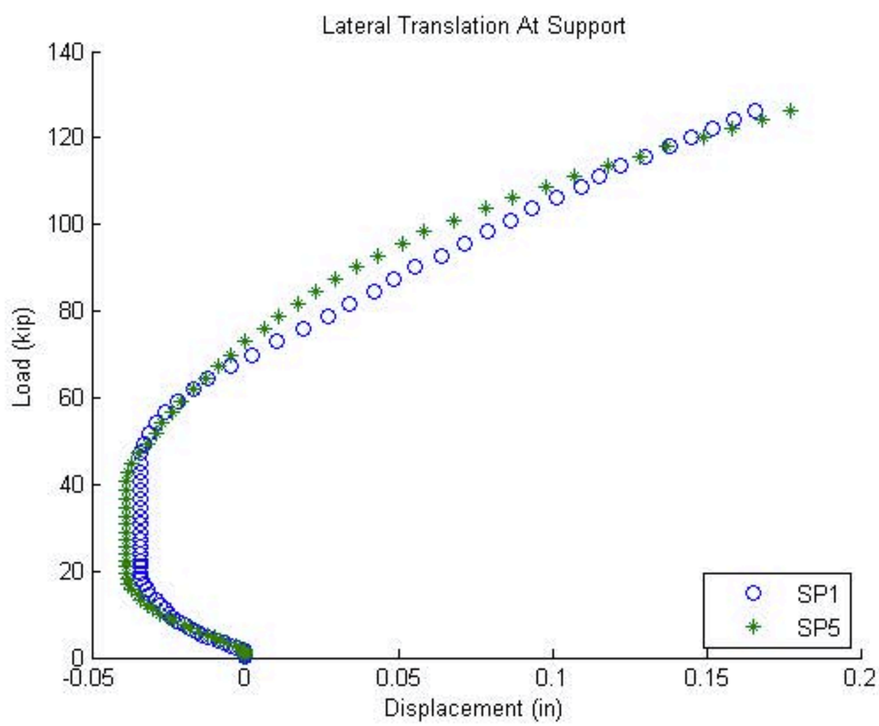

Test Results for Ultimate Loading of Pile F - 4FB

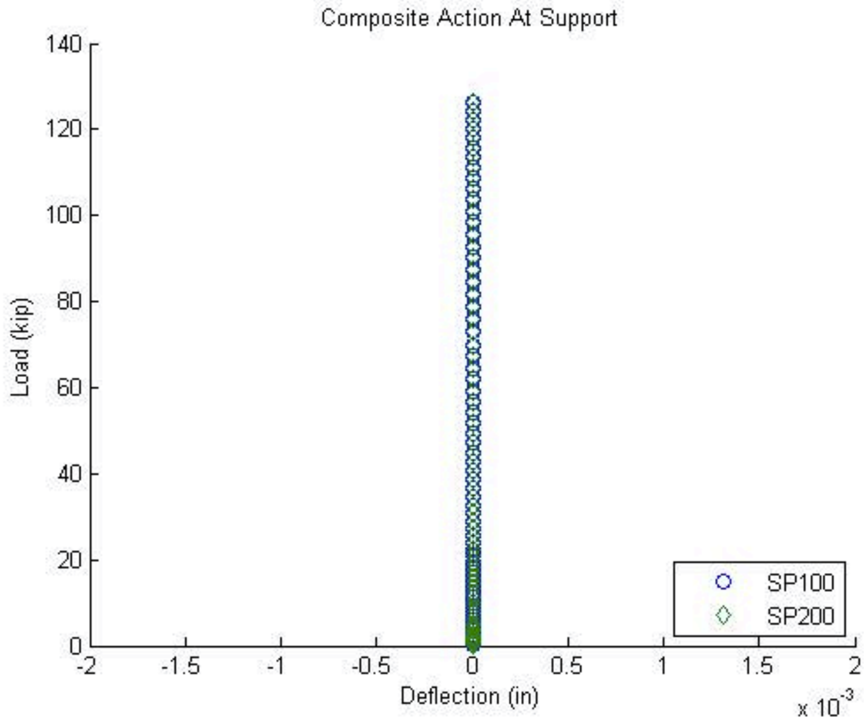

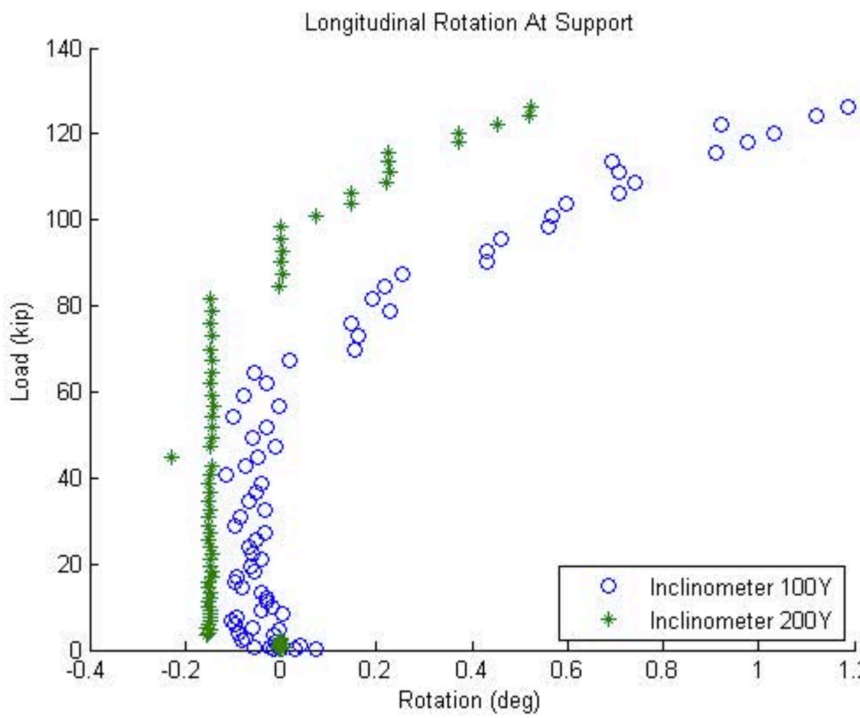

Test Results for Ultimate Loading of Pile F - 4FB

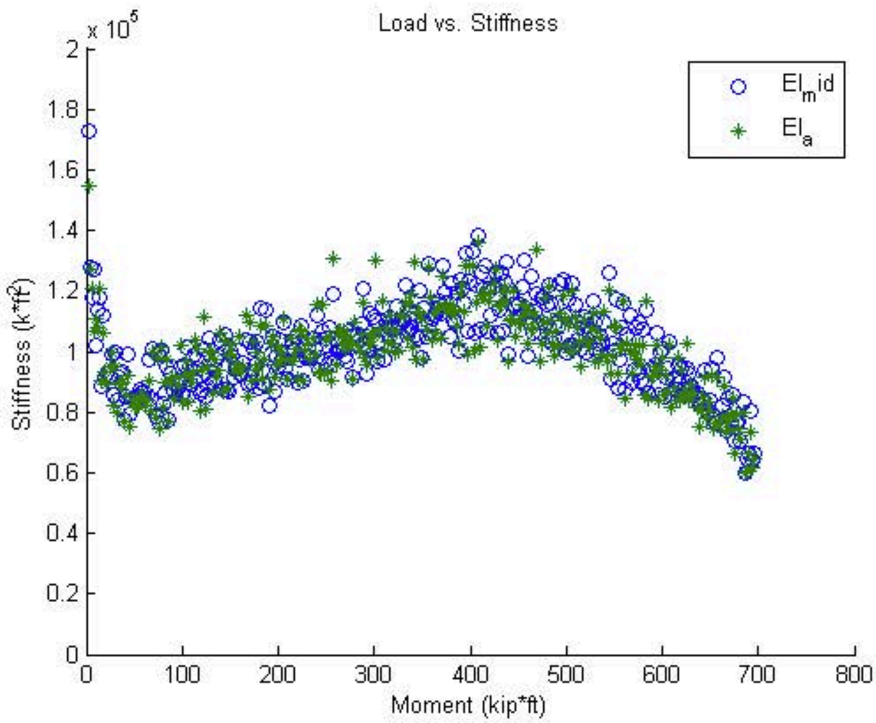

Appendix L: Test Results for First 10 Cycles of Pile F – 4FB

Test Results for First 10 Cycles of Pile F – 4FB

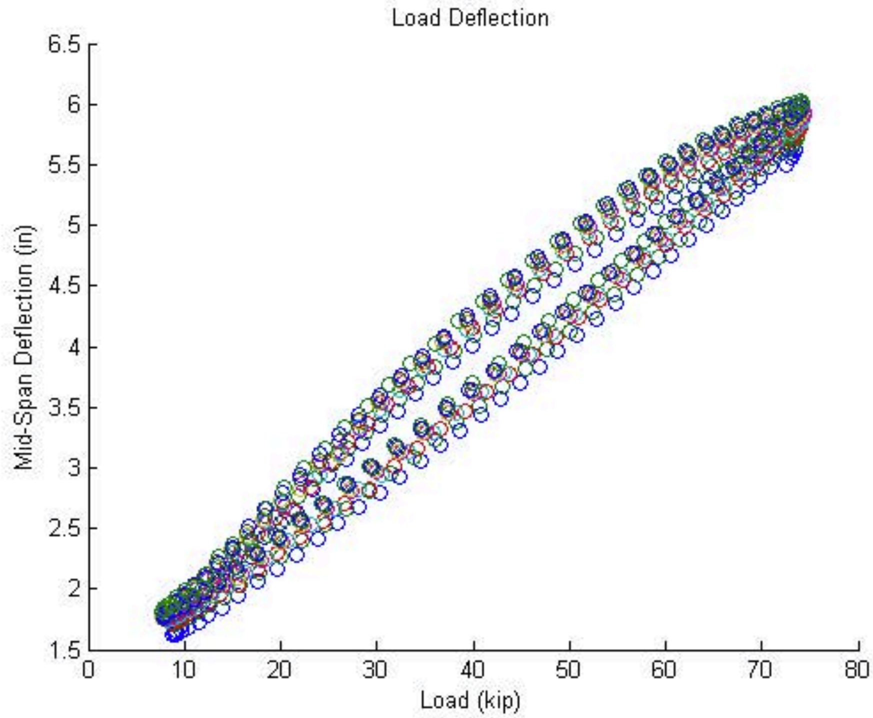

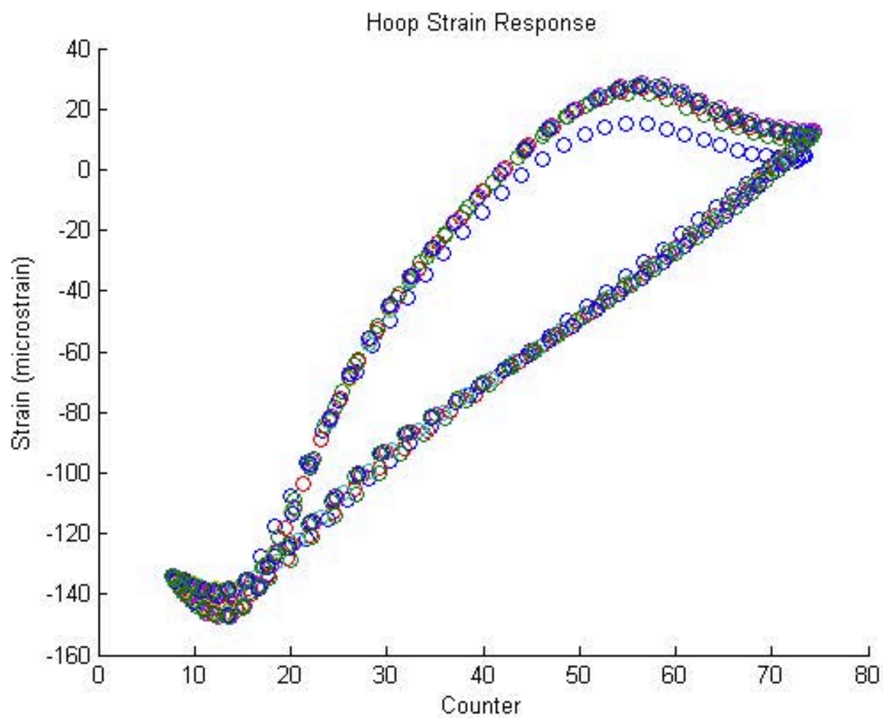

Test Results for First 10 Cycles of Pile F – 4FB

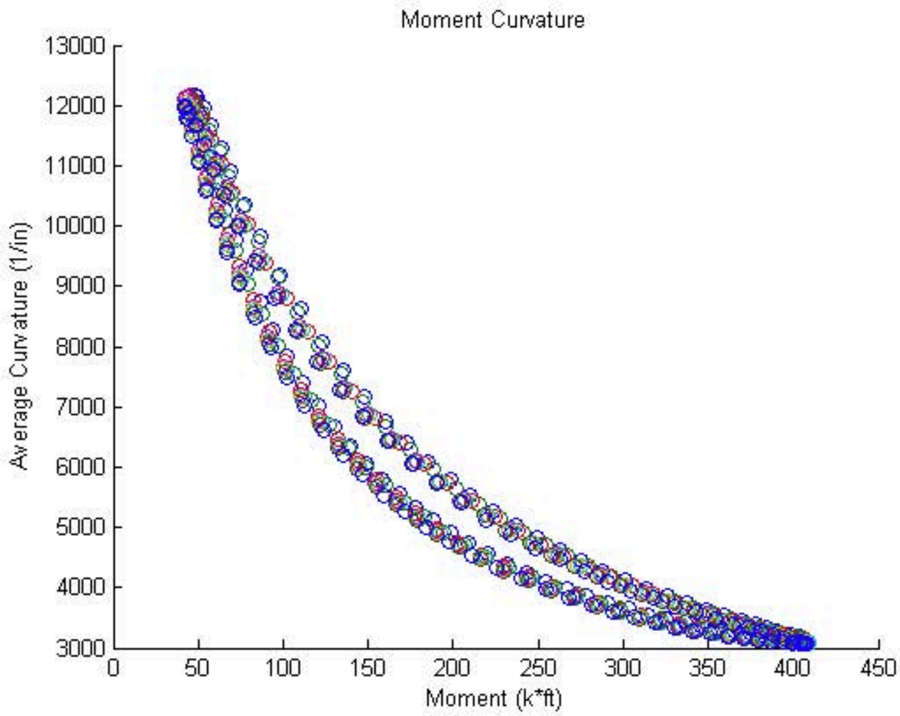

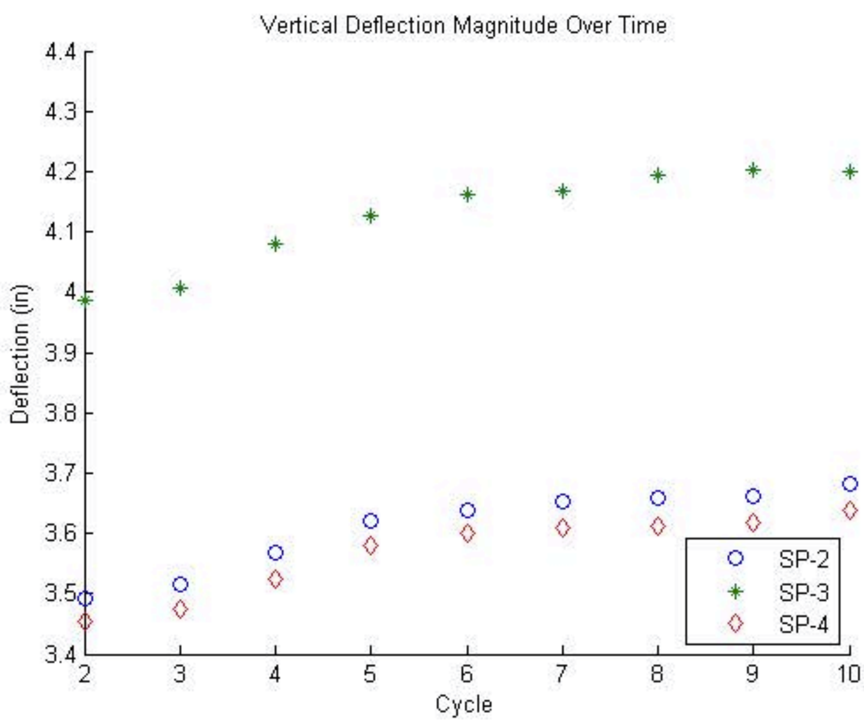

Test Results for First 10 Cycles of Pile F – 4FB

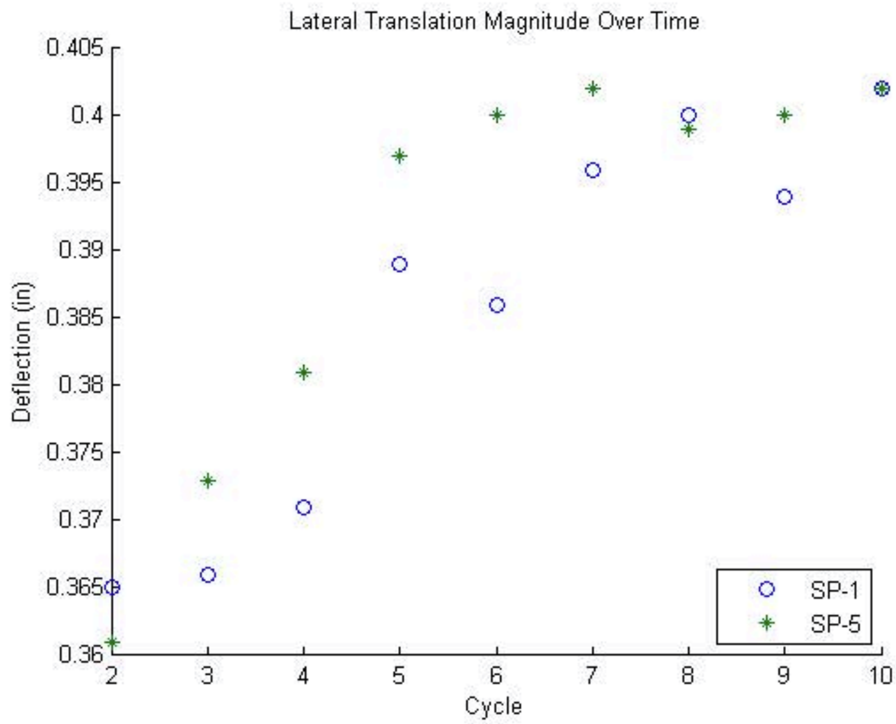

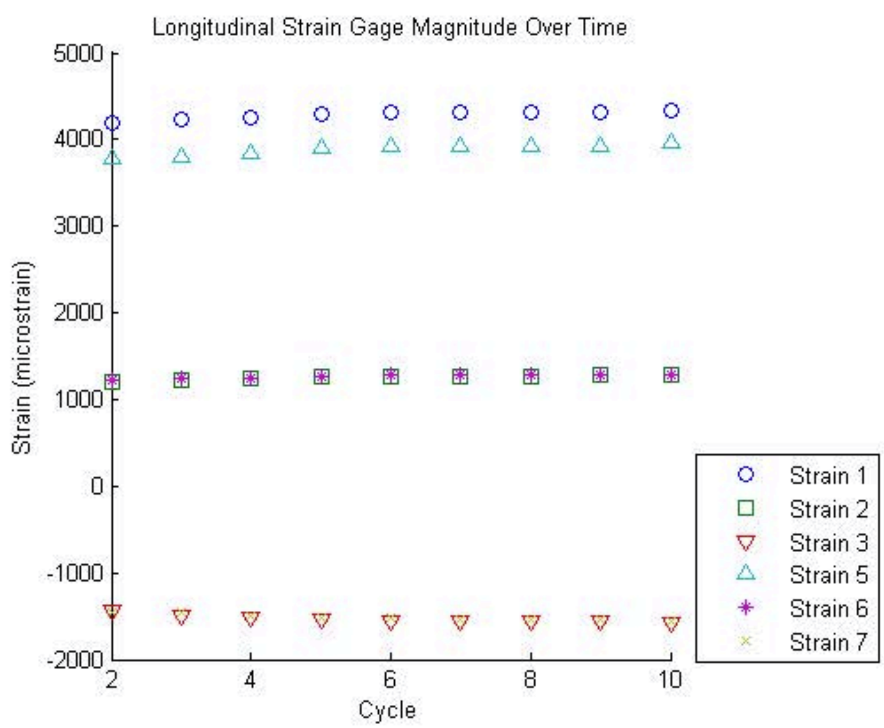

Test Results for First 10 Cycles of Pile F – 4FB

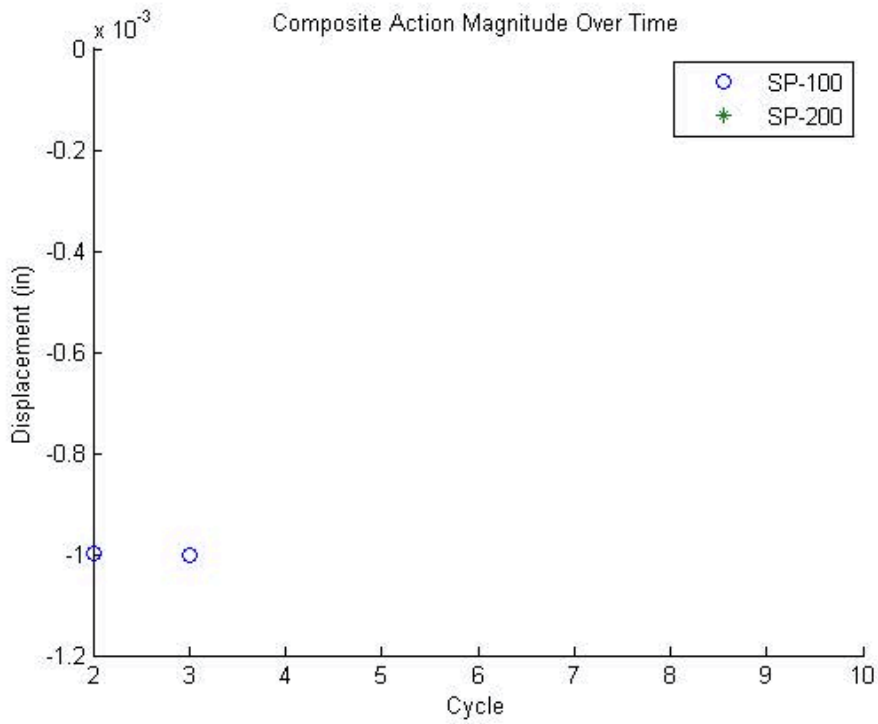

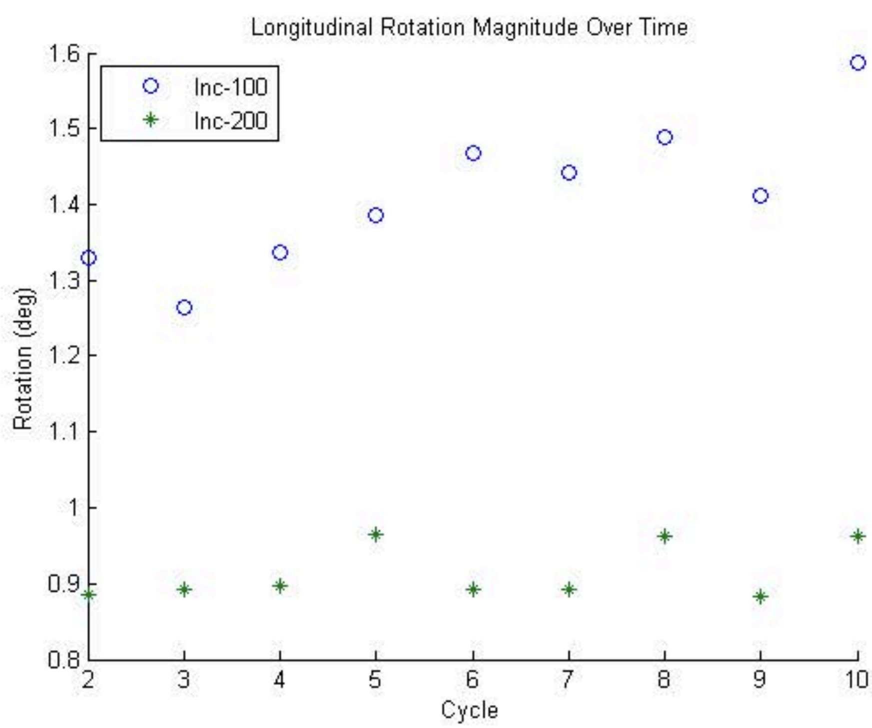

Test Results for First 10 Cycles of Pile F – 4FB

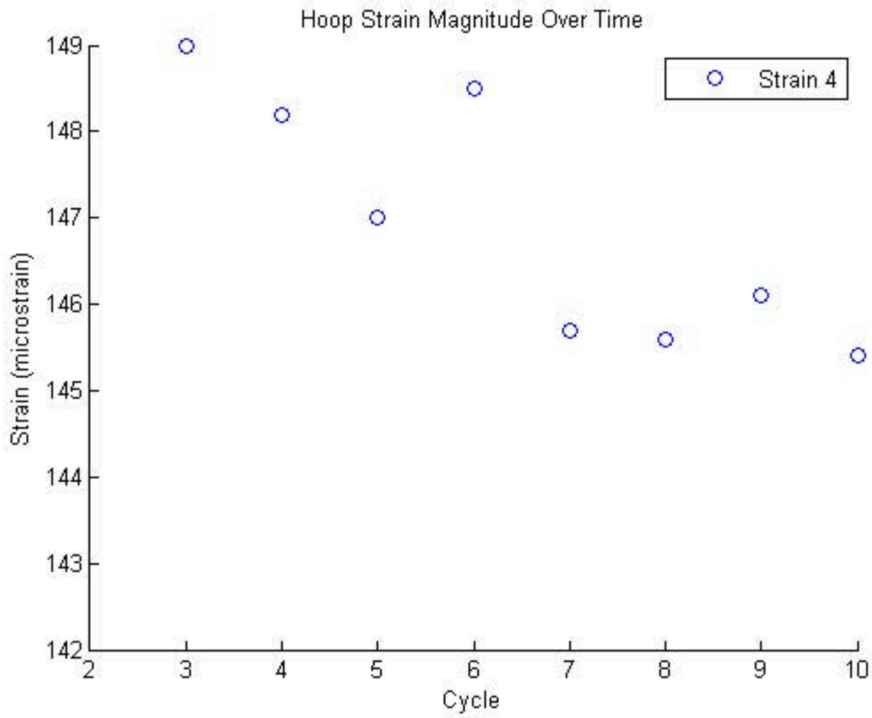

Appendix M: Test Results for Every 1,000 Cycles of Pile F – 4FB

Test Results for Every 1,000 Cycles of Pile F – 4FB

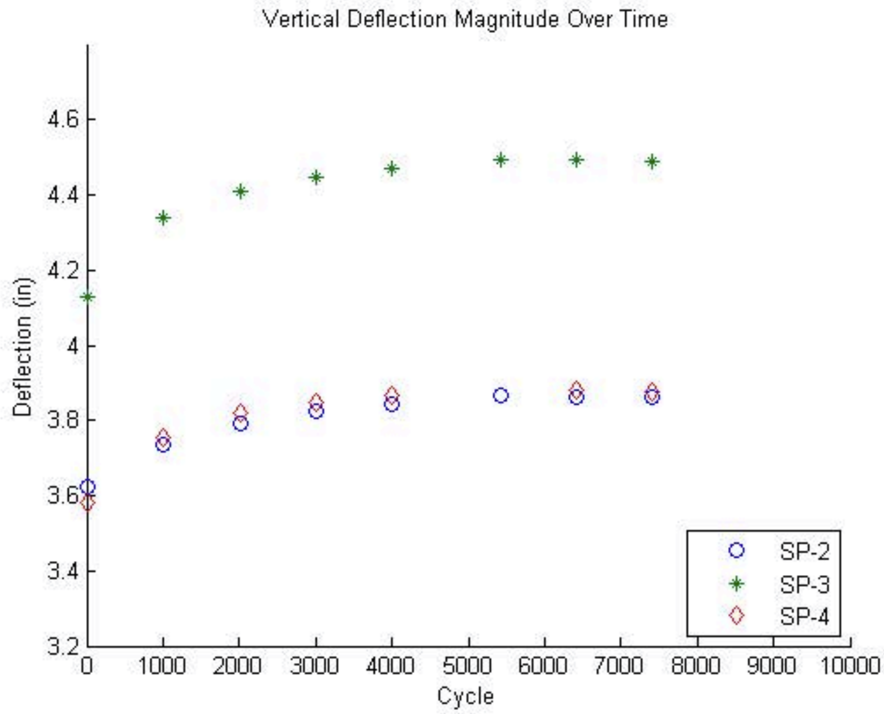

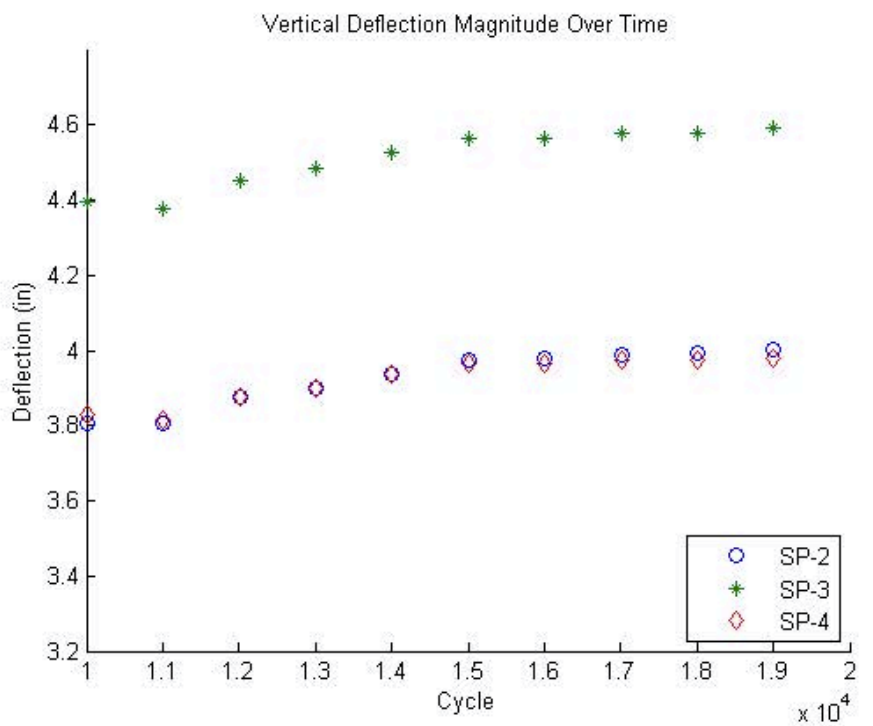

Test Results for Every 1,000 Cycles of Pile F – 4FB

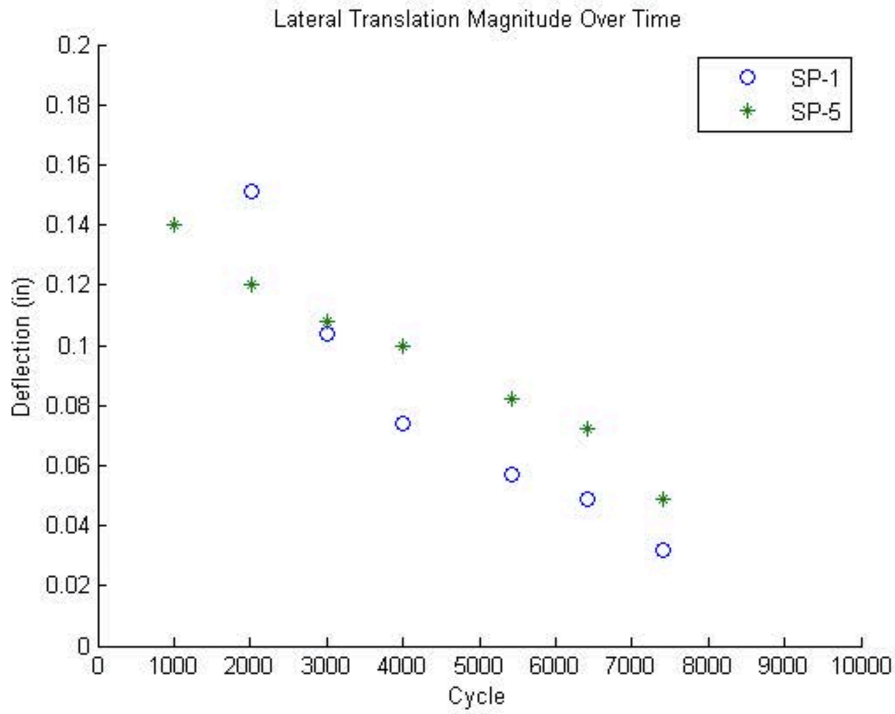

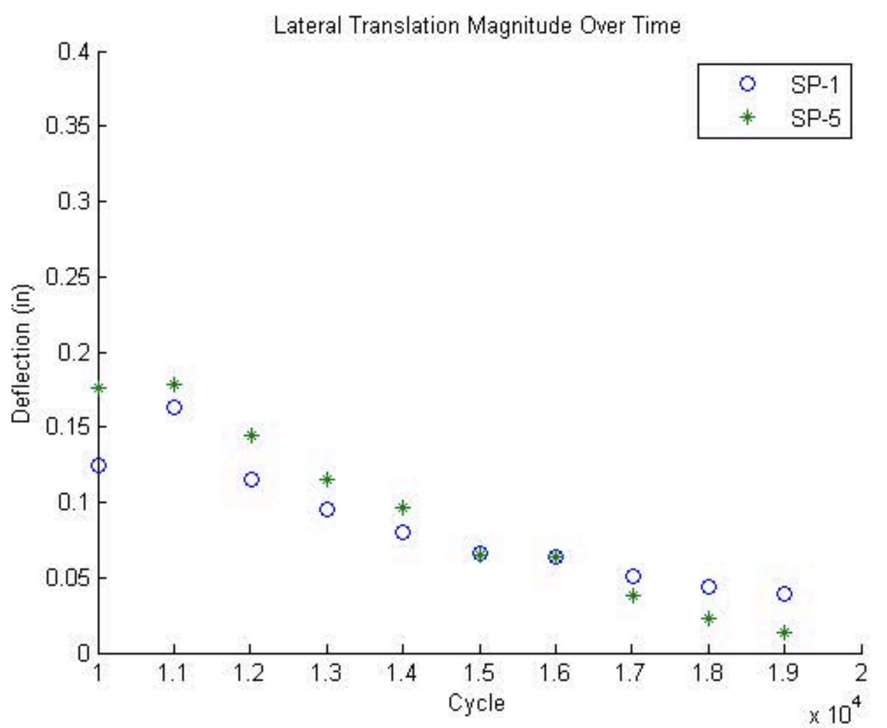

Test Results for Every 1,000 Cycles of Pile F – 4FB

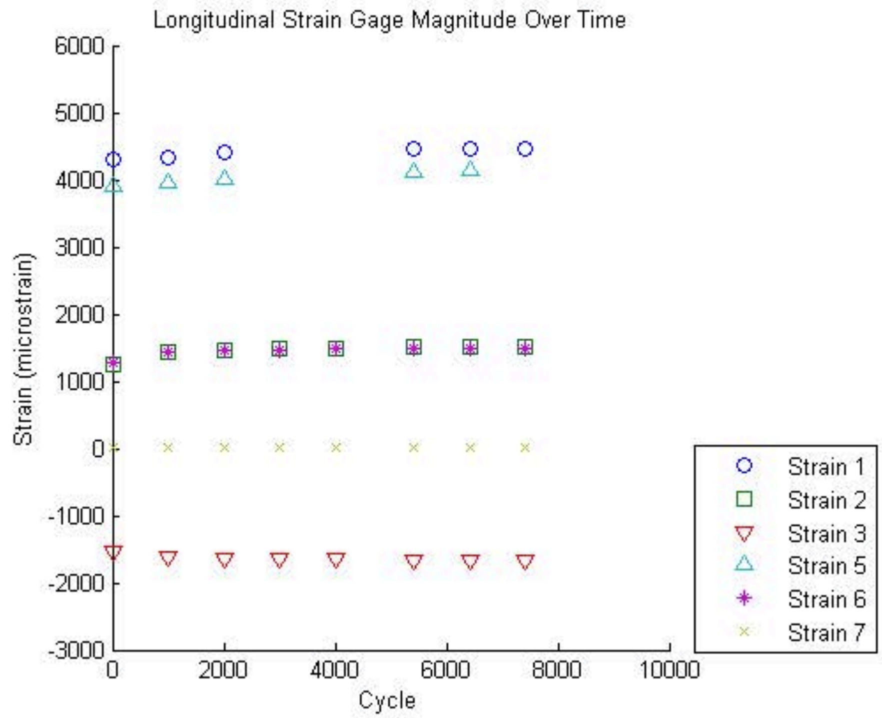

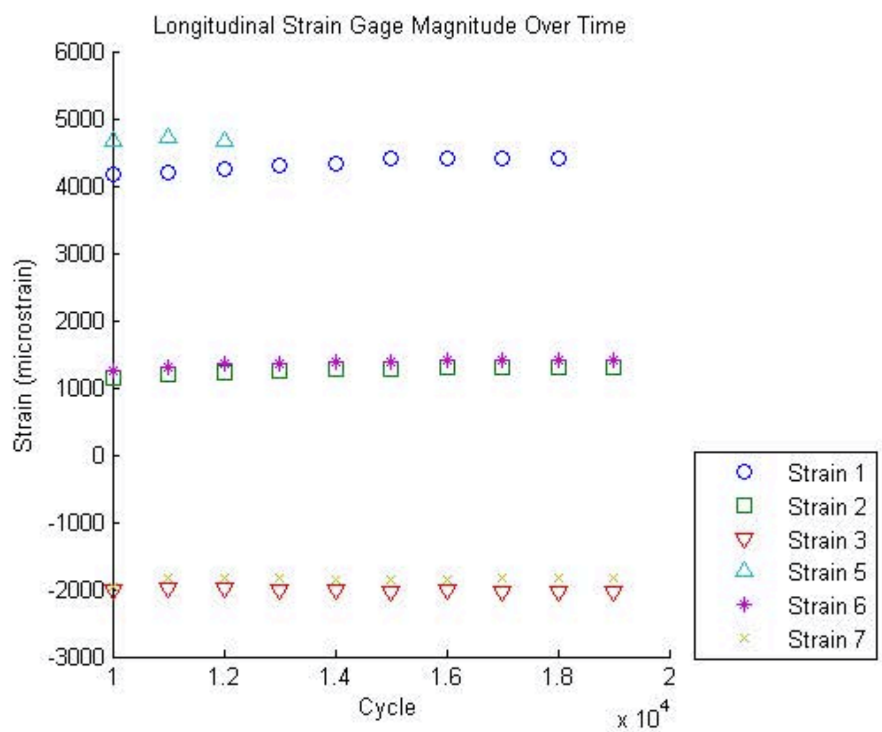

Test Results for Every 1,000 Cycles of Pile F – 4FB

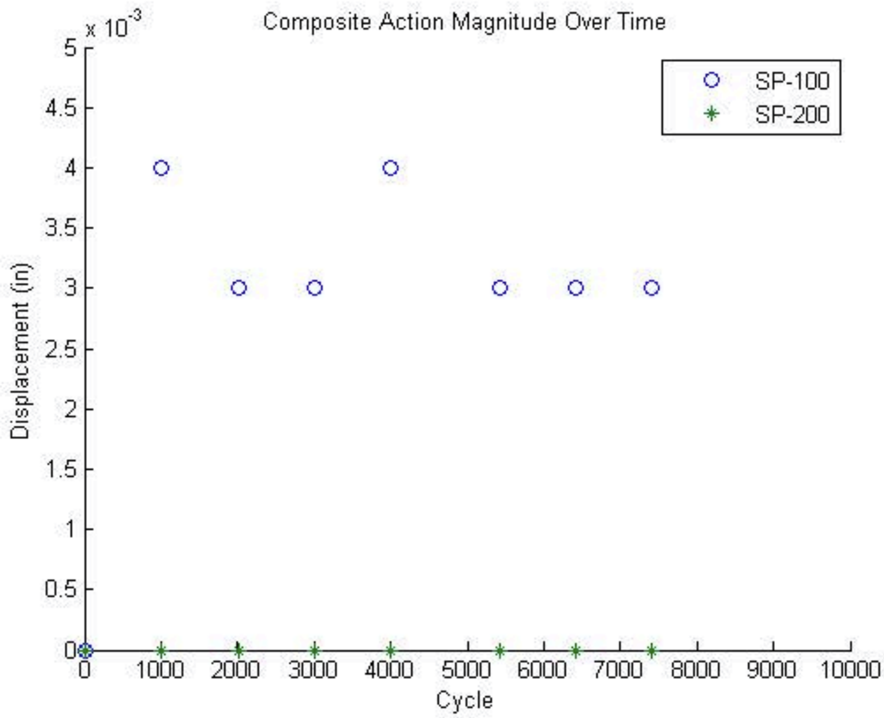

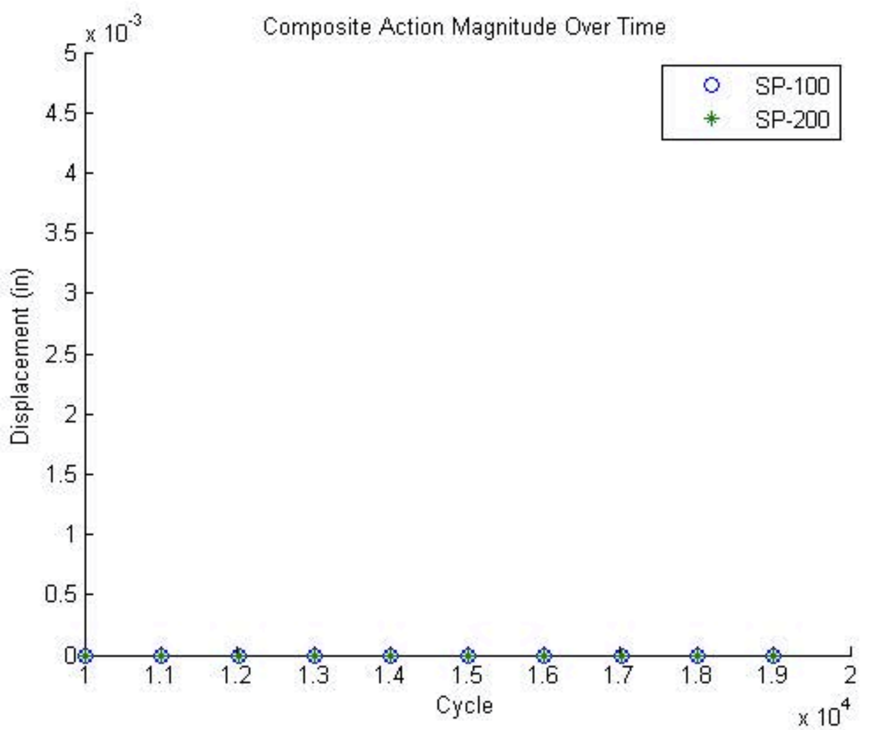

Test Results for Every 1,000 Cycles of Pile F – 4FB

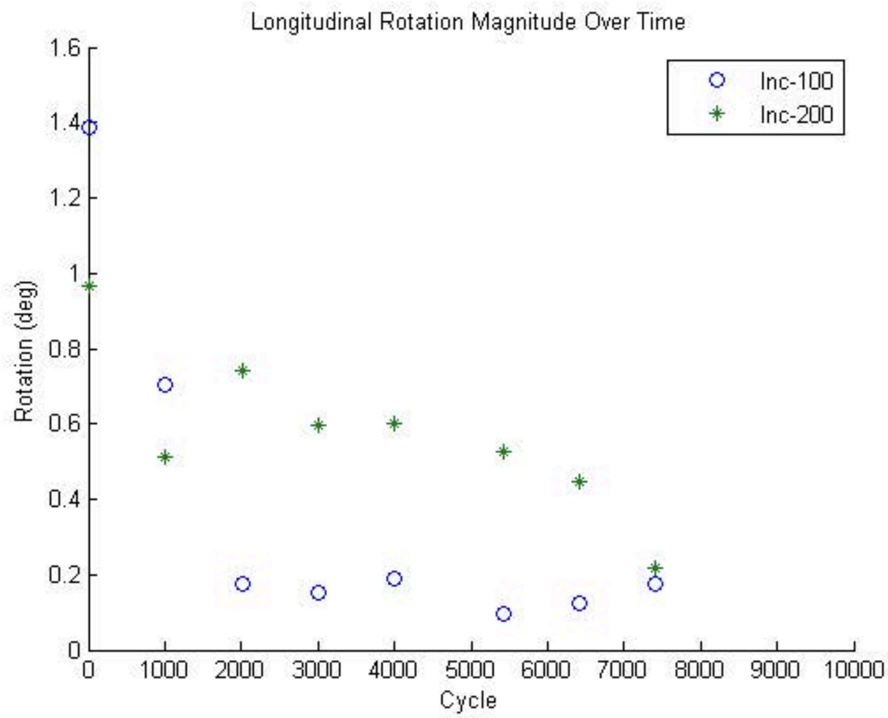

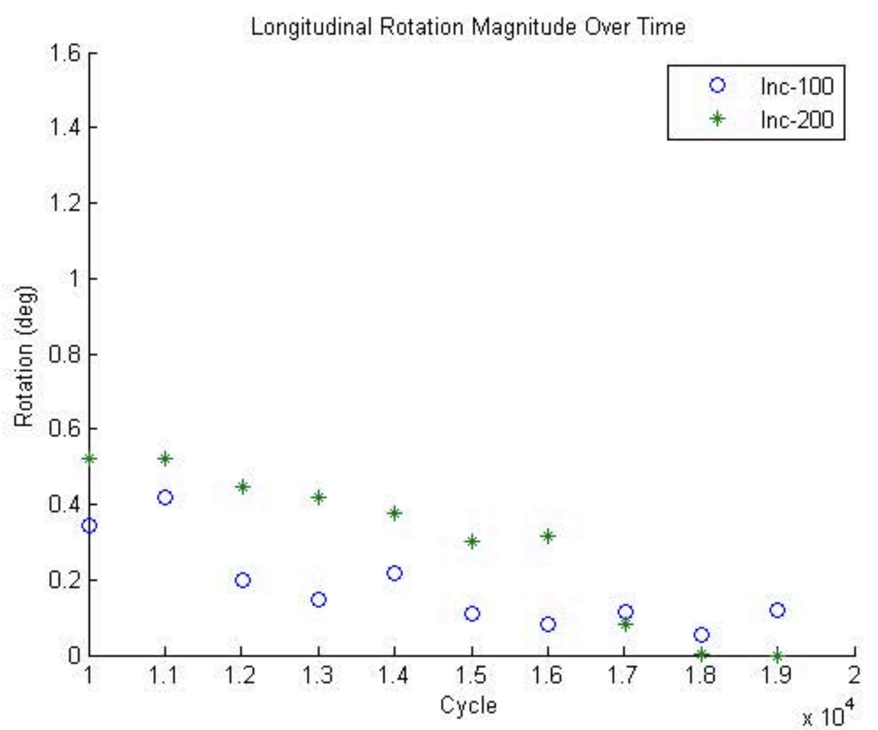

Test Results for Every 1,000 Cycles of Pile F – 4FB

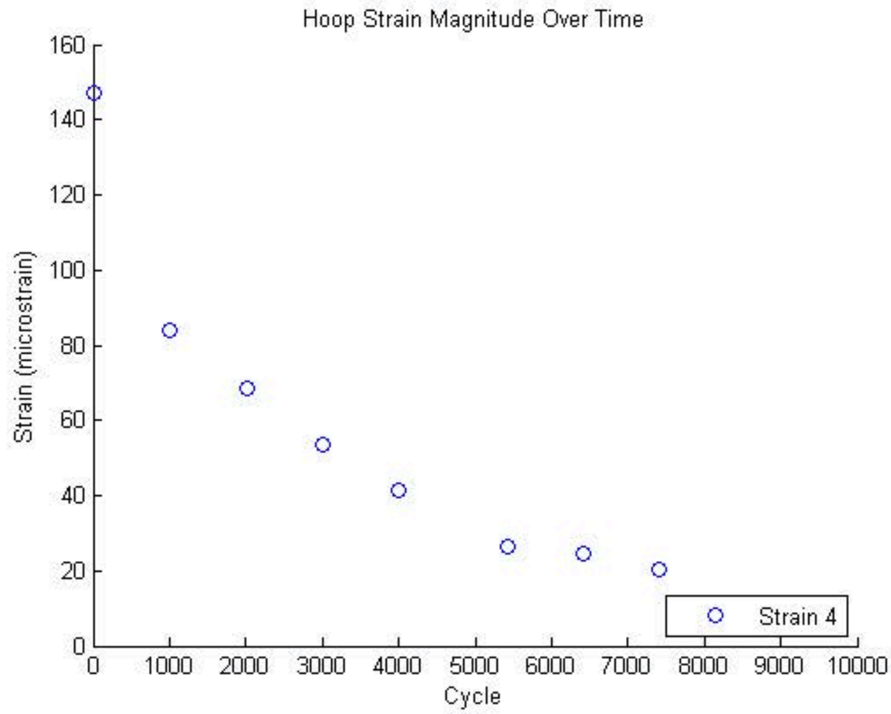

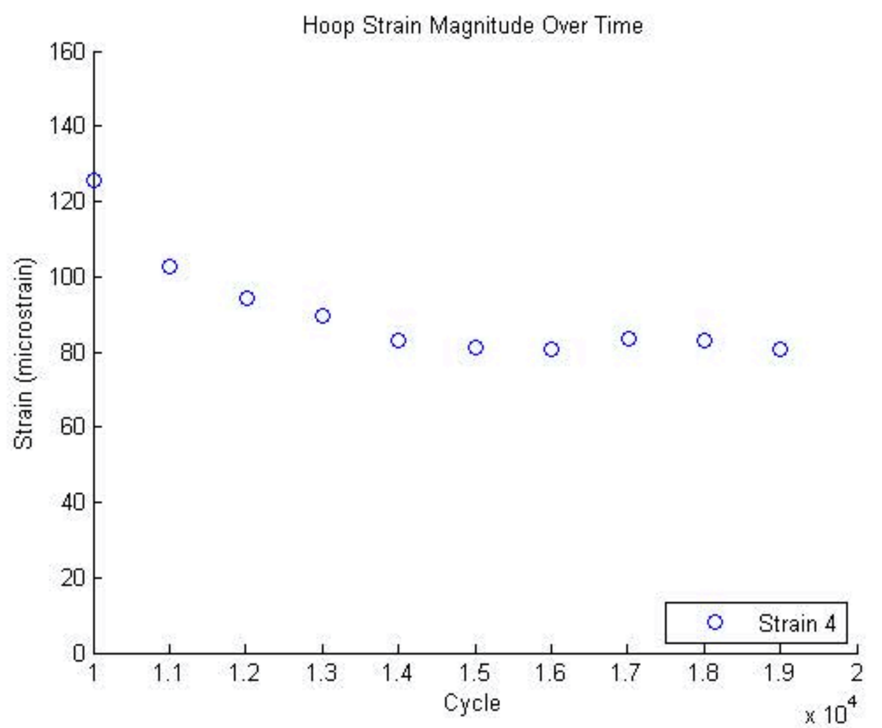

Appendix N: Test Results for Pile G – 4FB

Test Results for Pile G – 4FB

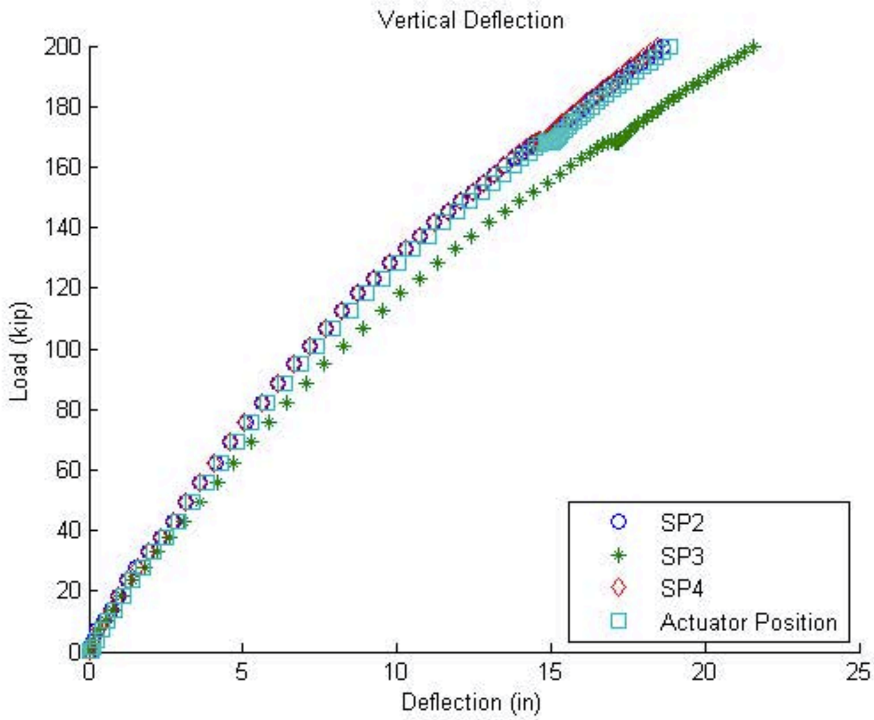

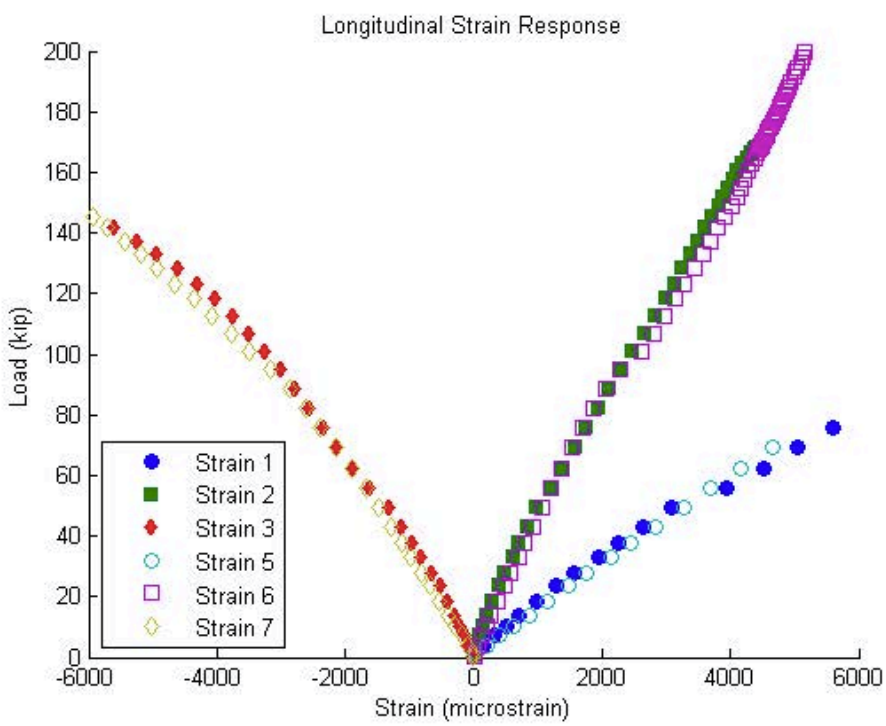

Test Results for Pile G – 4FB

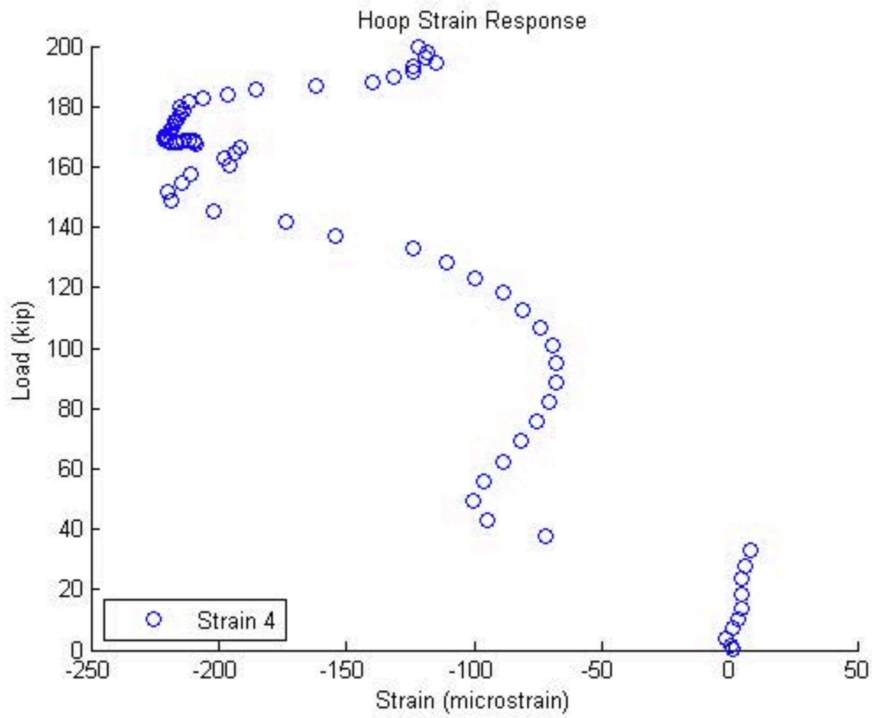

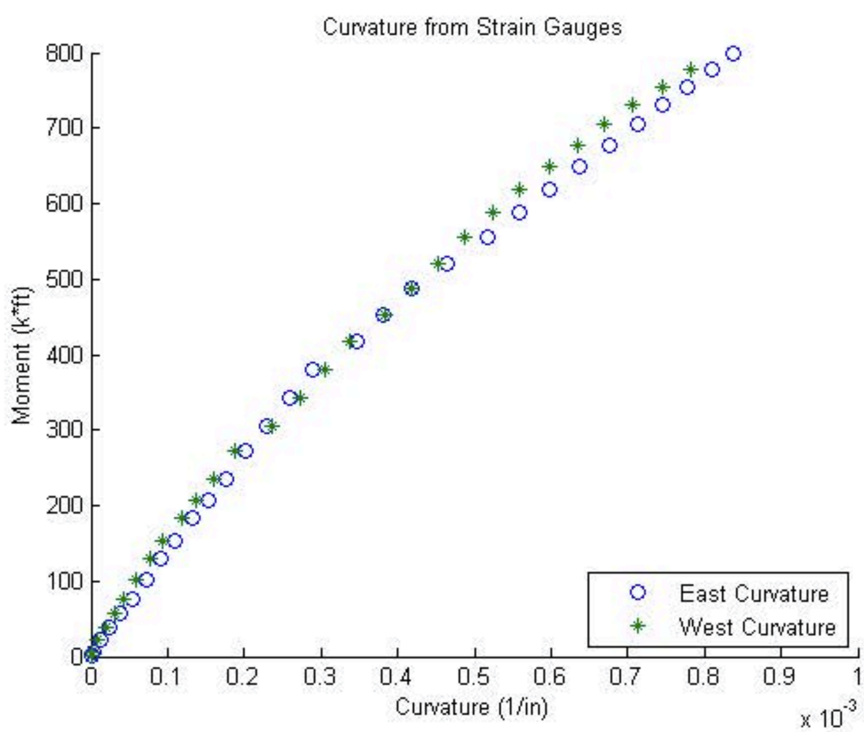

Test Results for Pile G – 4FB

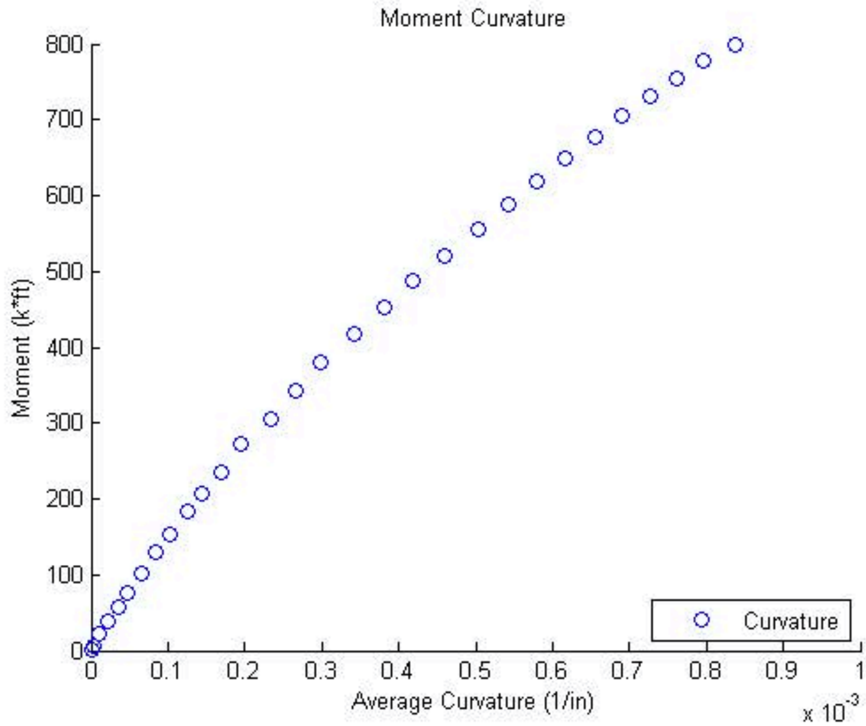

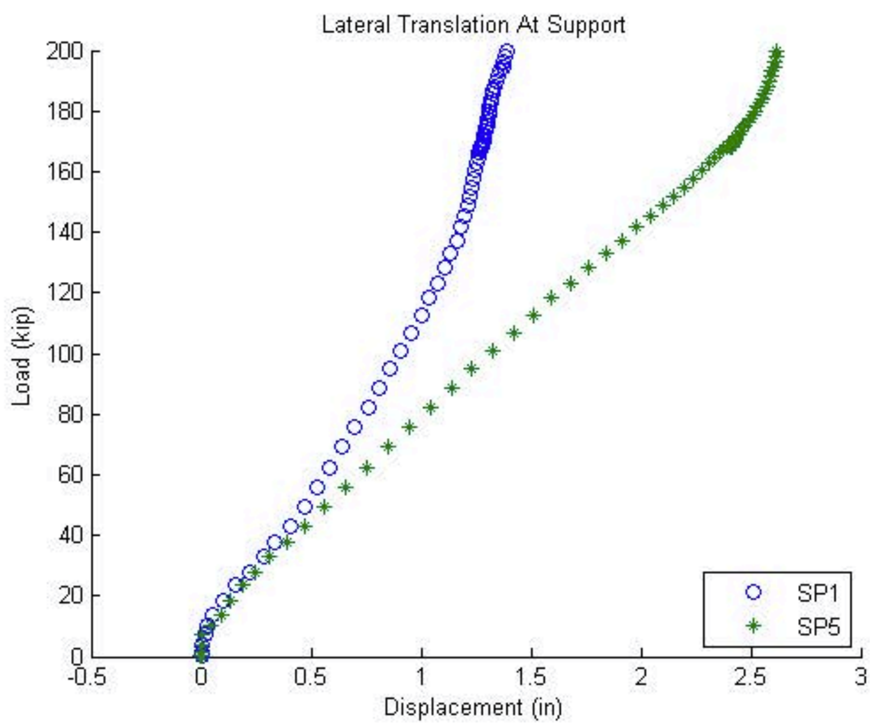

Test Results for Pile G – 4FB

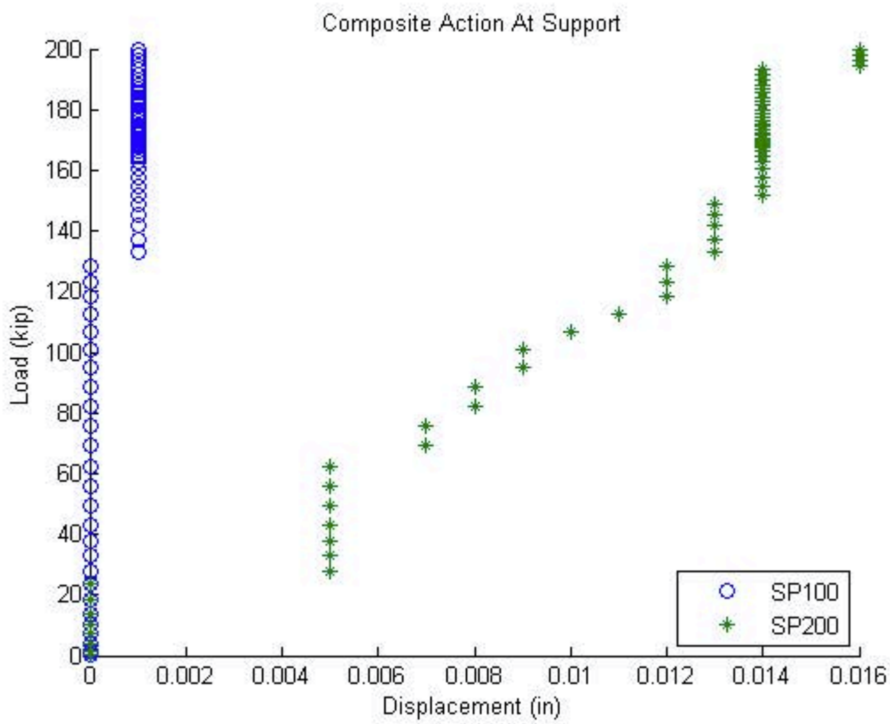

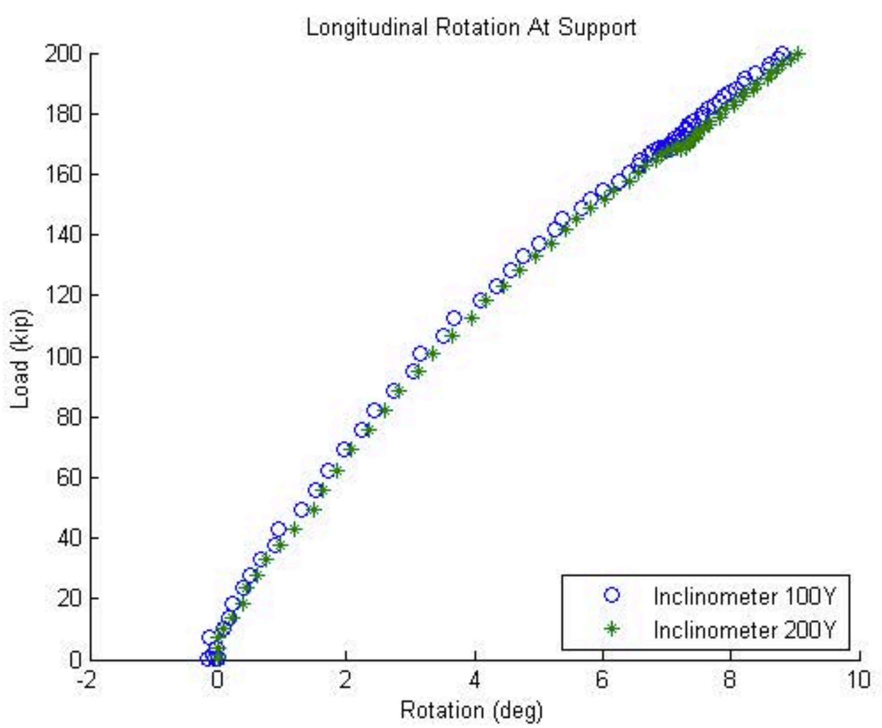

Test Results for Pile G – 4FB

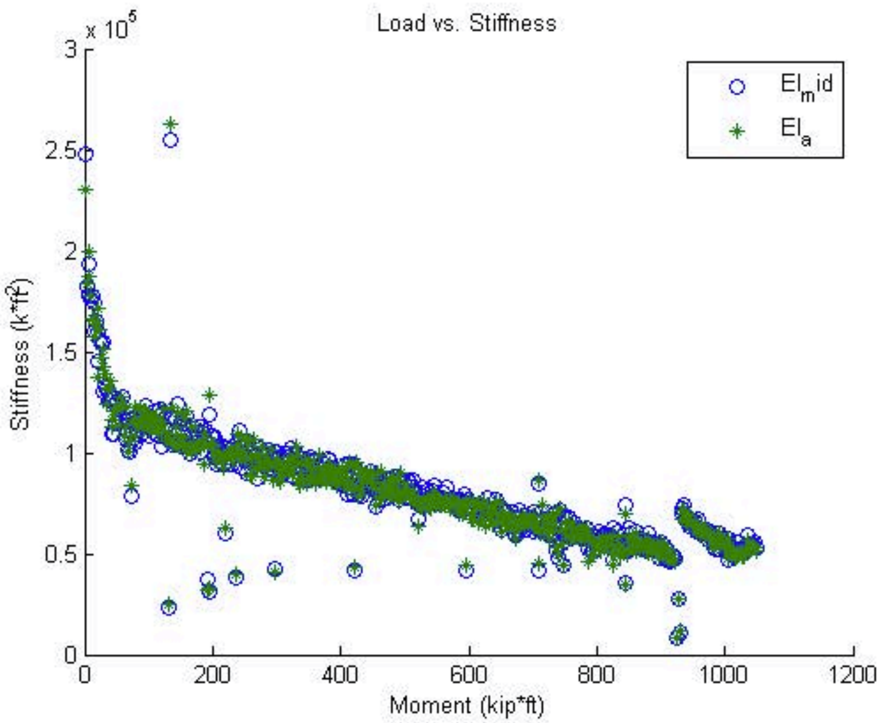

Appendix O: Test Results for Pile H – 4FB

Test Results for Pile H – 4FB

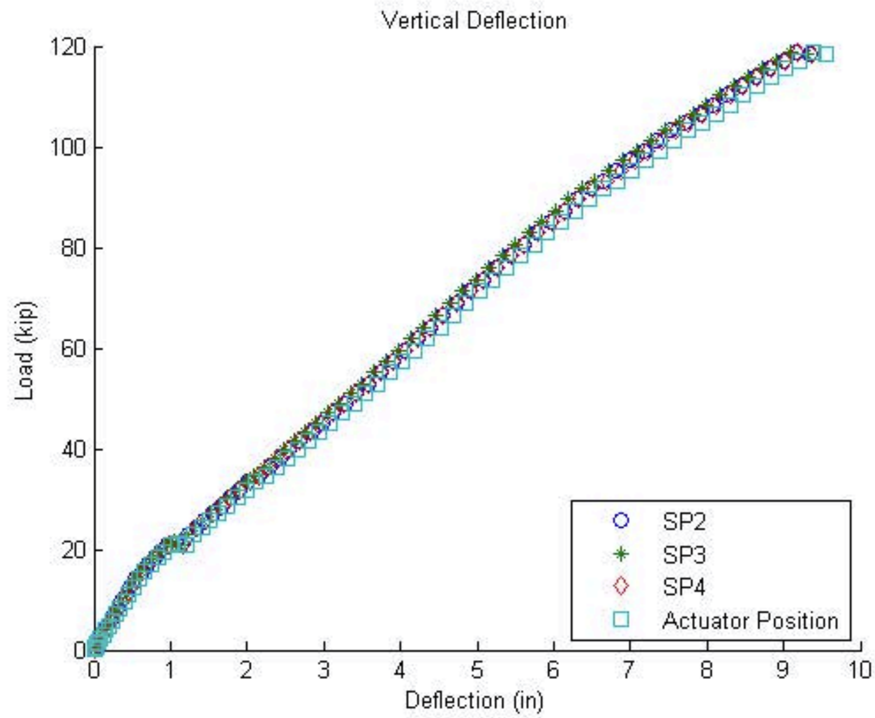

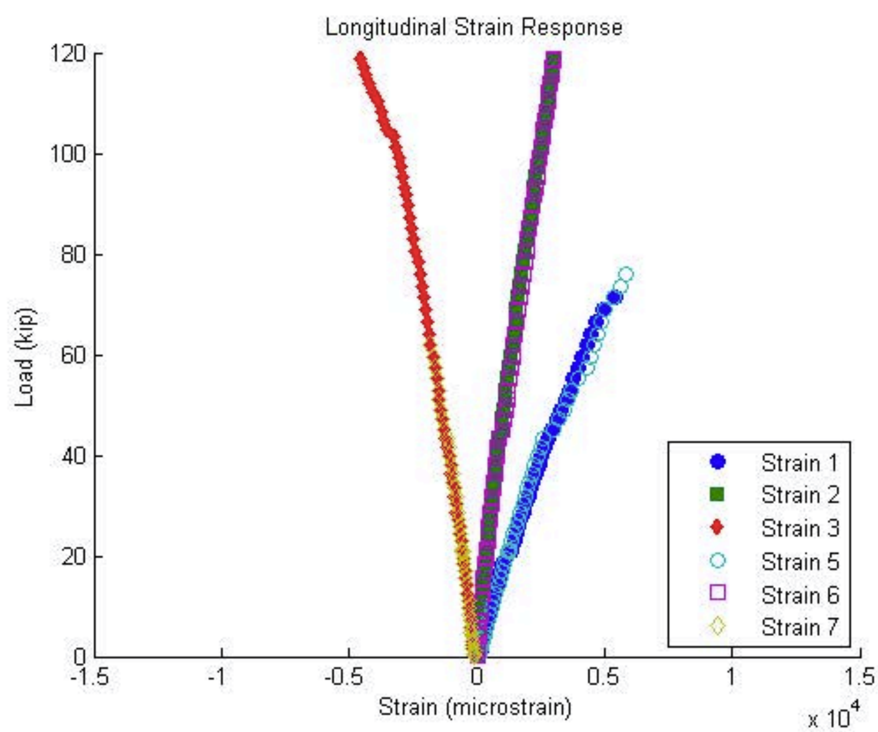

Test Results for Pile H – 4FB

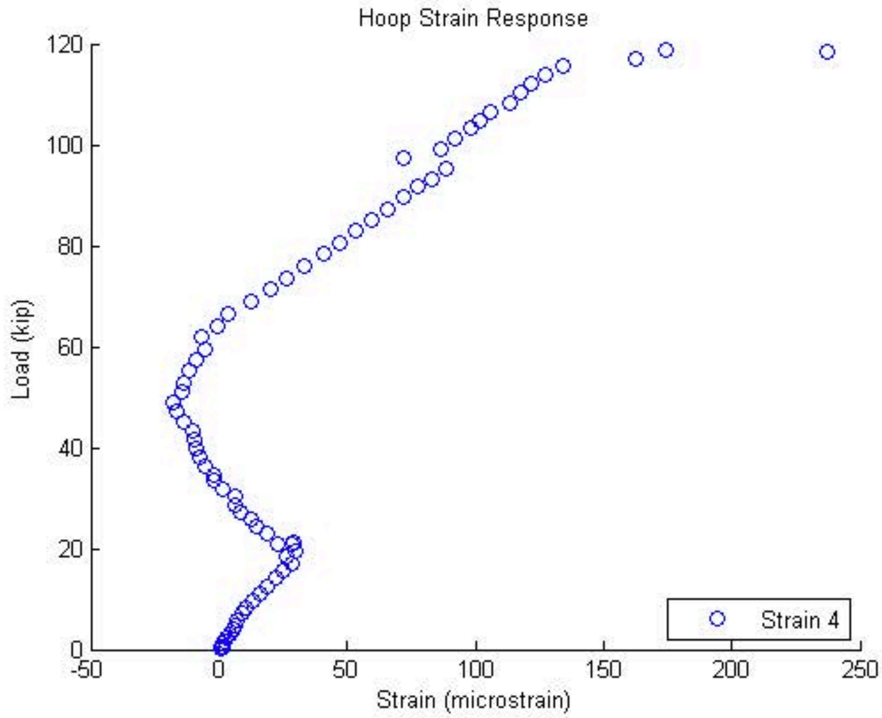

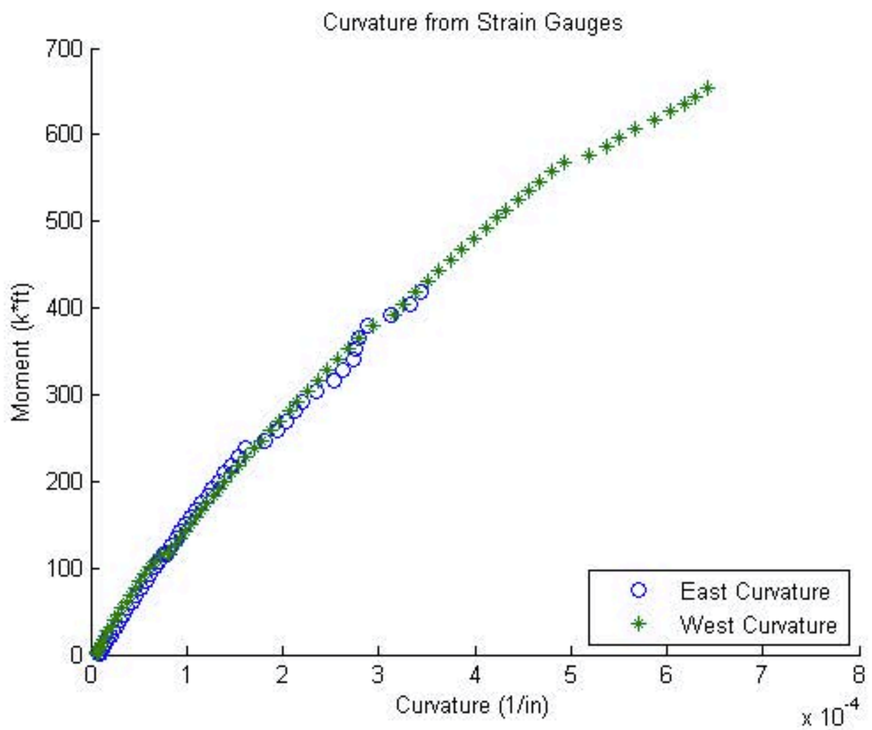

Test Results for Pile H – 4FB

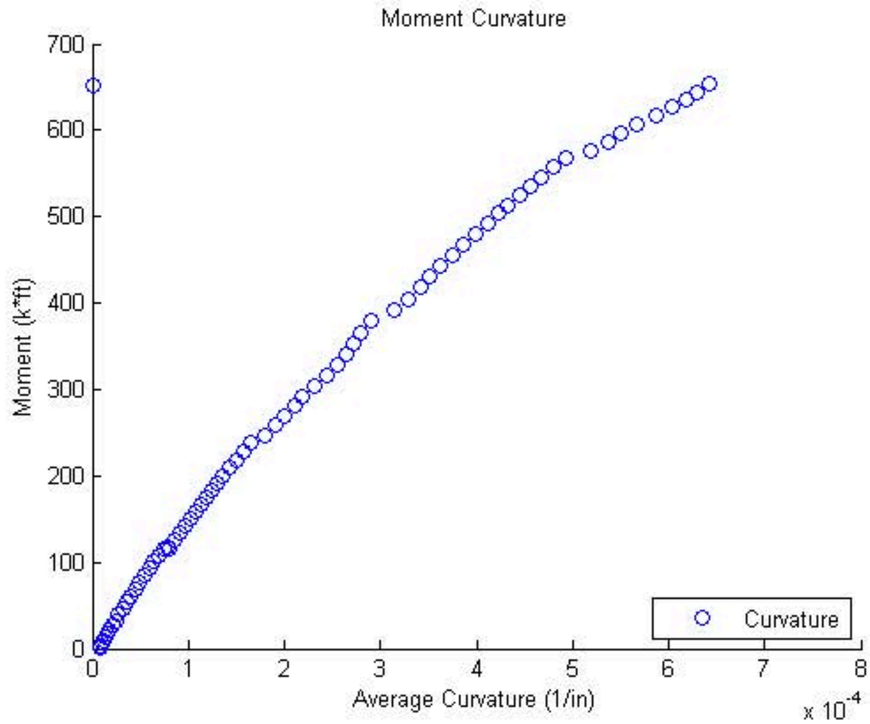

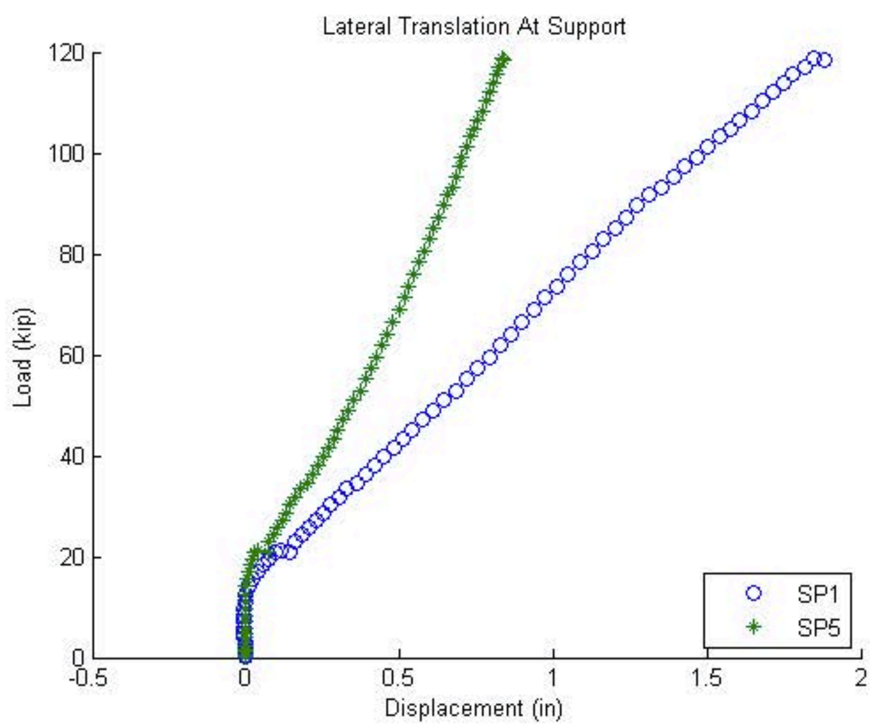

Test Results for Pile H – 4FB

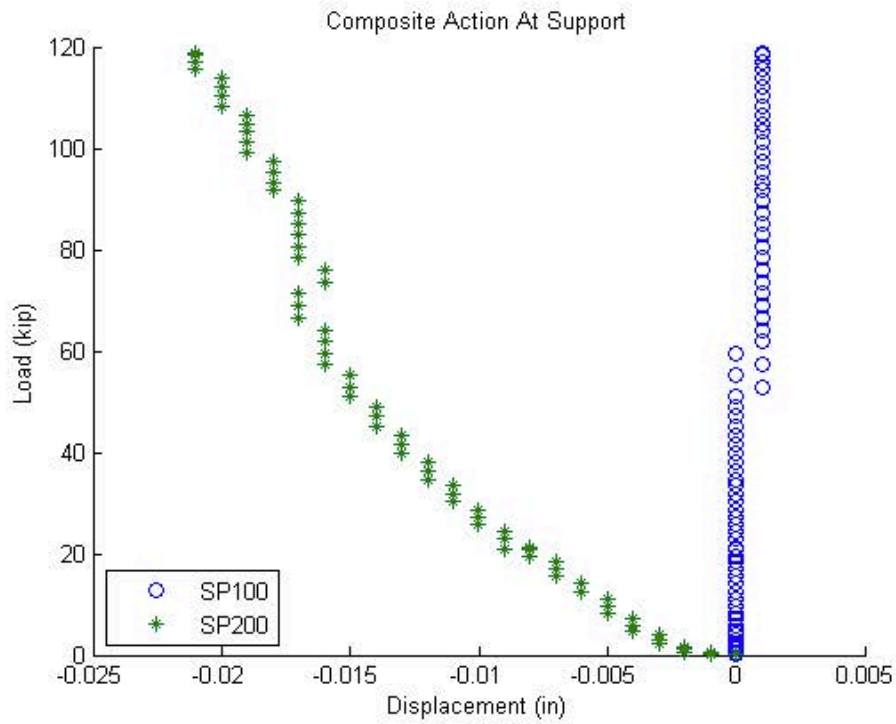

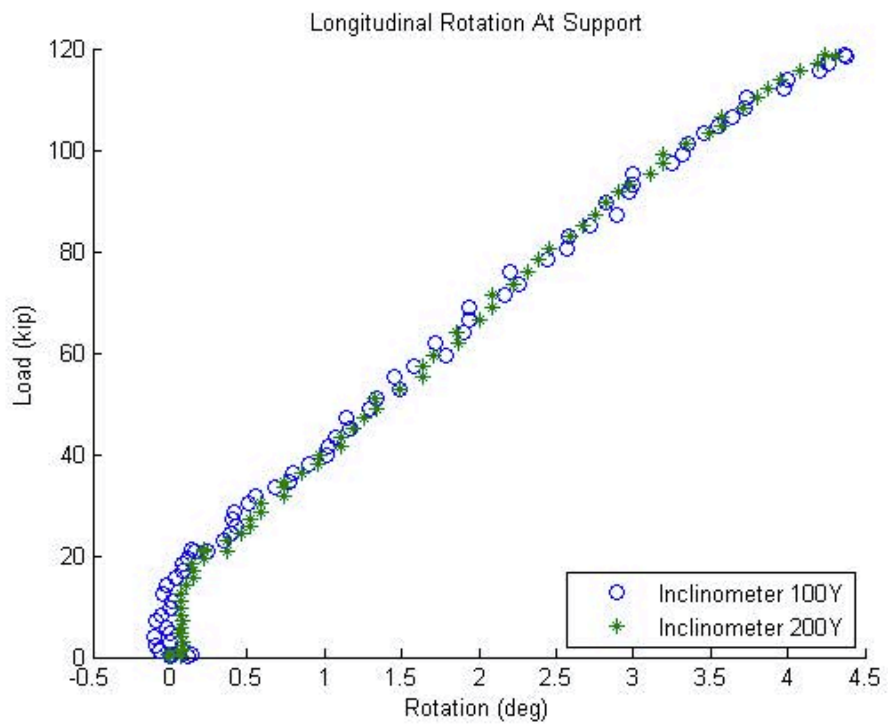

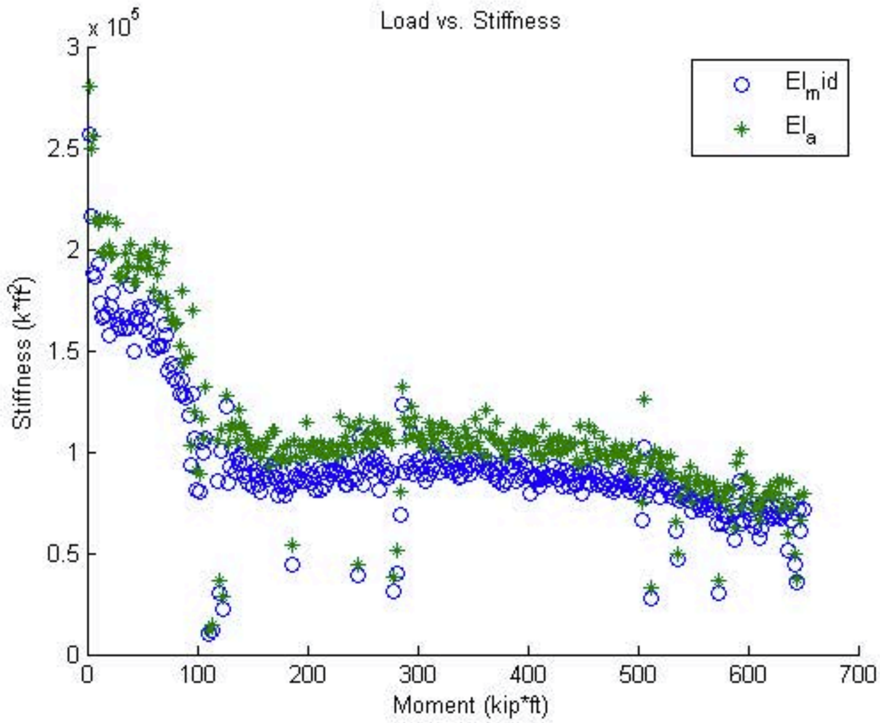
Load vs. Stiffness
x 10^5
3
2.5
2
1.5
1
0.5
0
Stiffness (k*ft^2)
EI_mid
EI_a
0
100
200
300
400
500
600
700
Moment (kip*ft)

Appendix P: Test Results for Pile I – 8HB

Test Results for Pile I – 8HB

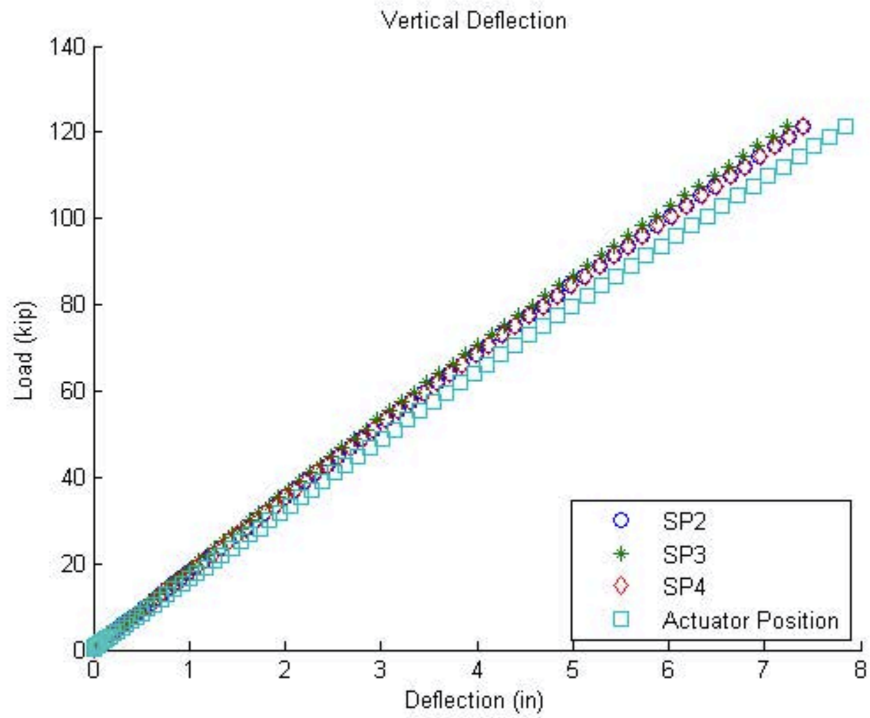

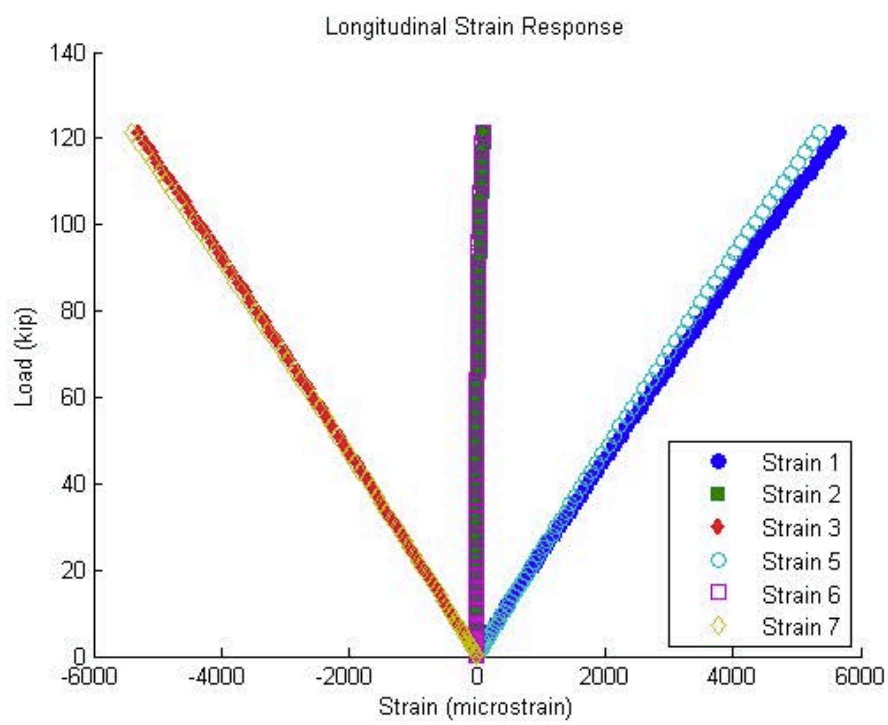

Test Results for Pile I – 8HB

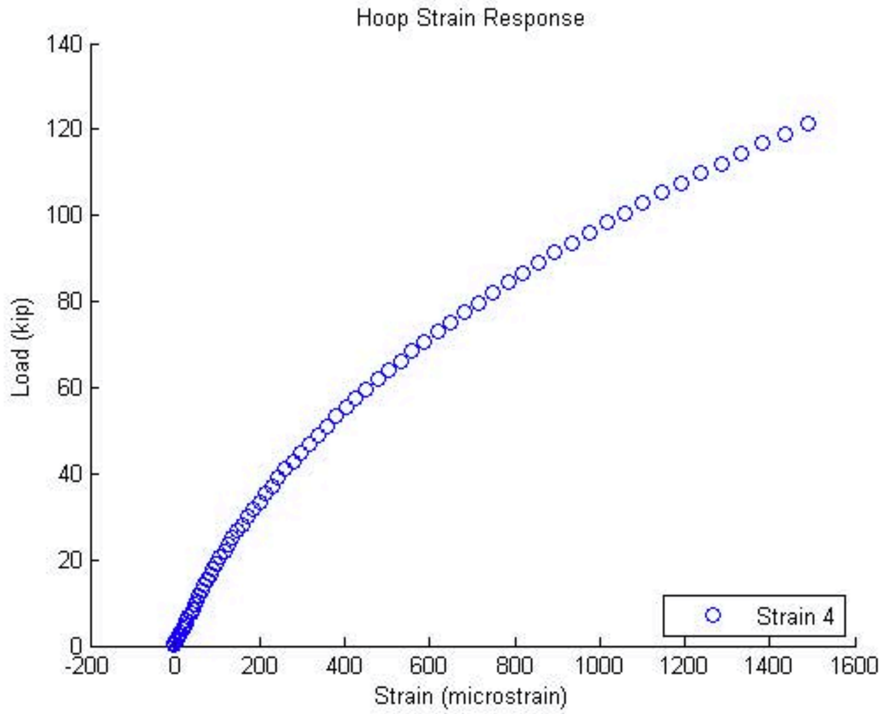

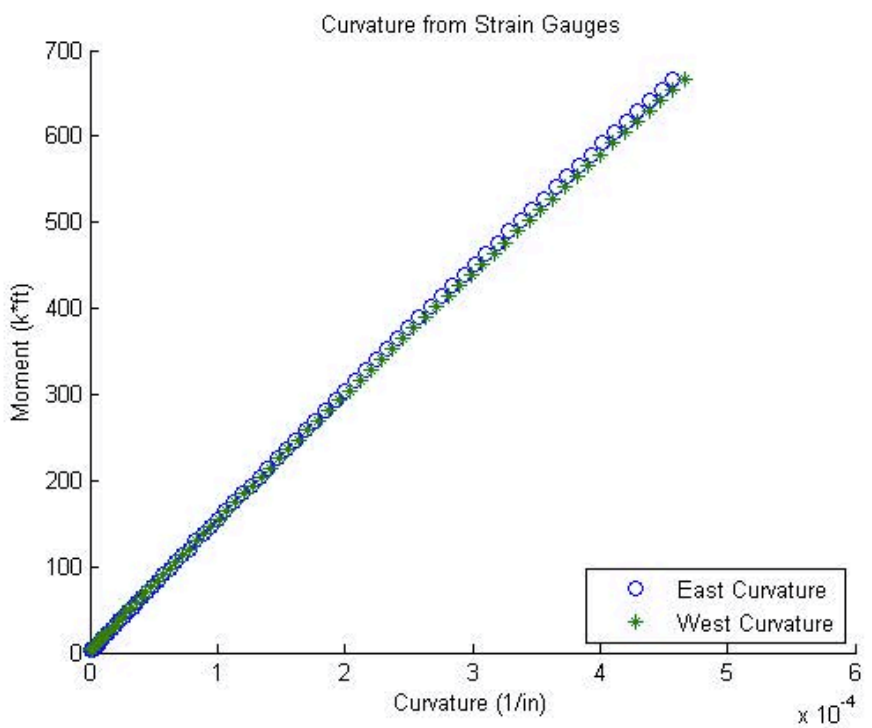

Test Results for Pile I – 8HB

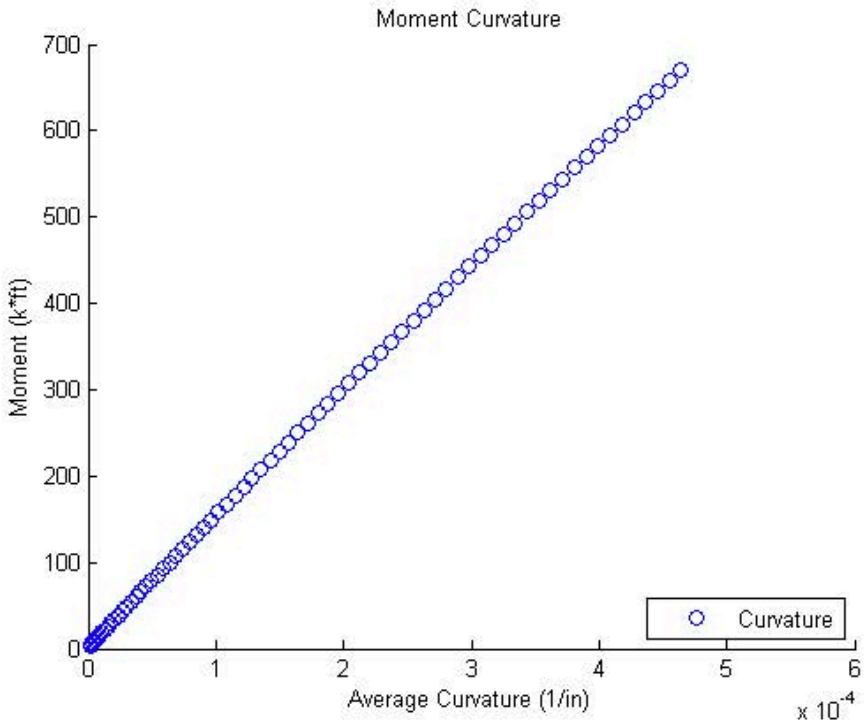

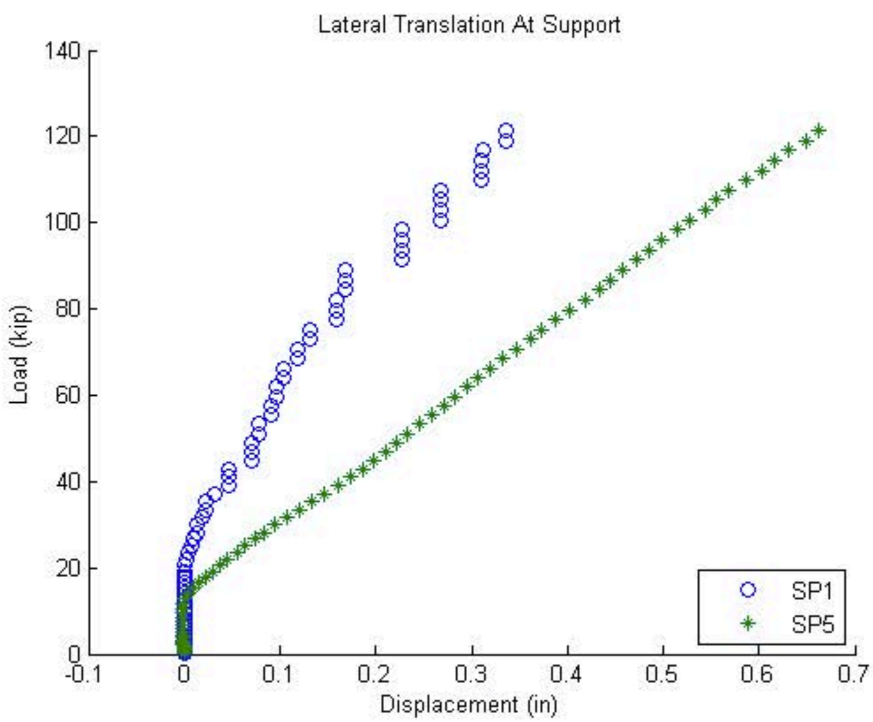

Test Results for Pile I – 8HB

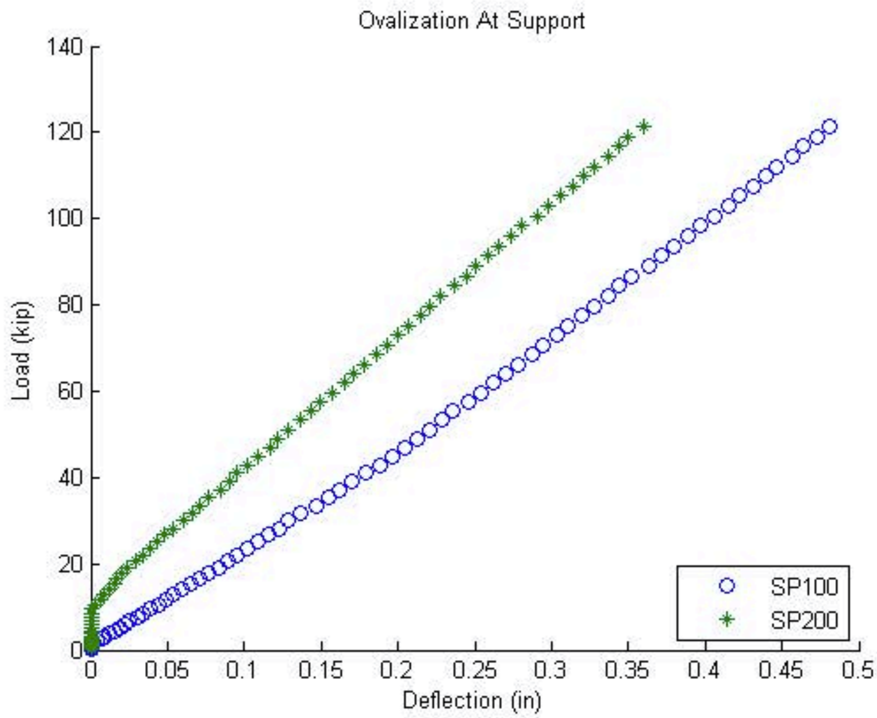

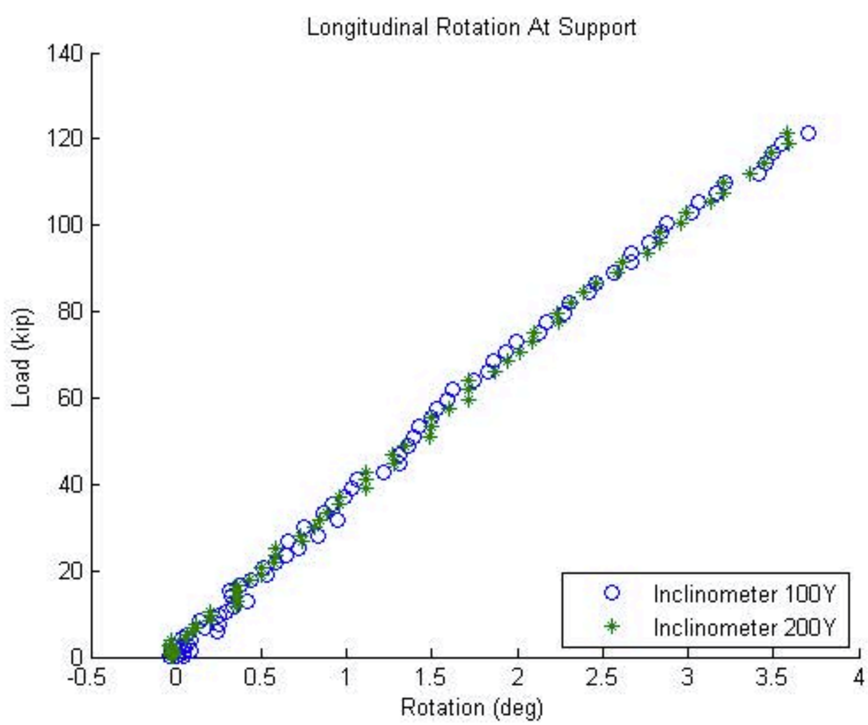

Appendix Q: Test Results for Pile J – 8HB

Test Results for Pile J – 8HB

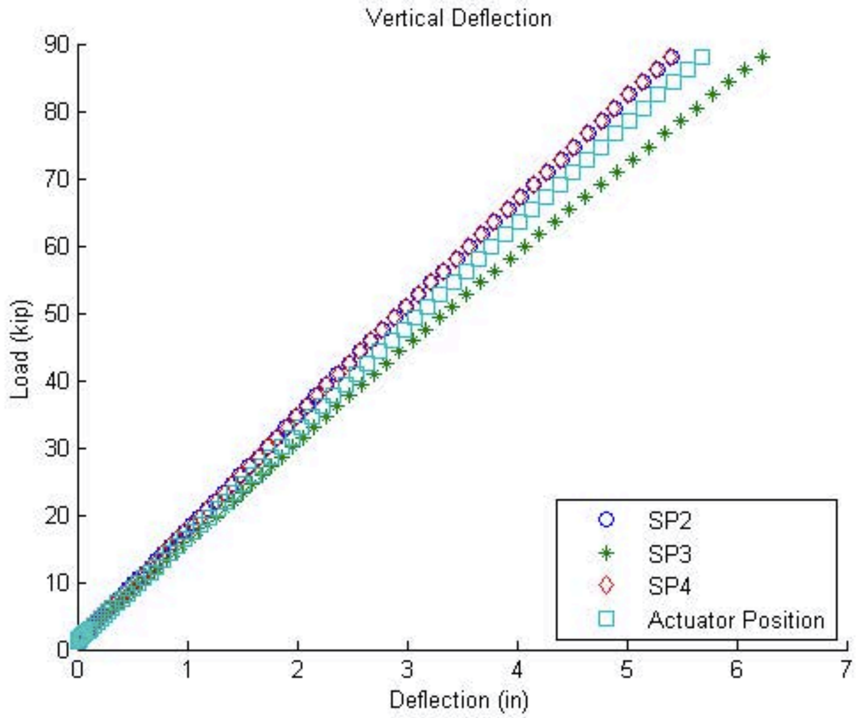

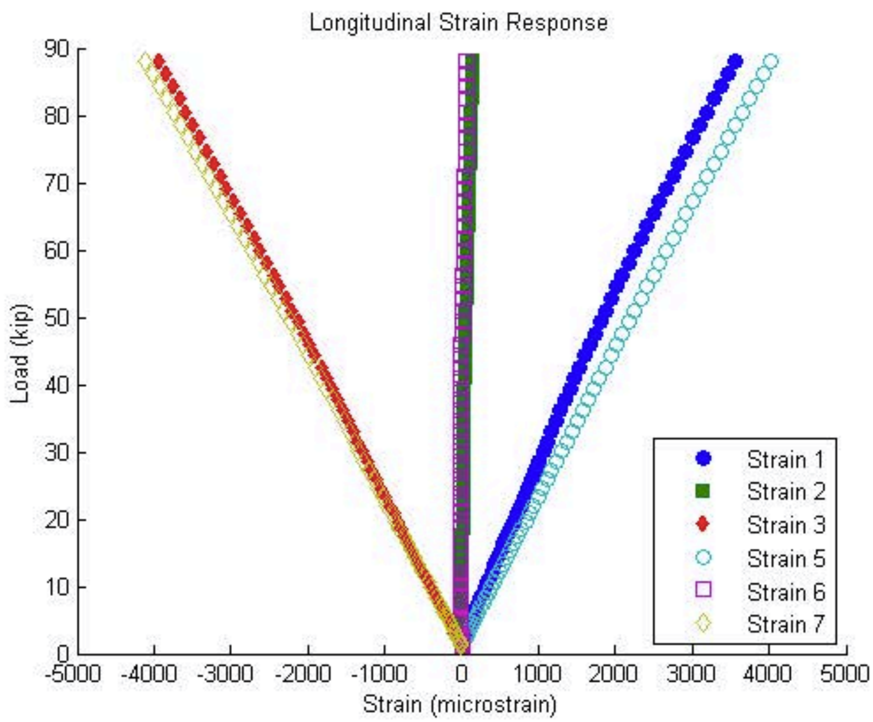

Test Results for Pile J – 8HB

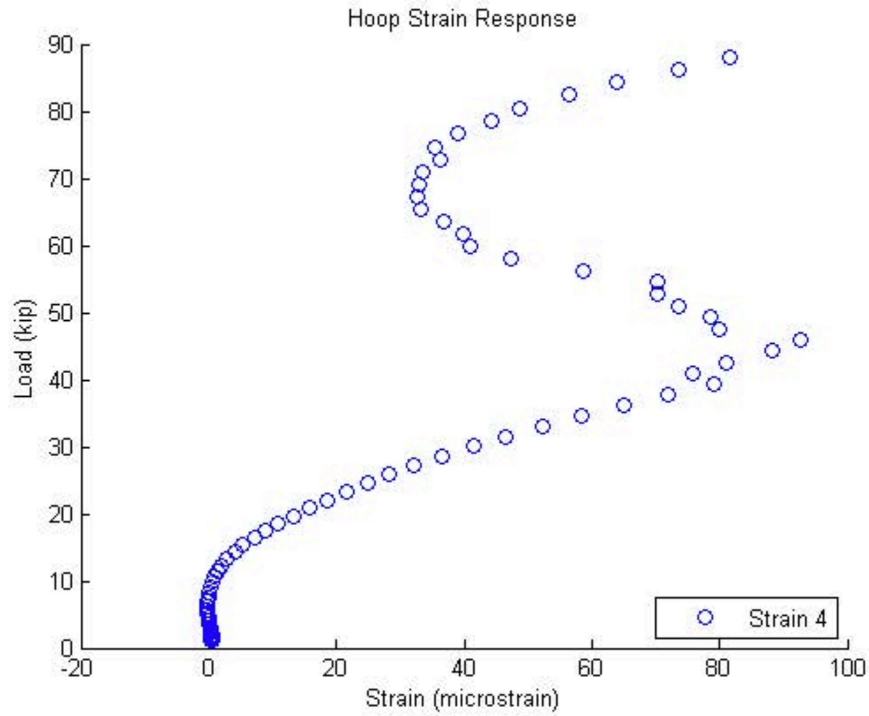

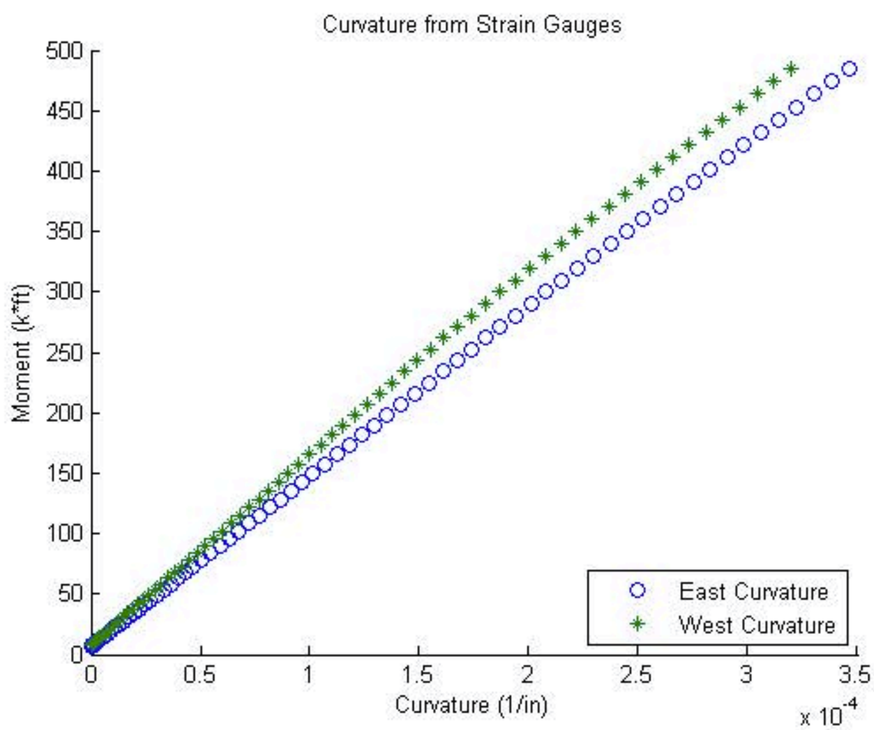

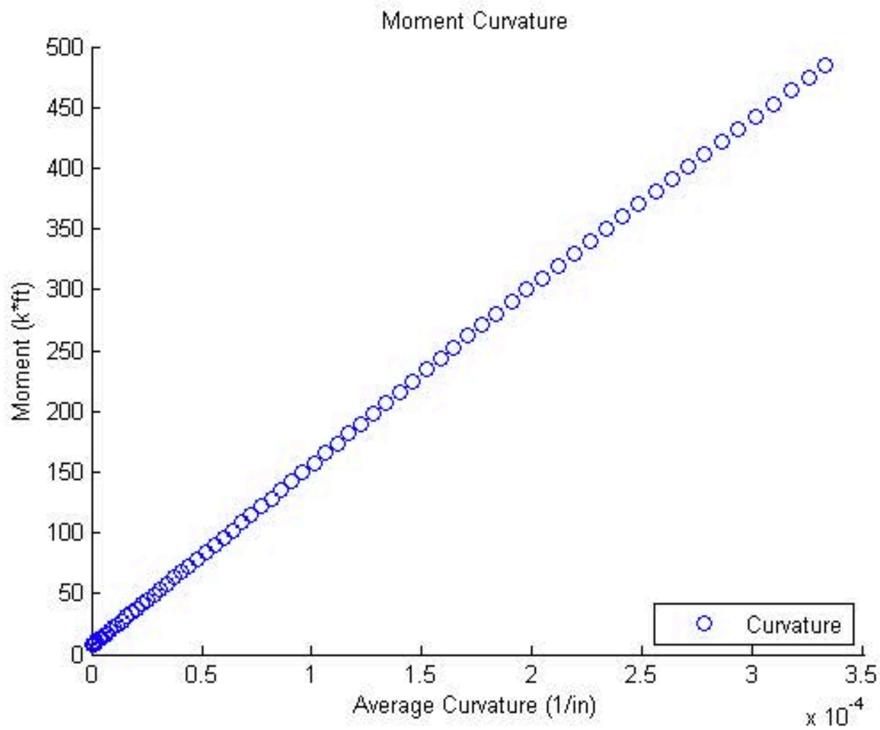
Moment Curvature
Moment (k*ft)
500
450
400
350
300
250
200
150
100
50
0
0
0.5
1
1.5
2
2.5
3
3.5
x 10^-4
Average Curvature (1/in)
Curvature

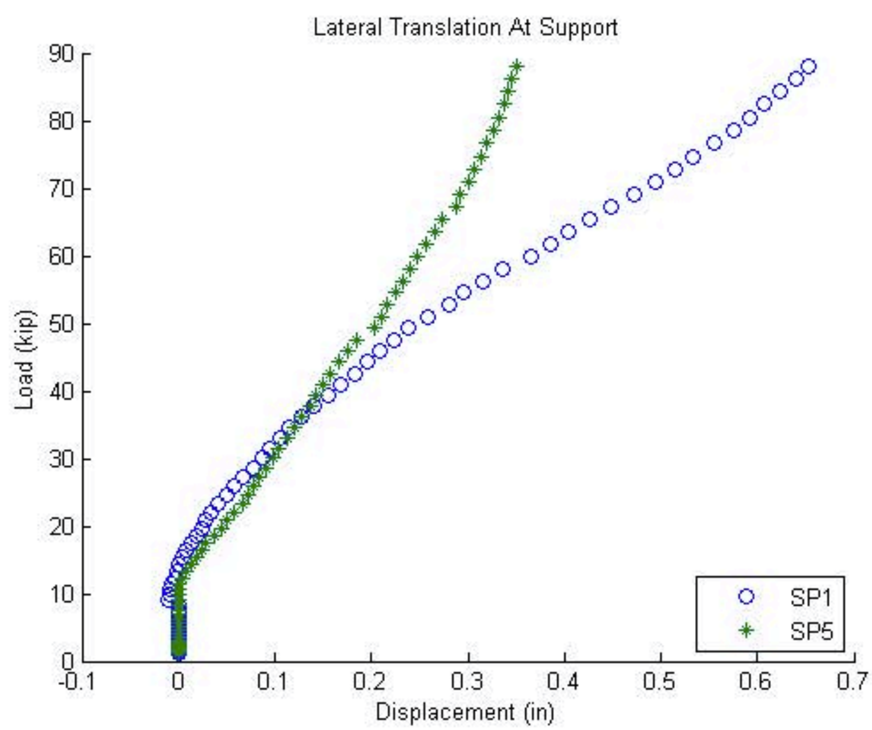
Lateral Translation At Support
Load (kip)
90
80
70
60
50
40
30
20
10
0
-0.1
0
0.1
0.2
0.3
0.4
0.5
0.6
0.7
Displacement (in)
SP1
SP5

Test Results for Pile J – 8HB

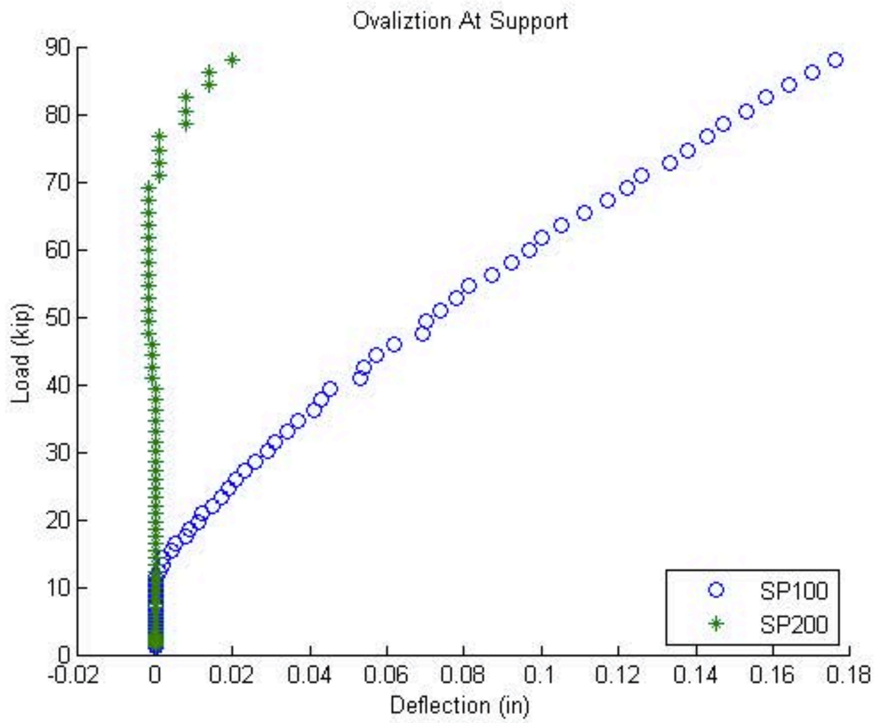

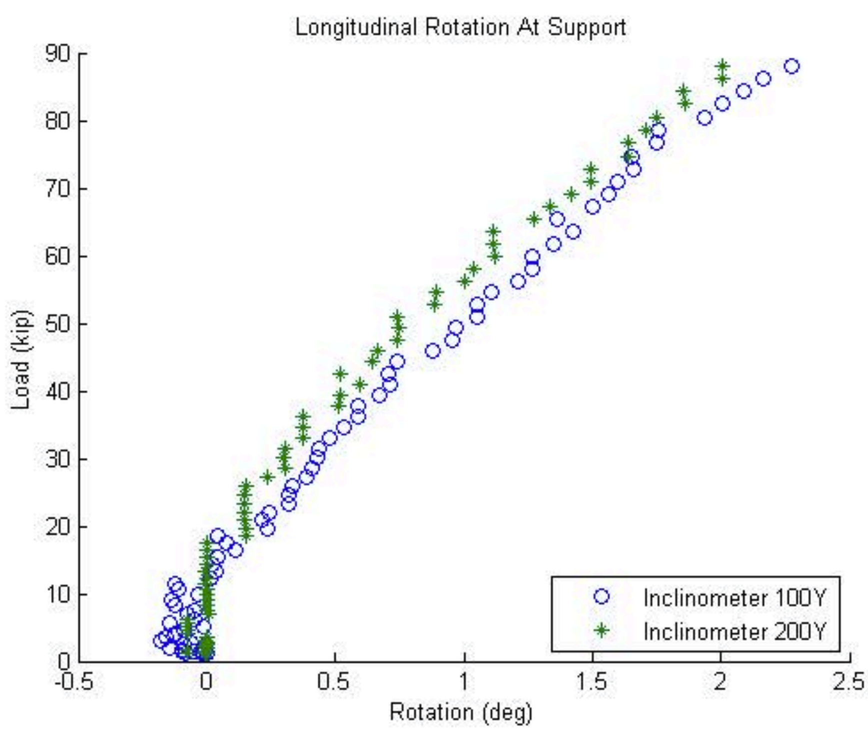

Appendix R: Summary of Hollow Pile Tests

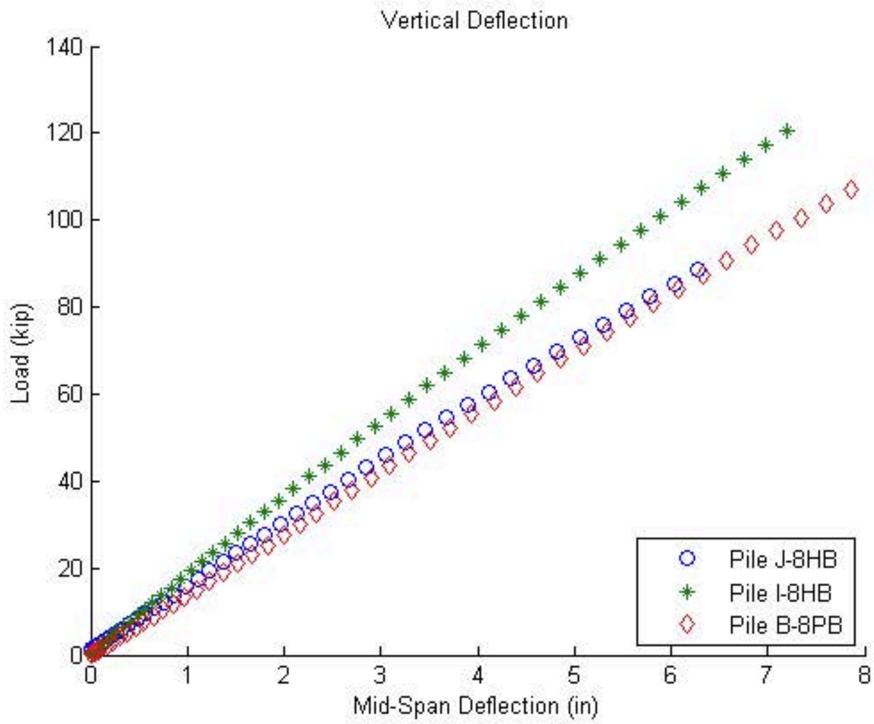
Vertical Deflection
Load (kip)
Mid-Span Deflection (in)
Pile J-8HB
Pile I-8HB
Pile B-8PB

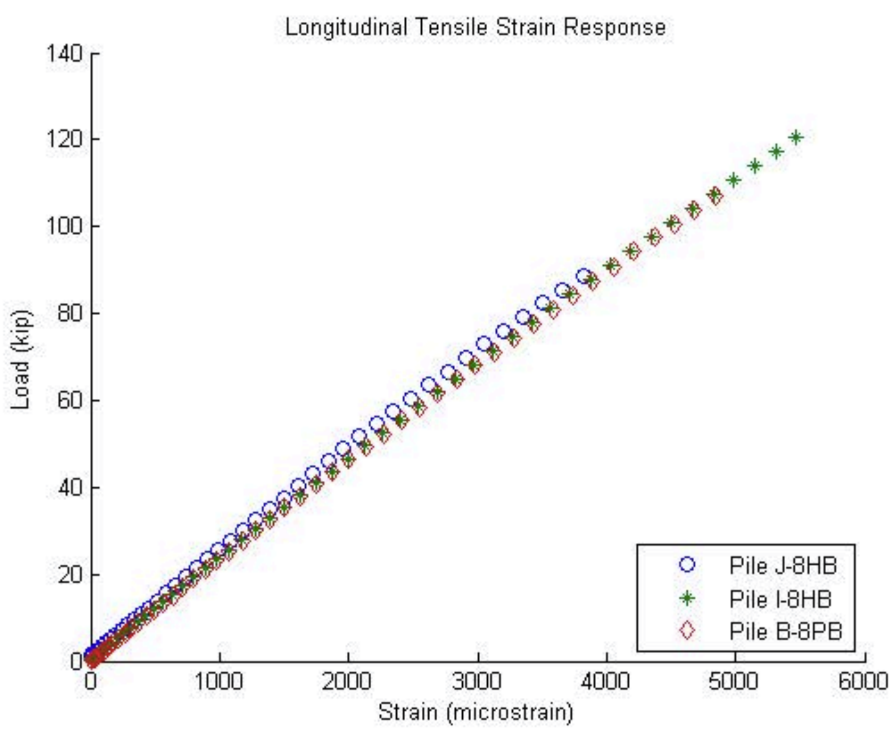
Longitudinal Tensile Strain Response
Load (kip)
Strain (microstrain)
Pile J-8HB
Pile I-8HB
Pile B-8PB

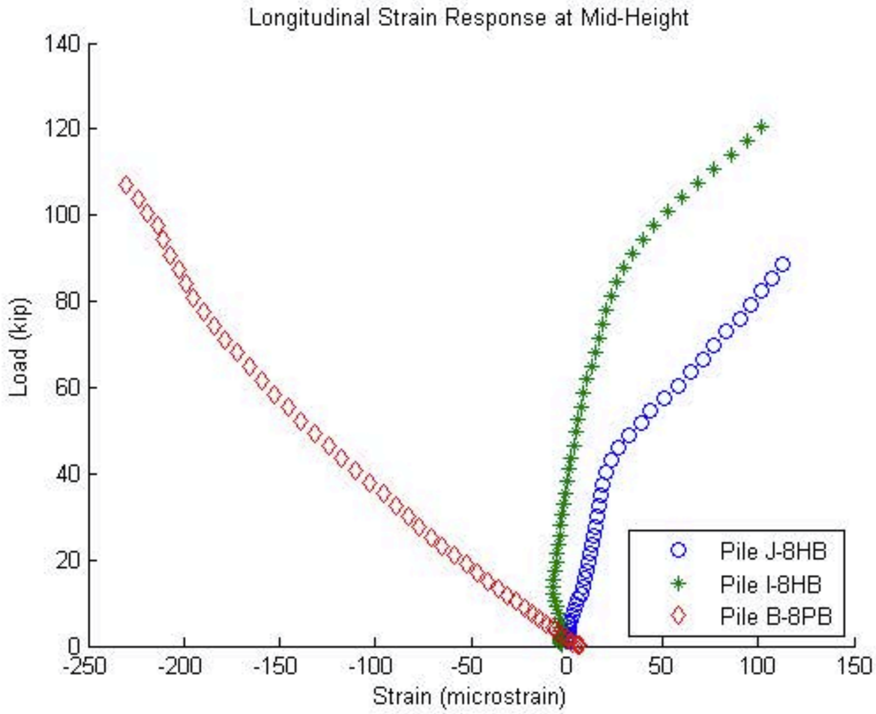
Longitudinal Strain Response at Mid-Height
Load (kip)
Strain (microstrain)
Pile J-8HB
Pile I-8HB
Pile B-8PB
140
120
100
80
60
40
20
0
-250
-200
-150
-100
-50
0
50
100
150

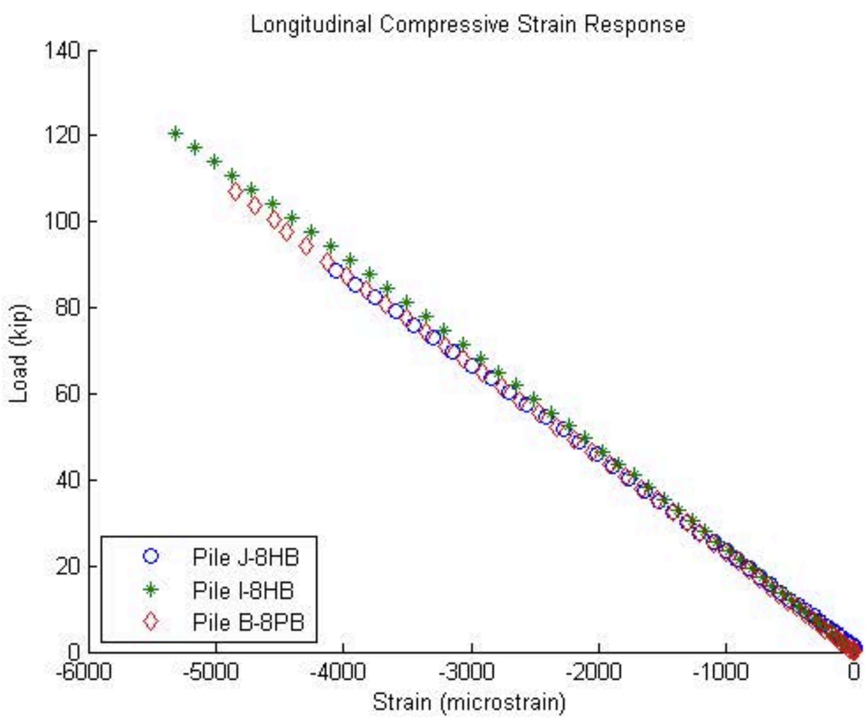
Longitudinal Compressive Strain Response
Load (kip)
Strain (microstrain)
Pile J-8HB
Pile I-8HB
Pile B-8PB
140
120
100
80
60
40
20
0
-6000
-5000
-4000
-3000
-2000
-1000
0

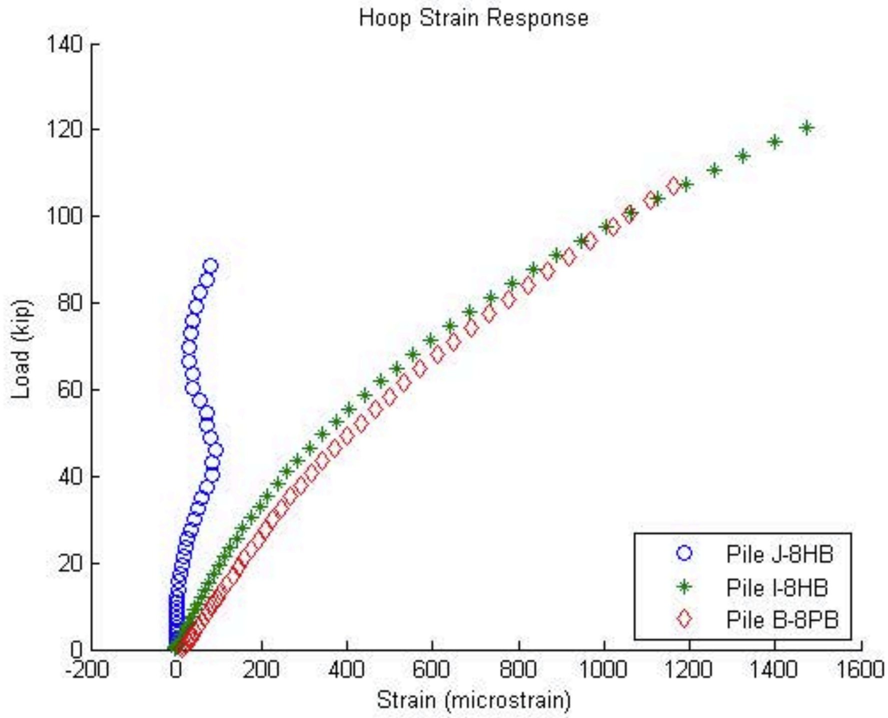
Hoop Strain Response
Load (kip)
Strain (microstrain)
140
120
100
80
60
40
20
0
-200
0
200
400
600
800
1000
1200
1400
1600
Pile J-8HB
Pile I-8HB
Pile B-8PB

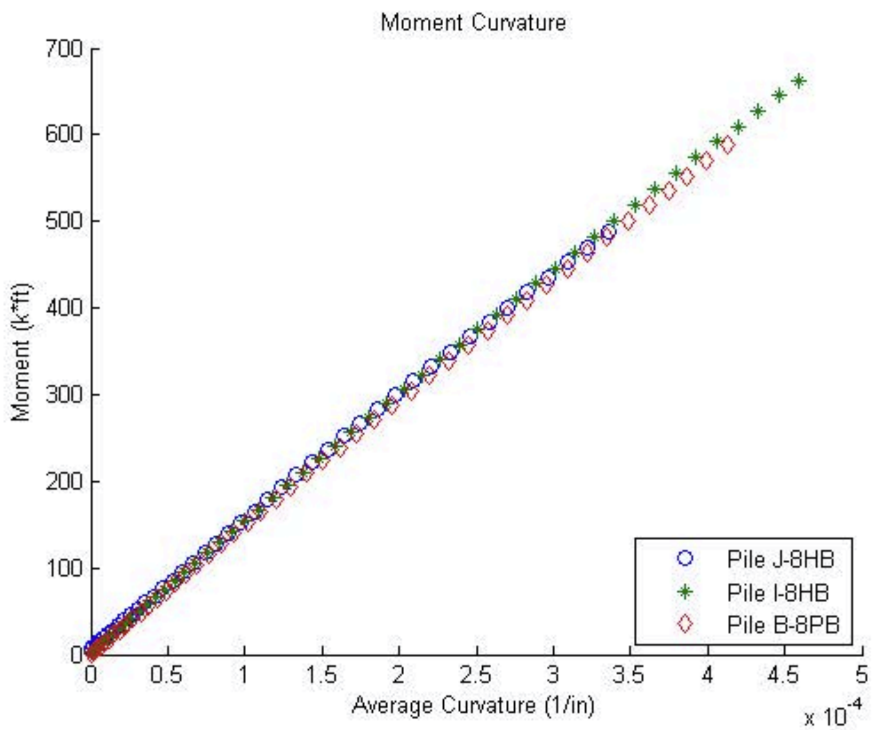
Moment Curvature
Moment (k*ft)
Average Curvature (1/in)
700
600
500
400
300
200
100
0
0
0.5
1
1.5
2
2.5
3
3.5
4
4.5
5
x 10^-4
Pile J-8HB
Pile I-8HB
Pile B-8PB

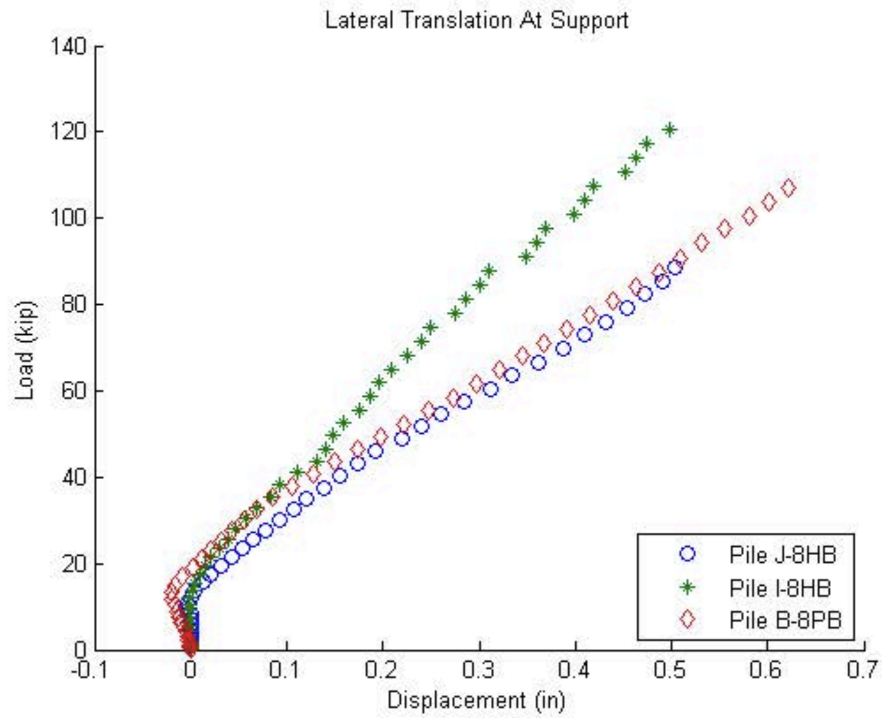
Lateral Translation At Support
Load (kip)
Displacement (in)
0
20
40
60
80
100
120
140
-0.1
0
0.1
0.2
0.3
0.4
0.5
0.6
0.7
Pile J-8HB
Pile I-8HB
Pile B-8PB

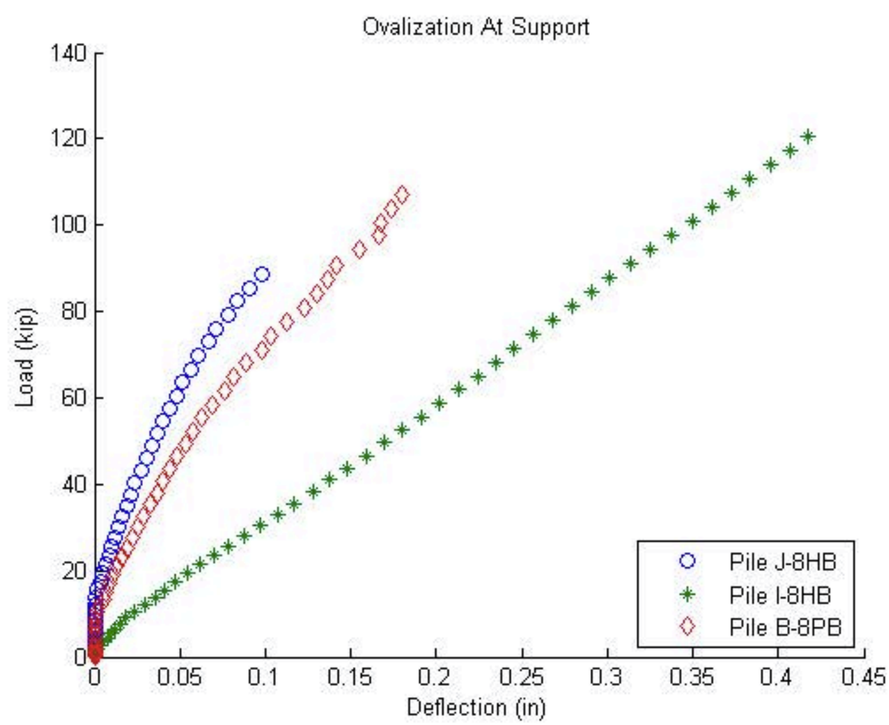
Ovalization At Support
Load (kip)
Deflection (in)
0
20
40
60
80
100
120
140
0
0.05
0.1
0.15
0.2
0.25
0.3
0.35
0.4
0.45
Pile J-8HB
Pile I-8HB
Pile B-8PB

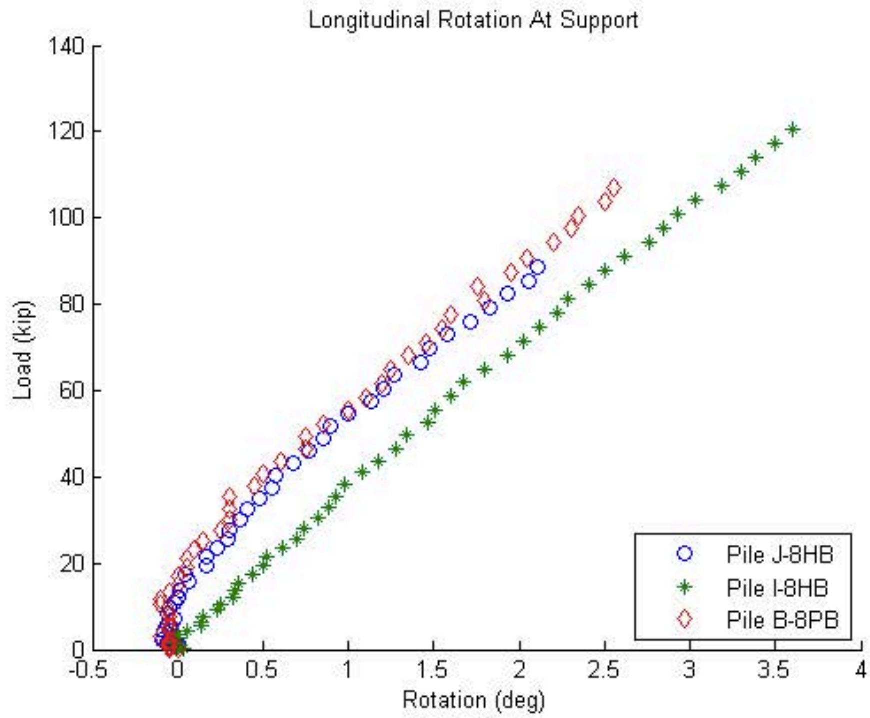
Longitudinal Rotation At Support
Load (kip)
Rotation (deg)
Pile J-8HB
Pile I-8HB
Pile B-8PB
140
120
100
80
60
40
20
0
-0.5
0
0.5
1
1.5
2
2.5
3
3.5
4

Appendix S: Summary of Concrete-Filled Pile Tests

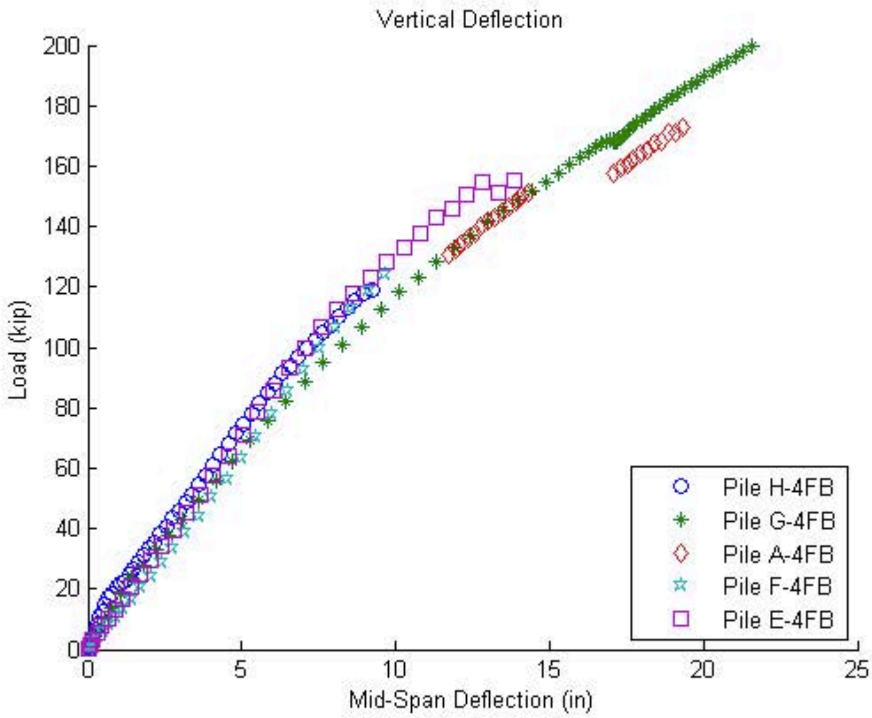
Vertical Deflection
Load (kip)
Mid-Span Deflection (in)
0
20
40
60
80
100
120
140
160
180
200
0
5
10
15
20
25
Pile H-4FB
Pile G-4FB
Pile A-4FB
Pile F-4FB
Pile E-4FB

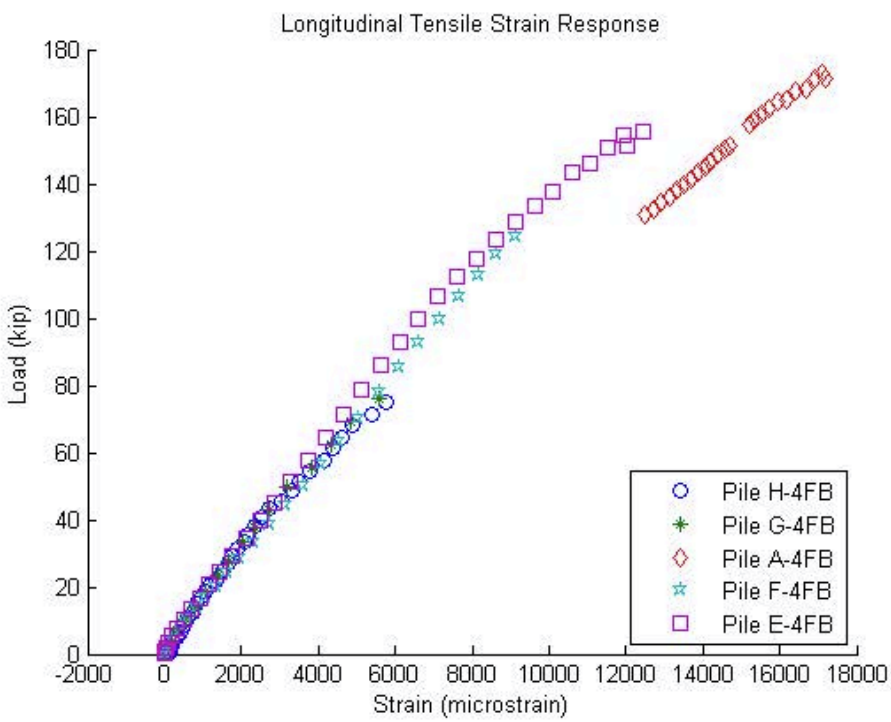
Longitudinal Tensile Strain Response
Load (kip)
Strain (microstrain)
0
20
40
60
80
100
120
140
160
180
-2000
0
2000
4000
6000
8000
10000
12000
14000
16000
18000
Pile H-4FB
Pile G-4FB
Pile A-4FB
Pile F-4FB
Pile E-4FB

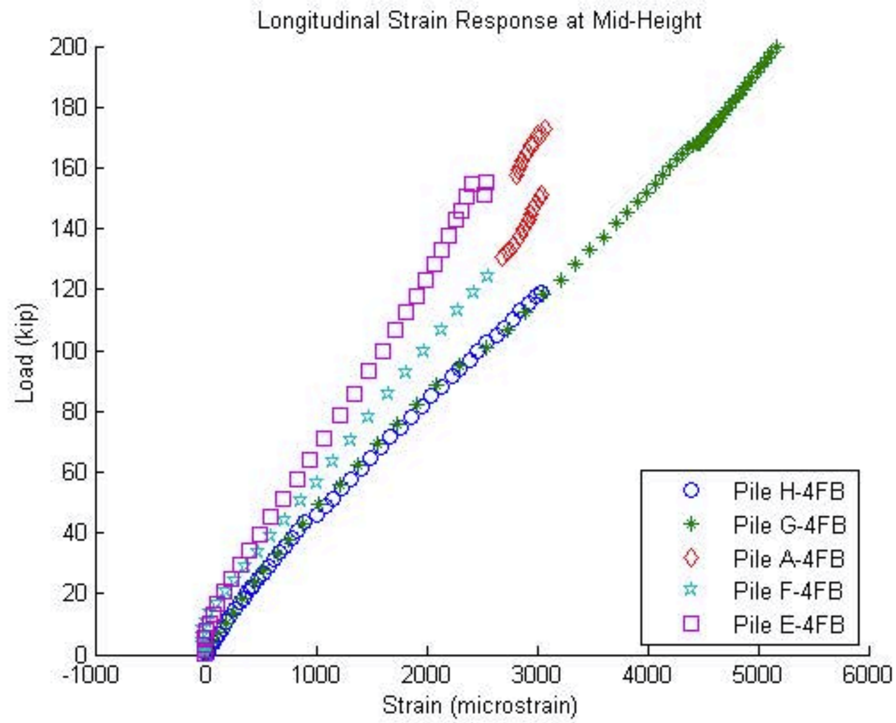
Longitudinal Strain Response at Mid-Height
Load (kip)
Strain (microstrain)
Pile H-4FB
Pile G-4FB
Pile A-4FB
Pile F-4FB
Pile E-4FB

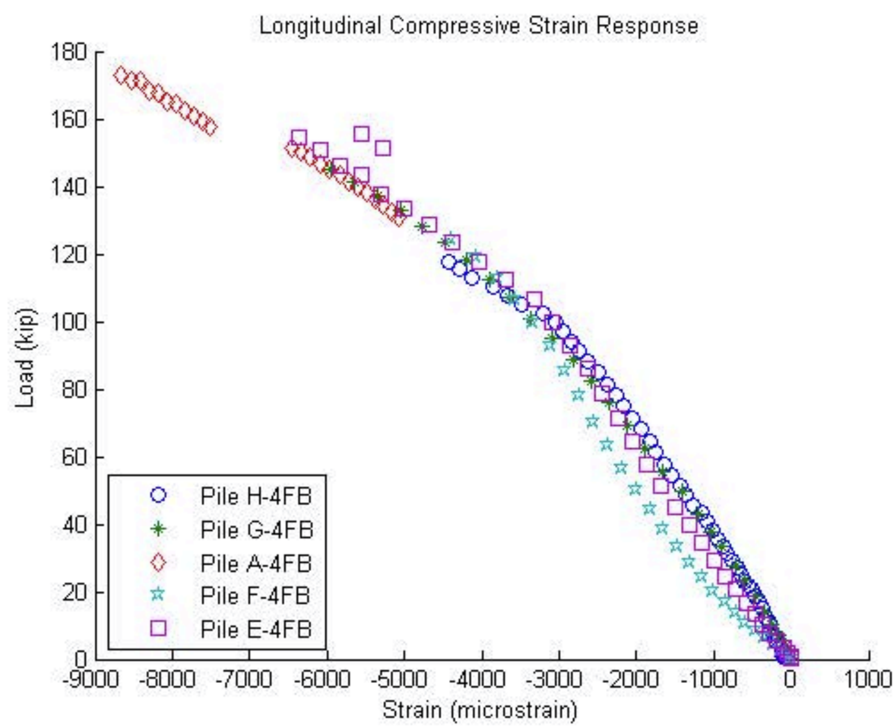
Longitudinal Compressive Strain Response
Load (kip)
Strain (microstrain)
Pile H-4FB
Pile G-4FB
Pile A-4FB
Pile F-4FB
Pile E-4FB

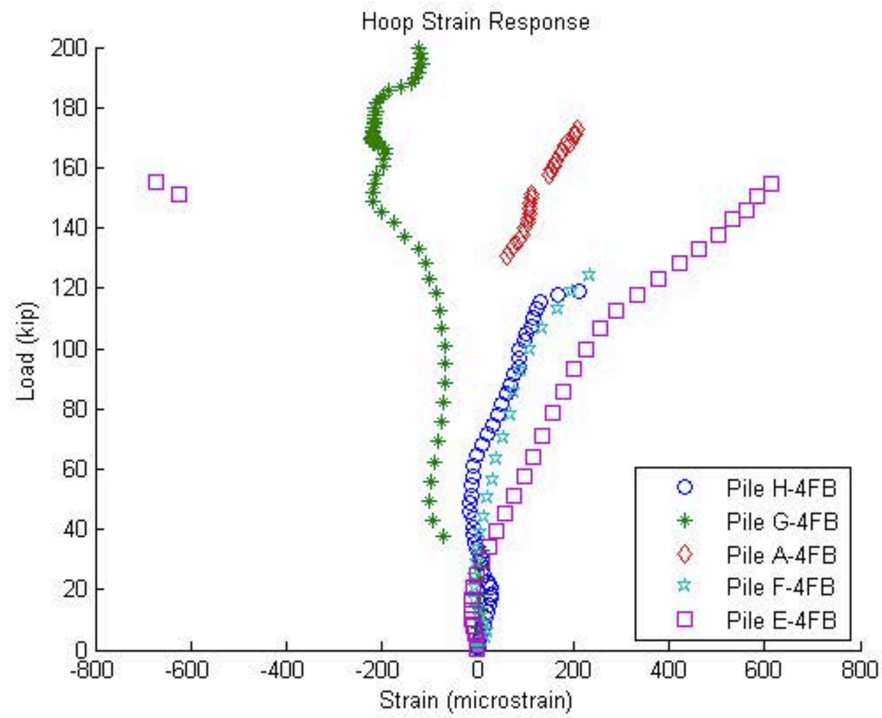
Hoop Strain Response
Load (kip)
Strain (microstrain)
200
180
160
140
120
100
80
60
40
20
0
-800
-600
-400
-200
0
200
400
600
800
Pile H-4FB
Pile G-4FB
Pile A-4FB
Pile F-4FB
Pile E-4FB

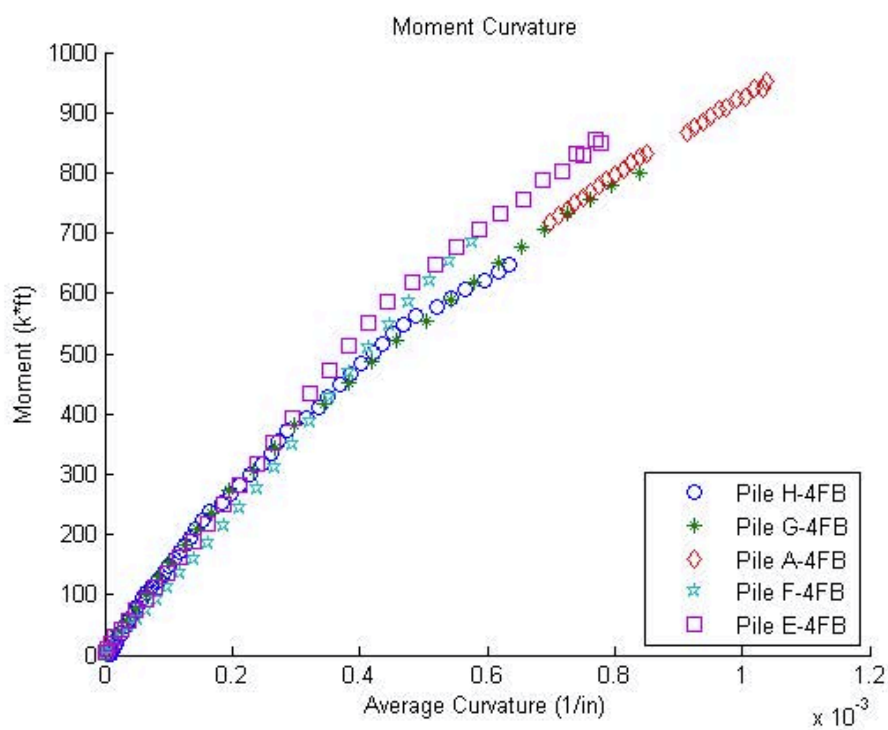
Moment Curvature
Moment (k*ft)
Average Curvature (1/in)
x 10-3
1000
900
800
700
600
500
400
300
200
100
0
0
0.2
0.4
0.6
0.8
1
1.2
Pile H-4FB
Pile G-4FB
Pile A-4FB
Pile F-4FB
Pile E-4FB

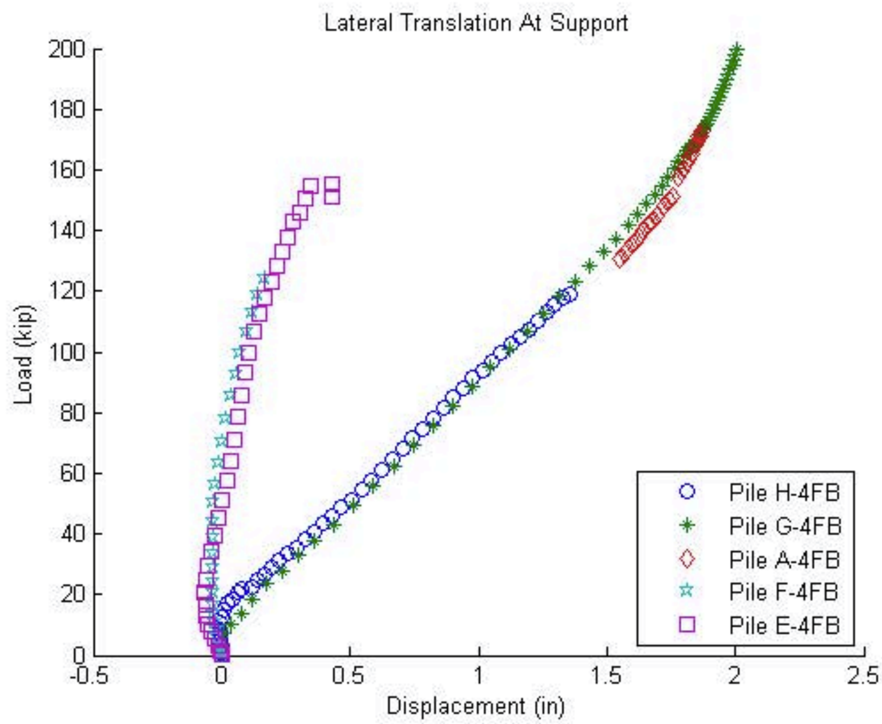
Lateral Translation At Support
Load (kip)
Displacement (in)
Pile H-4FB
Pile G-4FB
Pile A-4FB
Pile F-4FB
Pile E-4FB

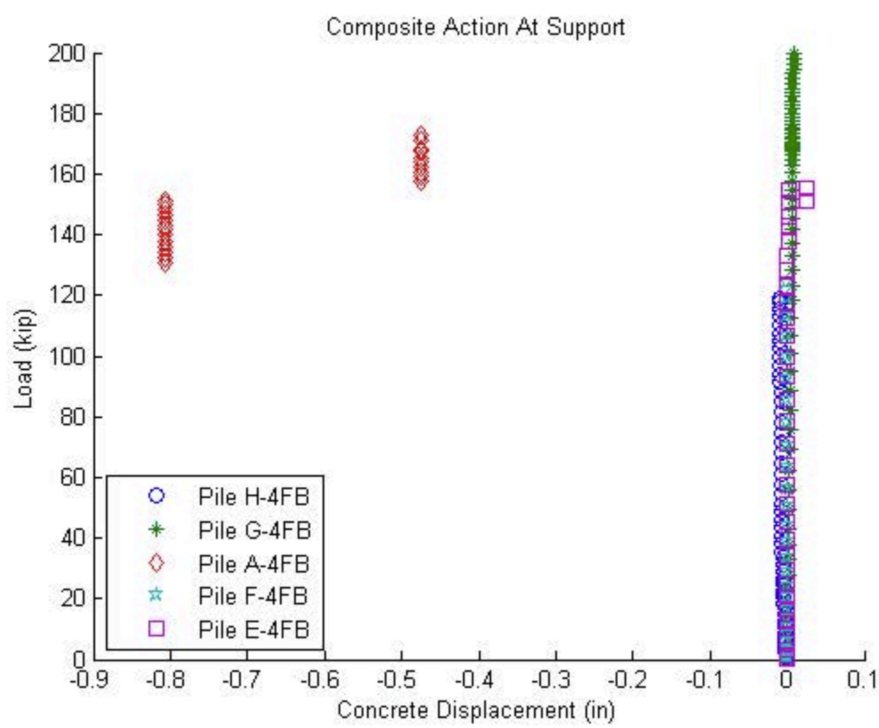
Composite Action At Support
Load (kip)
Concrete Displacement (in)
Pile H-4FB
Pile G-4FB
Pile A-4FB
Pile F-4FB
Pile E-4FB

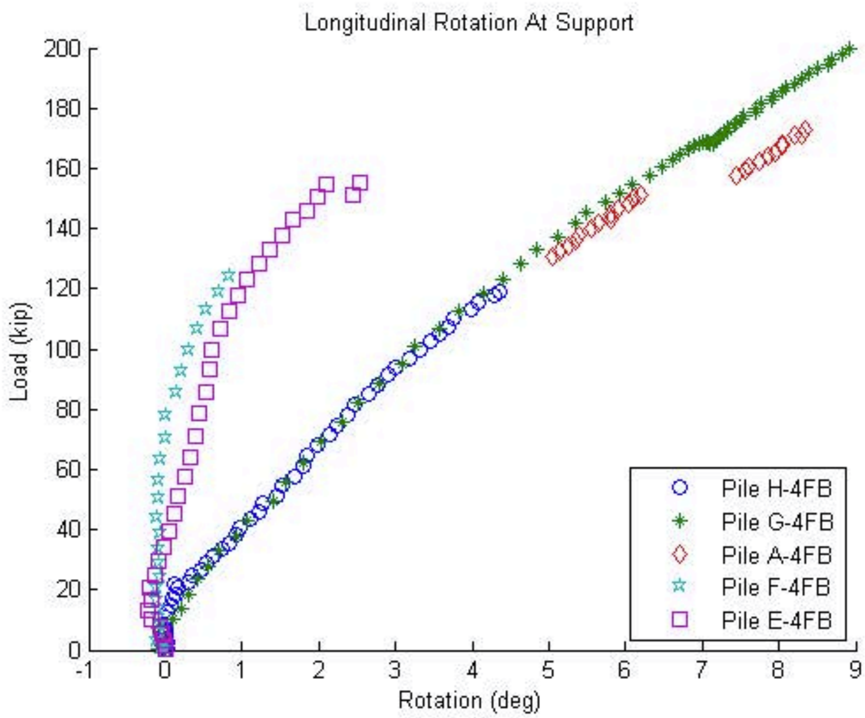
Longitudinal Rotation At Support
Load (kip)
Rotation (deg)
Pile H-4FB
Pile G-4FB
Pile A-4FB
Pile F-4FB
Pile E-4FB

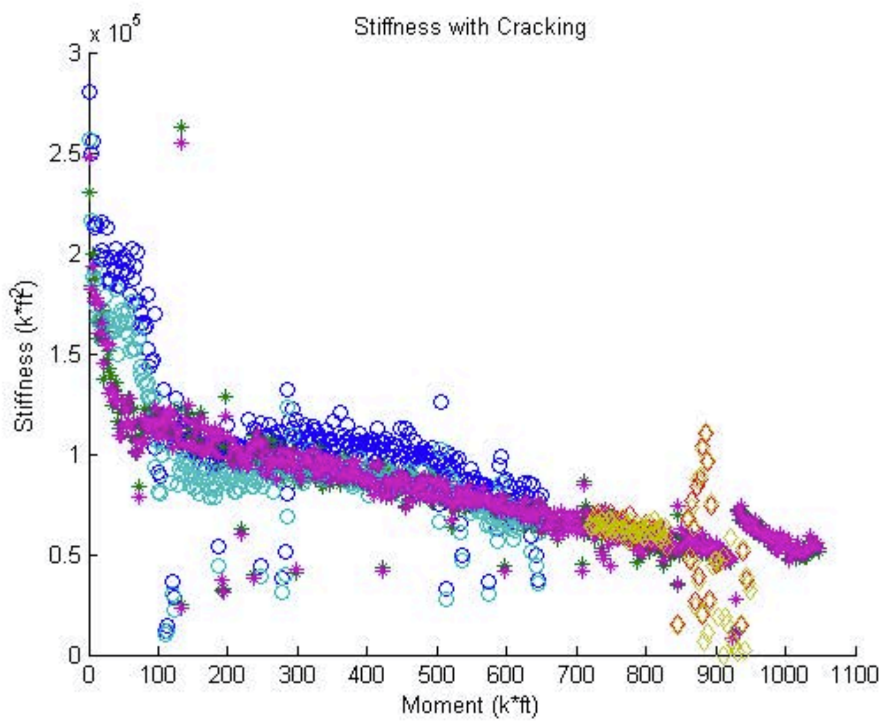
Stiffness with Cracking
x 10^5
Stiffness (k*ft^2)
Moment (k*ft)

Appendix T: Summary of Pile C Tests

Summary of Pile C Tests

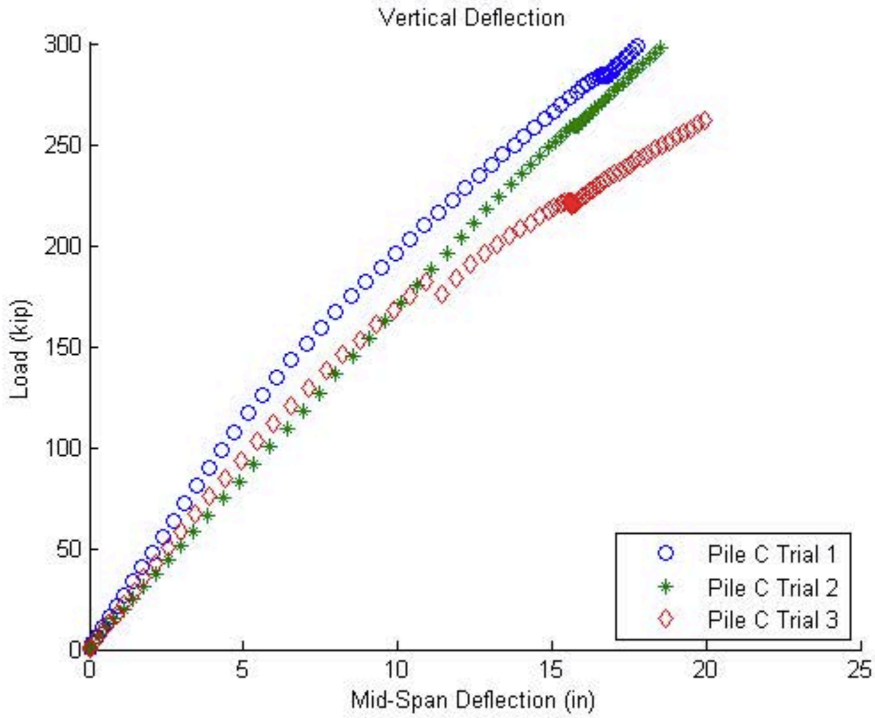

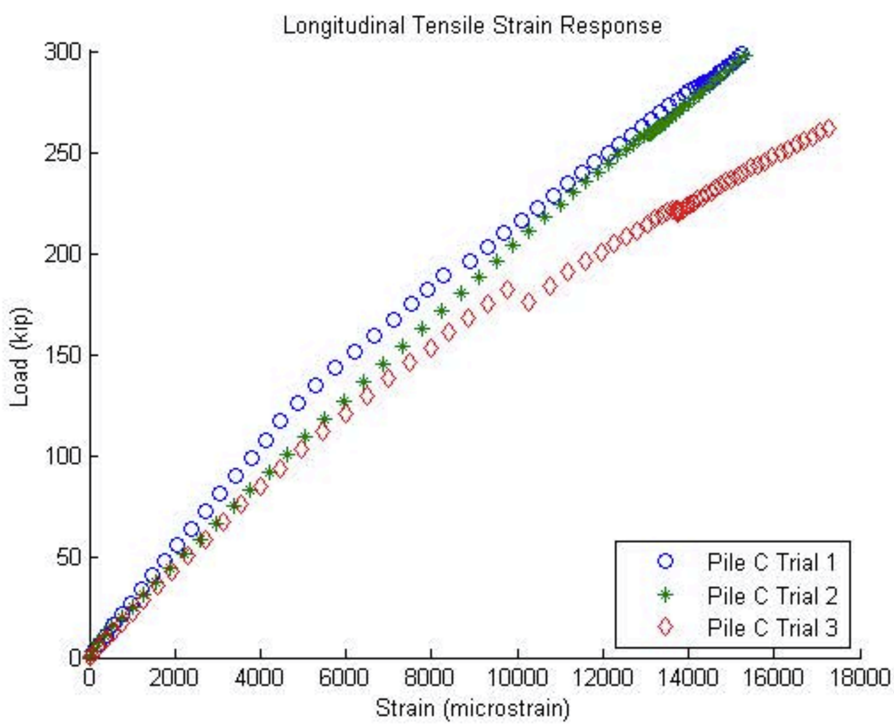

Summary of Pile C Tests

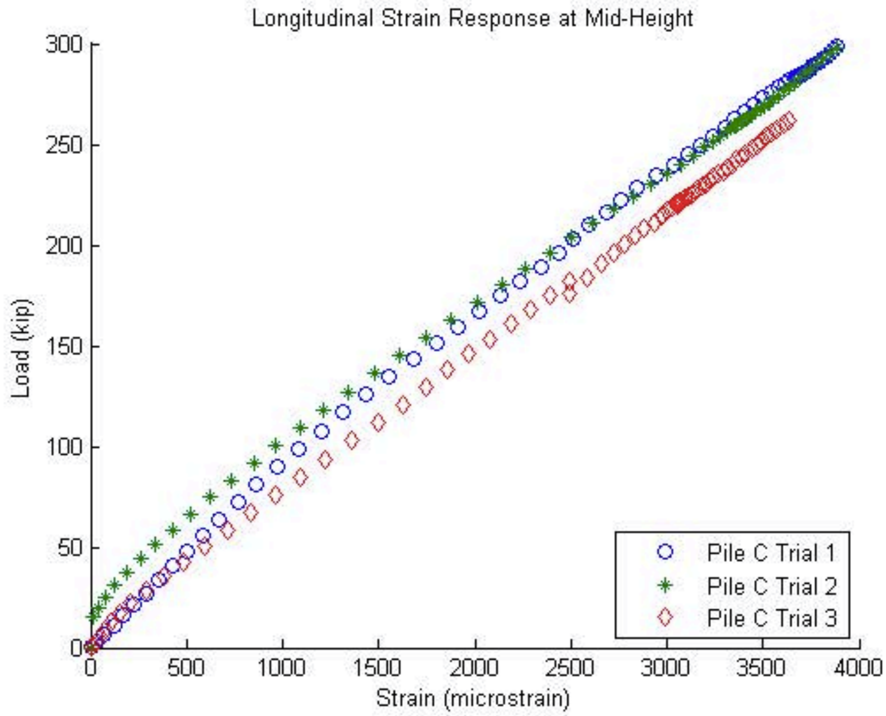

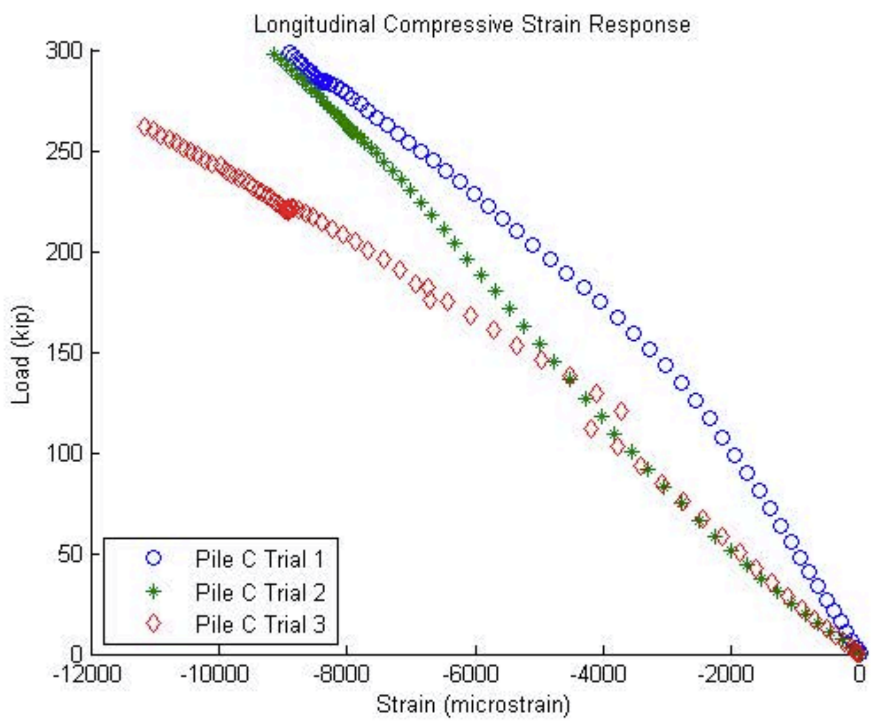

Summary of Pile C Tests

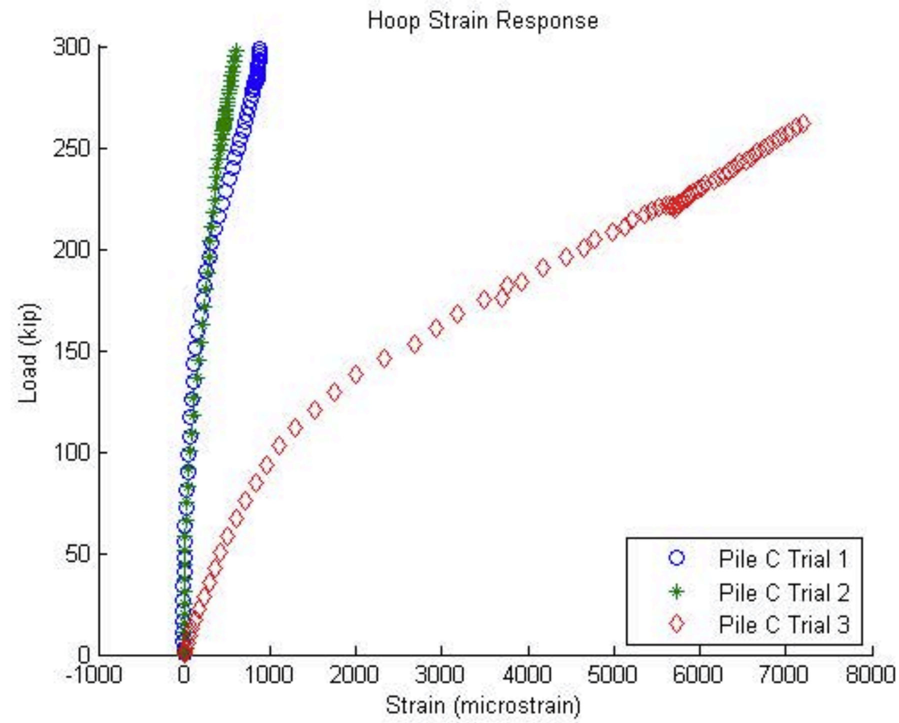

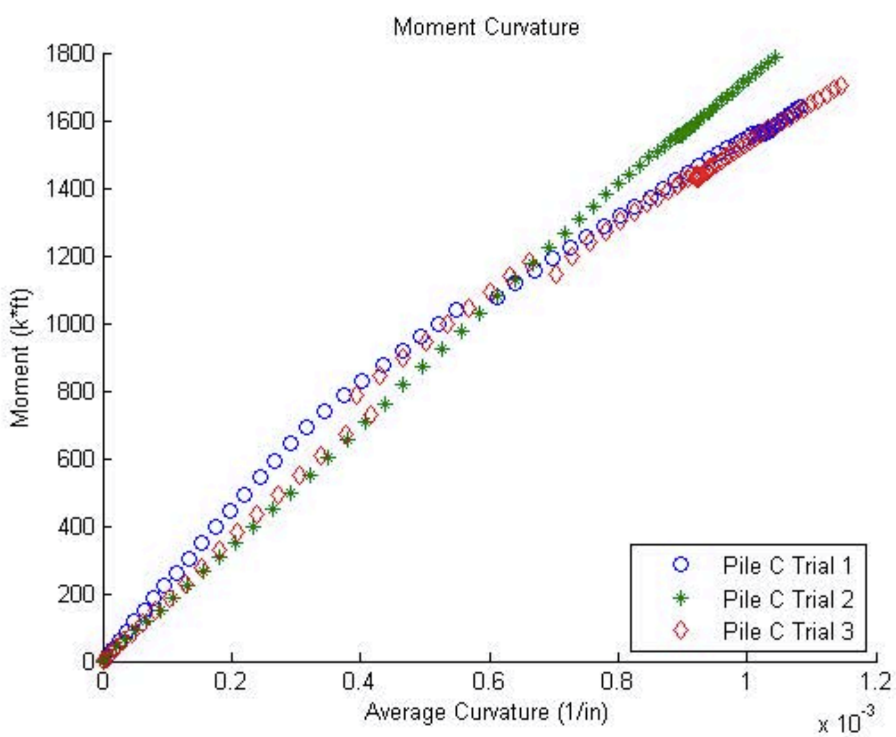

Summary of Pile C Tests

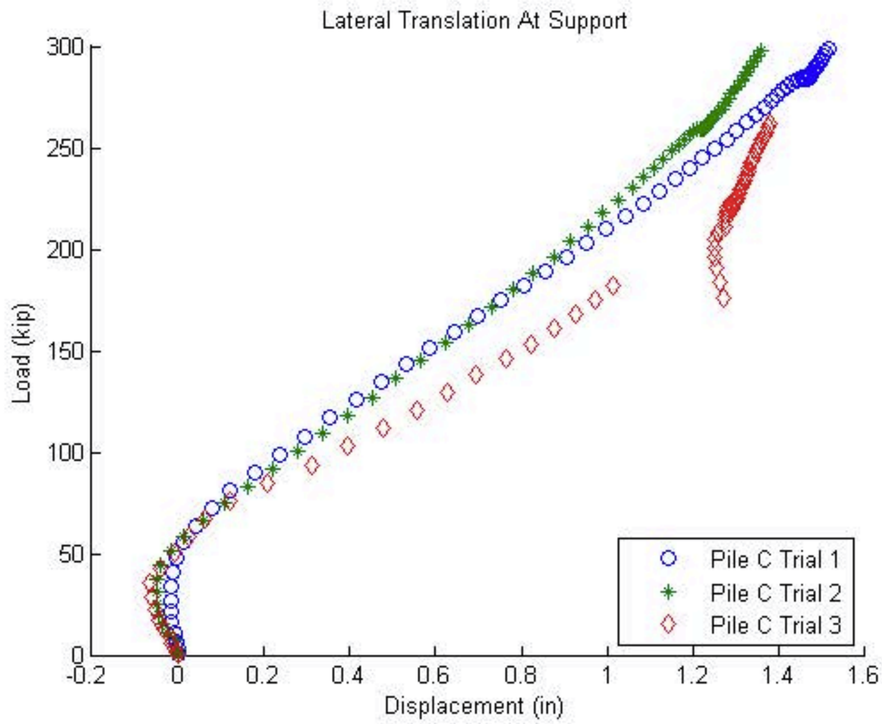

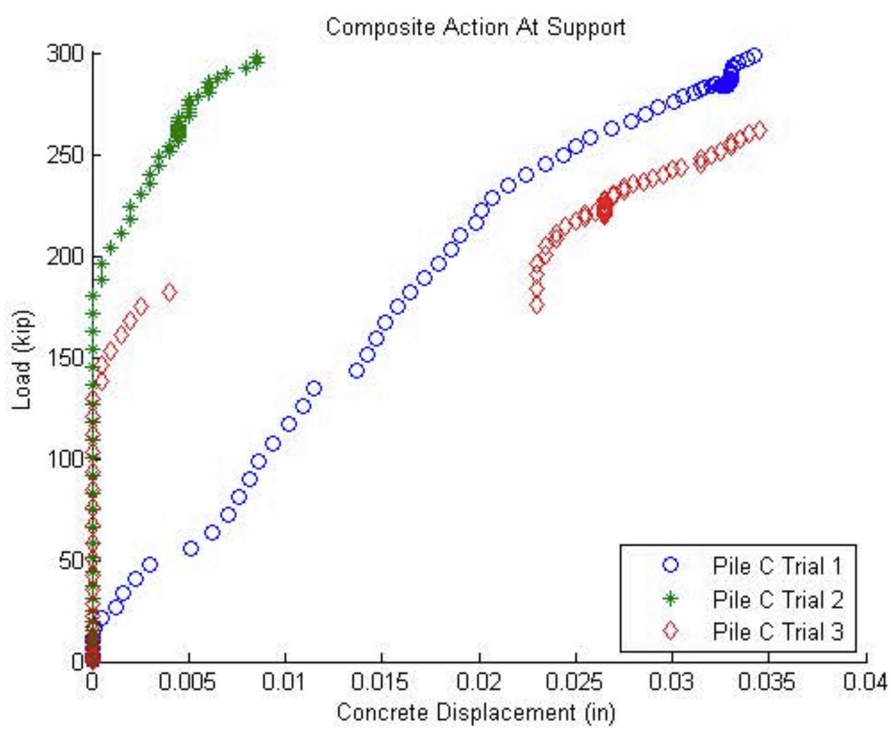

Summary of Pile C Tests